FINAL REPORT

Direct Push Chemical Sensors for DNAPL

ESTCP Project: ER-0109

JANUARY 2007

Stephen H. Lieberman
Space and Naval Warfare Systems Command

Environmental Security Technology Certification Program

Report Documentation Page

Form Approved
OMB No. 0704-0188

1. REPORT DATE	2. REPORT TYPE	3. DATES COVERED
JAN 2007		**00-00-2007 to 00-00-2007**

4. TITLE AND SUBTITLE	5a. CONTRACT NUMBER
Direct Push Chemical Sensors for DNAPL	5b. GRANT NUMBER
	5c. PROGRAM ELEMENT NUMBER
6. AUTHOR(S)	5d. PROJECT NUMBER
	5e. TASK NUMBER
	5f. WORK UNIT NUMBER
7. PERFORMING ORGANIZATION NAME(S) AND ADDRESS(ES) **Space and Naval Warfare Systems Command,4301 Pacific Highway,San Diego,CA,92110**	8. PERFORMING ORGANIZATION REPORT NUMBER
9. SPONSORING/MONITORING AGENCY NAME(S) AND ADDRESS(ES)	10. SPONSOR/MONITOR'S ACRONYM(S)
	11. SPONSOR/MONITOR'S REPORT NUMBER(S)

12. DISTRIBUTION/AVAILABILITY STATEMENT
Approved for public release; distribution unlimited

13. SUPPLEMENTARY NOTES

14. ABSTRACT

15. SUBJECT TERMS

16. SECURITY CLASSIFICATION OF:			17. LIMITATION OF ABSTRACT	18. NUMBER OF PAGES	19a. NAME OF RESPONSIBLE PERSON
a. REPORT	b. ABSTRACT	c. THIS PAGE			
unclassified	**unclassified**	**unclassified**	**Same as Report (SAR)**	**170**	

Table of Contents

Lists of Acronyms

AFCEE	Air Force Center for Environmental Excellence
ASTM	American Society for Testing and Materials
CLP	Contract Laboratory Program
Co-PI	Co Principal Investigator
CPT	Cone Penetrometer Test
CRDA	Cooperative Research and Development Agreement
DNAPL(s)	Dense Non-Aqueous Phase Liquids
DoD	Department of Defense
DOE	Department of Energy
DOIT	Demonstrating Onsite Innovative Technologies
DOT	Department of Transportation
DTI	Dakota Technologies, Inc.
ESTCP	Environmental Security Technology Certification Program
Georgia Tech	Georgia Institute of Technology
GeoVIS	Soil Video Imaging System
HRF	High Resolution Fluorescence
IAS	Initial Assessment Study
ITMS	Ion Trap Mass Spectrometer
LIF	Laser Induced Fluorescence
MCL	Maximum Allowable Contaminant Level
MIP	Membrane Interface Probe
MLLW	Mean Low Level Water
mm	millimeters
ms	milliseconds
NAPL	Non-Aqueous Phase Liquid
NAS	Naval Air Station
PCE	Tetrachloroethylene
PI	Principal Investigator
PWC	Public Works Center
QUAPP	Quality Assurance Project Plan
RI/RFI	Remedial Investigation/Remedial Feasibility Investigation
RPM	Remedial Program Manager
SCAPS	Site Characterization and Analysis Penetrometer System
SERDP	Strategic Environmental Research and Development Program
SPAWAR	Space and Naval Warfare
SSC	SPAWAR Systems Center

SSC-SD	SPAWAR System Center, San Diego
TCE	Trichloroethylene
TDS	Thermal Desorption Sampler
TSTG	Technology Specific Task Group
US EPA	United States Environmental Protection Agency
VOC(s)	Volatile Organic Compound(s)
WGA	Western Governors Association
XSD	Halogen Specific Detector

List of Figures

List of Tables

1 Introduction

1.1 Background

The Department of Defense (DoD) critically requires faster, cheaper, and more accurate procedures to characterize and monitor volatile organic compounds (VOCs) in the subsurface. Chlorinated solvents in the form of dense non-aqueous phase liquids (DNAPLs) pose the most serious challenge. Failure to adequately define DNAPLs source terms plagues many remediation efforts, wasting millions of dollars and possibly exacerbating the problem by redistributing the contaminant over a larger area. The inadequacy of current characterization techniques makes for highly uncertain clean-up time and cost estimates. With present methods it is likely that decades and tens of billions of dollars will be required to cleanup DoD sites.

Chlorinated solvents form DNAPLs because they are immiscible with and denser than water. Unlike petroleum hydrocarbons, DNAPLs sink as they travel through the vadose zone and into the ground water, leaving behind a trail of micro-globules in the soil matrix [1], [2]). The heterogeneously distributed "free-product" phase can continue to contaminate large volumes of groundwater for decades to centuries [3]. Tetrachloroethylene (PCE) has been detected in more than 10% of the wells tested in California [4]; the 5 ppb maximum allowable contaminant level (MCL) was exceeded in more than a quarter of the wells testing positive.

Defining the 3-dimensional subsurface distribution of VOCs traditionally relies on drilling, discrete sampling, and laboratory analysis. This strategy is messy, yields an incomplete picture, and the data are often suspect. Samples are extracted from the soil cores at widely separated intervals (typically several feet), the choice of where to sample is made arbitrarily, and volatiles are easily lost during the process. Unconsolidated sands and silty soils tend to flow in the saturated zone, resulting in poor retention of samples collected via split spoon below the water table.

The trial-and-error placement of soil borings and monitoring wells to locate the DNAPLs source terms is notoriously inefficient; even at intensely investigated DNAPL sites with high dissolved phase concentrations, direct detection of residual or free-phase DNAPL in the groundwater zone can be maddeningly rare [3]. For example, 328 monitoring wells were placed at Oak Ridge before free-phase product was finally observed. Methods that attempt to delineate DNAPL distributions by extrapolating the results from indirect methods, e.g., soil gas survey results, are generally unsuccessful. Non-invasive geophysical techniques that aim to "image" DNAPLs from the ground surface have not proved out [2] and breakthroughs do not appear imminent. The deeper the contamination, the lower will be the expected efficacy of any non-intrusive detection scheme.

Injection of solvents and/or surfactants can dissolve and mobilize DNAPLs, thereby complementing other remediation technologies such as steam thermal enhanced venting, sparging/venting, and in-well aeration; partitioning interwell tracer tests (PITT) can estimate the total contaminant mass. Removal efficiencies greater than 90% using surfactants at relatively homogenous sites, e.g., Hill AFB, have been reported [5]. But injection/extraction methodology is expensive and critically depends on a priori knowledge for design of the well field. As

Fountain cautions "Adequate site characterization is critical for evaluating the applicability of any DNAPL remediation technology and characterization of the DNAPL distribution is essential for both remediation design and performance evaluation… the ultimate level of clean up may be governed more by the hydrogeology than the technology."

The philosophy of minimally invasive methods embodied by the SCAPS program represents a major SERDP and ESTCP success story. For example, the SCAPS laser-induced fluorescence (LIF) technology for petroleum hydrocarbons (commercialized as the Rapid Optical Screening Tool) has been applied at hundreds of fuel-contaminated sites. Unfortunately, the LIF method cannot track dissolved phase plumes, the LIF data are screening in nature owing to soil matrix effects, and furthermore chlorinated solvents are not intrinsically luminescent. DoD urgently requires a direct push method (or combination of methods) that can definitively identify, verify, and quantitative VOCs in situations ranging from dissolved phase near the maximum contaminant levels (MCLs) to high-resolution characterization/delineation of DNAPL source zones. This ESTCP project, which retains the original SCAPS vision of continuous contaminant logging as a function of depth below ground surface, extends the original SCAPS approach to DNAPLs.

1.2 Objectives of the Demonstration

The objective of this effort is to demonstrate and validate (dem/val) an innovative suite of VOC characterization and verification tools, with emphasis on direct push deployment and DNAPL source term delineation. By bringing together several related and complementary techniques, the project allows site managers to intelligently choose the best arsenal of tools for any site in which subsurface VOC contamination is the issue. The reports emerging from this effort will accelerate acceptance in the government and private marketplace.

With the aid of SERDP funding, Dakota Technologies, Inc. (DTI) developed a halogen specific detector (XSD) which can be operated downhole behind a membrane interface probe (MIP) that samples the soil formation for VOCs. The MIP has undergone dem/val via an ESTCP project in which vapors are returned to an up hole detector [6], but moving the detector downhole and measuring while the direct push probe is continuously advanced will increase the spatial resolution of DNAPLs detection by an order of magnitude (from feet to inches). Even better spatial resolution (tenths of inches) will be obtained with a complementary High Resolution Fluorescence (HRF) sensing system that can be applied whenever the DNAPLs are fluorescent owing to dissolved petroleum products or humic substances. The ability of the characterization techniques to find DNAPLs will be verified via GeoVIS, an in situ video imaging system developed by the Navy.

1.3 Regulatory Drivers

There are numerous specific DoD Environmental requirements for improved methods for characterizing and cleaning up sites contaminated with chlorinate solvents. These include: Army 1A (1.1K Develop innovative alternative (and non invasive) techniques for sub-surface characterization; Navy 1.I.4.p (Improved remediation of soils contaminated with chlorinated hydrocarbons and other organics); Navy 1.III.1.K (Improved field analytical sensor toxicity

assays, methods and protocols to supplement traditional sampling and laboratory analysis; Air Force (numerous).

1.4 Stakeholder/End-User Issues

As stated previously, clean up of sites contaminated with chlorinated solvents have proven to be problematic. As a result, according to the Interstate Technology and Regulatory Cooperation Work Group DNAPL/Chemical Oxidation Work Team [7], "sites contaminated with DNAPL were often dealt with through a ground water containment strategy whereby the recalcitrant source material an/or the resultant plume of dissolved contaminants are physically contained and monitored over the long term to keep them from migrating further. Emerging in situ technologies are now being developed that actively target these DNAPL sources for elimination or substantial reduction…because the DNAPL source zone is targeted, additional characterization efforts, focused in the known or suspected source zone, are often needed to go beyond the conventional techniques used to delineate a dissolved plume." This study documents the performance of a suite of direct push sensor technologies that are designed to target these DNAPL source zones. This information gained from this evaluation will provide the stakeholder and end-users with cost and performance data on a novel approach for localizing DNAPL source zones.

2 Technology Description

2.1 XSD-MIP System

2.1.1 Design

The XSD-MIP (halogen-specific detector - membrane interface probe) sensor Figure 1 consists of several components housed in a downhole assembly that is advanced continuously through the subsurface. The assembly is mounted just behind the cone penetrometer tip and sleeve sensors. The main components of the XSD-MIP are; the MIP that samples the soil matrix for VOCs, a water removal system, and a halogen specific detector. As the heated membrane is advanced past the soil, the MIP continuously samples the VOCs that come across the membrane from the soil formation Figure 2. The effluents from the MIP are passed directly to the water removal system via a short (ca 6 inch) transfer line. By placing the drying system directly behind the MIP, the amount of water that condenses out in the transfer lines is greatly reduced if not eliminated.

Figure 1. Photograph of the downhole XSD (halogen specific detector), which relies on oxidative chemistry. The sample vapors pass through a reactor core whose temperature is set in the range 800-1100 C, which is high enough to break C-Cl bonds. A current is induced as the chlorine atoms pick up electrons at a ceramic element that is doped with an alkali metal.

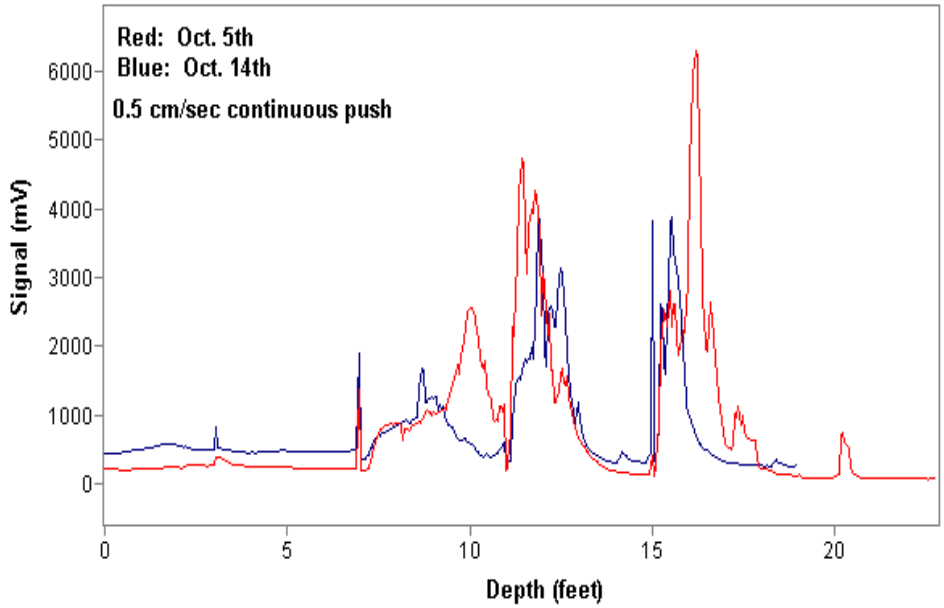

Figure 2. Experimental data from pushes of the XSD at a former dry cleaning site. The two pushes shown here were conducted two weeks apart. Effect of rod changes can be seen in "spikes" in log at 3, 7, 11, and 15 feet below ground surface. Highest PCE concentration seen in nearby well is ca. 5 mg/L.

After passing through the drying system, the gas stream passes into the XSD for analysis. The total distance that the effluents travel from the MIP to the detector is approximately eighteen inches, which corresponds to less than 2 seconds of lag time between sample collection and analysis. Since the probe is typically operated at advancement rates of 0.5-1.0 cm/sec the spatial distortion between collection and analysis is typically on the order of 1-2 inches.

Placing all of the sensing components of the XSD-MIP downhole offers several important advantages over systems where the sample is brought to the surface. First, the adsorption losses in the transfer lines are virtually eliminated with the short transfer lines. Second, the halogen detector's active sensing element operates at elevated temperatures (800-1000 °C), which

effectively warms the transfer lines and reduces the risk of analyte carryover or drag. Finally, depth correlation is straightforward since spatial distortion is only 1-2 inches. These features of the XSD-MIP effectively allow true dynamic logging of halogenated VOCs with depth.

2.1.2 Operation

To ensure that the XSD-MIP offers a representative measure of the subsurface contamination, several parameters must be held as constant as possible during operation. These parameters include:

- carrier gas flow rate and pressure
- XSD temperature
- MIP temperature
- advancement rate of the probe

To properly control both the pressure and flow rate, a pressure regulator and mass flow controller are used to maintain a constant carrier gas delivery to the MIP. Prior to field operation, both of these devices are set to an appropriate value (15-20 psig and 20-30 mL/min, respectively) and not changed during the entire data collection effort. These settings allow the transfer lines to be quickly swept free of analytes while not significantly diluting the analyte.

The XSD's temperature must be held constant to minimize variability in response. To maintain a constant temperature, a programmable power supply and temperature controller are used to actively monitor and control this detector. With this system, we are able to hold the detector's temperature at ± 0.5 ºC around the setpoint even when the probe is being advanced through varying geologic conditions. Transition from the vadose zone to the water table is a particularly challenging zone; MIP temperature drift in this region is typical. However, the XSD temperature control system manages to hold the temperature steady, even in this difficult zone.

As mentioned, when the probe is advanced into the subsurface, the MIP is constantly exposed to different soil and water conditions. These differing conditions require the MIP controller to be constantly adjusting the power to the MIP. While we have never been able to maintain a truly constant temperature of the MIP, our research has shown that as long as the temperature of the MIP is held at least 10-15 degrees above the boiling point of the suspected analytes, transport efficiency across the membrane is nominally constant. Most chlorinated VOCs have boiling points ranging from 40-120 ºC so we typically hold the MIP temperature between 130-140 ºC to minimize variability in transport efficiency. However, during the Camp Lejeune demonstration, the main contaminant was 1,1,2,2-tetrachloroethane (PCA), which has a boiling point of 146 ºC. Therefore, we chose to change the MIP operating temperature to 155 ºC to attempt to keep the temperature above PCA's boiling point. Unfortunately, the MIP controller was unable to maintain this temperature. Furthermore, the controller used was operated in PID (proportional/integral/derivative) mode, which further exacerbated the problem. These factors caused a variance in the MIP temperature of between 110-150 ºC, which is outside our normal operating range.

The advancement of direct push technology in continuous fashion is recognized as being superior to stop-and-go or discrete sampling techniques because of the ability to get a more continuous and representative picture of the subsurface contamination, including those subtle but important transition zones or narrow seams. Our research has shown that continuous

advancement results in more consistent results across varying soil types. Conditions at the surface of the MIP, such as temperature and pressure, have a great influence on the transport efficiency of the analyte across the membrane. Since the probe is continuously moving into fresh "undepleted" and unheated soil we maintain consistency (to the best of our ability) in the parameters that affect transport across the membrane. Stop and go sampling scenarios result in higher variances between clays and sands for instance, which have very different reactions to a "parked" MIP. By collecting data continuously with probe advancement, the XSD-MIP system reduces the variability in transport efficiencies caused by the changes in hydrostatic pressure with differing soil types.

While no instrument or methodology can address all the variables inherent with direct push technology, the XSD-MIP's design and operation addresses several of the issues inherent with this technology. Because of the advances made in the design and development of the XSD-MIP, we are convinced that the instrument can be used to accurately estimate the total halogen concentration in-situ and in real-time. Therefore we embarked on developing a calibration procedure that could be used during field operation to calibrate the instrument prior to each push. The following sections discuss the development of this calibration procedure and the ultimate results of these efforts.

2.1.3 Calibration Procedure

Dakota Technologies, Inc (DTI) has conducted extensive research in developing soil samples and probe advancement emulation systems for determining the most appropriate calibration technique. Our research has shown that consistently preparing soil samples for calibration is virtually impossible because of the variability in water content, sample mixing, volatile loss, sample presentation to the MIP, etc. Therefore, we chose to employ a flowing water solution (a calibration matrix easily produced) to consistently introduce calibration material to the MIP. This method was chosen because it closely simulates the membrane movement and exposure to saturated soil, which also flows continuously over the MIP in practice.

The original calibration method developed, referred to as the flowing sample method, was designed to efficiently and reproducibly flow aqueous calibration solutions over the MIP membrane. The main components of the system (Figure 3) are: (A) a water reservoir, (B) a calibration reservoir, (C) a switching valve, (D) a peristaltic pump, and (E) a flow cell. To collect data with the calibration apparatus, a flow cell (Figure 4) is secured over the MIP with a clamping system to eliminate leakage. A controlled flow of clean water is then passed over the membrane to simulate clean (no contaminate) conditions. After a certain interval, the system is switched to flow an analyte solution over the membrane. After stabilization of the detector signal, data is collected for at least two more minutes. Upon completion, clean water is again flowed over the membrane to clean out the flow cell and membrane for the following runs. This procedure was used to determine the correlation between chlorinated VOC concentrations and the detector's response (Figure 5). The solutions used for this experiment ranged from low ppm range to near the saturated level for TCE (Figure 6).

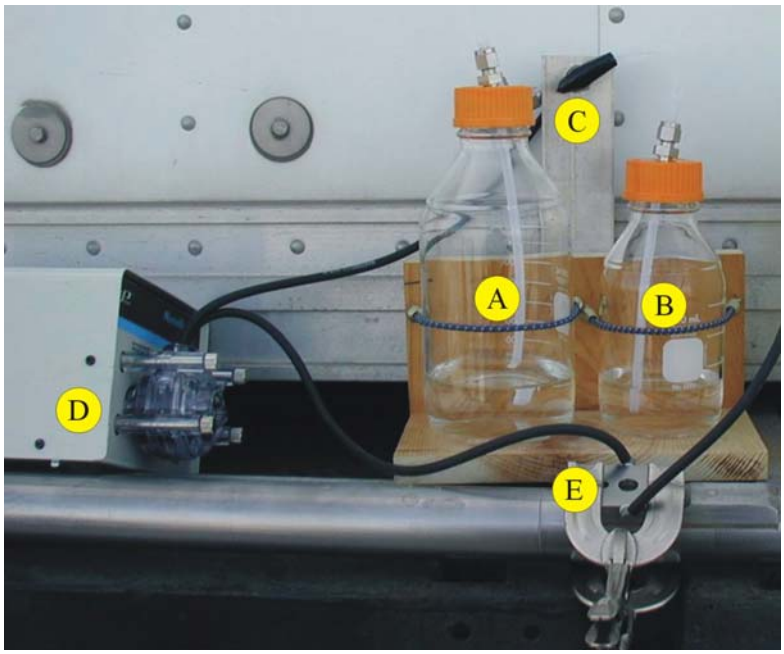

Figure 3. Dual reservoir flow cell system. The system consists of: (A) water reservoir, (B) calibration reservoir, (C) switching valve, (D) peristaltic pump, and (E) flow cell

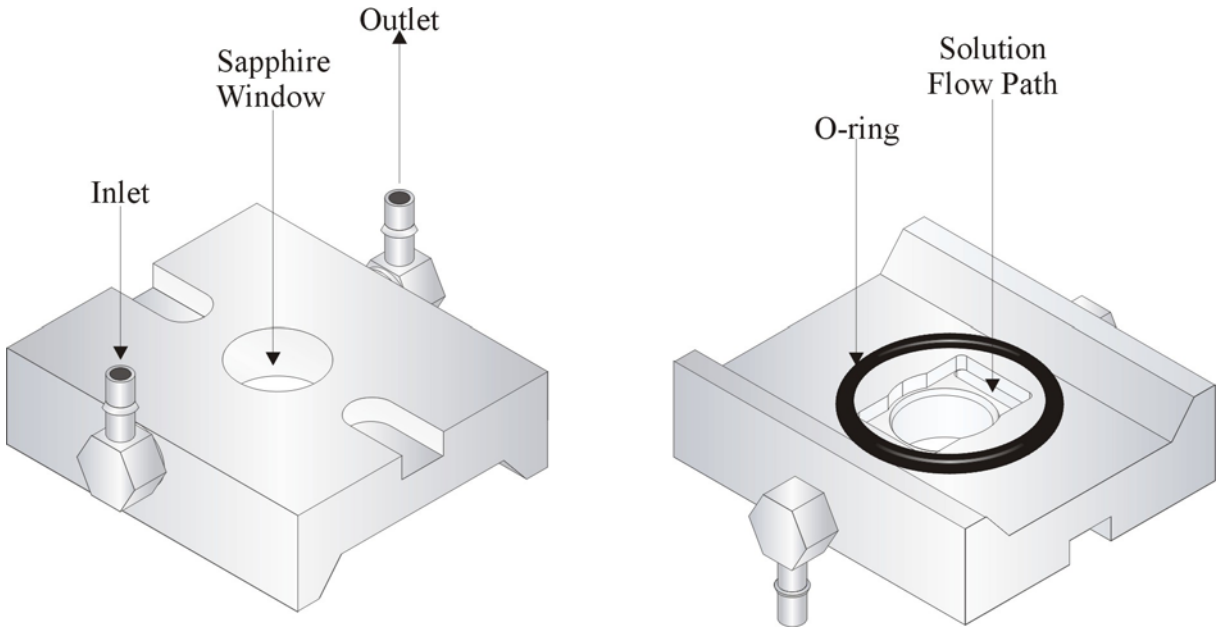

Figure 4. Schematic of the flow cell used to calibrate the XSD

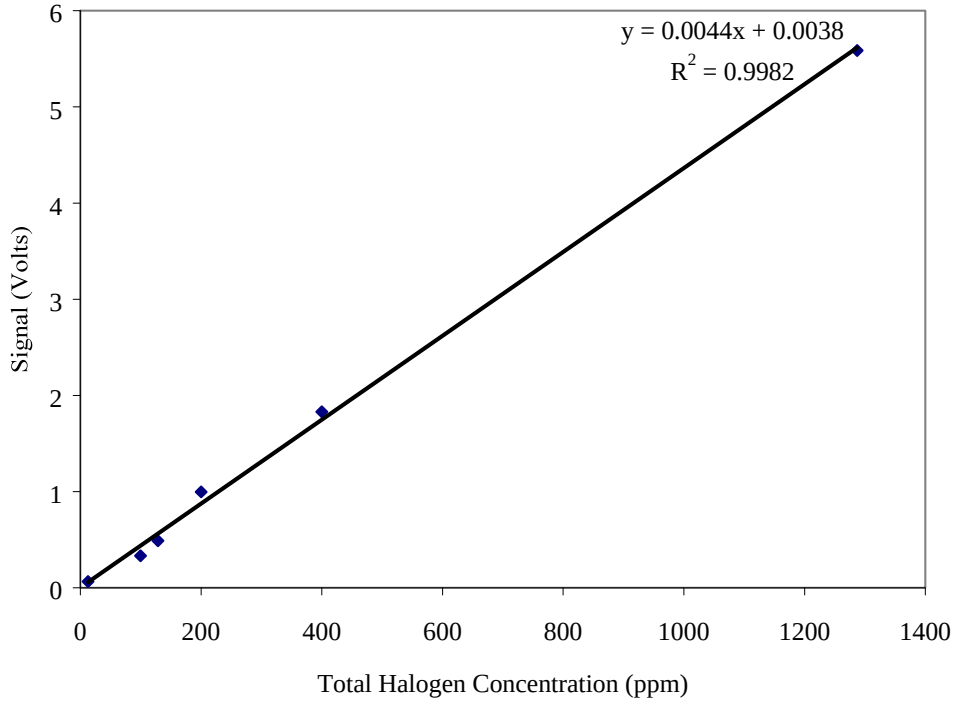

Figure 5. Correlation of XSD-MIP signal with TCE concentration

Table 1. Concentrations and signal levels of TCE solutions

TCE Concentration (ppm)	Signal (Volts)
12.9	0.065
100	0.334
128.7	0.490
200	0.997
400	1.831
1287	5.587

The correlation between the concentrations of the flowing solutions and the XSD-MIP signals are excellent (Table 1). This study clearly shows that the XSD-MIP responds linearly to halogen concentration introduced to its surface.

While the flowing sample method showed accurate correlation between concentration and signal, several drawbacks were encountered during the first ESTCP demonstration at North Island Naval Station (Jan. 2002). First, the system is bulky, requiring a large workspace to operate the instrument. Second, the flow cell requires several minutes to clean out after an analyte solution has been passed through it. Finally, a large amount of chlorinated waste is generated using the system that must be handled and disposed of properly. Because of these drawbacks, we determined that a simplified approach would be more suitable for field calibration.

The simplified approach that was developed, referred to as the aliquot injection method, uses the same cell (Figure 4) but does not require the dual reservoirs, the switching valve or the peristaltic pump. Rather, an aliquot of analyte solution is injected into the cell and allowed to boil. As soon as the signal levels reach their maximum levels, a pulse of compressed air is blown through the cell, which quickly cleans out the system. While the aliquot injection method is much simpler than the flowing sample method, it was crucial that we prove that the information obtained using the aliquot injection method could be directly correlated to the flowing system (which most closely emulates the subsurface) for accurate determination of analyte concentration.

To determine the correlation between the aliquot injection method and the flowing sample method, two common chlorinated VOCs, trichloroethylene (TCE) and 1,1,1-trichloroethane (TCA), were chosen as test compounds. To prepare solutions of these compounds, excess analyte was added to water and allowed to reach a saturated condition. GC analysis was then conducted on each of the solutions to determine their saturated concentration. Dilutions of these saturated solutions were then prepared and used for the subsequent tests. To assure that any variability in the membrane response was accounted for, a saturated TCE solution was injected through the cell several times prior to each analyte sample. The results of these standardizations were used to normalize all of the subsequent data. The aliquot injection and flowing solution methods were then used to generate data for each analyte sample.

To compare the data from the two different methods a means of determining the average signal was required. The average signal for the flowing sample method was determined by averaging the stabilized XSD-MIP's signal. However, determining an accurate average value for the aliquot injection method was more difficult. Research has shown that using the peak heights of the injected samples does not provide accurate results. Rather, we have found that using the peak area's for each sample injection is a much more effective means of determining the aliquot injection method's true response. The peak area is determined by summing the voltages over forty data points (~ 1 minute) for each injection. The results of these experiments are shown in Figure 6.

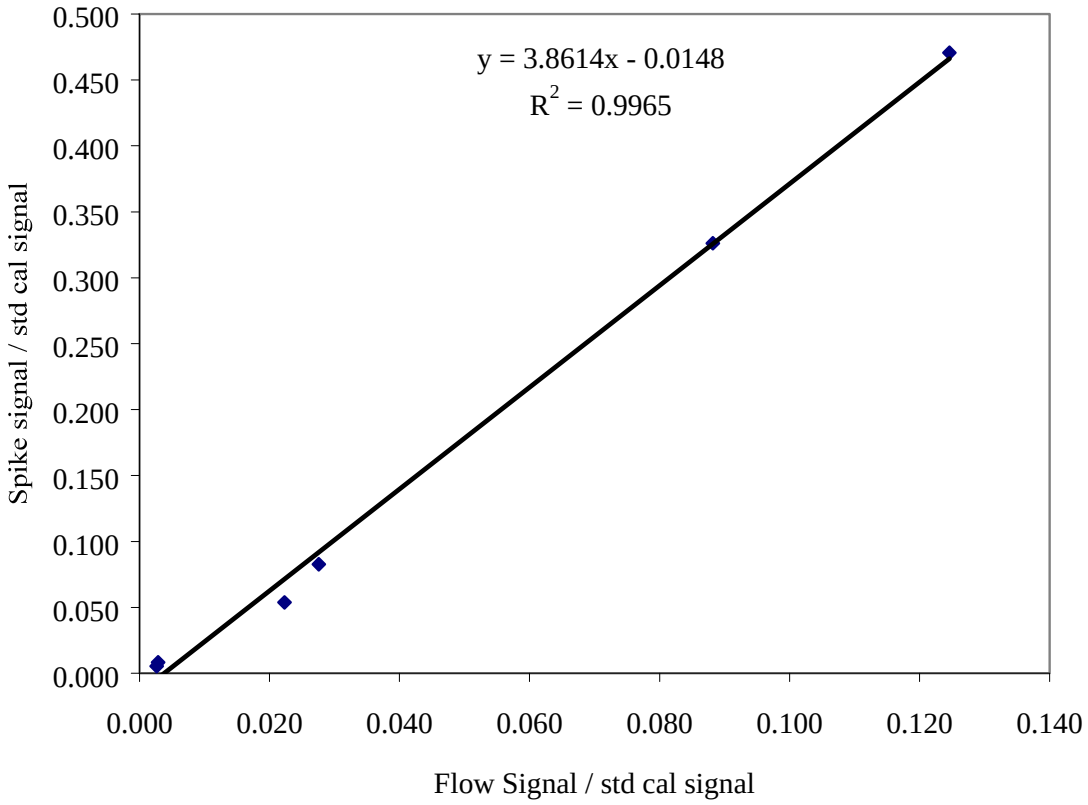

Figure 6. Correlation between aliquot injection method and flowing sample method

The correlation between the aliquot injection method and the flowing sample method is excellent. This experiment shows that the aliquot injection method can be used to ultimately measure the total halogen concentration of the calibration fluid from the XSD-MIP system's native voltage format. The equation that can be used to change the XSD signal voltage to a total halogen concentration is:

Equation 1. $$\text{Conc}_{\text{halogen}} = \left(\text{XSD Signal}_{\text{volts}} / \text{Peak Area}_{\text{std}}\right) \times \left(\text{Peak Area}_{\text{std}} / \text{Flow Signal}_{\text{std}}\right) \times \text{Conc}_{\text{std}}$$

Where:

$\text{Conc}_{\text{halogen}}$ = The Total Halogen Concentration
$\text{XSD Signal}_{\text{volts}}$ = XSD signal at a given data point
$\text{Peak Area}_{\text{std}}$ = Peak area of standard solution
$\text{Flow Signal}_{\text{std}}$ = Average flow signal for standard solution
Conc_{std} = Total halogen concentration of standard solution

For the purposes of our calibration procedure, the slope of the line in Figure 6 can be used for the second term, reducing the equation to:

Equation 2. $$\text{Conc}_{\text{halogen}} = 3.86 \times \left(\text{XSD Signal}_{\text{volts}} / \text{Peak Area}_{\text{std}}\right) \times \text{Conc}_{\text{std}}$$

Therefore, the only thing that is required to change the XSD signal collected during field operation to a total halogen concentration is to perform an injection of a standard solution prior to conducting an XSD-MIP push. Since the saturated TCE solution's concentration does not change appreciably, and its concentration has been determined with GC analysis, it is used as the standard solution used for the field calibration.

The final task in the calibration procedure was to determine if the XSD-MIP could be used on both single analyte solutions and solutions containing mixtures of analytes. The use of several different chlorinated VOCs in the same solution raises an aspect of the XSD-MIP system that must be explained. The XSD responds to the number of halogens in solution, so this must be taken into account. For example, if two equal concentration solutions were prepared, one containing TCE and the other PCE, the signal level from the PCE solution would be 4/3 that of the TCE solution. Therefore, one cannot simply plot the solution concentration but must rather plot the total halogen concentration. The total halogen concentration for a given analyte is determined by multiplying the solution concentration by the number of halogens on that analyte (2 for cis-DCE, 3 for TCE, 4 for PCE, etc.).

To show the ability of the XSD-MIP to accurately predict total halogen concentration, a series of single component solutions were prepared and analyzed using the aliquot injection method. After analysis of these solutions, several mixed analyte cocktail solutions were prepared and run on the XSD-MIP system. The results of the single component solutions were then plotted to determine an equation to predict the concentration of the multiple component solutions (Figure 7). This equation was then used to predict the total halogen concentration of the mixed analyte solutions.

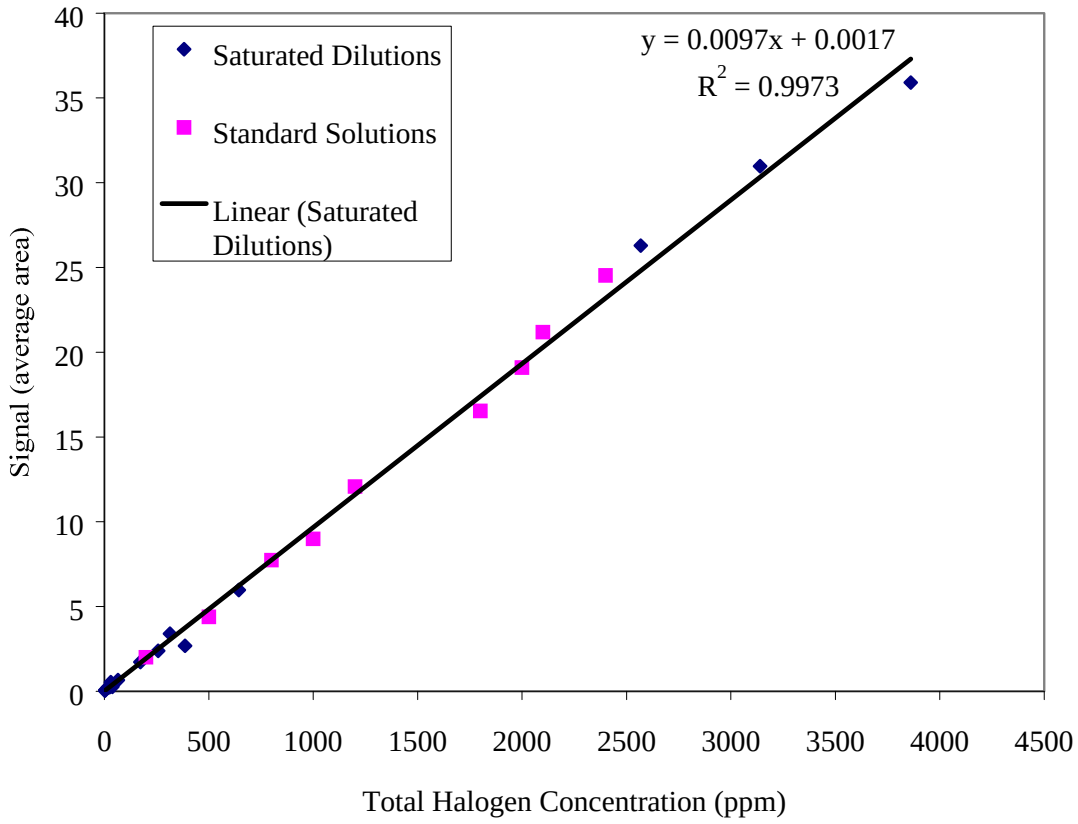

Figure 7. Peak Area versus total halogen concentration

Table 2. Total halogen concentrations for test solutions

Compounds Present	Solution Concentration x # of halogens	Total Halogen Concentration	Experimental Halogen Concentration
PCE CH2Cl2	25 ppm x 4 50 ppm x 2	200	207
CCl4 CH2Cl2	50 ppm x 4 150 ppm x 2	500	454
TCE CCl4 CH2Cl2	100 ppm x 3 100 ppm x 4 50 ppm x 2	800	800
CH2Cl2 1,1,2-TCA	200 ppm x 2 200 ppm x 3	1000	931
TCE CH2Cl2 1,1,1-TCA	150 ppm x 3 150 ppm x 2 150 ppm x 3	1200	1250
TCE 1,1,1-TCA 1,1,2-TCA	200 ppm x 3 200 ppm x 3 200 ppm x 3	1800	1711
TCE CCl4 1,1,1-TCA	200 ppm x 3 200 ppm x 4 200 ppm x 3	2000	1977
TCE CCl4	300 ppm x 3 300 ppm x 4	2100	2193
CCl4 CH2Cl2	400 ppm x 4 400 ppm x 2	2400	2539

2.1.3.1 Calibration solution

Water that is placed in constant contact with DNAPL (neat TCE in our case) reaches somewhat less than saturated concentrations because of the presence of DNAPL in the container. We have determined the concentration of aqueous solution in the presence of neat TCE is 1280 ppm by GC analysis. A large reservoir of this solution proves to be a convenient and repeatable source for calibrating the XSD and was used in the demonstration. Calibrating the XSD-MIP system to this nearly saturated concentration is referred to as the saturation response calibration (SRC).

2.1.3.2 Calibration procedure

The simplified aliquot approach discussed previously was used for calibration of the XSD-MIP system at Camp Lejeune. To calibrate the system, the flow cell was attached to the MIP membrane with customized Vise Grips. The data collection program was started and the signal vs. time and MIP temperature vs. time were monitored. Two minutes of baseline were collected, at which time a 1-milliliter aliquot of the SRC solution was injected into the flow cell system. As soon as the signal levels reached their maximum levels, a pulse of compressed air was blown through the cell, which quickly cleaned out the system. The signal levels were then allowed to return to baseline. Three replicate runs were then performed using the above procedure to produce a total of four SRC signals.

2.1.4 XSD optimization

Using the calibration procedure described above, the XSD-MIP system was adjusted to provide a 1/6 full-scale response (~1.5 V) when the SRC calibrant was applied to the system. This relatively low level (with respect to earlier field efforts) was chosen because the main contaminant at Camp Lejeune (1,1,2,2-tetrachloroethane or PCA) has a saturated level of approximately 2900 ppm. Since the XSD-MIP system acts as a halogen counter, the total halogen concentration of PCA is approximately 11600-ppm halogens or 3 times that of the TCE standard solution (1287 ppm or 3861 ppm halogens). Therefore, we set the XSD temperature such that any signal levels that exceeded ~5 V would be regarded as having the strong potential for being either high dissolved phase (DNAPL nearby) or DNAPL itself.

2.1.5 Field Data Collection Procedure

2.1.5.1 Initial startup of XSD-MIP system

The following startup procedure was used at the beginning of each day for the XSD-MIP system:

The flow rate of air to the carrier gas delivery line was set to 27 mL/min with a backing pressure of 15 psig. The carrier gas return line was immersed in water to confirm that the carrier gas was flowing through the entire system. If adequate airflow was present, the data collection program was then started and set to display the XSD signal vs. time and XSD temperature vs. time, while the MIP temperature was visually monitored. Next, the heater controllers for the XSD and MIP were turned on and allowed to come up to operating temperature (155 ºC for the MIP and 770 ºC for the XSD). Data collection was continued until the baseline XSD signal and XSD temperature had been stable for five minutes. The run was ended, the data file name was recorded, and the data file was saved to the hard drive and a floppy disk.

2.1.5.2 Field calibration of XSD-MIP system

Prior to an in situ measurement, a calibration of the system was done using the SRC solution and the aliquot injection method described above.

At the end of each push, the SRC data was used to normalize all field data to correct for any changes in responsivity and baseline. The SRC process allowed us to convert the XSD-MIP system's signal from its native data format (volts) to a total halogen concentration (ppm halogens). Application of this factor corrected for any system drift and changed the data to a format that could be readily compared to water sample data. This allowed us to view the entire

project data set in a normalized context at project completion with confidence that any drift in system responsivity had been accounted for. A description of the normalization procedure is given in a following section.

2.1.5.3 In situ measurement procedure for XSD-MIP system

The following procedure was used for all of the in situ measurements with the XSD-MIP system. First, both the XSD and MIP temperatures were checked to insure that they were at stable operating temperatures (155 ºC for the MIP and 770 ºC for the XSD). The MIP temperature was bumped up from the usual 135 ºC setting in an attempt to get better response for PCA due to its higher boiling, but the MIP was only able to sustain 115 to 125 ºC in the sub-surface. Next, the CPT tip was placed at ground surface and the CPT data acquisition program was zeroed. The data acquisition program was started and the probe was advanced at a rate of 1 foot per minute. The probe advancement was continued until either the maximum probe depth was achieved, the probe advancement was rejected, or the deepest suspected contamination level was surpassed. The run was ended, the data file name was recorded, and the data file was saved to the hard drive and a floppy disk.

After the completion of each push, the depth for that log was corrected. This offset was necessary because the software that collects the CPT information is written to use a 31.25-inch spacing from CPT tip to window. For the XSD system, the distance from the CPT tip to the MIP is 24 inches. By subtracting the first 7.25 inches of depth from the ground surface, the depth measurements are corrected for the XSD data.

2.1.5.4 Extraction procedure for XSD-MIP system

At the end of the push the probe was extracted from the subsurface while the MIP and XSD were still operating to maintain sufficient temperature to minimize water intrusion. Upon extraction, the MIP was cleaned off with steel brush, washed with distilled water, and visually inspected for membrane damage.

2.1.6 Data Processing

2.1.6.1 Data normalization process

At the end of each push the calibration run collected prior to the in situ measurement was used to normalize the log. First, the calibration run was background corrected by subtracting the average baseline signal collected at the start of the run. Next, the peak area's for each of the injections was calculated by summing the first forty points that made up each peak. These peak areas were then averaged to determine a mean value for that calibration run.

To convert the in situ measurements to a total halogen concentration, the logs were first background corrected using the average baseline signal collected at the start of the run. The appropriate correction factor and the concentration of the SRC solution (3861 ppm halogens) were then applied to each in-situ measurement using Equation 2. Table 3 shows the peak areas for each of the calibration runs and the correction factor that was applied to each in situ measurement.

Table 3. SRC signal for each profile, average SRC signal and correction factor used for normalization of in situ measurements

Calibration/Run Number	Peak Area	Correction Factor
1	15.32	972.8
2	9.22	1616.4
3	10.03	1485.9
4	14.98	994.9
5	15.22	979.2
6	9.3	1602.5
7	11.51	1294.8
8	8.78	1697.4
9	4.15	3591.2

2.1.6.2 Normalized XSD data

The nine XSD-MIP pushes performed at Camp Lejeune were done on a line in a known area of contamination (Figure 8). Pushes 1, 2, 3, 4, and 5 made up the horizontal length of the transect. Pushes 6, 7, and 8 were replicate pushes of 1, 3, and 2, respectively. These pushes were done approximately 1 foot away from the original probe locations. Finally, push 9 was performed approximately 200 feet east of push 5 in an area known to be contaminated with DNAPL. A description of the main features of each push is given below.

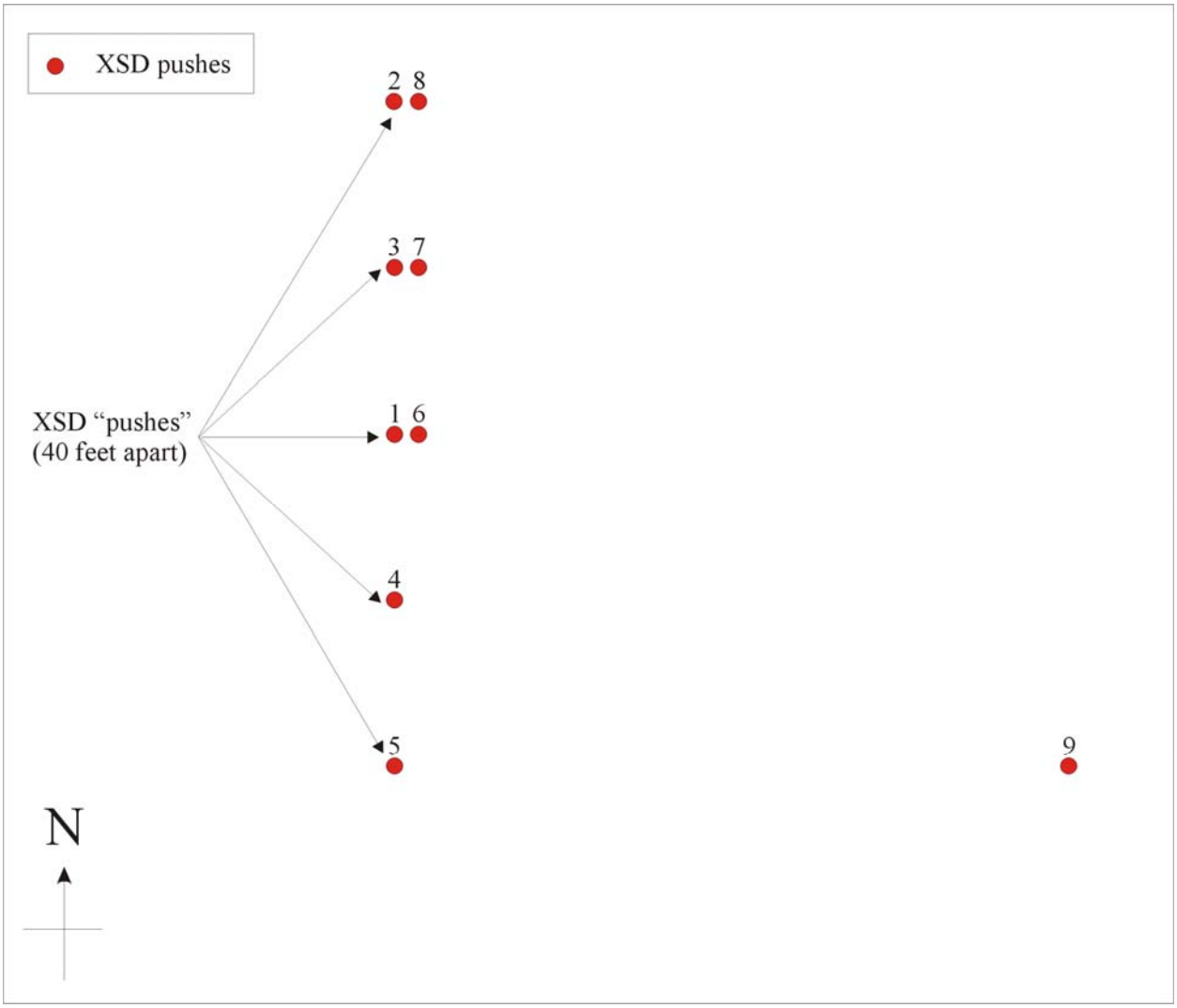

Figure 8. Map of XSD push locations at Camp Lejeune, North Carolina.

Numerous areas of contamination were noted in Push 1 (Figure 8). The largest continuous area ranged from ten to eighteen feet. Lower levels of contamination were noted from four to eight feet. The push was terminated at 18.15 feet.

2.2 Laser-Induced Fluorescence

The laser induced fluorescence (LIF) system used for the demonstration is a rapid optical screening tool (ROST) that was adapted for use in the SCAPS truck. The ROST system is typically deployed on Geoprobe-type direct push platforms that employ percussion hammering to reach depth. The ROST system was integrated with the dual window probe that SCAPS uses for LIF-GeoVIS work. The fiber optics from the SCAPS dual LIF-GeoVIS system was connected to the ROST system without modification. This section provides a description of the ROST system and provides background for understanding and interpreting the fluorescence data.

2.2.1 Polycyclic Aromatic Hydrocarbon (PAH) Fluorescence Principles

2.2.1.1 Laser-induced fluorescence (LIF)

Fluorescence spectroscopy is one of the most widely applied spectroscopic techniques in use today. It is, by nature, a fast, sensitive, and typically reversible process that makes it ideal for incorporation into a continuous screening technique that uses an optically transparent window as the conduit between the sensor and the analyte. Luminescence is the emission of light from any substance that returns to the ground state after being excited into an electronically excited state. If the bulk of the molecules emit their photons in less than a microsecond the emission is referred to as fluorescence. Emission that takes longer than this is called phosphorescence.

Fluorescence is typically observed in molecules that have an aromatic structure. One class of aromatics are the Polycyclic Aromatic Hydrocarbons (PAHs) found in quantity in typical petroleum products. The PAHs found in coal tars, creosotes and even sediments are also fluorescent, but they fluoresce much less efficiently than PAHs dissolved in more solvent-rich environments, such as the aliphatic body that makes up the bulk of fuels/petroleum. We have observed that the less solvent available, the less efficiently the PAHs fluoresce. PAHs found in chlorinated solvents typically exhibit fast lifetimes and lower response than PAHs dissolved in aliphatic solvents. In spite of this, the PAHs co-dissolved in chlorinated NAPL can still be coaxed into fluorescing well enough to allow in-situ LIF screening via a sapphire-windowed probe.

A plot of the relative distribution of the different colors (or energies) of the photons being emitted by an excited sample of PAH is called the spectrum (or spectra when referring to more than one). Figure 9 illustrates the concept of PAH absorbance and fluorescence spectra. The spectra of individual PAH species (such as naphthalene and anthracene) can contain enough structure (peaks and valleys) to be identified in simple mixtures in the lab. The fluorescence of PAHs in sediments however, is originating from such a wide variety and concentrations of PAHs and differing local environments (dissolved phase, sorbed to particles, microcrystals, etc.) that the resulting spectra are very broad and contain very little "structure" that one might use to determine which individual PAHs are responsible for the fluorescence. The spectra do shift enough to recognize that the distribution of species or environments are changing, but individual speciation is impossible.

Another property of fluorescence that can be measured is the varying amount of time it takes for the molecules to emit the photons after exposure to a pulsed excitation source, such as a laser, is illustrated in Figure 10. If we use a time sensitive detector to observe the number of photons being emitted over time, we can derive more information about the nature of the fluorophores and their environment. This decay time information contained within the waveform is measured with an oscilloscope. The different PAHs and the differing environments that exist in sediments all combine to change the decay times observed. This information is readily obtained when using a pulsed source such as the laser we used in this application. Our apparatus (described in the ROST System Description section allows us to investigate not only what colors are being emitted, but also how long it takes for the excited population of PAHs to emit the fluorescence photons. We use a patented method (U.S. Patent 5,828,452) of combining the photons from four regions of the emission spectrum optically collected over 20 nm wide sections of the emission spectra at 340, 390, 440, and 490 nm.

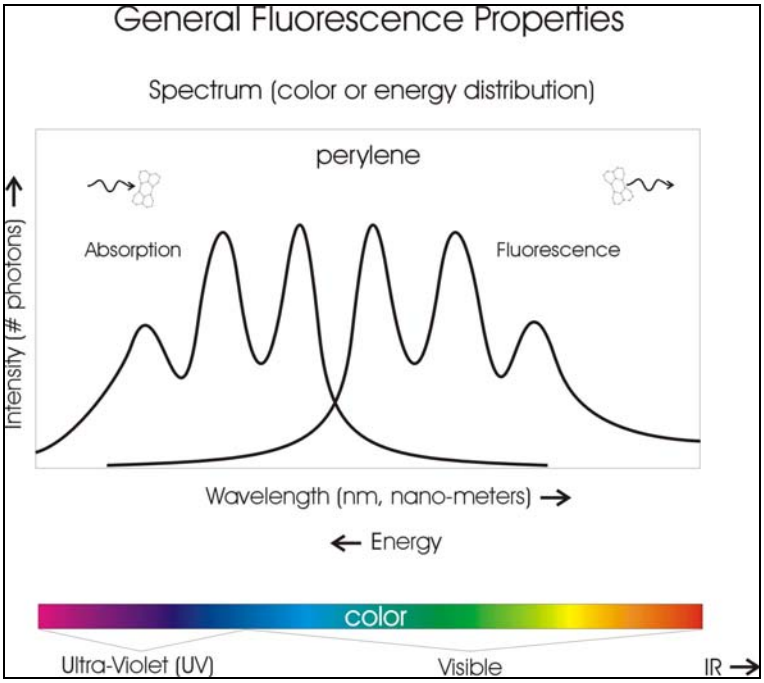

Figure 9. Spectral property of fluorescence

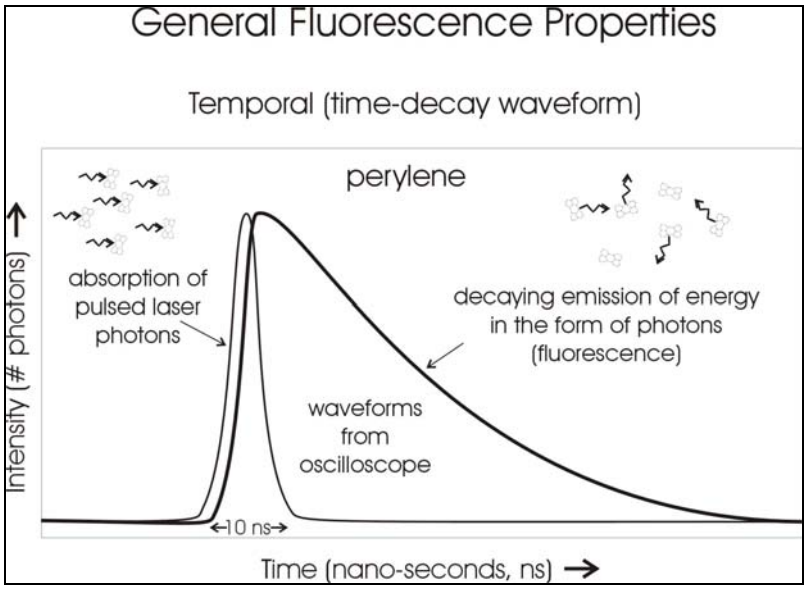

Figure 10. Temporal property of fluorescence

These four "channels" are delayed in time through successively longer fiber optic delay lines and eventually arrive at the detector (photomultiplier tube or PMT). The resulting oscilloscope waveform is a unique measurement of both the spectral and temporal components of the fluorescence. This allows us to simultaneously observe the spectral and temporal qualities of the fluorescence. This technique is described in detail later in this report. It is these multi-wavelength waveforms, measured continuously and stored vs. depth, that ultimately serve as our indicator of PAH concentration vs. depth in the sediment.

2.2.1.2 Interferences

Nature has co-deposited a myriad of additional fluorescent materials in soils that will also absorb the laser light and fluoresce intensely enough to complicate the measurement of the PAH fluorescence. Example materials include minerals such as calcites and a variety of biological materials. Both living organisms and their associated breakdown products (humic and fulvic acids) fluoresce well enough to interfere with the observation of the fluorescence of the target PAHs. This fluorescence, along with scattered excitation laser light and Raman light generated throughout the optical train (fiber optics) will ultimately make it back to the detector, mixed in with true PAH fluorescence, and must be accounted for in some fashion. Throughout this document we will refer to all these sources of non-PAH emitted photons as "background" fluorescence, even though the true source might well be non-fluorescent (scatter) in nature.

2.2.1.3 Understanding ROST Fluorescence Waveforms

Spectroscopic techniques involve probing the target matrix with light and learning about the contents of that matrix by analyzing the light that is emitted or absorbed by the target matrix. For screening tools it is crucial to glean as much information from this light as one can in as little time as possible. ROST accomplishes this task in a novel fashion. The fluorescence data from ROST is deceptively simple. There is a lot more going on in a ROST waveform than one would imagine at first glance. It is actually a two-dimensional data set that contains three-dimensional fluorescence information. To complicate this, some of the information is overlapping. A full description of the multi-wavelength waveform data follows in order to give the reader an understanding of the data acquired during this study.

2.2.1.4 PAH time decay waveforms

Each type of PAH molecule (such as phenanthrene, naphthalene, or anthracene) emits fluorescence over a unique time period after being excited by a pulsed excitation source such as the laser used in ROST. The emission starts out at maximum intensity, and then decays away at a rate unique to each type of PAH. The number of rings, the bonding between them, the amount of substitution on the rings, and other structural features of the molecule determine, to a great extent, the decay rate exhibited by a particular PAH. One class of molecule, the PCBs, have a structure that would seem to fluoresce well, but the chlorine substitution on the rings causes what is referred to as the heavy-atom effect, resulting in non-radiative relaxation from the excited state and a dramatic reduction in fluorescence. In fact the reduction is so significant that PCBs are essentially non-fluorescent molecules.

The environment in which the PAH exists also has a substantial influence on the decay rate. Quenching, which refers to any process that causes a decrease in the decay time (as well as the intensity) of the fluorescence, is dependent on conditions like oxygen levels, solvent availability, solvent viscosity, chlorinated molecules, and a myriad of other matrix dependent conditions. An example of this can be found with the fluorescence of PAHs in fuels (gasoline, diesel, or kerosene) vs. chlorinated solvents. The solvents can often contain more PAHs than the fuels, but the fluorescence lifetime is much shorter and the total fluorescence of fuels is often 2 to 3 orders of magnitude more intense. On the other hand, the fluorescence of chlorinated NAPL can also fluoresce just as intensely as POLs, so it’s difficult to predict how well chlorinated DNAPLs will fluoresce.

Figure 11 illustrates the differing decay times one might observe for four different PAHs, along with the time profile of the laser pulse that excited them. Now remember, these are large populations of PAHs being excited and while some begin emitting immediately, other individual PAH molecules "wait" many nanoseconds before emitting a photon. What is plotted here is a picture of the distribution of times that the PAHs are remaining in the excited state before emitting photons. Now in our case (sediments) we have many different PAHs of differing ring number and substitution levels. The bold curve in Figure 11 illustrates the fluorescence decay profile that would result if we observed the fluorescence of all four PAHs simultaneously. This is the fluorescence waveform that would result if all four different PAHs fluoresced with equal intensity (normalized to keep it on scale). This same concept is happening in the sediments. We are observing the sum of all the decay profiles for all the different PAHs that are absorbing and emitting photons with each pulse of the excitation laser. It should be noted that there is no predictable trend between decay rate and structure like the trend that exists between spectrum and structure as described below.

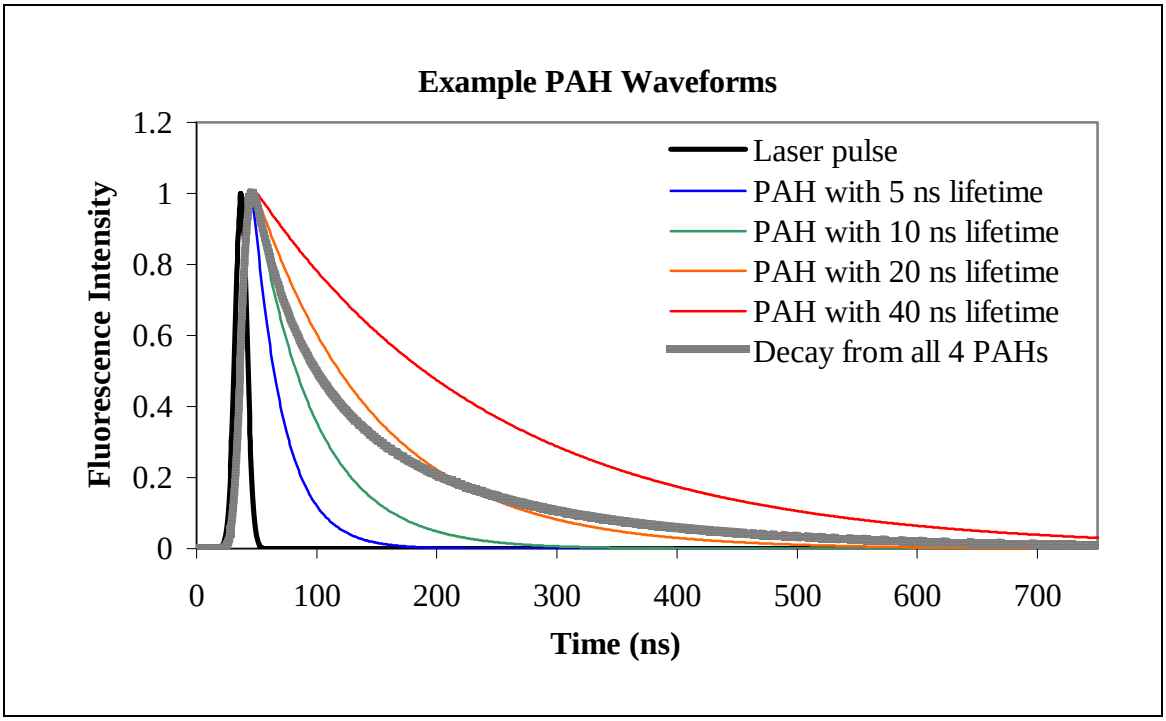

Figure 11. Temporal fluorescence examples

Of course the fluorescence decay profile observed in sediments is not made up of equal amounts of fluorescence from the various PAHs found in them. The wavelengths of light being emitted by (spectra) and the relative fluorescence yields of the different PAHs are all quite different, but the concept is still valid. The decay profile of the PAHs observed in the sediment results from the decay profiles of a mixture of different PAHs, along with fluorescence from other materials in the matrix.

2.2.1.5 PAH spectra

Let's take a look at the other property of the fluorescence emission of the same four example PAHs we showed in Figure 12. This time we'll examine not the time over which they fluoresce, but instead the distribution of energies found in the photons they emit. Remember that the

fluorescence emission spectrum of a pure PAH is simply a graphical representation of the energy distribution of photons that are emitted from a large population of the PAHs as they release energy that was absorbed from the excitation beam of light (in our case, a laser). Spectra of pure PAHs are typically acquired by dissolving a sample of the pure PAH in a pure solvent that does not fluoresce.

Figure 12 depicts the fluorescence emission spectra of the same four PAHs used in the temporal example in Figure 11. The laser wavelength is also shown in Figure 11, demonstrating the principle that fluorescence occurs at longer wavelength (lower energy) than the excitation wavelength (also known as Stokes' shift). The basic trend is toward longer wavelength emission as more rings are added or substitution increases. Naphthalene emits at around 340 nm and the spectra "red-shift" as the number of rings increase. Another general property of fluorescence is that for a pure PAH the emission spectrum remains the same irrespective of what wavelength of light is used to excite them (Kasha's rule). This is not true for mixtures however, because changing the excitation wavelength might well change which PAH are being excited and to what degree. The bold spectrum in Figure 12 is the combined spectra of all four PAHs. This is a simplified illustration of what generally happens if we observe the total fluorescence of a mixture of different PAHs. Any change in the relative amounts of the differing PAHs or changes in the matrix in which they exist will cause a change in the spectrum of light actually emitted.

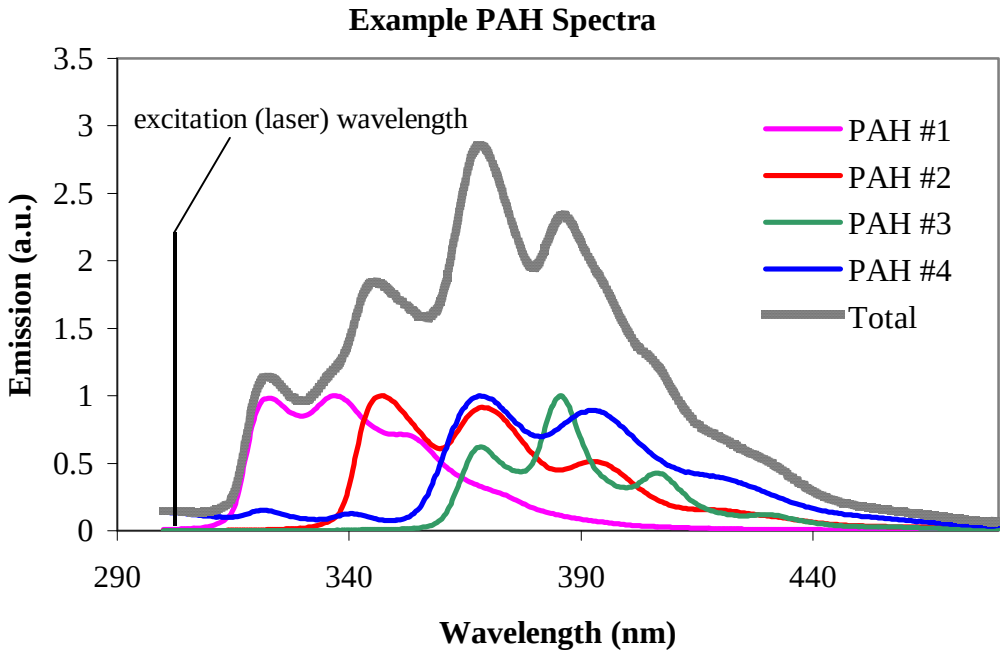

Figure 12. Spectral fluorescence examples

The fairly well defined structure (multiple peaks, valleys, and their various positions) of the spectra in Figure 12 suggests that perhaps one could use algorithms to extract information about the relative concentrations of the individual PAHs. While this is possible for very simple mixtures (2 to 3 PAHs) under controlled conditions, the algorithms quickly fail when many PAHs are present and interference fluorescence from humics, fulvics, and minerals is introduced.

At best, one is able to use the overall shape of the total fluorescence spectrum to predict the type of mixture (diesel, coal tar, crude oil, etc.) and, in fact, this is routinely accomplished in environmental fluorescence forensics.

2.2.1.6 PAH multi-wavelength waveform (MWW)

The fluorescence of PAHs has both a spectral and temporal component. Real-world environmental samples typically contain at least several (if not dozens) of different PAHs along with other fluorophores, and the PAH fluorescence spectra overlap to form broad and fairly featureless spectral and temporal emission (compared to pure PAH spectra). If we were to record the temporal decay waveforms across the entire spectrum we would record what is called a wavelength-time matrix (WTM) that would describe the fluorescence emission completely. To create this we scan the emission selection monochromator from wavelength to wavelength, monitoring the pulsed emission vs. time at each wavelength with an oscilloscope.

Figure 13 contains the WTMs of diesel, jet, creosote, and gasoline on sand at several thousand parts per million. The difference between the contaminants is clear and identification is straightforward. Dakota Technologies, Inc. (DTI) once employed these matrix style data sets to completely analyze the fluorescence of petroleum, oil, and lubricant (POL) contaminated soils. WTMs were (and still are) excellent for identifying/classifying the PAH fluorescence of environmental samples because of the unique information that both dimensions of PAH fluorescence exhibit when acquired in unison. While WTMs make different contaminants readily discernable from one another, they are 3-dimensional and large. Also, the screening tool must be held still while the measurement is being made. All of these qualities make WTMs unwieldy for environmental screening tools that are designed to continuously log (typically 1 Hz) the presence of PAHs vs. time or depth.

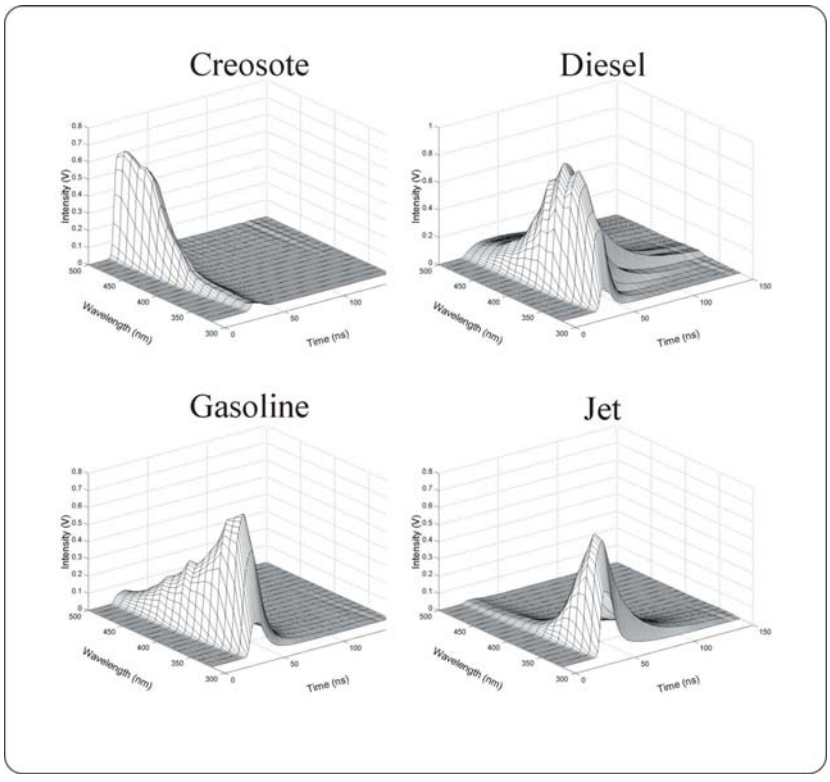

Figure 13. Example WTMs of common contaminants on sand

Because WTMs are so difficult to implement in screening mode, DTI developed (and patented) a multiple-wavelength waveform (MWW) technique that allows multi-dimensional PAH fluorescence measurements to be acquired "on the fly". Figure 14 illustrates the concept. Select regions of the spectrum are monitored for their temporal response. The responses are optically delayed and recombined, and the resulting responses converge to form a two-dimensional waveform. There is sometimes overlap between the "channels" with long decay times, and the spectral regions being monitored are fewer and farther between than WTMs, but the resulting waveform still retains a unique combination of spectral and temporal fluorescence information that makes speciation and identification of PAH mixtures possible. Figure 15 illustrates the unique waveform produced by a variety of common PAH-containing environmental contaminants.

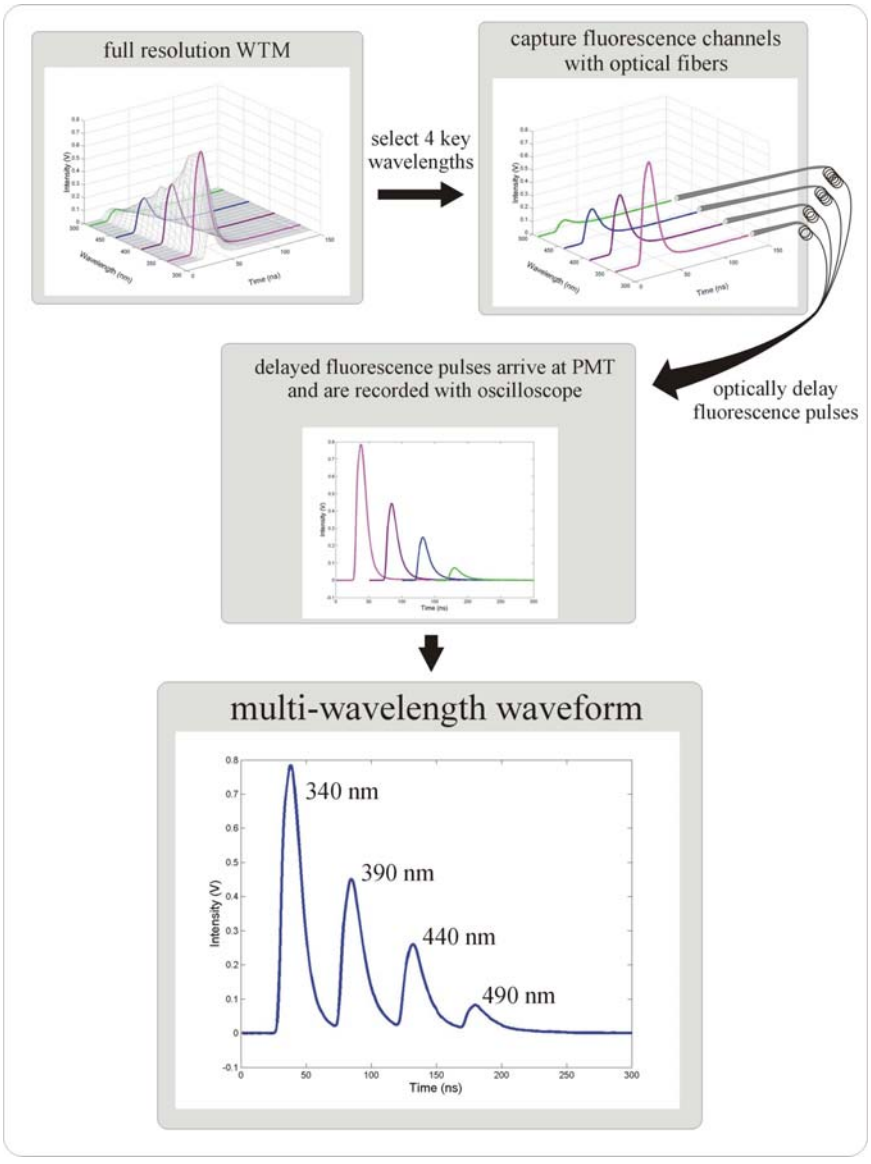

Figure 14. Multi-wavelength waveform concept

The ROST system acquires waveforms at ~1 Hz and logs them to the hard drive continuously. As described in section 2.2.3.1 below the waveforms are integrated to achieve a quantitative result that is plotted vs. depth. The shape of the waveform yields information on the nature of the fluorescing material. With experience the analyst learns to look for changes or similarities in the waveform and is able to assess changes in the analyte concentration or the matrix. For instance, are the decay times for the various channels changing due to changes in the PAHs or perhaps changes in oxygen levels that affect quenching? Is the emission shifting to shorter or longer wavelengths due to changes in the amount of degradation via biological activity, weathering, or volatilization? Is the first channel (closest to the laser) getting more or less contribution from laser scatter due to improper mirror alignment? These and a myriad of other questions and answers can be gleaned from the shape of this simple, yet informative, data format.

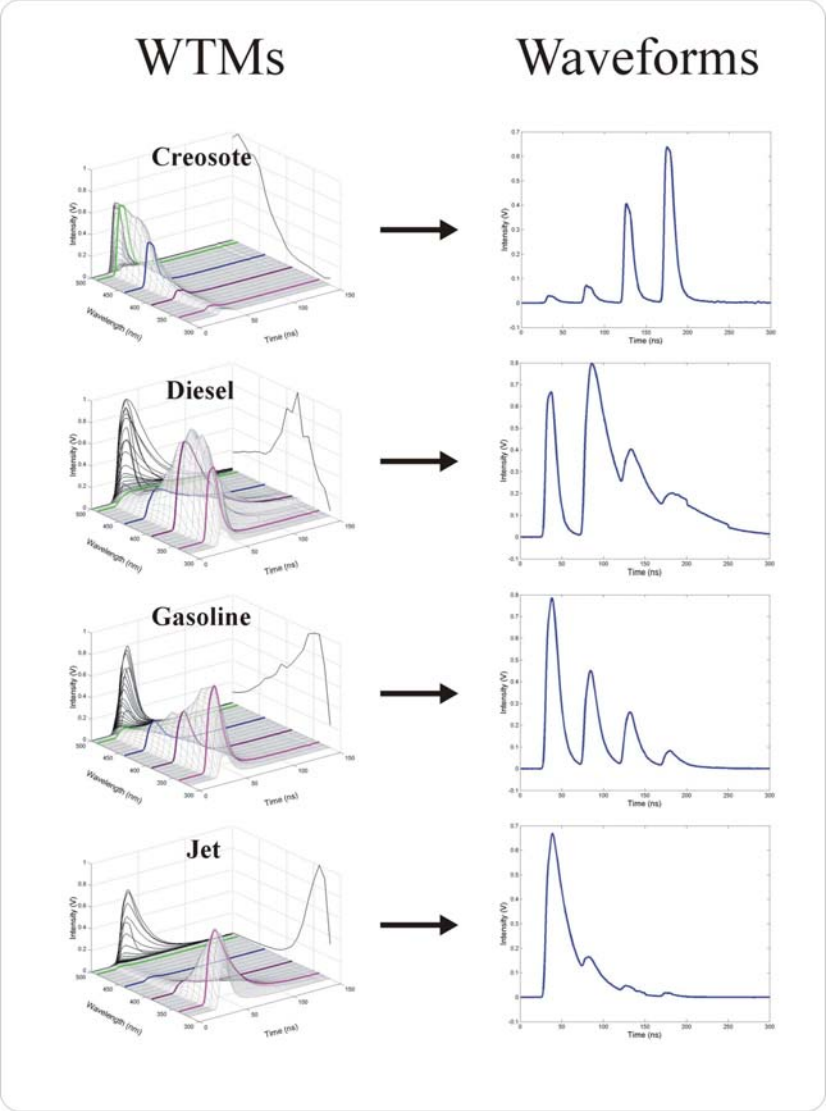

Figure 15. Waveforms of common contaminants

2.2.1.7 FVD colorization

The waveforms that are continuously logged vs. depth with ROST contain a wealth of information, but to make this information easily interpretable in fluorescence vs. depth (FVD) log format, we need to further reduce the data to a one-dimensional data set that we can plot vs.

depth. As discussed, the quantitative information is contained within the area under the waveform (total fluorescence) but how do we convert a waveform's shape into a singular entity? To accomplish this, DTI has developed and implemented a novel technique that effectively converts the shape of the waveforms into colors. These colors are then used to fill in the area under the FVD that represents the total fluorescence measured at each point in the FVD. Figure 16, derived from data from a coal tar delineation project, illustrates the technique of colorizing the FVD according to the shape of the waveforms.

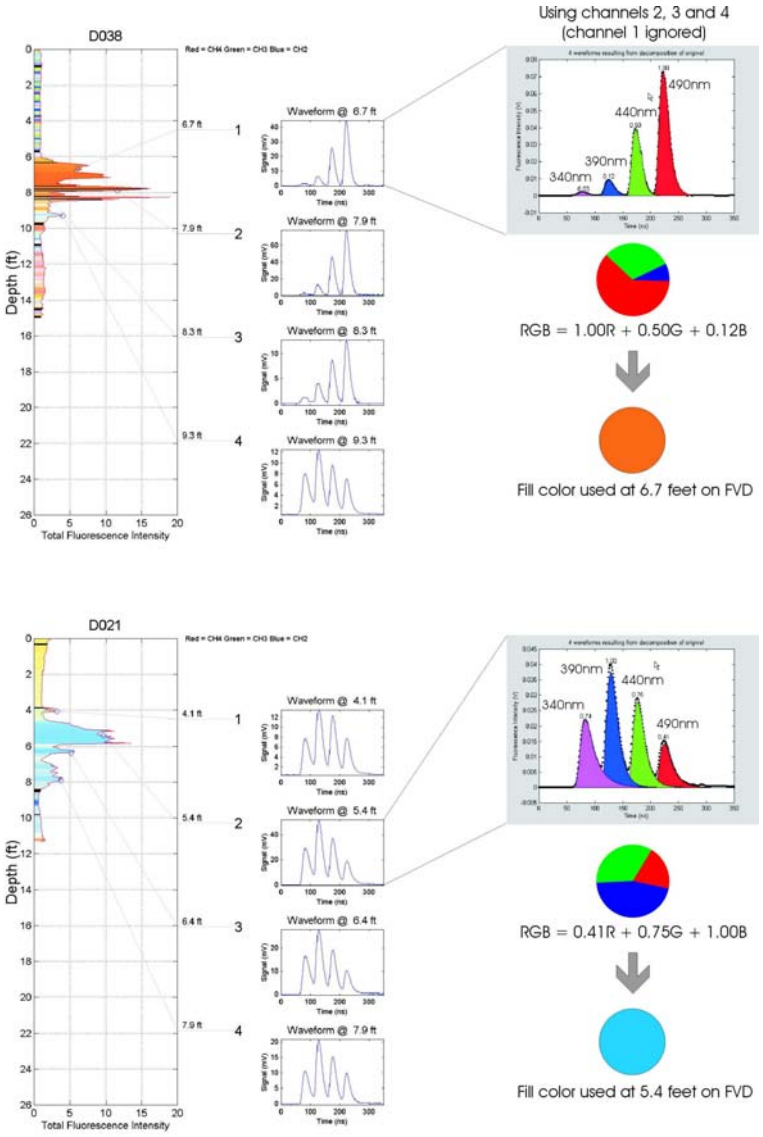

Figure 16. How color-coding is calculated

The result is a data presentation technique that allows the user to assess similarities or changes in the waveform shapes vs. depth by simply observing the colors that represent the shape of each and every waveform in the data set. This technique was used on the sediment measurements made in this project, both in the lab and in the field. It should be noted that the color black indicates that the algorithm that calculates the color failed to deconvolve the waveform successfully.

The colorization technique is limited to using three of the channels as a result of the red, green, and blue (RGB) color definition which computer colorization systems typically implement. A cyan, yellow, magenta, and black colorization system (CYMK) might allow the use of all four channels and is currently being considered as a replacement for RGB. The first three channels (340, 390, and 440 nm) were used to colorize the data in this study. The 490 nm channel was used in a quantitative sense, but was ignored for the colorization. It should be noted that a strictly temporal change (where only the decay times change, not the spectrum) would not necessarily result in a color change, since the ratios of the 3 channels used might remain constant even though the area under the waveform itself will increase or decrease.

An added benefit of this technique is that it provides insight in situations where non-linear response behavior is encountered. Many contaminants such as coal tars, heavy crudes, and creosotes do not fluoresce with concentration in a linear fashion. For instance, a 10 fold increase in PAH concentration might produce very little or no increase in total fluorescence intensity. However, a spectral or temporal shift often does continue to occur with changes in concentration due to energy transfer, photon cycling, and other phenomenon. The color of the FVD fill continues to darken or shift in color, acting as an indicator of a change in the fluorescence of the sample, alerting the analyst to a possible increase in concentration. While this technique is less than analytical it does provide the analyst with additional insight into the distribution of PAHs in the soil vs. depth.

2.2.2 ROST System Description

The ROST system is contained in a rugedized shipping container as shown in Figure 17. The system actually consists of a variety of sub-systems that are described in detail in this section.

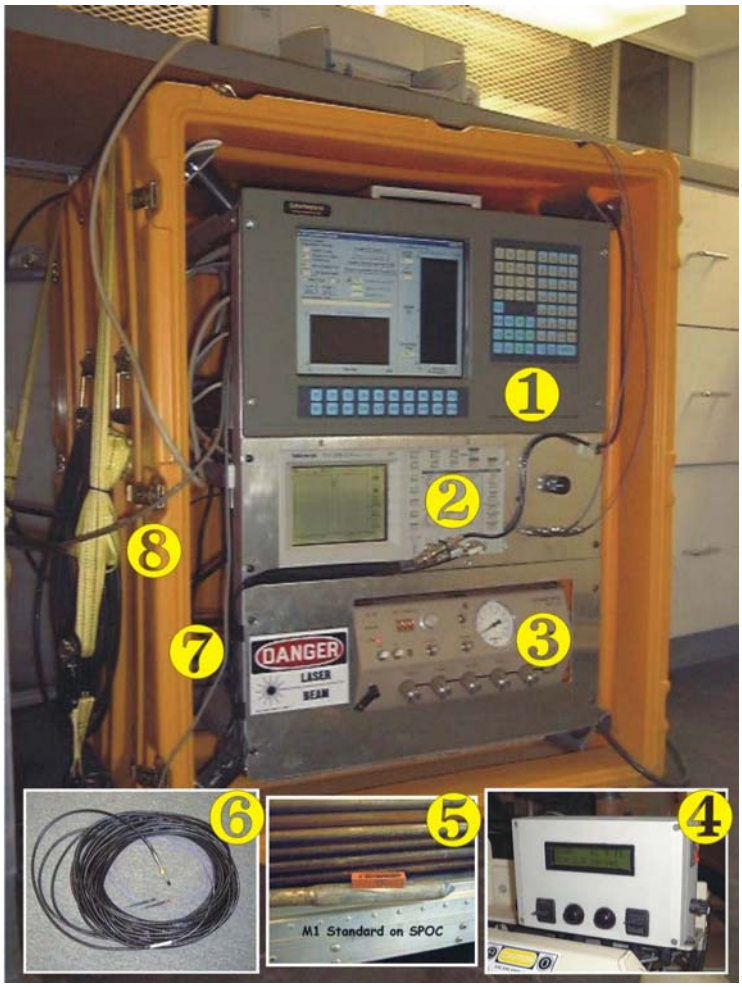

Figure 17. ROST system and key peripheral devices

2.2.2.1.1 Laser

The ROST system employs a pulsed XeCl excimer laser (MPB Technologies PSX-100) that generates very fast pulses of 308 nm light at 50 Hz. Each pulse measures less than 10 billionths (10 ns) of a second wide at half height. The 308 nm wavelength efficiently excites the vast majority of PAHs that are contained within the sediments being screened. A beamsplitter directs a small portion of the beam to an energy meter to monitor excitation pulse energy. A photodiode is positioned near the beamsplitter and serves as the trigger source for the time-resolved fluorescence measurement that takes place with the oscilloscope. A lens is used to launch the laser light into a fiber optic for delivery to the subsurface.

2.2.2.1.2 Fiber optic cable

The SCAPS dual windowed probe utilizes a single combined umbilical cable that houses the video, cone, and LIF fiber optics in one durable package. The fiber optic cable consists of two silica/silica 365-micron core diameter optical fibers. One fiber delivers the excitation pulse while the other serves to return a portion of the resulting fluorescence to the surface for measurement. Both fibers are SMA terminated at the surface.

2.2.2.1.3 Shock-protected optical compartment (SPOC)

DTI typically uses a SPOC with its Geoprobe to jackhammer the LIF probe into the sub-surface to delineate typical POL spills. Fibers terminated into a standard optical mount would shatter or cleave instantly under the shock and vibration of the jackhammer. DTI developed and built the SPOC that employs proprietary elastomer supports, in combination with Swagelock fittings, to insure long-term stability of the optical alignment along with protection against breakage. The SPOC contains a parabolic mirror that acts to turn the excitation beam 90 degrees.

The SCAPS dual windowed sub was used in place of the SPOC during the tests at North Island. It employs a bend in the fiber optics instead of a mirror allowing for greater signal strength. The SCAPS probe uses a compound angle polish that dramatically reduces the scattered laser light being collected compared with the fiber alignment system used previously on SCAPS systems. We were pleased with the very low background signals achieved during the North Island demo.

2.2.2.1.4 Emission detection system

The collection fiber returns the entire spectrum of light ("white light") that is collected from the sediment surface. Since this is a multi-channel (multi-wavelength) detection system, we must disperse the white light. To accomplish this, the collection fiber is butt-coupled directly into an Acton SP150 imaging monochromator where a series of mirrors and a 600 groove/mm grating act to disperse the white light into a "rainbow" that can sampled (four regions at 340, 390, 440, and 490 nm) for detection.

Before the light is dispersed by the monochromator the laser light (308 nm) must be removed and the amount of fluorescence light must be controlled. If not rejected, the relatively intense laser light that accompanies the fluorescence bounces around the interior surfaces of the monochromator and ultimately ends up in the detector. The detector does not differentiate between laser light and fluorescence, so this laser light must be filtered out. To achieve this, a cutoff long-pass filter (320 nm CFLP) is arranged immediately inside the monochromator, rejecting the vast majority of laser light, but passing the lower energy (longer wavelength) fluorescence. Butt-coupling of the fiber to the monochromator eliminates the slits that are usually found on the entrance of a monochromator. These slits are designed to control bandpass and the amount of light that enters the monochromator to avoid saturating the detector. The ROST system employs a neutral density filter wheel for controlling light levels instead. By selecting an appropriate optical density filter the light levels can be controlled with precision. The reference emitter signal (M1, described later) was attenuated in these studies while the PAH fluorescence was passed through without filtering due to its relatively low intensity compared to standard POLs.

The fluorescence passes through the CFLP and neutral density filter wheel assembly and is ultimately dispersed into a rainbow of light on the back plate of the monochromator. The polished faces of four fiber optics are located on this plate and are arranged to "pick off" four regions of the spectrum where PAHs fluoresce with varying intensity, depending on the number of rings and substitution level of the PAHs being observed. Rotating the grating allows selection of different regions, but always with 50 nm between channels because the space between fibers is not adjustable. ROST uses 340, 390, 440, and 490 nm under standard conditions and these wavelengths were used here.

At this point if all four fiber optics were of the same length and were directed into the detector (PMT), we would observe all four channels combined into a single decay curve (waveform). To achieve separation of the four channels we must time delay the photons so that they strike the detector at different times. To achieve this the fiber optics are all made 10 m longer than the next. The fibers are 2, 12, 22, and 32 m long for the 340, 390, 440, and 490 nm wavelengths, successively, delaying each channel by approximately 50 ns. These four fibers are then terminated in a single large core SMA fitting which couples to a large diameter (1500 micron) fiber optic that is 0.33 meters in length. This large diameter fiber is taken through a relatively sharp bend that serves to "mix" the four fiber optic beams into one homogeneous beam. The large fiber is attached to a mount that directs the light at the photocathode of the PMT detector.

The dynode chain of the PMT is held at a –900 V bias with a high voltage power supply. This bias accelerates and multiplies the electrons that are ejected from the photocathode when the photons strike the surface. The PMT detector (Hamamatsu R928) essentially converts the pulse of photons into a pulse of electrical current. The pulse is actually a train of 4 pulses that results from each channel's photons arriving at the PMT in succession.

2.2.2.1.5 Oscilloscope

The pulse of electrical current is very short lived. In fact, the entire train of pulses (the waveform) arrives in less than 250 ns. A very fast device is required to accurately record the current pulse. The ROST system employs a 100 MHz Tektronix® TDS 220 digital storage oscilloscope capable of 1 billion samples per second (1 GS) to record the waveforms. A 50-ohm terminator at the input of the fluorescence channel converts the current to a voltage, allowing measurement of a voltage vs. time waveform that represents the arrival of the photons at the PMT. A second channel of the oscilloscope is used to monitor an energy meter (a much slower measurement) before each test, to log the laser energy performance for maintenance/service tracking purposes. The fluorescence waveforms are displayed on the oscilloscope in real time and are retrieved from the oscilloscope via general-purpose interface bus (GPIB) for storage and analysis. Approximately 50 laser shots are averaged for each sampling point along the test, which ends up being equivalent to a 1 Hz waveform storage rate. At the slower probe advancement speed used in these studies (when halogen specific detector (XSD) results indicated possible NAPL presence), the vertical data density averaged 0.5 to 1.5 mm.

2.2.2.1.6 Control computer

A rack-mounted industrial computer is used to control the ROST system and log the data to hard drive. The computer controls the monochromator, the oscilloscope, a differential GPS beacon, and the depth control and acquisition module (DCAM). The host computer program was written in Visual Basic 5. The software provides a real time display of the test results while the test is in progress and generates a full color picture of the log at the end of the test. The waveforms are continuously logged to the hard drive while a total FVD log is created by integrating the entire fluorescence waveform and plotting its intensity vs. depth. The final data analysis and display was done on a separate workstation in the office.

2.2.2.1.7 DCAM

DTI typically employs a depth control and acquisition module (DCAM) specifically designed for use with Geoprobes. An alternative method needed to be used for integration with the SCAPS system. The SCAPS video recording system receives a RS-232 data string from the CPT control system. This data string contains the depth information necessary to tag the data to the correct

depth below ground surface. A serial data tap was put in place and the ROST data acquisition code was modified to receive the string and parse the depth information. This allows the ROST computer system to monitor the depth without modification of the SCAPS system.

2.2.3 SOP/Calibration

2.2.3.1 Calibration and normalization

The ROST system response depends on a host of factors. These include laser energy, fiber termination quality, neutral density filter selection, sapphire window quality, and fiber length, just to name a few. To account for changes in these over time and location, a single point calibration and system check is performed immediately prior to each push. The sapphire window is cleaned and a check is made to ensure that there is no discernable signal being generated as a result of a contaminated window. A reference emitter (called M1) is placed on the sapphire window and the average response from 500 laser shots is measured. The M1 solution is permanently stored in a quartz cuvette for convenience and the measurement takes place through the wall of the cleaned cuvette. This proprietary mix of hydrocarbons fluoresces efficiently across the entire system and serves as both an indicator of system function and as a data normalization benchmark.

The total fluorescence intensity (area under the waveform) of M1 serves to normalize the data from the push that immediately follows the reference emitter measurement. All the FVD logs are presented as a percentage of the signal achieved with M1. The area under every waveform in the data set is integrated, resulting in a picovolt-seconds unit (picoseconds * V or pVs). These values are divided by the pVs measured for M1, and the result is multiplied by 100. The result is a log with x-axis units of percent of M1. This creates a normalized data set that takes into account the entire system performance, from end to end (laser to oscilloscope). The shape of the M1 waveform also acts to guide the operator in assessing proper alignment of the detection system. The relative contribution for each channel and the shape of M1 waveform is monitored for consistency to insure that the waveforms remain consistent from day to day.

2.3 Soil Video Imaging System

The microscopic color video imaging system Figure 18 incorporated into a cone penetrometer push probe has been successfully deployed at several sites by the Navy. Micro-scale globules of apparent residual DNAPL have been observed (Figure 19), but these observations must be confirmed. *In situ* video microscopy in conjunction with geotechnical soil classification data is seen as an outstanding means to assess how DNAPLS are distributed in the environment, aiding the intelligent choice of remediation method.

Several organizations, including the Navy, DTI, Fugro Geosciences, Inc., Applied Research Associates, and Westinghouse Savannah River, have previously noted elevated fluorescence levels at sites in which the presence of DNAPLs is suspected or known. The indirect fluorescence method relies on fluorophores (such as fuel hydrocarbons) that may be co-dissolved in the DNAPL. Questions remain about the method's generality and the optimal choice of wavelengths. The fluorescence approach that will be applied here improves upon past efforts in several ways. One is that much higher spatial resolution (ca. 2 mm) will be obtained by tightly focusing the excitation beam on the soil matrix and be reducing data acquisition times to about

200 ms. The high resolution fluorescence sensor will be integrated with the GeoVIS for simultaneous collection of video microscopy and indirect fluorescence data.

Figure 18. . Photograph of downhole video imaging system probe. Soil in contact with the sapphire window is illuminated with scattered light from white LEDs. The soil is imaged through a lens system coupled to a color CCD camera. The video signal is returned to the surface where it can be viewed in real-time and recorded using a video recorder or stored digitally.

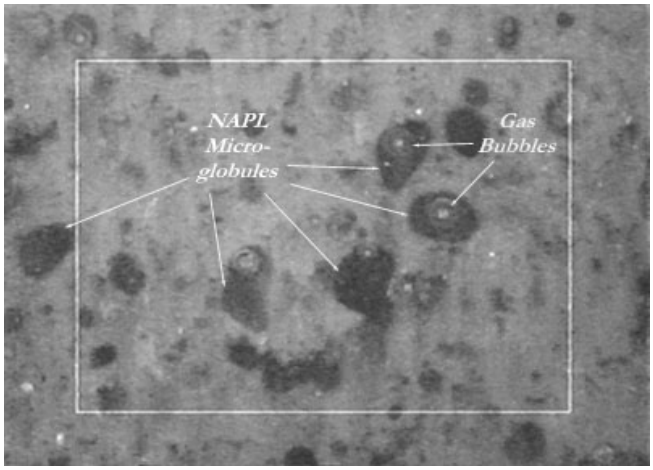

Figure 19. *In situ* image of soil showing NAPL micro-globules (dark objects) and associated gas bubbles. White box on image is 2 x 2.5 mm electronic reference scale.

2.4 Previous Testing of the Technology

All of the sensor technologies have undergone the appropriate small-scale field-testing to prove they are rugged enough and sufficiently mature to advance to the dem/val stage. The Membrane Interface Probe (MIP), which serves, as the sampling front end for the XSD is commercially

available. DTI has successfully pushed the XSD on several occasions at a various test sites. A total of more than 30 penetrations to depths of more than 40 feet have been completed without problems. Although the XSD sensor has been pushed at several sites (including the dry cleaning site shown in Figure 2) only limited validation data is available. The most extensive validation data set is from a test conducted at Offutt AFB in Omaha, NE.

At Offutt, XSD data was collected using a Geoprobe percussion push vehicle. The Geoprobe vehicle was operated in push mode to continuously advance the sensor at 0.5 cm/sec. All pertinent information for each push was collected with a PC and DTI's in-house software. The software simultaneously collects MIP temperature, XSD temperature, time, depth, and XSD signal. To allow the user to immediately see the results of the push, the software plots XSD signal versus depth and MIP temperature versus depth as the probe is being advance. XSD results were compared with results from laboratory analyses of water samples collected from monitoring wells located close to the push locations. Because the laboratory results were from samples collected at discrete depths and the XSD data was collected continuously, XSD data was averaged over the depth range that corresponded to the depth of the discrete sample. To obtain a signal representative of only chlorinated contamination, an average of the baseline signal was subtracted from the averaged XSD signal. The region that best represented a baseline region was the last foot of each push. Averaged XSD values were then plotted against the concentrations from the lab data (Figure 20). (It should be noted the laboratory data was derived from samples collected over a two-month period.). Figure 20 shows that the XSD data correlates well with the laboratory results from water samples collected from nearby monitoring wells.

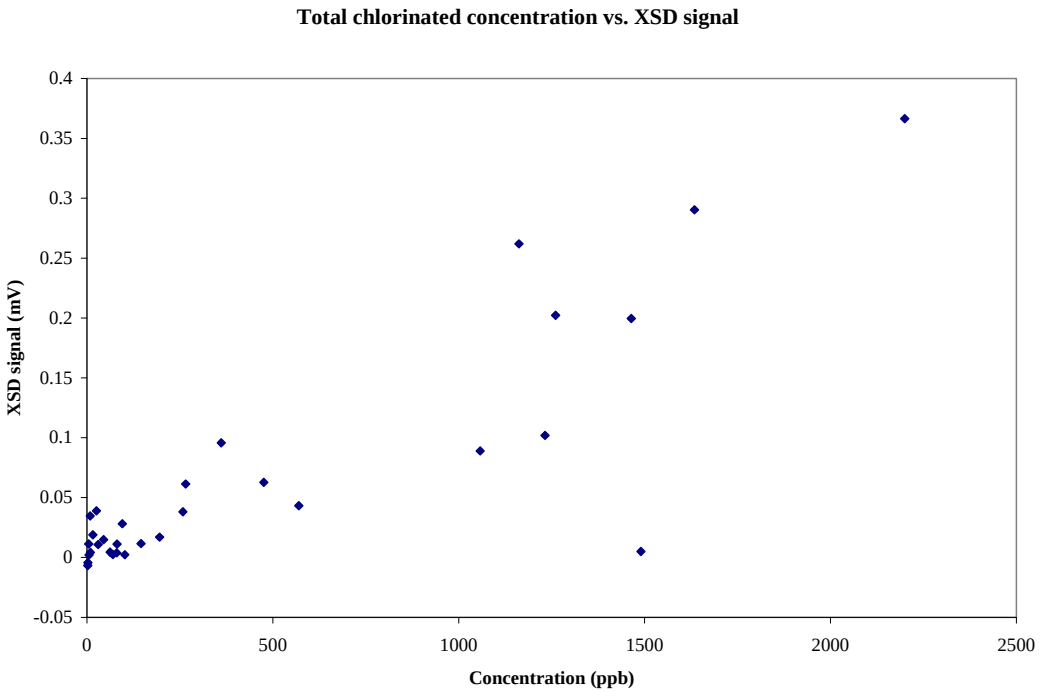

Figure 20. Correlation of XSD data with laboratory analysis of water samples collected from nearby monitoring well.

The Navy has deployed the video camera at several sites. Fluorescence detection through a sapphire window interface on a direct push probe is commonly performed. Prior to this study the HRF has not been used in conjunction with the video imaging system.

2.5 Factors Affecting Cost and Performance

The cost and performance of direct push in situ sensor are always subject to factors related to site specific conditions, as are conventional site characterization methods. At certain sites geological conditions (presence of cobbles or bedrock) may impede or limit the ability to push sensors into the ground. Changes in lithology (presence of silts and clay) may also affect the effectiveness of the MIP as a sampling device.

2.6 Advantages and Limitations of the Technology

Traditionally, characterization of DNAPL contaminated sites has depended on collection of soil and water samples followed by subsequent laboratory analyses [7]. The presence of DNAPLs (free phase product) is usually inferred from the presence of dissolved phase concentrations at or near solubility limits in aqueous samples or from the presence of free phase product in monitoring wells. There are almost no documented cases where DNAPL source zones have been directly identified ([3]). Because of the difficult sampling problem, localizing DNAPL source zones has proven to very problematic. In order to improve the capability for characterizing DNAPL source zones several workers have recently adapted in situ sampling systems to direct push systems. These include (1) a thermal desorption sampler (TDS) that captures a known volume of subsurface soil in situ and then heats the sample chamber and purges the VOC contaminants and transports the contaminants to the surface [6] and (2) a membrane interface probe (MIP) that uses a heated membrane to transfer VOC contaminants from the subsurface soil to the a carrier gas. The carrier gas then that transports the sample to a detector at the surface.

The primary advantage of direct push based sensor technologies is that they provide information in real-time while the site investigation is ongoing. Real-time information facilitates optimization/modification of sampling plans without waiting days or weeks for results from the laboratory and helps eliminate the need for iterative sampling efforts that are often required to fill in data gaps. Direct push sensor systems also generally provide much higher vertical spatial resolutions that are useful for resolving thin contaminant layers that might easily be missed with conventional sampling strategies.

The primary advantage of the sensor suite demonstrated in this effort is that it is the first approach that provides real-time in situ detection (using a downhole chemical sensor) of DNAPLs in the subsurface. In addition to providing direct chemical information on chlorinated hydrocarbons in subsurface soils the in situ fluorescence and video imaging systems will also provide direct information on how the DNAPL is distributed in the soil matrix (i.e., free phase mobile product versus residual phase product on the soil matrix.). A significant advantage of the downhole XSD detector is that it eliminates the requirement for transfer lines for transporting the analyte from the sampling system to a surface mounted detection system (such as that used with the Thermal Desorption Sampler (TDS) that was interfaced with an Ion Trap Mass Spectrometer (ITMS) ([6]). One of the main advantages of the downhole detector system over systems that

utilize “up hole” detectors is that problems associated with carryover or “memory” effects that arise when the probe is pushed through zones of high level contamination are minimized. Experience with the TDS/ITMS system showed that 50 minute purging times were required to reduce the contaminant level down to 99.8% of the initial value and that overnight purging or complete breakdown and cleaning would be required to reduce carry over to a background equivalent to the typical detection limit of the systems. It is clear that sample carryover in transfer lines often necessitates lengthy purging of transfer lines that may results in considerable delay to field operations and significant extra costs.

Experience with other direct push chemical sensors (e.g., fluorescence and video imaging systems suggest that it is unlikely that that the outside of the MIP probe will fouled by free product that smears the probe surface as it is pushed through a pool of free DNAPL. Previous work has shown that the outside surface of the probes tends to be self-polishing (i.e., self cleaning) due to the abrasion of the probe surface with the soil. If there is any evidence of carryover, it is expected that the XSD signal would be at or near saturation levels, indicating the presence of free product. In the event that saturation occurs the probe will be advanced very slowly and the heated MIP should completely volatilize any residual DNAPL over a period of a few minutes, allowing us to proceed. Again, we believe that MIP, which is heated directly, is much less prone to fouling than the transfer tubing which receives a large “dose” of analyte. The short distance between the MIP and the XSD (1 foot vs. 120 feet with uphole detectors) is expected to dramatically reduce the long wait times typically experienced with the MIP exposure to product due to contamination of the entire length of tubing in the trunk line.

Although the XSD exhibits specific response to chlorinated species with approximately 5000:1 selectivity relative to petroleum hydrocarbons, the XSD-MIP it is not capable of speciating between chlorinated compounds in either the DNAPL or dissolved (aqueous) phase. The data generated by the XSD-MIP indicates total chlorinated hydrocarbon transferred across the MIP vs. depth. This detailed spatial information can then be used as a guide for collection of discrete laboratory methods that can be used to differentiate between multiple species. The XSD-MIP data allows one to make informed sampling decisions (how many, how deep, where) in a straightforward and cost-effective manner, eliminating the costly and ineffective “stabs in the dark” that are used currently.

3 Demonstration Design

3.1 Performance Objectives

Performance objectives for this demonstration/validation are listed in Table 4.

Table 4. Performance Objectives

Type of Performance Objective	Primary Performance Criteria	Expected Performance (Metric)
Qualitative	1. Ability to detect DNAPL source zones	Improved capability for localizing DNAPL source zones
	2. Capability to resolve small spatial scale variations in DNAPL distributions	Improved capability for localizing small scale spatial variations in DNAPL distributions
	2. Time required for delineating DNAPL source zones	Reduction in time required for delineating DNAPL source zones
	3. Ease of use	Operator acceptance
Quantitative	1. Detection of DNAPL micro globules via high-resolution fluorescence and video imaging	Accuracy >80% <15% false positives/negatives
	2. Dynamic Range of XSD	10^4 (10^2-10^6ppb)

3.2 Selecting Test Site(s)

The ideal test site is one in which DNAPLs is present, but under conditions where the ability of traditional techniques to efficiently locate the source terms is in question

Several practical and logistical factors must be considered when selecting individual test sites, these include the following criteria:

· The US Department of Defense (DoD) (as site owner) agrees to allow access to the site for the demonstration.

· The site is accessible to the direct push vehicle.

· The soils at the site have been contaminated by DNAPLs that are representative of other DoD sites and detectable by the DNAPL sensor technologies to be evaluate.

The soil types at the site consist of unconsolidated sediments of native sands, silts, clays, and gravel. These soil types are suitable for CPT pushing and present appropriate matrices for the DNAPL sensor technologies to be evaluated in this dem/val.

- The soil contaminant levels identified during previous investigations range from below analytical laboratory detection limits to heavily impacted. These data indicate contamination in the subsurface in concentration ranges comparable with the DNAPL sensing technologies to be demonstrated.

Baseline data will likely be available on most, if not all, the sites, but conclusively establishing that DNAPLs source terms have been located in these challenging situations will not be trivial owing to the weaknesses of traditional methodology. The sensors tested here may individually provide characteristic DNAPLs signatures, which can be verified by comparison to push data made outside the DNAPLs contamination zones. More likely, the combined data from the suite of sensors will provide a level of certainty far greater than has been possible heretofore. Owing to the importance and complexity of the problem, we plan to consult with other experts to assist with site selection, data interpretation, and assessing the performance of the new characterization technology against traditional site characterization approaches.

3.3 Test Site Description

Demonstrations efforts were conducted at three sites: (1)Naval Air Station North Island, IR Site 9, Coronado, CA; (2) Marine Corps Base, Camp Lejeune, Site 89, which is located in Onslow County, North Carolina Camp Lejeune, South Carolina, and (3)Travis Air Force Base. Details of each site are as follows:

3.3.1 Naval Air Station North Island (NAS North Island) IR Site 9

IR Site 9 is located at Naval Air Station North Island (NAS North Island) in San Diego County California (Figure 21). This site was selected because it meets most of the criteria listed in Section 3.2 and it is located near the SSC-SD laboratory, which will facilitate integration of the new sensors with the SCAPS platform and system shakedown. IR Site 9 operated as a chemical waste disposal area from approximately the 1940's through the early 1970's. No records were kept of the amounts of chemicals deposited at this site. Based on a 1978 estimate of wastes generated at NAS North Island, it has been estimated [8] that somewhere 8 to 32 million gallons of waste were deposited at the site. These wastes included paints, solvents, caustics, acids and oils. Unknown quantities of chlorinated solvents were disposed of in unlined trenches at the site for several decades. The volume of waste liquids disposed of a Site 9 resulted in the formation of a NAPL layer located in the capillary fringe above the ground water table between 9 and 11 feet below ground surface (bgs). The NAPL is a mixture of hydrophobic fluids comprised of up to 20% trichloroethylene (TCE) by weight. The location of Site 9 is shown in Figure 22.

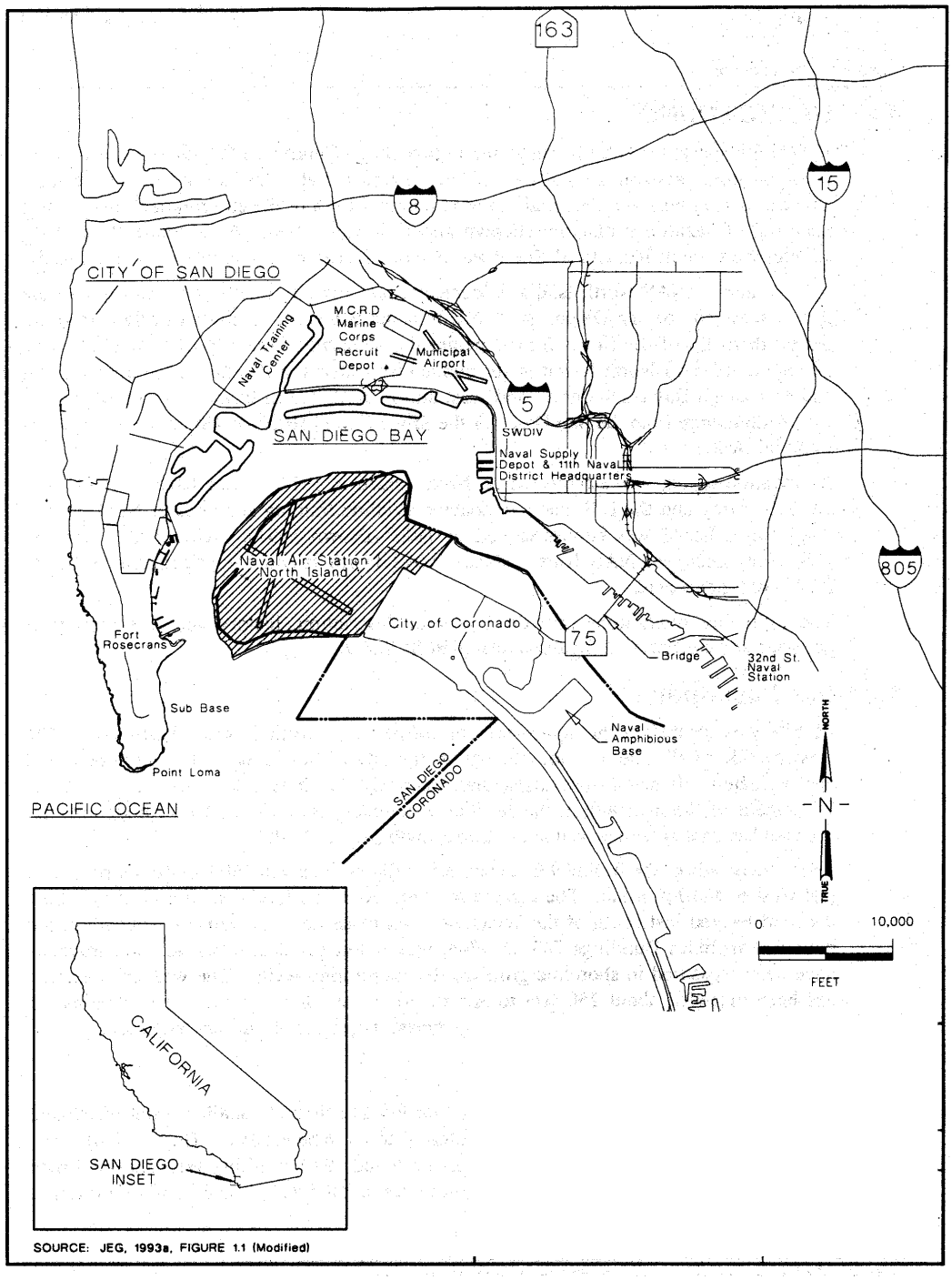

Figure 21. NAS North Island Vicinity Map.

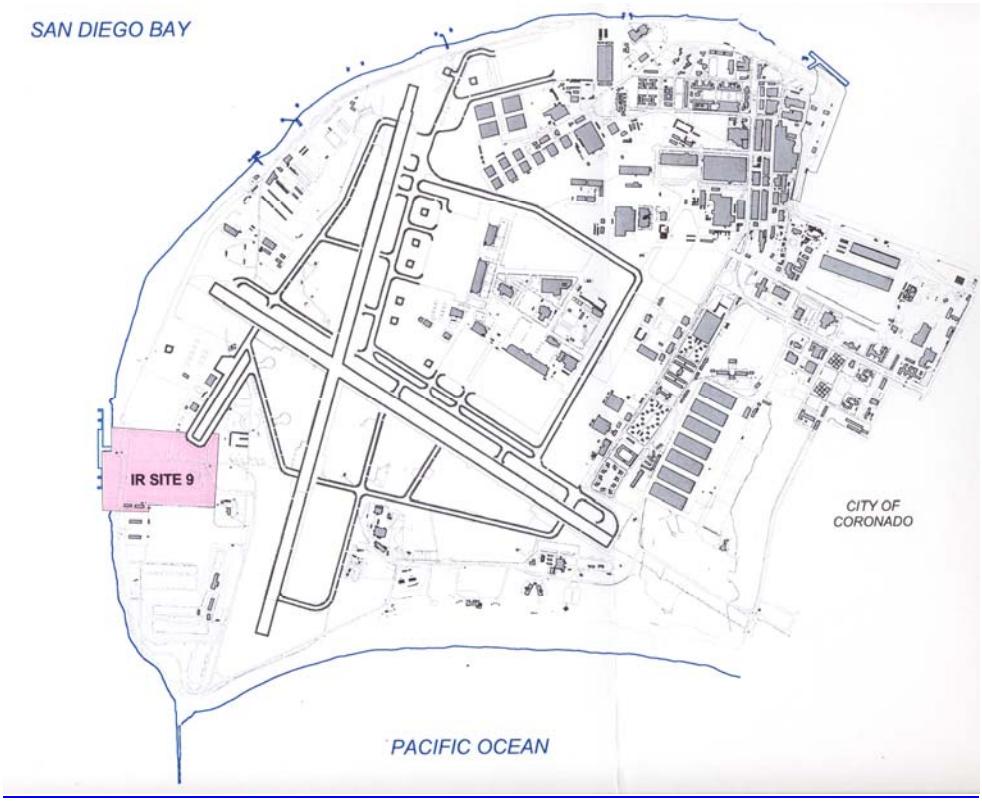

Figure 22. Site 9 location map.

The physical characteristics of North Island have been described in detail in previous reports [9]. In general North Island is characterized by low topographic relief with an average elevation of approximately 23 feet above mean low level water depth (MLLW). The area within the IR Site 9 boundary ranges from about 10 to 23.5 feet above MLLW. Surficial geological units mapped at NAS North Island include older natural deposits, which have been described as Pleistocene Bay Point Formation [10], Holocene beach sand and artificial fill.

In late 1998, the Site Characterization and Analysis Penetrometer System (SCAPS), using Laser Induced Fluorescence (LIF), identified a large volume of light non-aqueous phase liquid (LNAPL) floating on the groundwater beneath the site. Figure 23 shows a plume map generated from the SCAPS data. LNAPL plume was discovered to contain a significant weight fraction of chlorinated solvents. The chlorinated solvents consisted primarily of TCE, which was measured at approximately 20% by weight.

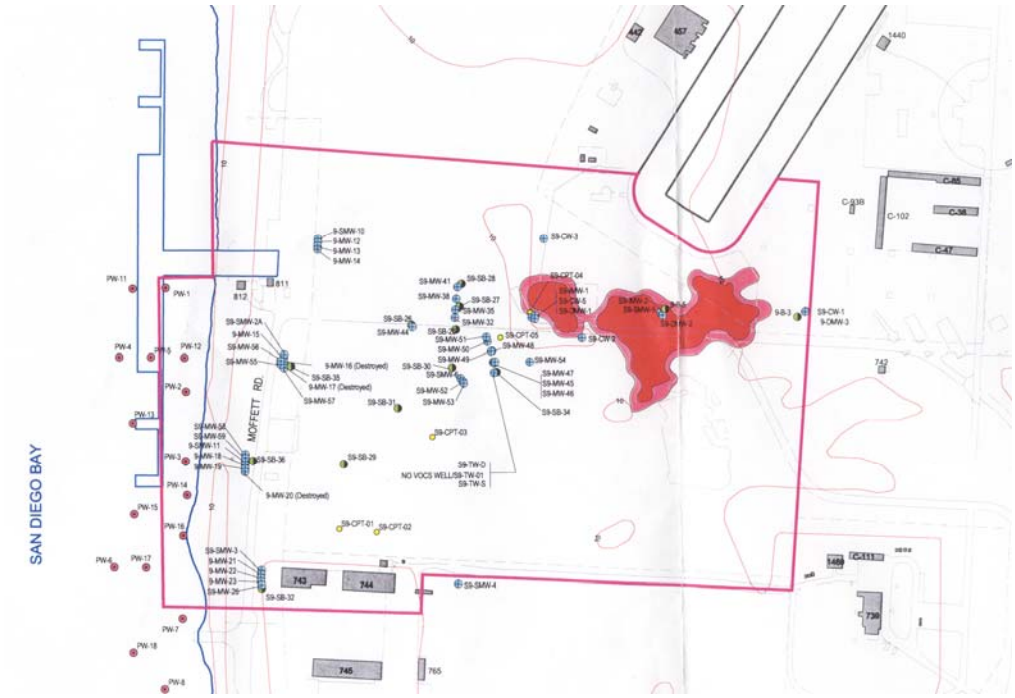

Figure 23. Expanded plan map of IR sit 9 showing NAPL plume boundaries.

IR Site 9 has been the subject of multiple investigations beginning with the initial assessment study (IAS) in 1983[8]. Ten areas of concern were identified during the RI/RFI (JEG 1995). See Figure 24. Removal action work is currently ongoing. A soil vapor extraction system (SVE) shown in Figure 25 was recently operated in Areas 1, 3 and 8. The system is being modified to use steam injection for continued treatment of contaminated soils because contaminant levels remained high at several locations and a light non-aqueous phase liquid was discovered.

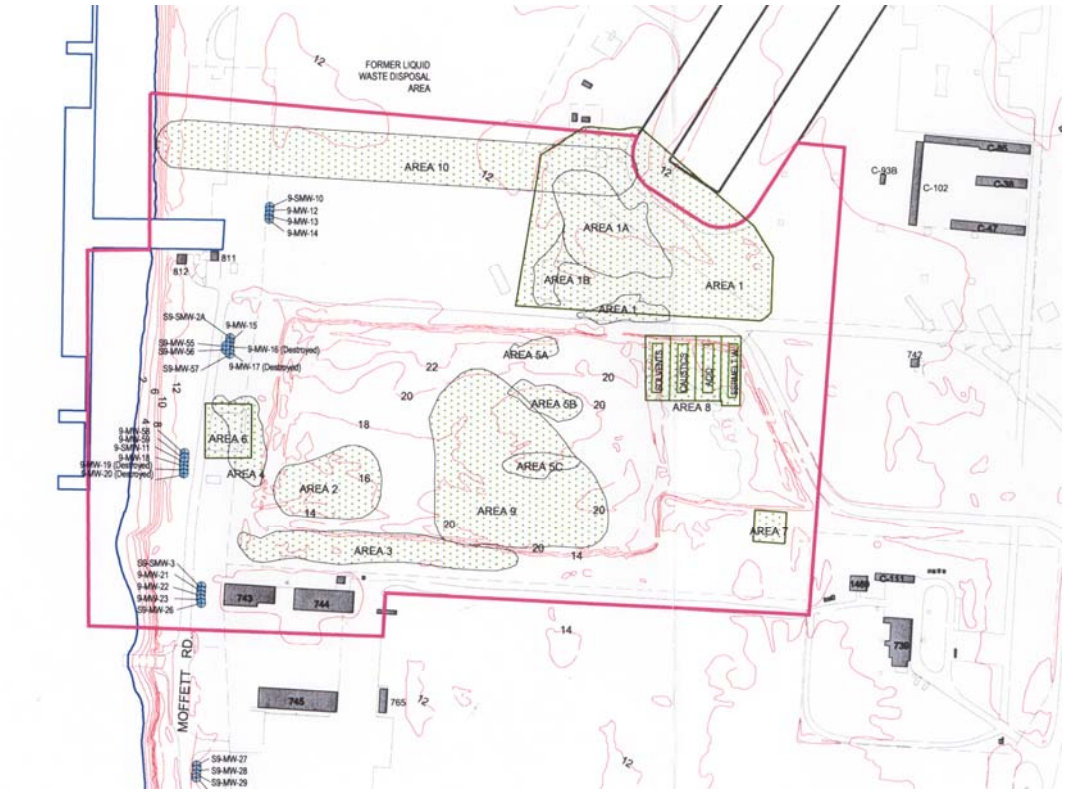

Figure 24. IR Site 9 Area Map.

Figure 25. Photograph of IR Site 9 showing plumbing used for SVE system.

3.3.2 Marine Corps Base, Camp Lejeune, Site 89

This section discusses the history and characteristics of the second demonstration site, Site 89, Marine Corps Base, Camp Lejeune is located in Onslow County, North Carolina, (Figure 26). Site descriptions reported here have been extracted from the Remedial Investigation (RI) report prepared by Baker Environmental [11].

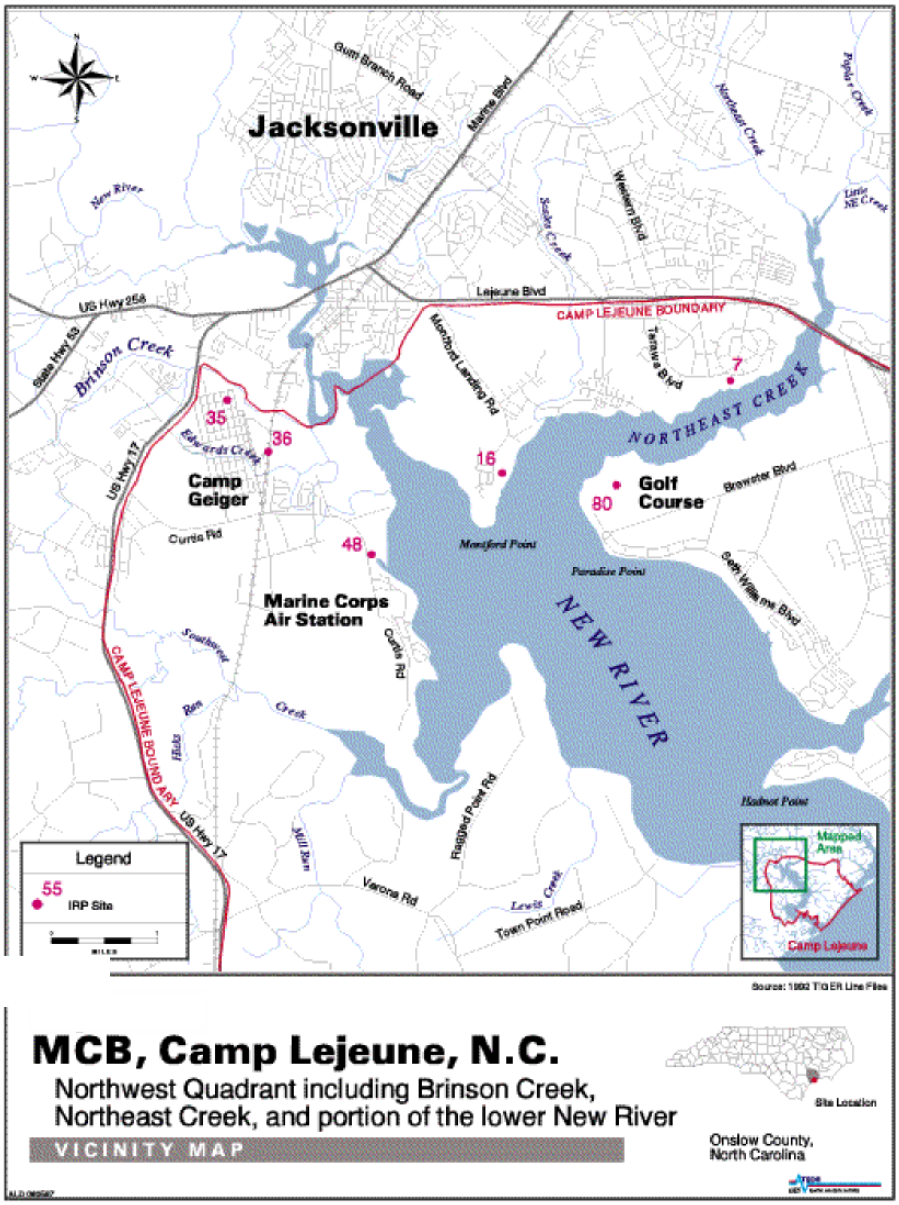

(from http://www.atsdr.cdc.gov/HAC/PHA/usmclejeune/clej_p2b.html)

Figure 26. Camp Lejeune Vicinity Map.

Site 89 is located near the intersection of "G"and Eighth Streets, formerly the Defense Reauthorization and Marketing Office (DRMO) area of Camp Geiger (Figure 27 and Figure 28). Site 89 is the larger of the two sites within OU 16. It encompasses a significant portion of Camp Geiger, which includes all of the DRMO and additional area to the south and east. Originally, site investigations focused on a small area within the DRMO that contained an underground storage tank (UST), which was identified as STC-868. The UST was a steel 550-gallon waste oil tank located between Building STC-867 (a soil storage facility) and an elevated wash rack. The tank was installed in 1983 and used for the storage of waste oil. This UST was reportedly closed by removal in 1993. Initially, two monitoring wells were installed in the area of the former UST by R.E. Wright Associates, Inc. (R.E. Wright). Based upon elevated levels of both total petroleum hydrocarbons (TPH) and oil and grease (O&G), a third well was installed in June 1994. The major finding of the initial UST investigation at Site 89 was the detection of several chlorinated solvents in the groundwater. The presence of chlorinated compounds during the initial investigation demonstrated that impact to the groundwater involved compounds not normally associated with a petroleum UST site. Historical records research of the area show that relocated to an asphalt paved area immediately north of the former DRMO facility. The findings of the initial UST investigation led to the inclusion of Site 89 into MCB, Camp Lejeune's IR Program. The IR Program focuses on non-UST sites and provides the framework for a more complex and detailed environmental investigations at the base. The current area of Site 89 has expanded to include more than the former UST area. The site presently includes the entire DRMO and additional area outside the DRMO fence, including the wooded areas to the south and the east. The approximate site boundary is displayed on Figure 29.

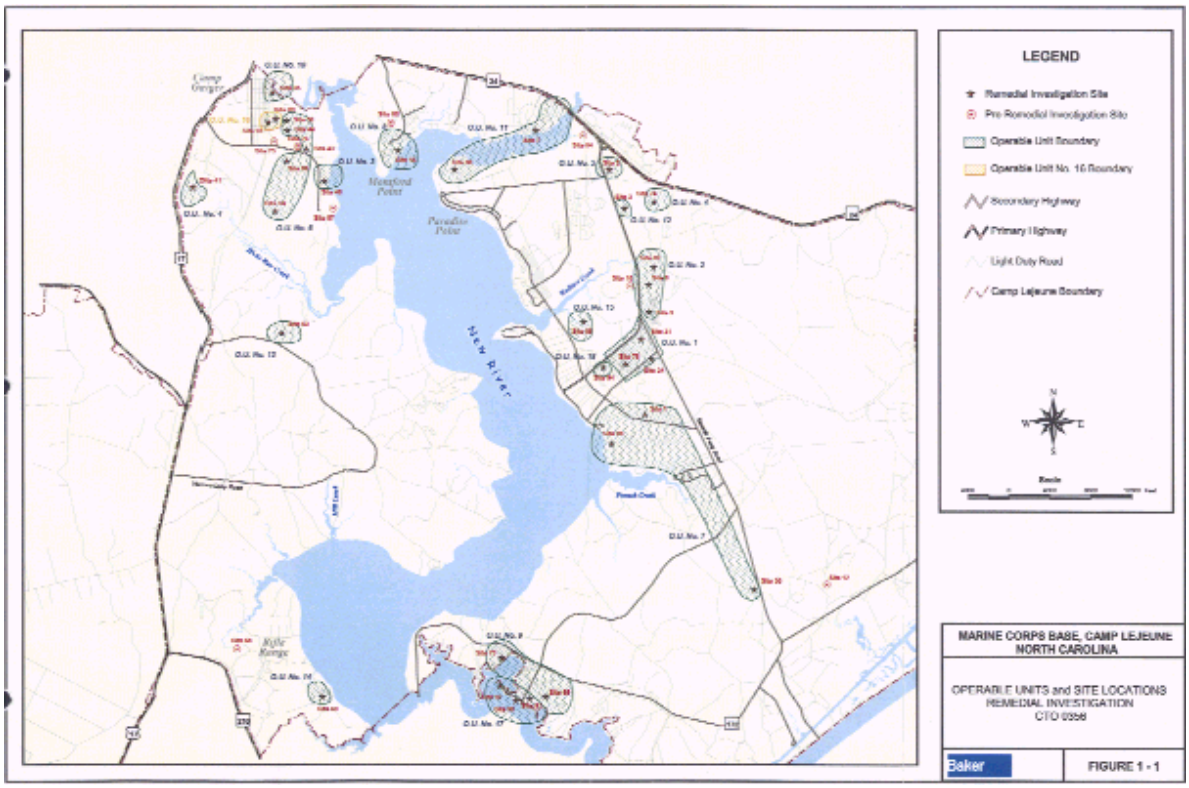

Figure 27. Site 89 Location map.

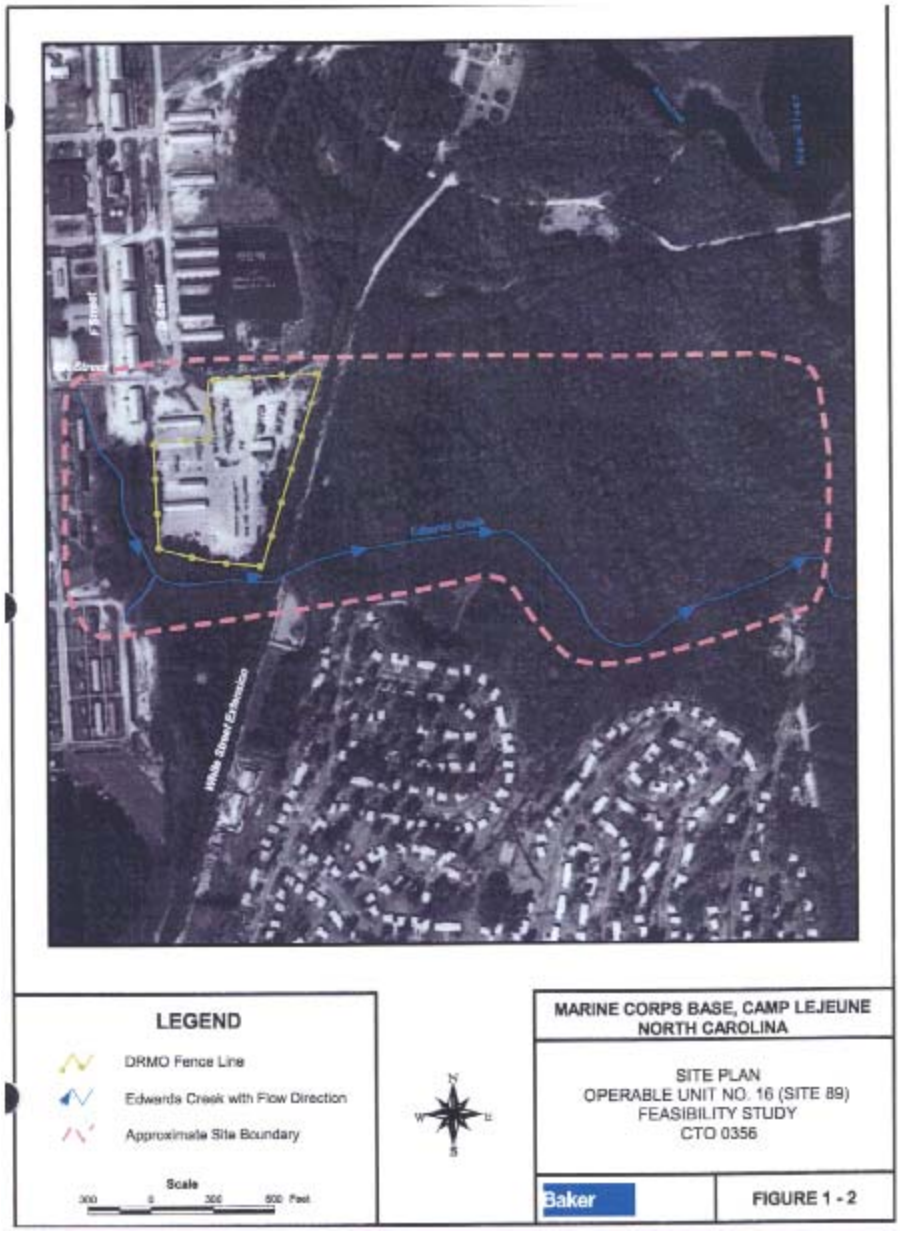

Figure 28. Site 89 Area Map showing approximate site boundary, Edward Creek flow direction and DRMO fence line.

The majority of the western portion of Site 89 is primarily covered by asphalt, roads, and gravel parking areas. The eastern portion of Site 89, is heavily wooded, as is the area immediately south of the DRMO. Edwards Creek is the nearest surface water body, located along the western and southern portions of the site. The stream is located approximately 525 feet south of the former UST location. The land surface of Site 89 slopes in the direction of Edwards Creek, which begins as a series of drainage ditches within Camp Geiger. The stream begins near 8th Street and flows south for a short distance before turning to the west, where it tends to widen as it flows through the wooded area of Site 89. The eastern portion of the stream flows through a low-lying swampy area.

The geology of OU No. 16 (Sites 89 and 93) is described together because of the close proximity of these sites. The geology is also placed in context of the regional geology, as described in the

"Hydrogeologic Framework of U.S. Marine Corps Base at Camp Lejeune, North Carolina"[12]. A fairly consistent depositional sequence was observed in the borings throughout Sites 89 and 93. This observed sequence is similar to the generalized North Carolina coastal plain sequence, which shows that the Yorktown, Eastover, and Pungo River Formations lie between the Undifferentiated and Belgrade Formations. The Yorktown, Eastover, and Pungo River Formations, however, have not been identified at Camp Lejeune. During the RI, the Undifferentiated and River Bend Formations were encountered. The Belgrade Formation did not appear to be consistent at OU No. 16; however, a description of this unit has been included. It appears that the shallow temporary wells installed during this investigation are screened in the Undifferentiated Formation (surficial aquifer) and the intermediate wells are screened in the upper portions of the River Bend Formation (Castle Hayne aquifer). The Undifferentiated Formation is comprised of loose to medium dense sands and soft to medium stiff clay. This formation is comprised of several units of Holocene and Pleistocene ages and can consist of a fine to coarse sand, with lesser amounts of silt and clay. At Sites 89 and 93, this formation typically extends to a depth between 20 and 30 feet below ground surface (bgs). The silt and clay lenses present within this formation may be correlated to the regional geology as the Belgrade Formation, or Castle Hayne confining unit. This unit, however, did not appear consistent at Sites 89 and 93.

The Belgrade Formation is comprised of fine sand with some shell fragments, silt, and clay of the Miocene age. Identifying this formation at OU No. 16 was difficult due to its inconsistency. Overall, the Undifferentiated Formation (surficial aquifer) appears to lie immediately above the River Bend Formation (upper portion of the Castle Hayne aquifer), with little to no presence of the Belgrade Formation (Castle Hayne confining unit). The inconsistent nature of the Belgrade Formation suggests that a significant hydraulic connection exists between the Undifferentiated Formation (surficial aquifer) and the upper portions of the River Bend Formation (Castle Hayne aquifer). At best, the Belgrade Formation at OU No. 16 can be classified as a semi-confining unit or a "retarding layer", as it is laterally discontinuous and does not exhibit completely confining conditions to the River Bend Formation below (Castle Hayne aquifer). Beneath the Undifferentiated Formation and the limited Belgrade Formation lies the River Bend Formation (upper potion of the Castle Hayne aquifer). This unit, which is predominantly composed of dense to very dense shell and fossil fragments interbedded with calcareous sands, is present at OU No. 16 approximately 25 to 50 feet bgs.

The surficial aquifer resides within the Undifferentiated Formation, the Castle Hayne confining unit resides within the Belgrade Formation, and the Castle Hayne aquifer resides within the River Bend Formation. United States Geological Society (USGS) documents the thickness of the surficial aquifer to be 18 to 23 feet and the thickness of the Castle Hayne confining layer as 4 to 7 feet in the vicinity of OU No. 16 (based on RI supply well boring logs). This places the elevation of the Castle Hayne confining unit from 0 to 8 feet above mean sea level (msl), although a definite confining layer which separates the surficial aquifer from the Castle Hayne aquifer is not present at OU No. 16. General descriptions of the 1993 USGS document and site-specific geologic conditions place the top of the Castle Hayne aquifer at approximately -10 feet msl.

Groundwater levels within RI monitoring wells ranged from 2.15 feet below msl to 13.52 feet above msl. Groundwater level measurements for Sites 89 and 93 are presented within the RI; however, three groundwater elevation maps are included herein for the shallow monitoring wells,

intermediate monitoring wells, and the deep monitoring wells. The groundwater elevation data suggest that the flow patterns observed for the surficial and upper portions of the Castle Hayne aquifers display similar trends. Overall, elevations are higher in the northern portion of the OU, with decreasing elevations in the direction of Edwards Creek and in the wooded area to the east. Groundwater flow in the surficial aquifer shows a pronounced localized flow to the south as Edwards Creek serves as a groundwater discharge boundary. Edwards Creek effects flow within the surficial aquifer and upper portions of the Castle Hayne aquifer more than in the deeper portion of the aquifer. Groundwater flow in the upper portions of the Castle Hayne is affected somewhat by the local discharge area of Edwards Creek, but there is also a trend eastward demonstrating the effects of the surface water bodies associated with the New River. The New River, located east of the OU, apparently influences the groundwater flow of the deeper portions of the Castle Hayne aquifer, causing groundwater at depth to move east, toward the river. Groundwater head differentials between the shallow and intermediate wells were evaluated to determine if a vertical component of flow underlies the OU. In general, elevations in shallow temporary wells are greater than the associated elevation in the intermediate temporary wells in those wells located north of Edwards Creek. This data demonstrates a downward component of groundwater movement from the surficial aquifer to the Castle Hayne aquifer north of Edwards Creek. This information supports the assumption that confining conditions of the Castle Hayne aquifer in this area are not likely.

Prior to 1987, the southern area of the DRMO yard was used for heavy vehicle storage and maintenance. Base personnel reported heavy use of solvents during that time. The solvents included acetone, trichloroethene (TCE), and methyl ethyl ketone. DRMO operations have been in this location since 1990. In the early 1990s fuel bladders (mobile storage tanks) were placed on site with the intent that the bladders be shredded and subsequently disposed following their use. The bladders ranged in size from 600 gallons to 20,000 gallons and were used in training exercises for helicopter refueling. Base personnel reported that the bladders were emptied, cleaned with solvents, re-emptied, and capped prior to storage at the DRMO. Acetone was reportedly used, and possibly 1,1,2,2-PCA. The bladders were stored for 3 to 4 years in a pile approximately 75 feet in diameter by 25 feet high. The pile was located west of what is now the oil changing area. A shredder was brought on site and located immediately north of the bladder pile. The bladders were shredded into small cubes and placed into roll-off boxes. During shredding operations liquids were observed escaping from the bladders. These liquids were not contained or removed. [13].

Three previous investigations have been completed at Site 89, including:

- Phase I and II Remedial Investigation (RI) - August 1996 and May 1997
- MCB, Camp Lejeune Monitoring Program - April 1999
- Immediate Response Field Effort - June/July 1999

In April of 1999, 1,1,2,2-tetrachloroethane (PCA) was found at a concentration of 30 mg/L in a groundwater sample collected from monitoring well IR89-MW02. There were no detections of this contaminant at any location within the DRMO yard before this sampling event. PCA is a chlorinated solvent and has some similar physical properties as trichloroethylene (TCE) and tetrachloroethylene (PCE); however, PCA water solubility is greater (~3000 mg/L at 25oC), its vapor pressure lower (~6mmHg at 25^{o}C), and its viscosity (1.8cP at 25^{o}C) are greater than for water.

Subsequent soil samples collected from Site 89 have confirmed the presence of PCA in the near surface soils. A recent MIP based sample collection effort directed the collection of soil samples that contained NAPL. Mark DeJohn (Baker Engineering and Energy) supplied Figure 29 and noted that "…free DNAPL was observed in 89-MW17, IS21, IS23, and IS25." Approximately 0.5 feet of DNAPL was found in 89-MW17 after installation and during development. An additional 2 feet of DNAPL was detected several weeks after the initial recovery of DNAPL in 89-MW17. Currently, IT Corporation periodically pumps out the DNAPL in the 89-MW17 and only trace amounts of DNAPL have been observed in the well.

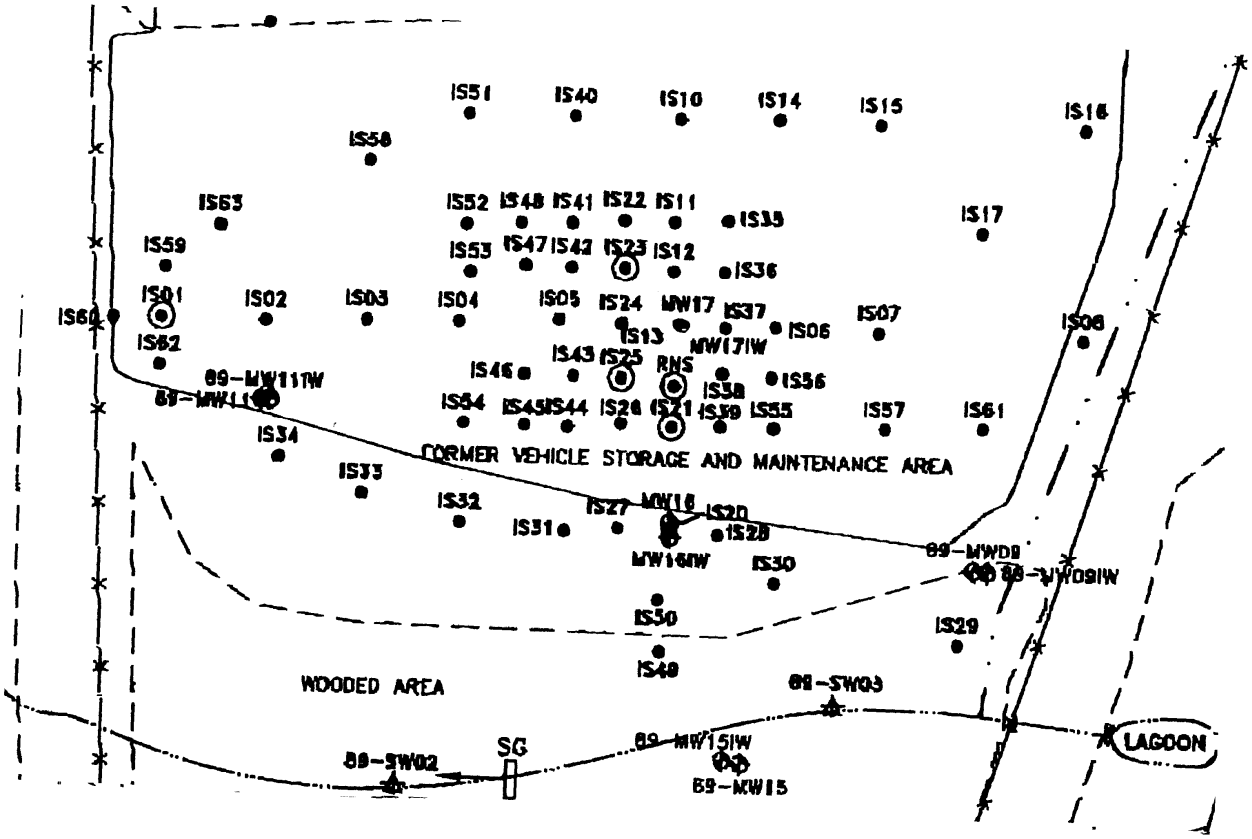

Figure 29. Site 89 Layout and Investigation Locations.

3.3.2.1 Travis AFB

This section discusses the history and characteristics of Site DP039 at Travis Air Force Base. Site DP039 is located on Travis Air Force Base in Solano County, California, (Figure 30). Site descriptions reported here have been extracted from the Groundwater Sampling Report prepared by CH2M Hill.

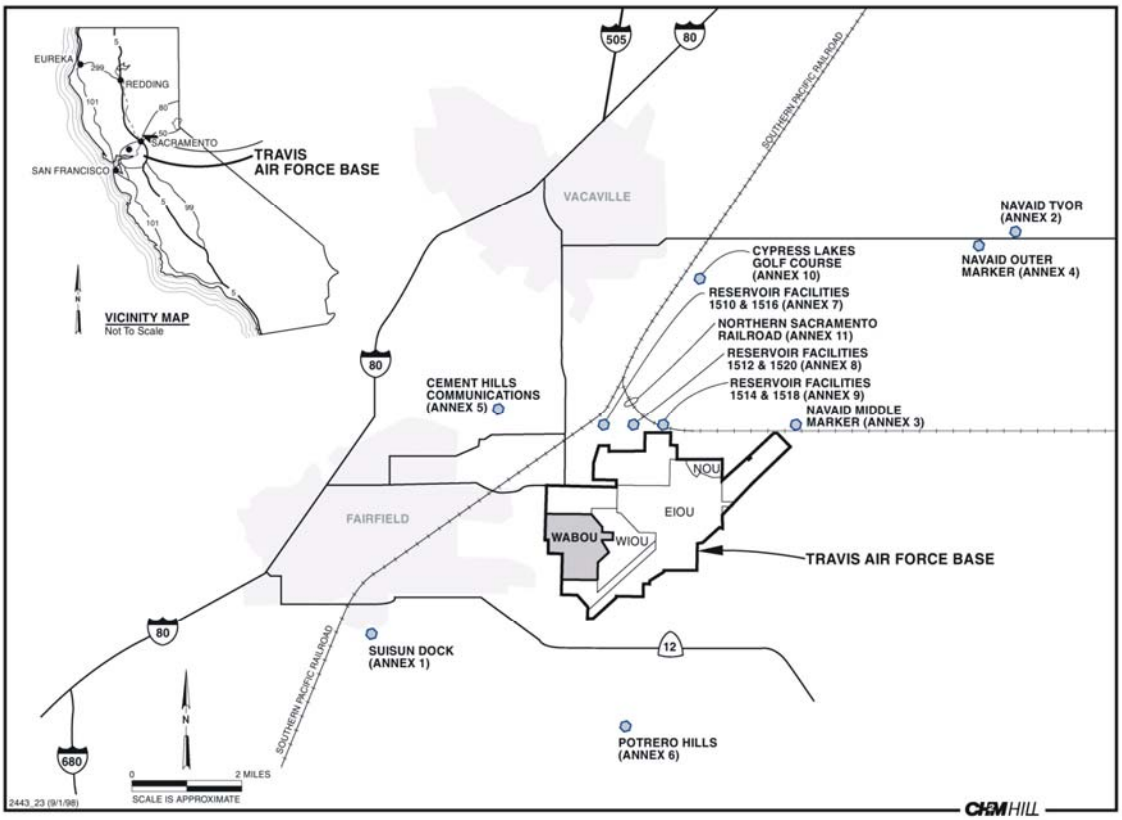

Figure 30. Travis AFB Vicinity Map

Site DP039 (Building 755) is located in the northern portion of the West/Annexes/Basewide Operable Unit (WABOU) on the north side of Ellis Drive, about 1,000 feet east of Dixon Avenue (see Figure 31 and Figure 32). Historically, Building 755 was used for testing rocket engines with rocket propulsion fuel. Since 1968, however, Building 755 has been the location of the Travis AFB Battery and Electric Shop. The DP039 site consists of a former rock-filled acid-neutralization sump located approximately 65 feet west of Building 755, and a former leach field southwest of the sump.

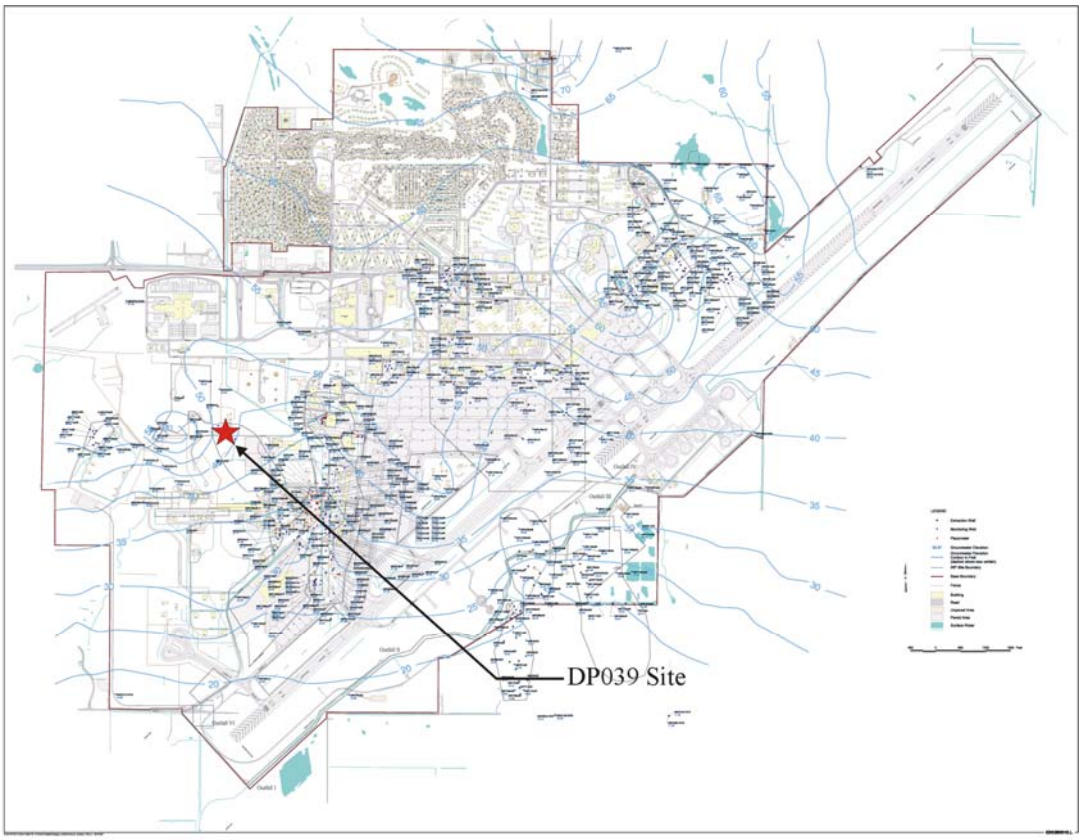

Figure 31. Site DP039 Location map

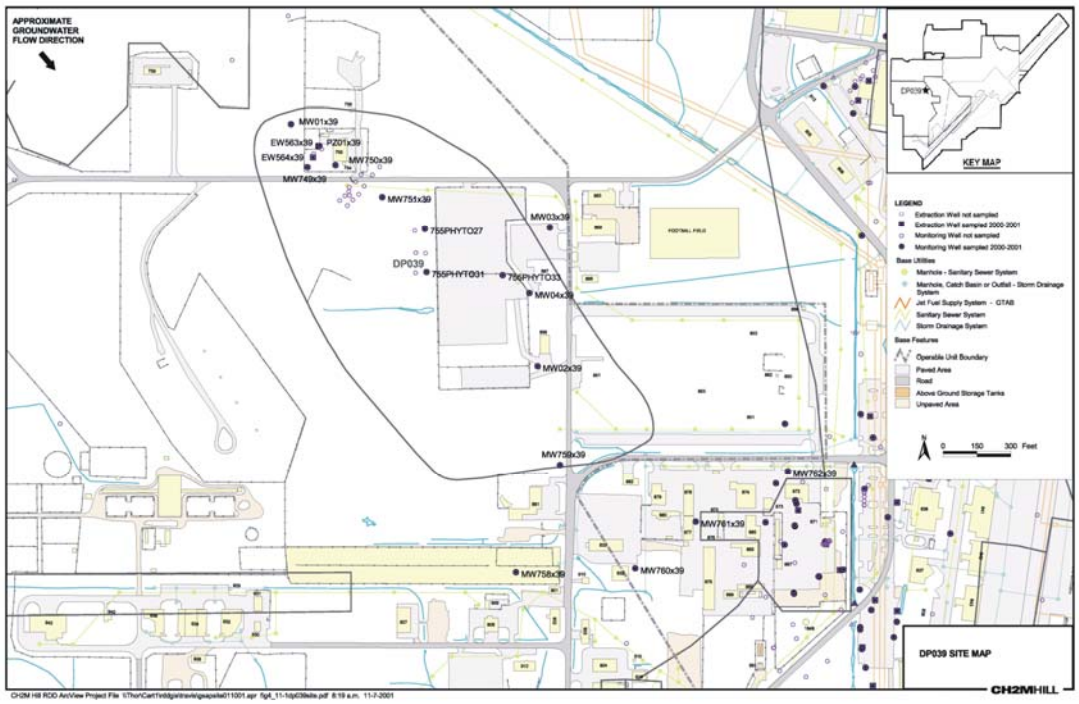

Figure 32. Site DP039 Area Map showing approximate site boundary, monitoring wells, and groundwater flow direction

Operations at Building 755 include recharging and dismantling lead-acid and nickel-cadmium batteries. Rinsate from recharged batteries and battery wastes is neutralized, collected in drums, and transported to an accumulation point at Building 1365 for disposal. The Electric Shop also services and tests constant speed drives. These drives are drained of oil and wiped clean. Waste oil is containerized and disposed offsite. Generators have also been cleaned and tested in the Electric Shop since 1968. The cleaning and testing generates waste oil, which is containerized and transported for off base disposal.

In the past, chlorinated solvents were also used for cleaning generators. Prior to 1978, battery acid solutions and solvents were reportedly discharged into a sink inside Building 755 that drained into the sump and leach field. This practice was discontinued in 1978, when the pipeline to the sump was dismantled and reconnected to the sanitary sewer system. Solvent wastes were also containerized and transported for off base disposal after 1978. The sump and leach field have been inactive since then.

In July 1993, the sump was removed and disposed of off base. The sump was 8 feet long, 8 feet wide, and 4 feet deep. The sump area was lined with visqueen and backfilled with clean soil. Figure 32 shows the site features and the location of the monitoring wells at Site DP039.

Geologic data collected during investigations at DP039 indicate that the subsurface geology at DP039 is highly heterogeneous, varying from clays and silts to sands with little or no horizontal continuity of layers. Relatively permeable sands and silty/clayey sands are encountered primarily as thin zones, ranging from 2 to 5 feet in thickness. Bedrock was encountered on the eastern side of the site at depths ranging from 35 to 55 feet bgs. The bedrock plunges to the east and becomes progressively deeper in that direction. The subsurface geology at DP039 should be viewed as a single complex, heterogeneous hydrogeologic system of unconsolidated sediments. No clearly defined, laterally extensive layers of discrete aquifers or aquitards are present.

The depth to groundwater ranged from about 9 to 27 feet bgs in May 2001. Groundwater hydrographs indicate that the groundwater elevation has been declining at DP039 since about 1997. The decline is pronounced at MW01x39, located at the source area where groundwater extraction has been occurring. In this area, the water table has declined about 10 feet. However, the water table has also declined about 5 feet in wells located beyond the range of the extraction system, such as MW02x30, MW03x39, and MW04x39. On a seasonal basis, the water table fluctuates from about 2 to 4 feet.

As shown on Figure 32, groundwater flows in a predominantly southeasterly direction at DP039. This flow direction is likely caused by a ridge of the Tehama Formation, which forms a topographic high point west and northwest of the site. Groundwater flows away from this ridge toward a bedrock trough filled with Younger Alluvium located east of the site. The alluvium is relatively more permeable than the ridge. In the southeastern part of the site, the groundwater flow direction curves toward the south and joins the regional flow direction.

The horizontal gradient ranges from about 0.01 foot/foot to 0.003 foot/foot at DP039, with an average gradient of about 0.008 foot/foot. The vertical gradient is uncertain at DP039. However, over most of Travis AFB the vertical gradient is negligible, except in the vicinity of extraction wells.

The WABOU RI concluded that VOCs are present in groundwater at and downgradient of the former sump area. TCE concentrations beneath the sump were sufficiently elevated to imply that residual concentrations of liquid-phase TCE were present beneath the sump. A groundwater TCE plume is now known to extend over 2,000 feet downgradient from the former sump.

A pre-design investigation was performed in the downgradient portion of the plume, as part of a preliminary assessment of natural attenuation at DP039. This investigation included the installation of several new downgradient-monitoring wells. A DP039NAAW was then prepared, which specifies ongoing monitoring during the interim period as part of the MNA assessment.

Three treatability studies have been performed or are currently underway at DP039. A Vacuum Dewatering Treatability Study has been completed, and assessed the effectiveness of a 2-Phase groundwater and soil vapor extraction system at removing VOCs at the former sump area. Over the duration of the study, 495 pounds of total VOC mass were removed from the source area. However, because of the short duration of this treatability study, the contractors estimate that there is still significant DNAPL present at DP039 and current technologies are inadequate to determine the amount present.

A Reactive Wall Treatability Study is currently underway by the Air Force. A subsurface iron filings reactive wall was constructed downgradient from the source area to assess its effectiveness at reducing dissolved VOC concentrations in groundwater. Data will be collected as part of the study through 2002, and are not currently available.

A Phytoremediation Treatability Study is also in progress at DP039. The purpose of this study is to assess the use of engineered tree plantings to hydraulically control and remove VOC mass from the groundwater.

3.4 Pre-Demonstration Testing and Analysis

Pre-demonstration activities were conducted by SSC-SD, Dakota Technologies, Inc. and Georgia Institute of Technology (Georgia Tech) before each demonstration. These activities included pre-demonstration site visits, demonstration plan preparation, logistics planning, existing site data evaluation, laboratory and analytical methods review and subcontract procurement of laboratories.

3.5 Testing and Evaluation Plan

3.5.1 Demonstration Installation and Start-Up

The SCAPS truck mounted CPT platform is a stand-alone, roll-on, roll-off unit requiring no outside utilities during operation. No special structures, either temporary or permanent are required for operation. All power is supplied from a generator operated off the truck diesel motor and is regulated through an uninterruptible power supply with a bank of batteries. An

external electrical power input is also available. A hydraulic system, integrated into the truck, provides the force to insert the probe into the ground and also powers the grout pump. Water, from onboard tanks, is consumed in the steam cleaning system and during grouting. A local source of water is required for refilling the onboard tanks. Another consumable is grout. These items may be acquired locally or carried along in the SCAPS support vehicles. Steam cleaning rinsate water is collected in DOT rated 208 liters (55 gallon) drums and handled as potentially hazardous waste. Operations yield approximately half a drum of rinsate waste a day. Wastewater disposal is coordinated with the responsible party for the site and handled locally after results of sampling are obtained.

The SSC-SD program manager communicated regularly with the demonstration participants and coordinated all field activities associated with this demonstration and to resolve any logistical, technical, or QA issues that may arise as the demonstration progresses. The successful implementation of the demonstration will require detailed coordination and constant communication among all demonstration participants. SSC-SD will coordinate, in conjunction with Dakota Technologies, Inc. and Georgia Tech the acquisition and availability of all equipment needed for fieldwork associated with this demonstration.

3.5.2 Period of Operation

3.5.2.1 NAS North Island

The demonstration was conducted in January of 2002.

3.5.2.2 Camp Lejeune

The demonstration was conducted in October of 2002.

3.5.2.3 Travis AFB

The demonstration was conducted in May of 2003.

3.5.3 Amount/Treatment Rate of Material to be Treated

NA

3.5.4 Residuals Handling

Direct push sensor technologies do not bring significant quantities of soil to the surface as is common with conventional drilling methods. The primary investigation-derived waste that will be generated during this effort is the rinsate from the steam cleaning of the rods and probe during retraction. The steam cleaning waste will be collect in 55-gallon drums, and the drums will be labeled and disposed of appropriately as discussed above.

3.5.5 Operating Parameters for the Technology

The three sensor technologies that were demonstrated as part of this effort are designed to be deployed from a direct push sensor platform. The XSD sensor will be pushed continuously at a rate of approximately 0.5-2.0 cm/sec. The GeoVIS soil video imaging system and the high-resolution fluorescence sensor were pushed continuously at a rate of 10 cm/min. The standard 20-ton cone penetrometer system normally requires two people in the push room (one rod handler plus one hydraulic system operator). A minimum of one technician is required to operate either the XSD probe or the HRF/GeoVIS probe.

3.5.6 Experimental Design

The ability of the XSD/MIP sensor system and the HRF/GeoVIS system to accurately delineate DNAPL source zones was accomplished by (1) correlating observed distributions of chlorinated hydrocarbons indicated by in situ XSD data with concentrations of chlorinated hydrocarbons measured on soil and water samples using standard laboratory methods and (2) confirming the presence of likely NAPL source zones identified via XSD screening and indicated by HRF/GeoVIS sensor by direct visual inspections of soil samples and/or treatment of a the soil samples with Sudan Red dye followed by visual inspection.

In situ XSD results are compared against laboratory results from both soil and water samples because systematic differences between *in situ* measurements versus sampling of soil or water followed subsequent laboratory measurement precludes rigorous quantitative comparisons. On one hand, as indicated earlier in Section 2.1, in situ XSD/MIP measurement detects chlorinated hydrocarbons from multiple phases including gas, water, NAPL phases, and may also included chlorinated hyrdrocarbons sorbed onto soil. This “in situ” extraction is somewhat analogous to the “purge and trap” sample extraction process that occurs when subsurface soil samples are collected and sent to a laboratory for analysis by EPA Methods. However, a major difference between the in situ MIP extract and the analysis of a laboratory sample extract is that the laboratory extract is from a known mass of soil, while the MIP extract is from an unknown volume (since the extraction is performed in-situ, there is no way to know the mass of soil from which the sample was actually extracted from). Another issue that complicates direct comparisons is that the solute mass from the laboratory sample may underestimate of the in-situ mass due to losses that occur during sample handling. This difficulty was first reported during the completion of the SCAPS Membrane Interface Probe Demonstration/Validation effort [14].

In addition to variability that arises from sampling handling, spatial variability in the subsurface distribution of contaminants also complicates comparisons of *in situ* versus laboratory methods. For this reason, comparison of in situ XSD/MIP measurements with laboratory measurement of groundwater samples may provide a more accurate method of comparing subsurface contaminant distributions derived via in situ versus laboratory methods. Because groundwater samples represent a larger subsurface volume (a more integrated sample) than soil samples, effects of small scale variability that are unavoidable when comparing the MIP sample volume to a discrete soil sample from a nearby location are minimized. In contrast, a water sample collected from a temporary monitoring well represents a small volume of ground water that is greater than the MIP sample volume, but both samples are from phase that is in equilibrium with the NAPL

phase. Furthermore, lower solute losses are expected during handling of water samples because the solute is in equilibrium within the water phase.

In summary, the goal of this effort is to evaluate the effectiveness of an integrated suite of in situ sensors as field screening tools for determining the presence and location of NAPL in the subsurface. There is no claim regarding the ability to quantify subsurface contaminant concentrations to a degree equal to that of conventional sample collection followed by off–site analysis. The use of conventional analytical techniques is proposed for verifying an in-situ finding or claim of NAPL. It is important to note that the objective of this study is not to provide a rigorous comparison of in situ sensors versus standard laboratory methods, but rather to demonstrate the capability of the technologies presented here to effectively identify and localize DNAPL source zones in the subsurface. This is an important distinction, because numerous studies and workshops have repeatedly pointed out the deficiencies of the standard methods for localizing DNAPL source zones (e.g., [7]). Therefore, in this demonstration, the ability of the sensors tested here to accurately delineate DNAPL source zones are evaluated from direct comparisons of in situ sensor measurements with measurements of discrete water and soil samples collected not because the standard methods represent an accepted method of finding DNAPL in the subsurface but because they provide a means of validating the presence of chlorinated hydrocarbon contamination derived from observed sensor response. Details of the comparisons are listed in Table 5.

In-situ direct sensing measurements will be completed on the centimeter scale, while depth discrete soil and water samples will achieve 10s of centimeter resolution at best. As a result of the difference in sample density, the in-situ results will be averaged over the depth interval corresponding to the discrete soil or water sample for direct comparison. Qualitative evaluation of the capability of the HRF and GeoVIS sensor systems for identifying and delineating the presence of NAPL microglobules will be evaluated using a combination of direct visual inspection of soil cores for evidence of free product and/or treatment of a the soil core with Sudan Red dye followed by visual inspection to identify NAPL [15].

Table 5. Data Quality Objectives.

		Data Quality Objective		
Sensor	**Standard Method**	**Evaluation Criteria**	**Accuracy**	**False Positives/False Negatives**
XSD	8260b (GC/MS)	Semi-Quantitative	Linear correlation > $R^2 > 0.8$	N/A
HRF	Visual/Sudan Red	Semi-Quantitative	80%	<15%
GeoVIS	Visual/Sudan Red	Semi-Quantitative	80%	<15%

3.5.7 Sampling Plan

To evaluate the data acquired by the three direct push DNAPL sensing technologies, measurements are compared directly to data derived from conventional analytical methods performed on water and soil samples collected in the immediate vicinity of the push data. This is accomplished by completing a series of sensor pushes and direct push temporary monitoring wells/soil borings along a transect that traverses from an area that is heavily impacted to an areas that is not impacted with DNAPL contamination. A proposed transect is shown schematically in Figure 33. Approximately six sets of co-located pushes (one SCAPS XSD sensor push, one SCAPS HRF/GeoVIS push, and one or more CPT validation pushes for collection of soil and water samples) will be performed along the transect. Each of these CPT pushes will be positioned so that the three pushes form a triangle that is approximately 12 inches on a side. By minimizing the distance between pushes spatial heterogeneity in contaminant levels will be minimized. After measurements/sampling each CPT push hole will be backfilled with a dilute Portland cement, bentonite, and Sikament mixture.

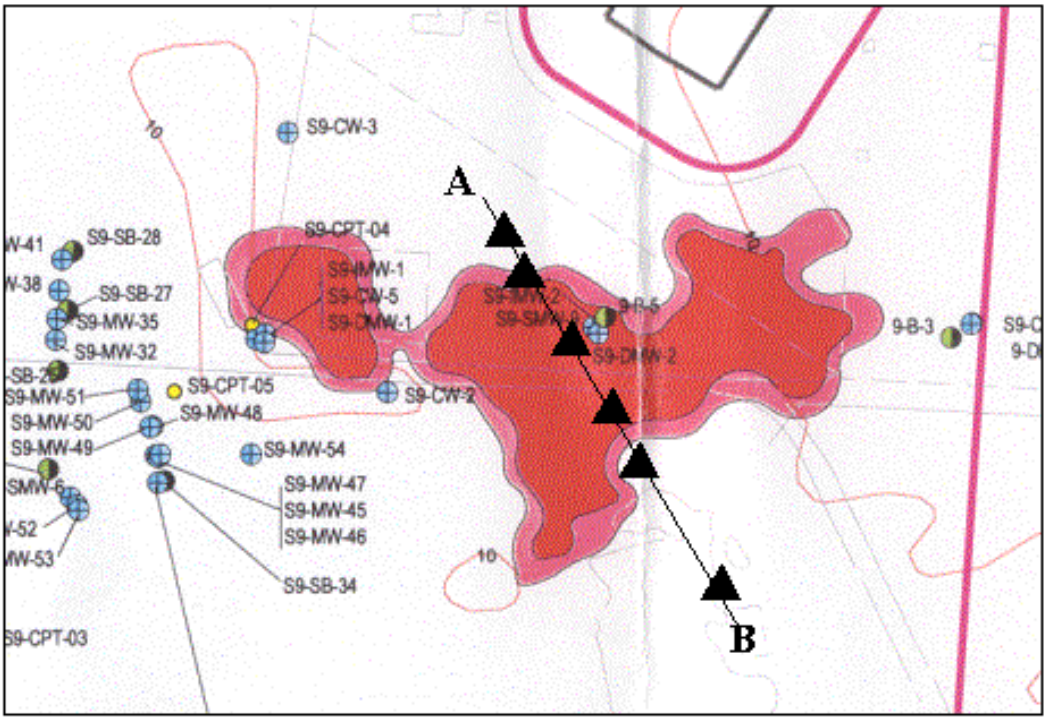

Figure 33. Proposed sampling transect

After the real-time XSD and HRF/GeoVIS sensor data have been collected from each set of push holes, soil and water confirmation samples will be collected.

3.5.7.1 Collection, Preservation, and Analysis of Soil Samples

Soil samples were collected using a direct-push Vertek soil sampler (Applied Research Associates, Inc., South Royalton, VT), which collects a soil core that is 1.4 inches in diameter

and 21 inches long. The soil sampler was assembled with 3, 6 inch long stainless-steel sleeves, a core catcher, and a retractable tip. The soil sampler was then pushed to the target depth, the sampler tip retracted, and sampler pushed approximately 30 inches to fill the stainless-steel sleeves with soil. The soil sampler was then retrieved from the subsurface and a 5-gram sub-sample was collected from the middle stainless-steel sleeve. The soil sample was immediately placed into a 40 mL vial that contained 5 mL of methanol per U.S. EPA method 5035. The methanol filled vials were prepared by Columbia Analytical Services, Canoga Park, CA and used as delivered. Each vial was sealed after filling with soil by wiping the lip of the vial with a dry, lint-free paper towel (Kimwipes), and then affixing a screw thread cap with Teflon lined septum. The soil and methanol were mixed by hand and the vial was placed in an insulated cooler on ice until shipped to Columbia Analytical Services for analysis by U.S. EPA method 8260B. Method 8260B involves purging volatile organic compounds from a sample for analysis by a gas chromatograph equipped with a mass spectrometer.

3.5.7.2 Soil Sample Dye Test Procedure

A dye test was performed on a soil sub-sample from each soil core, which was collected from within 3 inches of the soil sub-sample collected for EPA 8260B analysis. A 5-gram soil sub-sample was placed into a 20 mL clear glass vial and approximately 10 mL of deionized water was added to cover the soil. A small amount (<0.1 g) of Oil Red O (Fisher Scientific, Suwanee, GA) hydrophobic dye (i.e., a xylylazo-naphthol compound) was then added to the 20 mL vial and the vial sealed with a screw thread cap. The 20 mL vial was hand mixed for one minute and the dye color noted. If the dye color changed from brown to bright red, a positive dye test result was noted, while no change in dye color was noted as a negative dye test result. An additional dye test was performed by adding dye crystals directly to the entire soil core when the 20 mL vial test was negative. The whole-core dye test was performed to determine if small NAPL drops were present, which may have been missed in the 5-gram sub-sample.

3.5.7.3 Collection and Analysis of Water Samples

Water samples from the subsurface were collected using a 36 inch long section of 3/4 inch diameter Schedule 40 PVC microwell screen with 0.010 inch intake slots (GeoInsight, Las Cruces, NM). Each microwell screen was individually packaged in plastic wrap and used as delivered. An aluminum tip equipped with a foam ring (GeoInsight, Las Cruces, NM) was attached to the microwell screen and the screen/tip assembly inserted into a section of direct-push pipe. The foam ring served to prevent water and NAPL from entering the push pipe and microwell screen during subsurface installation. The aluminum tip and microwell screen were pushed into the subsurface to a predetermined depth, the direct-push pipe was then retracted approximately 2 feet to expose the microwell screen to the subsurface. Ground water filled the push pipe and once the water elevation was stable, a disposable Teflon bailer was slowly lowered into the push pipe and a water sample was collected. No water was purged from the push pipe prior to collecting the water sample. The bailer contents were then transferred into a 40 mL vial provided by Columbia Analytical Services and the vial was sealed with a screw thread cap fitted with a Teflon lined septum. The vials were stored within an insulated cooler on ice until shipped to Columbia Analytical Services for analysis by U.S. EPA method 8260B (U.S. EPA, 1996a).

Once the water sample was collected, the direct-push pipe was removed from the ground and the well screen abandoned in place. The push-pipe exterior was decontaminated by rinsing with hot water and the push-pipe interior was decontaminated using a steam rinse followed by a deionized water rinse. All rinsewater was collected into a 55-gallon drum for proper storage and disposal.

3.5.7.4 Borehole Abandonment Procedure

Each direct-push borehole was sealed with a cement grout mixture using a tremie grouting method. The tremie grouting method consisted of pushing a probe to maximum borehole depth and injecting grout through the probe tip while retracting the push pipe.

3.5.7.5 Investigation Derived Waste

Two 55-gallon drums filled with rinsewater (no solids) were produced during the demonstration. The drums were sealed, labeled as investigation derived waste, and picked up by The Shaw Corporation to be managed under the NAS North Island, Installation Restoration program

3.5.7.6 Modification of sampling plan for Camp Lejeune.

Based on results obtained during the first demonstration at NAS North Island and subsequent discussions that took place at the May 2002 IPR several sensor pushes will be conducted in close proximity to each other in addition the transect of approximately six sampling locations describe in the test plan [16]. This data will provide a basis for quantifying small-scale spatial variability observed between closely spaced pushes.

3.5.7.7 Modification of the sampling plan for Travis AFB

The main modification during the 3rd field demonstrations was to demonstrate that the XSD-MIP could be transitioned from a cone penetrometer test (CPT) platform to an anchored (when necessary) Geoprobe platform. A secondary goal of this demonstration was to show that the XSD-MIP system could be effectively used to completely map the source term area of a halogenated VOC site.

Transitioning from a CPT platform to an anchored Geoprobe platform makes economic sense because of the limited availability of CPT platform and their high capital and maintenance costs. To fully realize the broad application of the XSD-MIP system, it is imperative that the system be deployed from a more cost-effective and generalized platform. Geoprobe Systems (Salina, KS) direct push machines fulfill this requirement because of their lower cost as well as their widespread use around the world. DTI owns and operates a Geoprobe system so the transition process can be carried out entirely at DTI's facilities prior to mobilization.

The transect approach taken in the previous two demonstrations was successful in validating the performance of the XSD-MIP system. However, the transect approach limits the ability to demonstrate the XSD-MIP system's ability to quickly map the source term(s) of a halogenated VOC site. Site DP039 was selected for the third demonstration site because DNAPL is present but some of the source areas are unknown. This provides an ideal opportunity to demonstrate the

XSD-MIP's speed, adaptability, and efficacy for delineating source terms in a more site wide manner as opposed to a single transect. Since the emphasis of this demonstration will be to map DNAPL plume area(s), numerous pushes (30-40) will be conducted. Because the DP039 source area is relatively small (Figure 34), this number of pushes will be adequate to completely characterize the site.

Figure 34. Picture of the source term area at the DP039 site

The initial proposed transect for the DP039 site is shown in Figure 35. The North end of the transect (marked A) is the area where the Phase II vacuum dewatering study was conducted and most of the free phase product has been removed. The center portion of the transect is part of the old leech field for the former sump and a likely location for additional DNAPL source terms. The South end of the transect was the area where a Phase I vacuum dewatering study was conducted and some DNAPL removed. Discussions with base personnel indicated that this area still has DNAPL present. Uncontaminated areas are located to the north of the purposed transect and will be investigated to confirm the XSD-MIP system is operating properly.

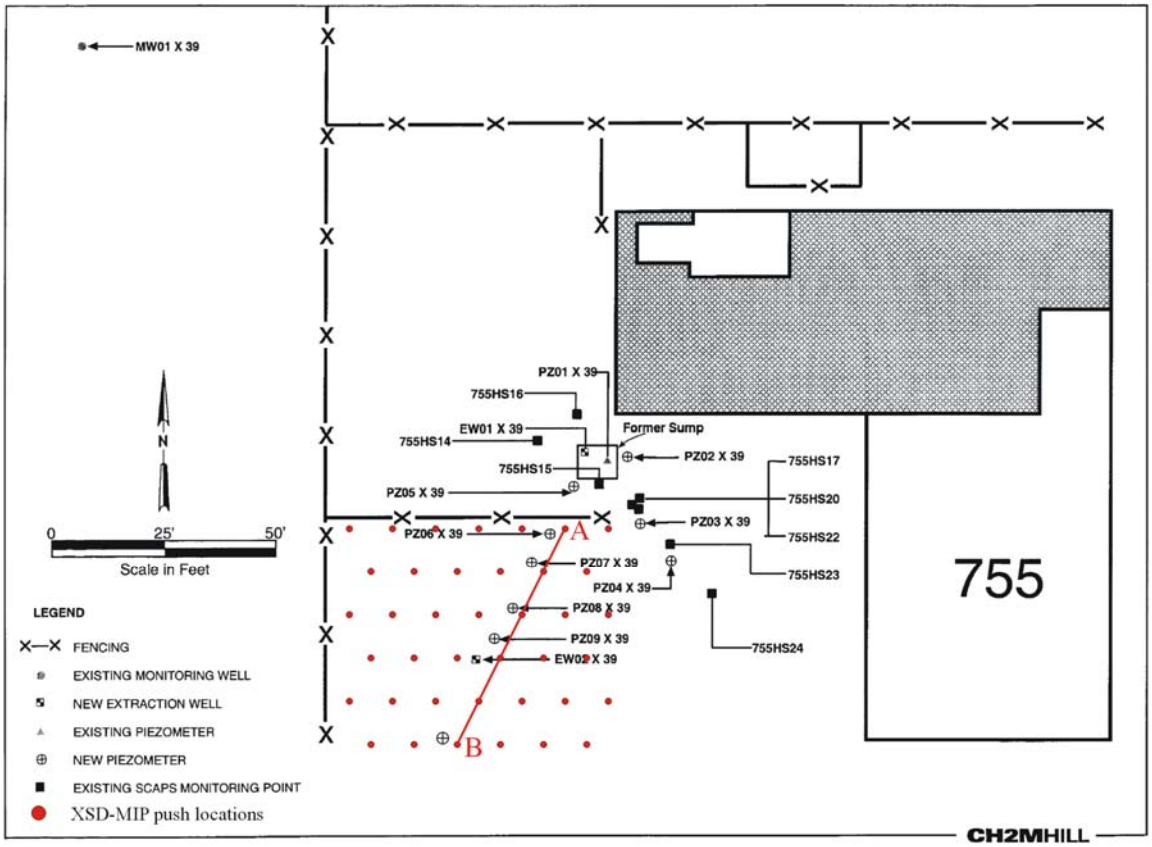

Figure 35. Site DP039 Layout and Investigation Locations

Based on the low water recovery experienced during the second demonstration, which had similar soil conditions to this site, we propose to validate the pushes with water samples collected from existing monitoring wells. DTI will conduct the initial penetrations near five existing monitoring wells and compare the XSD-MIP's results with the concentration of water across the screened interval of these monitoring wells. Splits of these samples will also be analyzed using the XSD-MIP system and the same procedure as was employed during the first two demonstrations. The remainder of the XSD-MIP pushes will be used to determine any other likely DNAPL areas in this area. For these pushes, we will continue to fill in the proposed push locations as shown in Figure 36. For these pushes, soil samples and subsequent dye tests will be used for DNAPL confirmation.

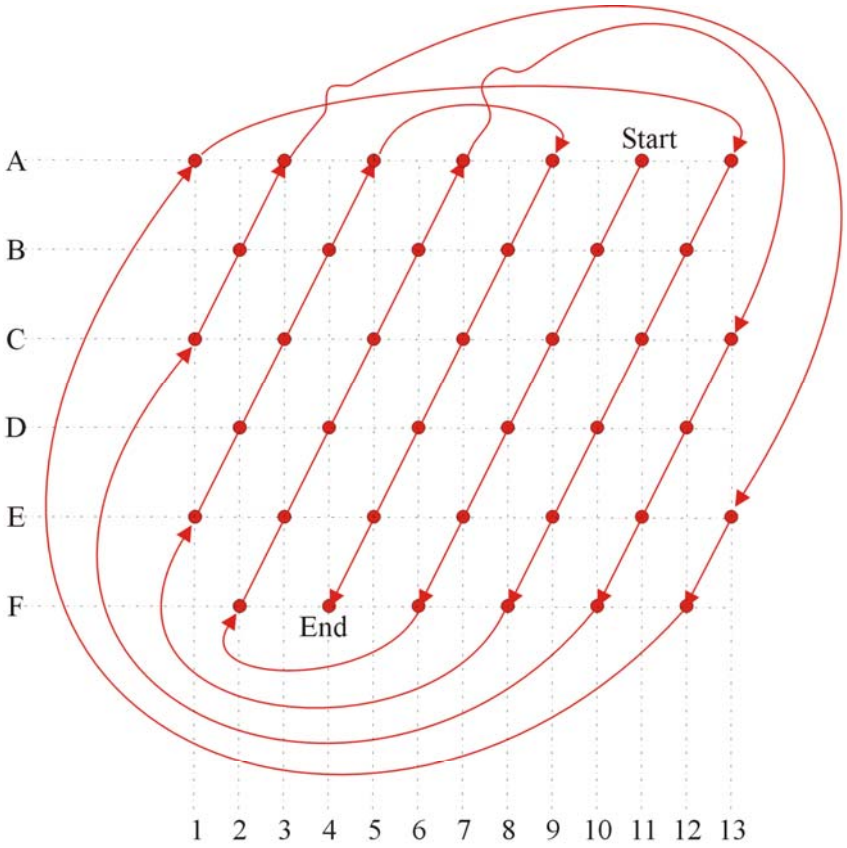

Push Number	Location	Push Number	Location	Push Number	Location
1	A 11	14	D 12	27	E 9
2	B 10	15	E 11	28	F 8
3	C 9	16	F 10	29	E 1
4	D 8	17	C 1	30	D 2
5	E 7	18	B 2	31	C 3
6	F 6	19	A 3	32	B 4
7	F 2	20	E 13	33	A 5
8	E 3	21	F 12	34	A 9
9	D 4	22	A 1	35	B 8
10	C 5	23	A 13	36	C 7
11	B 6	24	B 12	37	D 6
12	A 7	25	C 11	38	E 5
13	C 13	26	D 10	39	F 4

Figure 36. Proposed push locations and order for characterization of DP039 site

3.5.8 Demobilization

Because direct push sensor systems usually roll onto the site in a self-contained wheeled vehicle, demobilization is usually very simple. Demobilization primarily involves on-site packing of equipment and return travel of the push vehicle to its home base (in this case either San Diego, California or Fargo, North Dakota). For some demonstrations sensor equipment may be packed and shipped separately to the individual technologist laboratory.

3.6 Selection of the Analytical/testing Methods

US EPA SW-846 Method 8260b for DNAPLs have been selected as the confirmatory analytical method for comparison with the XSD sensor for measurement of DNAPLs in soils. The 8260b method has been chosen because of its widespread and generally accepted use in delineating the extent of DNAPL soil contamination. This is the most comparable analytical method corresponding to the objective of demonstrating rapid field screening using the XSD Sensor. This US EPA Method is in Appendix A.

Qualitative evaluation of the capability of the HRF and GeoVIS sensor systems for identifying and delineating the presence of NAPL microglobules will be evaluated using a combination of direct visual inspection of soil cores for evidence of free product and/or treatment of a the soil core with Sudan Red dye followed by visual inspection to identify NAPL [15].

3.7 Selection of Analytical/Testing Laboratory

To assess the performance of the DNAPL sensor technologies, the data generated using the sensor technologies is compared to data obtained using conventional sample collection and analytical methods. A certified laboratory was selected to provide confirmatory analytical services. The analytical laboratory was selected based on its experience with QA procedures; analytical result reporting requirements, data quality parameters, etc. The selected analytical laboratory was not affiliated with SSC-SD or any of the demonstration team members. It is important that the selected analytical laboratory be able to report data in contract laboratory program (CLP) format in order to insure that the data acquired during these demonstrations is in a form familiar to the regulatory community. Upon selection, the analytical laboratory's US EPA certification, standard operating procedures and QA/QC (Quality assurance/ quality control) procedures will be submitted as an addendum to this demonstration plan.

4 Performance Assessment

4.1 Performance Criteria

Performance criteria to be evaluated as part of this demonstration are listed in Table 6.

Table 6. Performance Objectives.

Performance Criteria	Description	Primary or Secondary
Factors Affecting Technology Performance	Contaminant, Hydrogeology, Soil Type, Push-rate, Presence of mixed contaminants	Primary
Versatility	Includes assessment of performance for different geological conditions, different suites of contaminants, different push systems	Primary
Hazardous Materials	Hazardous materials introduced by technology	Secondary
Process Waste	Includes any waste produced by the technology	Secondary
Reliability	Includes breakdown of equipment, sample carry-over, sensitivity to changes in soil type	Secondary
Ease of Use	Includes number of personnel required to operate equipment, skill levels of personnel, amount of data processing/post processing required	Primary
Maintenance	Includes requirements and frequency for required calibration/maintenance and level of training required for maintenance personnel	Secondary
Scale-up Constraints	Issues related to scale up for full implementation	Secondary

4.2 Performance Confirmation Methods

4.2.1.1.1 Performance Criteria	**Expected Performance Metric (pre demo)**	**Performance Confirmation Method**
PRIMARY CRITERIA(Performance Objectives) (Qualitative)		
Ability to detect DNAPL source zones	Improved capability for localizing DNAPL source zones	Comparison with concentrations from US EPA method 8260b, visual identification of DNAPL in confirmation samples
Capability to resolve small scale variations in DNAPL distributions	Improved capability for localizing small scale variations in DNAPL distributions	Comparison of distributions derived from push data with data from discrete samples
Time required for delineating DNAPL source zones	Reduction in time for delineating DNAPLS sources zones with direct push sensors	Comparison with discrete sample collection and laboratory analysis
PRIMARY CRITERIA (Performance Objectives) (Quantitative)		
Detection of DNAPL miroglobules via HRF and video imaging	Accuracy >80%, <15% false positives/negatives	Compare with visual observations/Sudan Red shaker test
Dynamic Range of XSD detector (semi-quantitative)	10^4 (10^2 ppb-10^6ppb) aqueous phase	Compare with US EPA Method 8260b
SECONDARY PERFORMANCE CRITERIA (Qualitative)		
Reliability	Expect sensors to be robust, with minimal sample carryover	Field records
Ease of Use	Operator experience	Experience from demonstration
Versatility - applicable to different geological conditions - use with different push systems	Yes Yes	Experience from demonstration
Maintenance - required	None	Experience from demonstration
Process Waste - Generated	None	Field experience/analysis of steam cleaning effluent

4.3 Data Analysis, Interpretation and Evaluation

4.3.1 NAS North Island

4.3.1.1 XSD Data

4.3.1.1.1 Initial startup of MIP-XSD system

The following startup procedure was used at the beginning of each day for the XSD-MIP system.

The flow rate of air to the system was set to 30 mL/min with a backing pressure of 15 psig. The carrier gas return line was immersed in water to confirm that the carrier gas was flowing through the entire system. If adequate airflow was present, the data collection program was then started and set to display the XSD signal vs. time and XSD temperature vs. time, while the MIP temperature was visually monitored. Next, the heater controllers for the XSD and MIP were turned on and allowed to come up to operating temperature (140 ºC for the MIP and 900 ºC for the XSD). Data collection was continued until the baseline XSD signal and XSD temperature had been stable for five minutes. The run was ended, the data file name was recorded, and the data file was saved to the hard drive and a floppy disk.

4.3.1.1.2 Field calibration of MIP-XSD system

Prior to an in situ measurement, a calibration of the system was done using the SRC solution and the dual reservoir flow cell system described above.

At the end of the field demonstration, the SRC data was used to normalize all field data to correct for the inevitable changes in responsivity and baseline. The SRC process yielded a unitless correction factor for each unique location probed. Application of this factor corrected for system drift but allowed us to retain the XSD-MIP data's native data format (volts). This allowed us to view the entire project data set in a normalized context at project completion with confidence that any drift in system responsivity had been accounted for. A description of the normalization procedure is given in a following section.

4.3.1.1.3 In situ measurement procedure for MIP-XSD system

The following procedure was used for all of the in situ measurements with the XSD-MIP system. First, both the XSD and MIP temperatures were checked to insure that they were at stable operating temperatures (140 ºC for the MIP and 900 ºC for the XSD). Next, the CPT tip was placed six inches from ground surface and the CPT data acquisition program was zeroed. This offset was necessary because the software that collects the CPT information is written to use a 31-inch spacing from CPT tip to window. For the XSD system, the distance from the CPT tip to the MIP is 25 inches. By zeroing the system 6 inches from the ground surface, the depth measurements for the XSD system would be correct. The data acquisition program was started and the probe was advanced at 1 foot per minute. The probe advancement was continued until either the maximum probe depth was achieved, the probe advancement was rejected, or the deepest suspected contamination level was surpassed. The run was ended, the data file name was recorded, and the data file was saved to the hard drive and a floppy disk.

4.3.1.1.4 Extraction procedure for MIP-XSD system

At the end of the push the probe was extracted from the subsurface while the MIP and XSD were still operating to maintain sufficient temperature to minimize water intrusion. Upon extraction, the MIP was cleaned off with steel brush, washed with distilled water, and visually inspected for membrane damage.

4.3.1.1.5 Data Processing

4.3.1.1.5.1 Data normalization process

At the end of the field demonstration the SRC profiles collected prior to each in situ measurement were used to normalize the logs. First, each SRC profile was background corrected by subtracting the average baseline signal collected at the start of the run. Next, the average SRC signal for each profile was found over the range in the profile where the SRC solution was producing a stable signal. The mean SRC value was then calculated by finding the average of all of the individual SRC averages. Finally, the mean SRC analyte signal was divided by the average SRC value for each SRC profile in order to create a correction factor for each in situ profile. Table 7 shows the SRC signal for each profile, the average SRC signal, and the correction factor that was applied to each in situ measurement.

Each in situ measurement was then background corrected using the average baseline signal collected at the start of the run. Finally, the unitless correction factors were applied to the in situ profiles to yield normalized profiles of the XSD data. The change in the average calibration signal between runs four and five were caused by the necessity of changing MIP membranes.

Table 7. SRC signal for each profile, average SRC signal and correction factor used for normalization of in situ measurements

Calibration/Run Number	Average Baseline Signal	Average Signal and Baseline	Average Calibration Signal	Correction Factor
2	0.339	6.953	6.614	0.956
3	1.033	8.141	7.108	0.890
4	0.286	7.889	7.603	0.832
5	0.596	6.460	5.865	1.079
6	0.296	4.732	4.436	1.426
		Average of all calibrations	6.325	

4.3.1.1.5.2 Normalized XSD data

Using the average SRC value (6.325 volts) the regions where DNAPLs were suspected was found. In this subroutine, the computer program went through the data and plotted all points that were above the average SRC value. Since all of the profiles were normalized, this allowed us to use this value to find the regions DNAPLs were indicated with the XSD. These points are shown as red circles in the following sections. Pushes 2, 3, and 6 all indicated areas where DNAPL could be present. A description of the main features of each push is given below.

Push 1a and b were rejected at 5.8 and 1.7 feet respectively. No contamination was encountered in either push.

Numerous areas of contamination were noted in Push 2 (Figure 37). The largest continuous area ranged from three to seventeen feet. Thin layers of contamination were noted at 22.7, 24, 24.7, 25.9, 28.1, 29-31.3, 32.2, 32.7 and 33.4 – 33.6 feet. The regions suspected of being indicative of DNAPLs are: 9.2 – 11.5, 12 – 12.3, and 21.2 – 32.8 feet. The push was terminated at 33.9 feet.

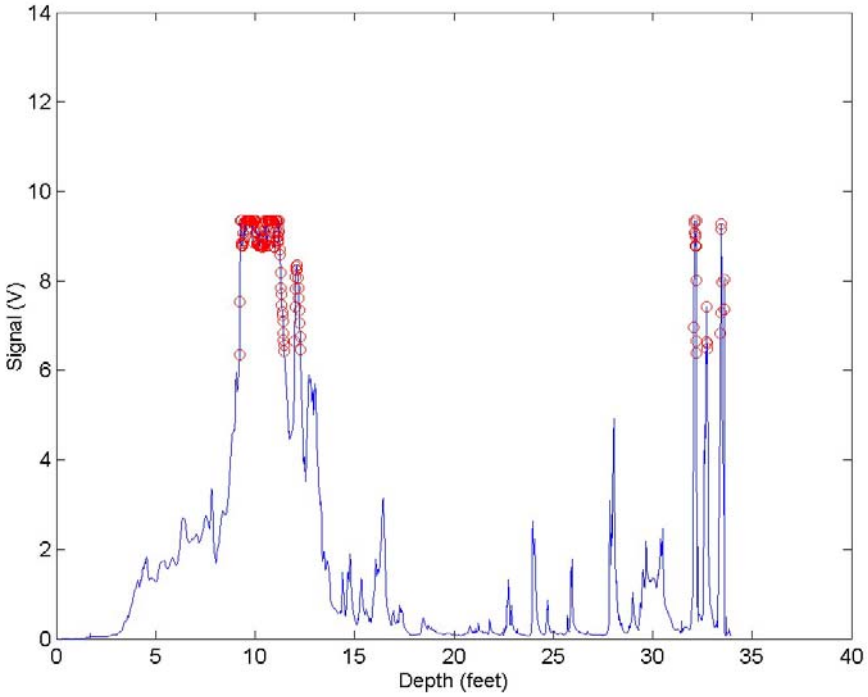

Figure 37. XSD Push 2 profile

Some areas of contamination were noted in Push 3 (Figure 38). The largest continuous area ranged from one to sixteen feet. Several thin layers of contamination were noted at 21.1, 25.2, 25.6, 28.3, 29.2, 29.9, and 30.3 feet. The regions suspected of being indicative of DNAPLs are: 9.1 – 10.5, 11.3 – 11.6, and 12.1 – 12.2 feet. The push was terminated at 30.3 feet.

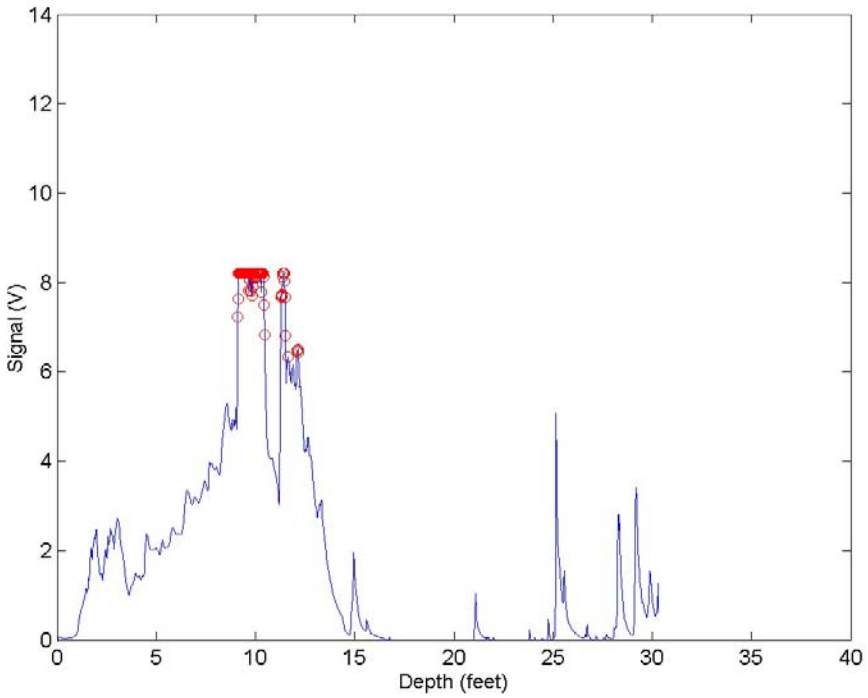

Figure 38. XSD Push 3 profile

Two moderate areas of contamination were noted in Push 3 (Figure 38). The largest continuous area ranged from one to sixteen feet. The other contaminated region noted was from 27 to 30.7 feet. No suspected DNAPL regions were indicated in this push. The push was terminated at 30.7 feet.

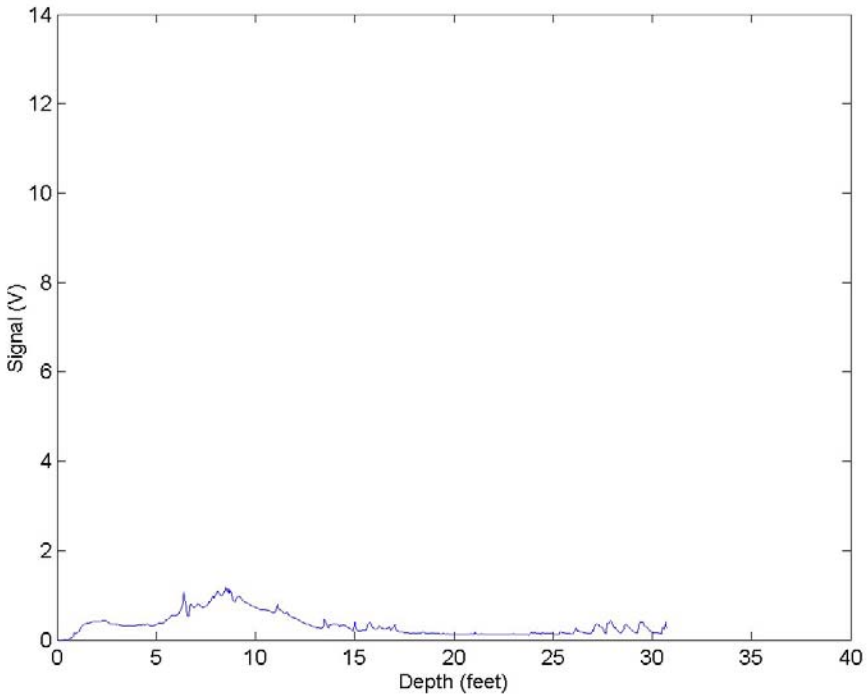

Figure 39. XSD Push 4 profile.

No contaminated regions were noted during Push 5 (Figure 40). The push was terminated at 37.5 feet.

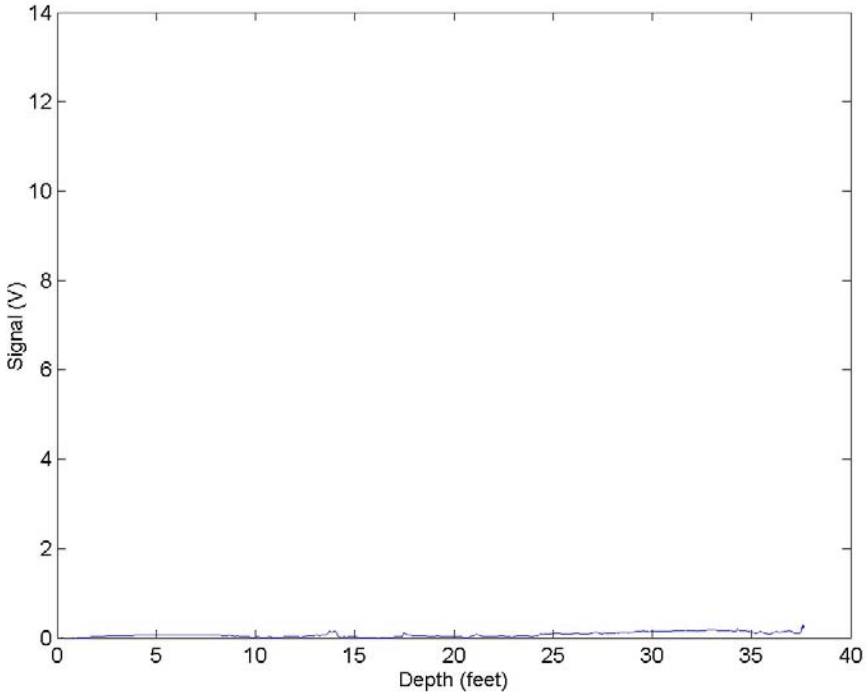

Figure 40. XSD Push 5 profile.

Several areas of contamination were noted in Push 6 (Figure 41). Thin layers of contamination were noted at 10.1, 11.1, 17, and 18.1 feet. The largest continuous area ranged from 28 to 36.8 feet. The regions suspected of being indicative of DNAPLs are: 16.9 - 17, 29.5 – 31.3, 33.4 – 33.5, 34.2 – 35.4, and 36.6 – 36.8 feet. The push was terminated at 36.8 feet.

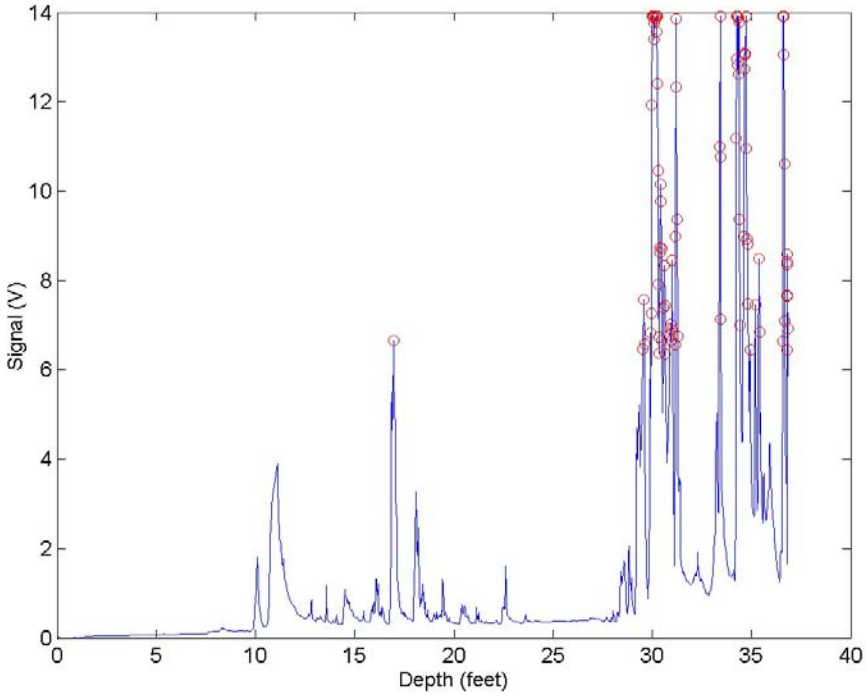

Figure 41. XSD Push 6 profile.

Transect of XSD pushes (Figure 42) and results of the water sample data (blue "tees"). The amplitude of the "tee" indicates the total halogen concentration (normalized to the XSD's 15-volt scale). The width of the "tee" denotes the depth interval over which the water samples were collected.

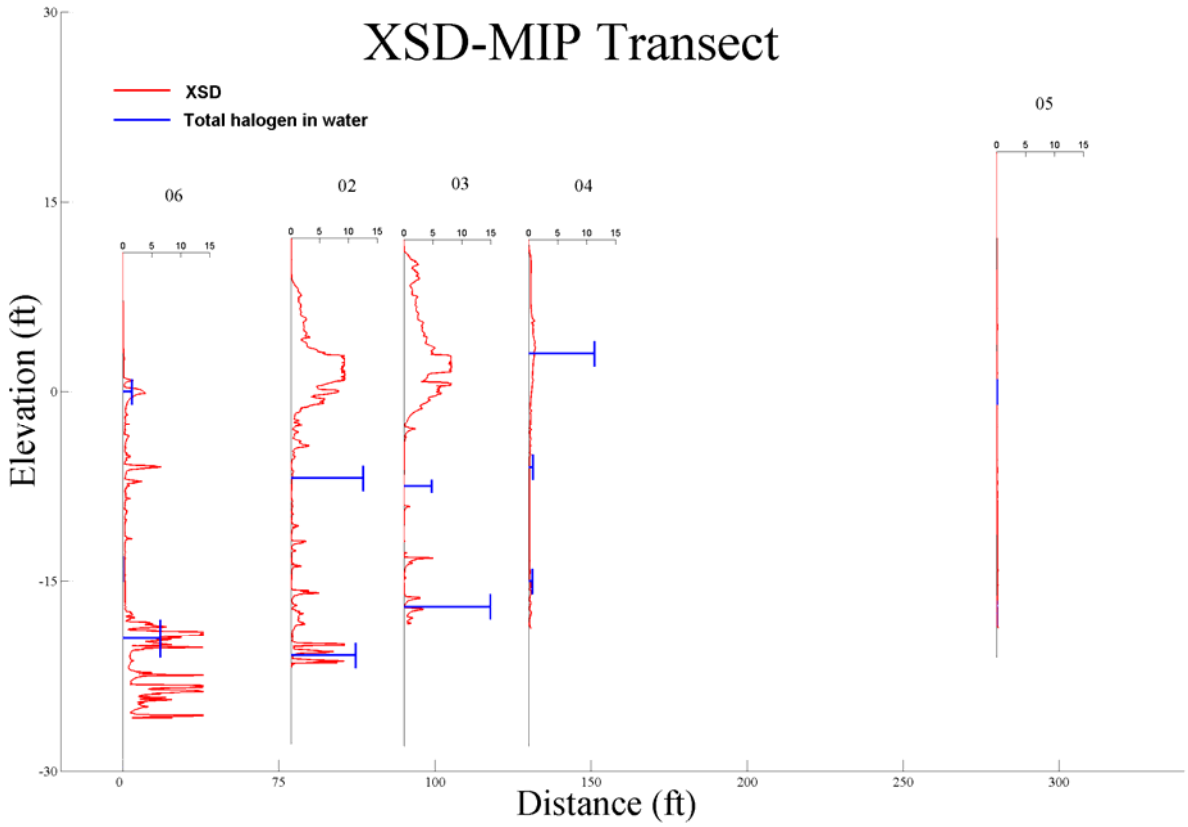

Figure 42. Transect of all XSD pushes at North Island IR site 9

4.3.1.1.6 Comparison of In situ Measurements with Laboratory Water Samples

A comparison of the in situ XSD measurements with the water samples was undertaken to identify any correlation. Since the water sample data was collected over discrete depth intervals and our data was collected continuously, the method to correlate our data was to average the XSD signal over the depth range of the water samples. The push locations, depth regions, halogenated concentration, and averaged XSD signals are shown in Table 8.

Table 8. North Island Water sample and XSD results at selected depths

XSD Push number	Depth (feet)	Total halogenated concentration (ppm)	Average XSD signal (V)
02	9 – 11	1834380	8.748
02	18 – 20	1839.24	0.168
02	32 – 34	1652	2.840
03	19 – 20	706.5	-0.064
03	28 – 30	2189.6	0.987
04	8 – 10	1672	0.941
04	17 – 19	112.6	0.166
04	26 – 28	108.4	0.240
05	18 – 20	24.58	0.038
05	35.5 – 37.5	0	0.119
06	10 – 12	240	1.254
06	24 – 26	0	0.364
06	29 – 32	952.8	5.391

A clarification must be made about the way we handled the water sample data. The XSD responses to most halogenated species, consequently all halogenated compounds must be taken into account in the correlation. Furthermore, the XSD signal is directly related to the number of halogen atoms on a molecule. For example, equal concentrations of trichloroethylene (TCE) and perchloroethylene (PCE) would not give the same signal level, rather, the signal from PCE would be 4/3 as strong as from TCE since the PCE contains four chlorine atoms while TCE only has three. To account for the varying number of halogen atoms, the concentrations of each halogenated species was multiplied by their respective halogen number (3 for TCE, 4 for PCE, etc.). These values were then summed to give a total halogenated concentration. In most cases, the major contributor to the total halogenated concentration was TCE, however, there were notable exceptions. For example, the main contributor for push 6 at the 29-32 feet depth region was cis-1, 2-dichloroethene. Figure 43 shows a scatter plot of the XSD signals vs. total halogenated concentration.

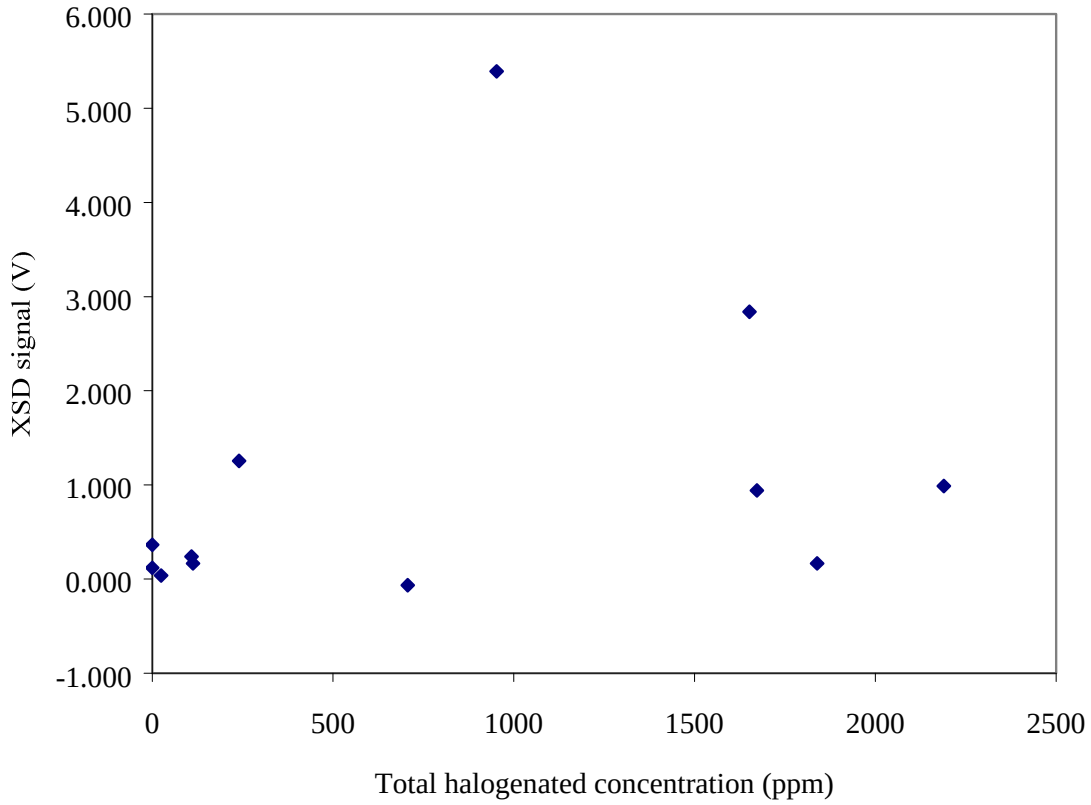

Figure 43. Total halogenated concentration vs. XSD signal

The correlation between the water sample data and the XSD signal levels was inconclusive. One of the most probable reasons for the inconclusive correlation is that since the XSD signal was averaged over the entire sampled depth range and the contaminated regions were quite narrow, the average XSD value was effectively diluted. Also, at two of the push locations the water samples had to be taken under a heavily impacted area, which raises the concern about cross-contamination of the lower sampled areas. To prove that the XSD-MIP system reacts linearly to increasing halogen concentration, splits of the water samples taken at the North Island site were analyzed with the XSD-MIP system in the laboratory. The procedure and results are discussed in the next sections.

4.3.1.1.7 Laboratory Analysis of Water Samples with XSD-MIP System

To evaluate whether the XSD-MIP system reacted linearly to the water samples collected at the site, splits were run on the XSD-MIP system in the laboratory. Because of the sample size (40 mL per location) the flow cell system could not be used in its normal mode of operation. Rather, a modification to the sample introduction method was developed so that the samples could be run under a standardized procedure. The method developed for running the water samples was to inject a 500 μL aliquot sample into the flow cell and then push it through the flow cell with a burst of compressed air. The resulting signal's peak height was taken as the value for the corresponding sample. Since only small amounts of sample were injected, it was imperative that the solution evenly wetted the membrane as it passed through the flow cell. Even wetting was

visually monitored and any sample injections that did not evenly wet the membrane were discarded. Multiple injections of each sample were run and averaged to minimize variability.

4.3.1.1.8 Calibration Procedure Prior to Water Sample Analysis

Prior to running the water samples, a four-point calibration was done using dilutions of a saturated TCE solution. Since the membrane that was used for these studies had been used in the field, the transport ability had increased due to some of the Teflon coating being worn off. Therefore, the calibration could only be done from 550 ppm to 11 ppm TCE (see Figure 44).

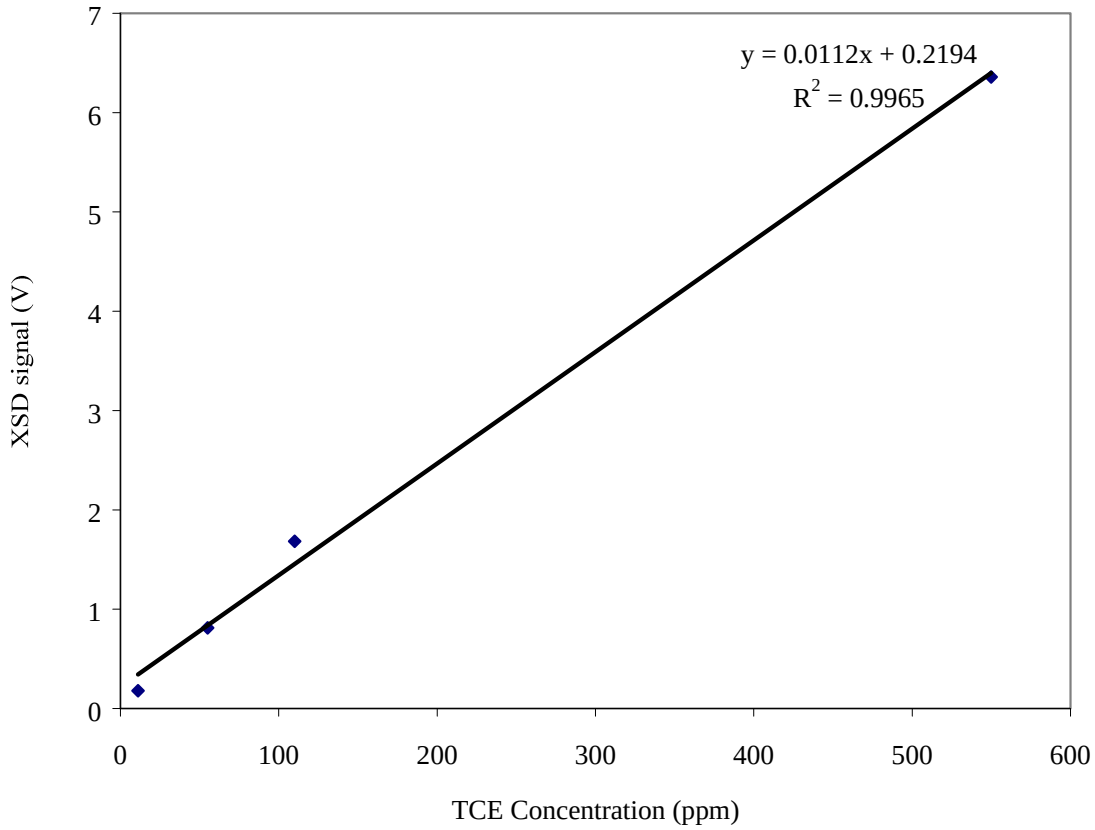

Figure 44. Four point calibration of XSD-MIP system

4.3.1.1.9 Water Sample Analysis

Prior to the introduction of each water sample a single point calibration was done using multiple aliquots of a 110-ppm TCE solution. The results of each calibration were used to normalize the corresponding water sample data.

Immediately following the calibration solution aliquots, the water samples were placed on the membrane. Again multiple sample aliquots were done to find an average value for the water samples.

To keep the sample concentrations within the range of the calibration, four of the samples were diluted by a factor of two. The original concentrations were calculated by multiplying by 2.

Figure 45 shows the comparison of the laboratory water sample data with the XSD-MIP values for each sample location

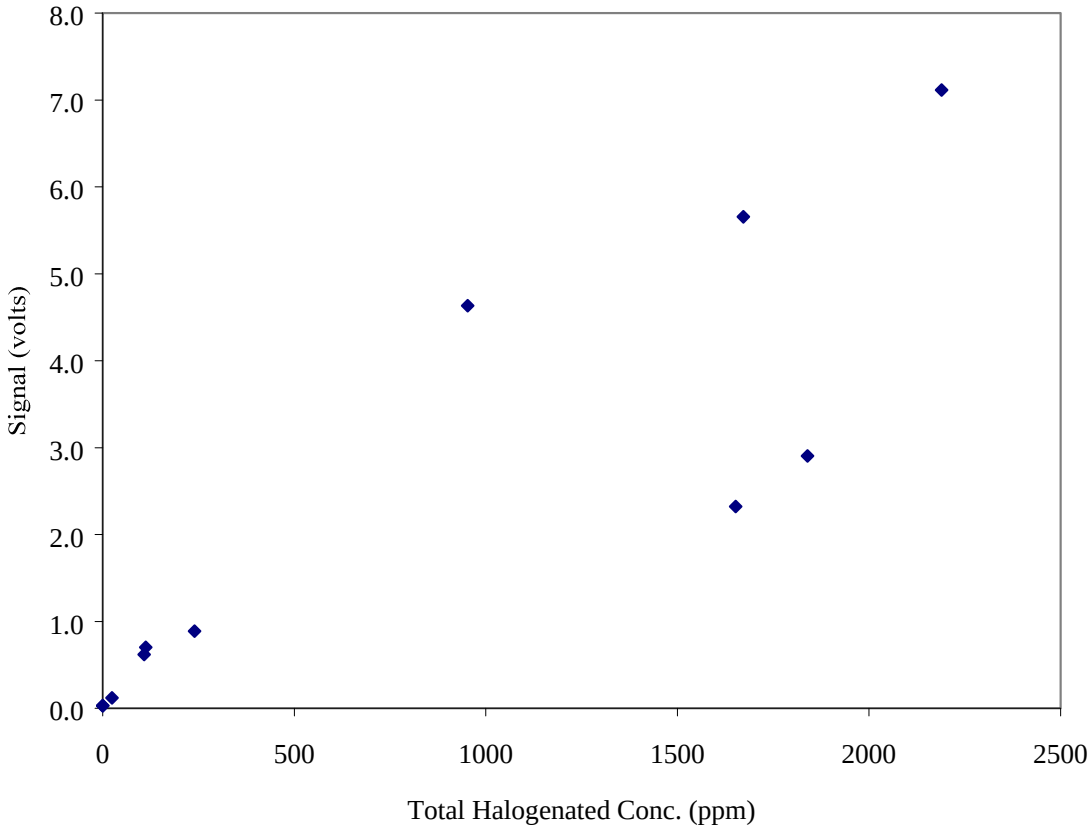

Figure 45. Comparison of laboratory water sample concentrations with XSD-MIP signals on water sample splits

It can be seen that there is good correlation between the laboratory water sample analysis and the XSD-MIP analysis. Only two points significantly deviated from the rest. Both of these data points were from the Push 02 location and taken at 18-20 and 28-30 feet respectively. Both of these locations were under the heavily impacted region.

In situ sensor measurements were completed at 6 locations in the region of Site 9 where NAPL had been previously identified (Figure 46). Four of the locations were located in an area thought to contain NAPL (NI01 through NI 04), while two of the places were located in areas thought to be free of NAPL (NI05 and NI06). The XSD/MIP probe was used at all six locations with a duplicate measurement completed at NI02. Two attempts were made to advance the XSD/MIP probe at location NI01; however, the maximum depth achieved was 5.8 feet due to the presence of an unidentified subsurface obstacle. After the XSD/MIP measurements were completed, the LIF/GeoVIS probe was used at four of the six locations including NI02, NI03, NI04, and NI06 targeting specific depth intervals based on XSD/MIP results.

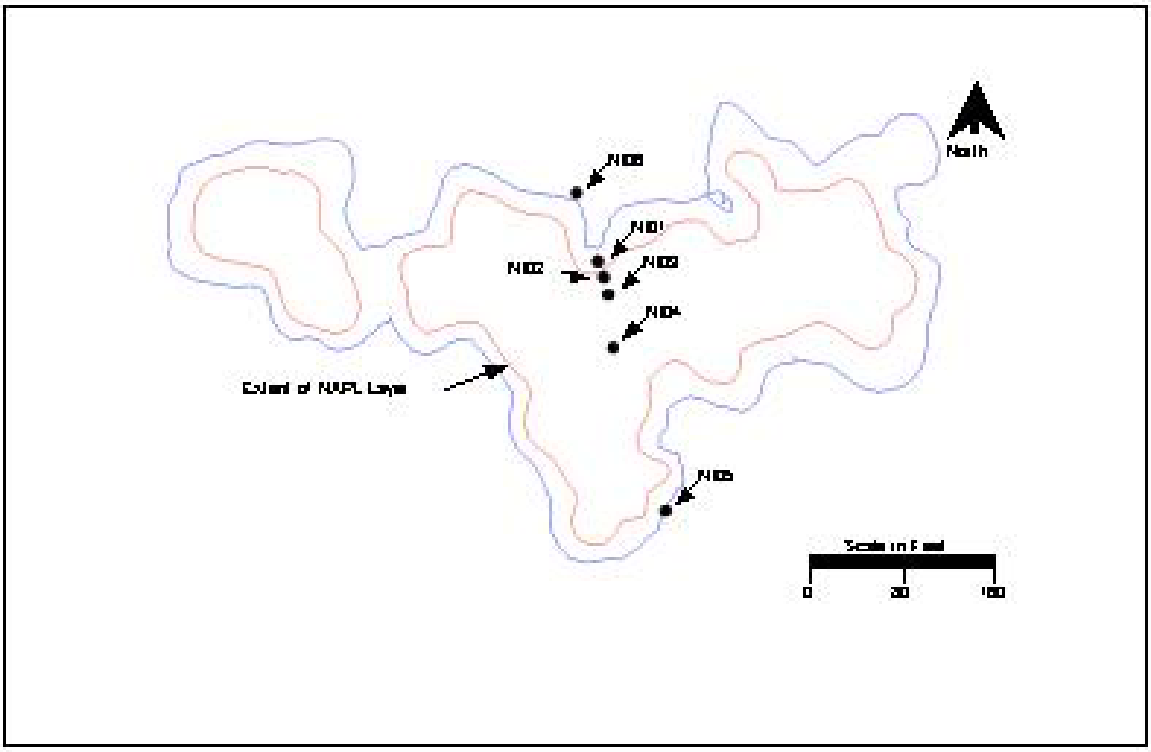

Figure 46. Site 9 NAPL Distribution and In Situ Sensor Transect

4.3.1.2 LIF Data

A total of four LIF logs were acquired on January 9th at the North Island demonstration site. Table 9 summarizes the basic statistics of the logs. These logs are very large in comparison to the 1.0-1.5 MB typical size for ROST files.

Table 9. LIF logs collected at North Island in January 2002

	NIGVLIF02.fvd	NIGVLIF03.fvd	NIGVLIF04.fvd	NIGVLIF06.fvd
Start Time	8:20 a.m.	10:30 a.m.	2:04 p.m.	4:04 p.m.
File Size	13.8 MB	13.2 MB	8.4 MB	10.9 MB
# of data points	4,338	4,198	2,672	3,453
Max depth achieved	33.8	30.8	29.1	33.5
Maximum response (LIF)	173% @ 9.8 ft	425%@ 9.4 ft	286% @ 8.7 ft	8.5% @ 28.8 ft

The XSD and colorized LIF data were printed in the field and were used to guide the sampling effort in the field.

4.3.1.2.1 Data Analysis

As discussed earlier, the depth information for ROST was provided via a RS-232 data-tap of the depth feed to the GeoVIS recording system. The data stream being sent is accurate for the GeoVIS video window, which is located 3.125" below the LIF window. This required that the LIF data be depth adjusted to 3.125" less than originally recorded. Unfortunately, the resolution of the depth data stream was rounded to the nearest 0.1 foot. This wasn't nearly adequate enough resolution to properly encode the LIF data since the data density was on the order of 0.003 ft (during the slower GeoVIS/high resolution push mode). As a work-around for this phase, constant velocity was assumed between all the depths recorded and a linear interpolation of depth was done for the ROST data stream where duplicate depths were recorded. The LIF depth data was then converted to the nearest 0.001 ft.

Figure 47 illustrates the relative location and quantitative (total fluorescence intensity) of the logs generated on the North Island transect. Location #5 (NA) is shown for reference against XSD log #5. The transect view shows a highly fluorescent material at the water table (LNAPL) with relatively small responses interspersed at depth where possible DNAPL were suspected.

Figure 48, Figure 49, Figure 50 and Figure 51 contain the depth corrected, interpolated and colorized logs acquired on the North Island transect. Waveforms from selected points along the log are shown to the right of the log. Log # 2, 3, and 4 all showed very high levels of fluorescence in the 6-14 ft region where a floating (LNAPL) mixed product was found in previous site investigations. The waveforms in this suspected LNAPL zone are all fairly similar, with a slight shift in color (and therefore, spectra) from one end of the transect to the other. The colorization, described earlier in this report, aids in the interpretation of the logs by pointing out similarities or differences in the waveforms. The color (waveform shapes) of the LNAPL shifts from yellow to green-orange as one moves south along the transect, indicating a change in the make-up of the LNAPL. One possible reason for this shift is a change in the chlorinated fraction of the LNAPL along the transect. Another reason could be a change in PAH concentration simply as a result of the varying source of the originally dumped products. The black color indicates a failure of the colorization algorithm due to clipped or highly unusual waveforms. GEOVISLIF03 contains unusually high amounts of black colorization due to clipping of the waveforms that resulted from very high signal levels (beyond the maximum set range of the oscilloscope).

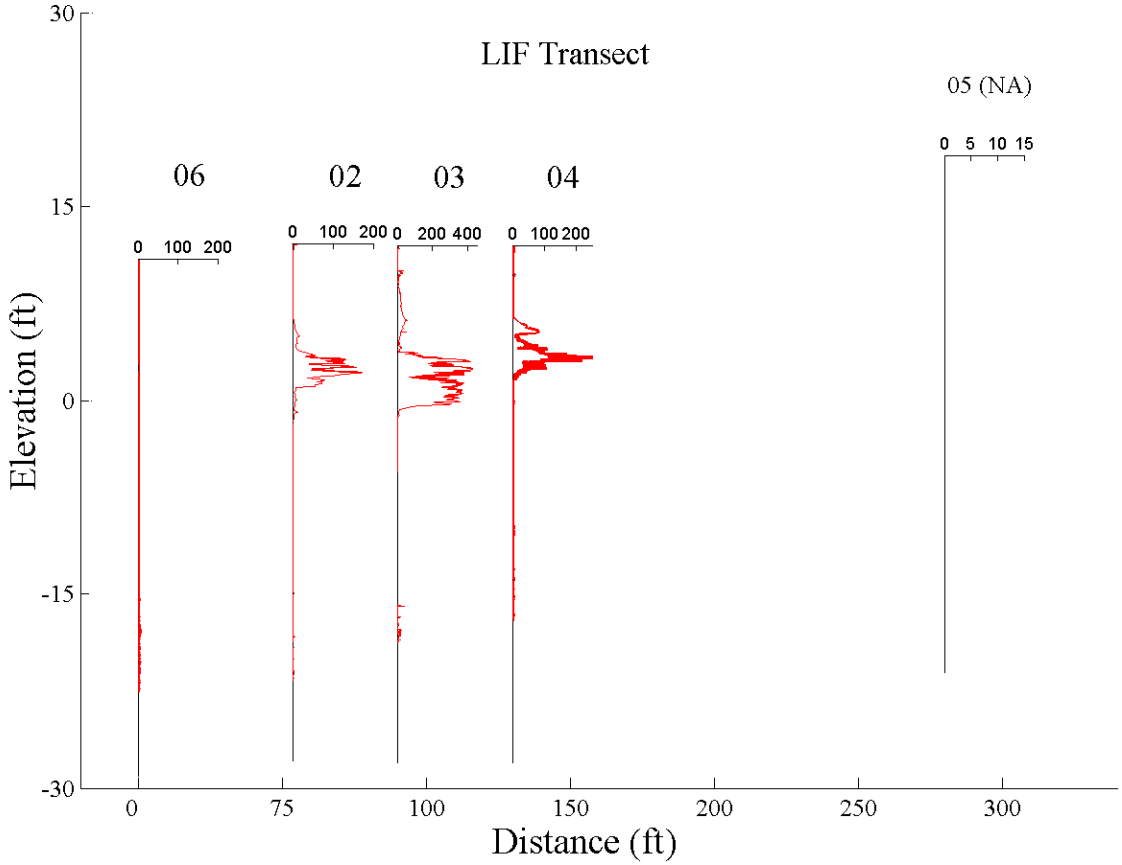

Figure 47. Transect of LIF response for transect at North Island

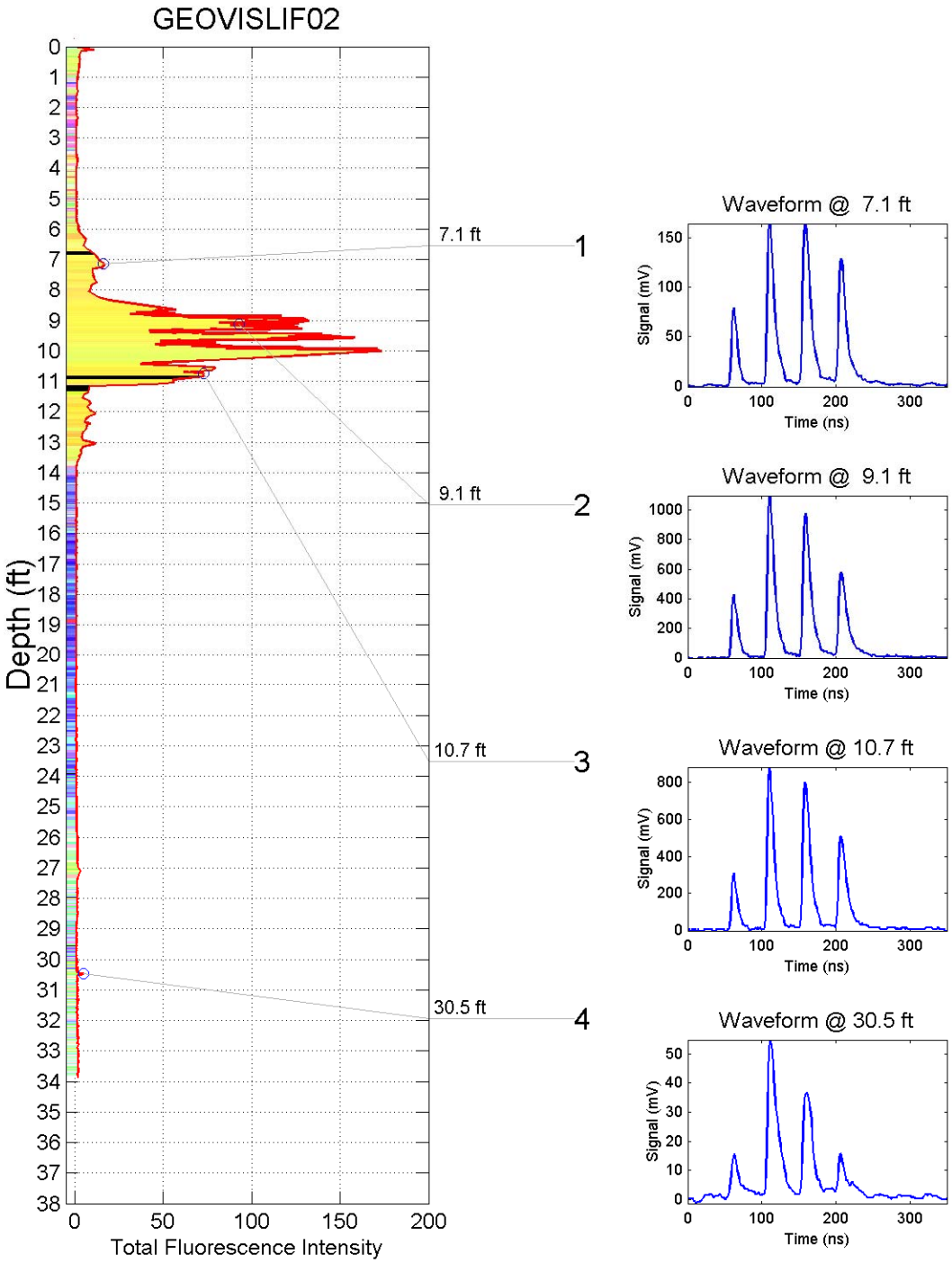

Figure 48. Colorized FVD from location #2

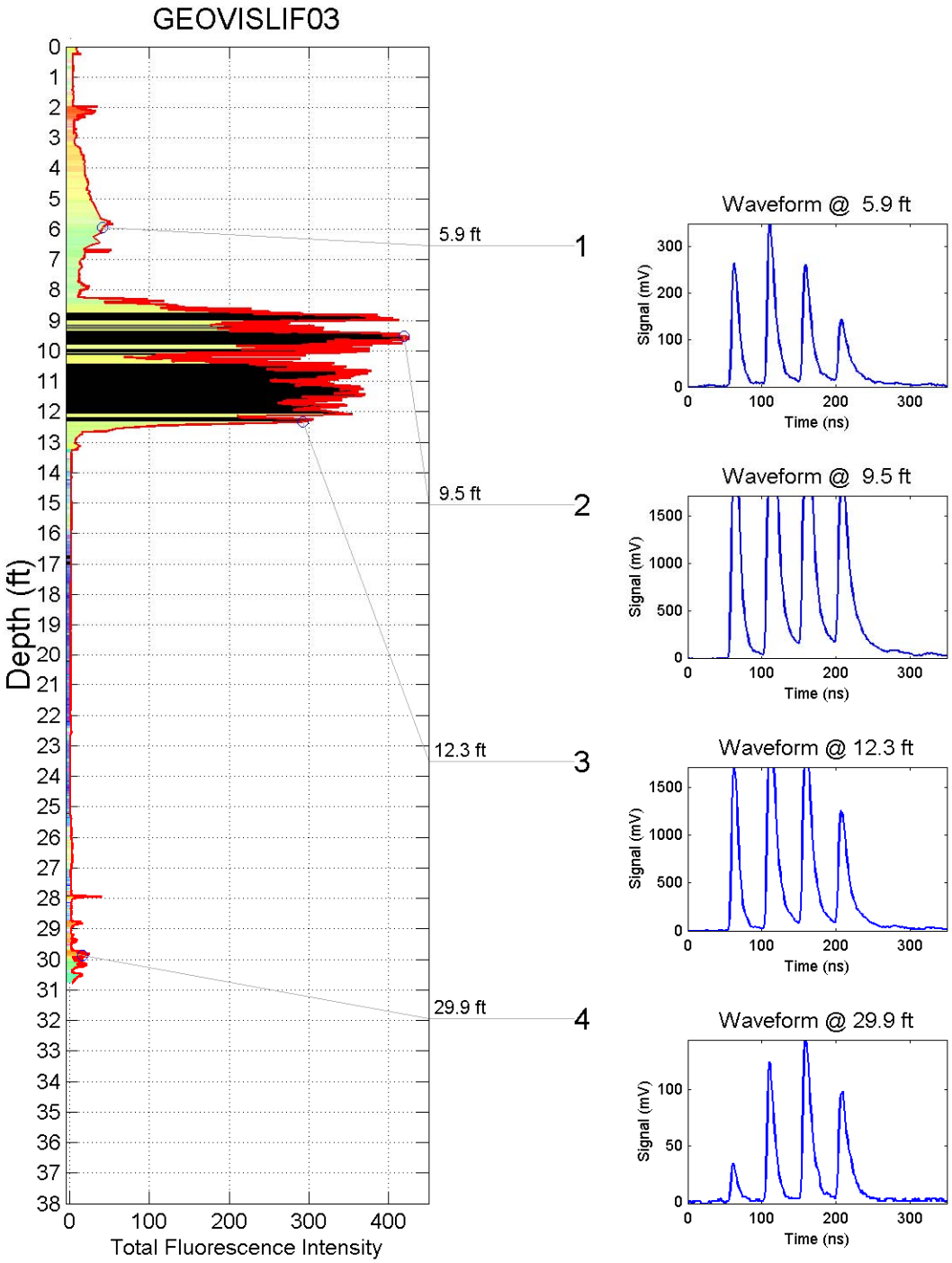

Figure 49. Colorized FVD from location #3

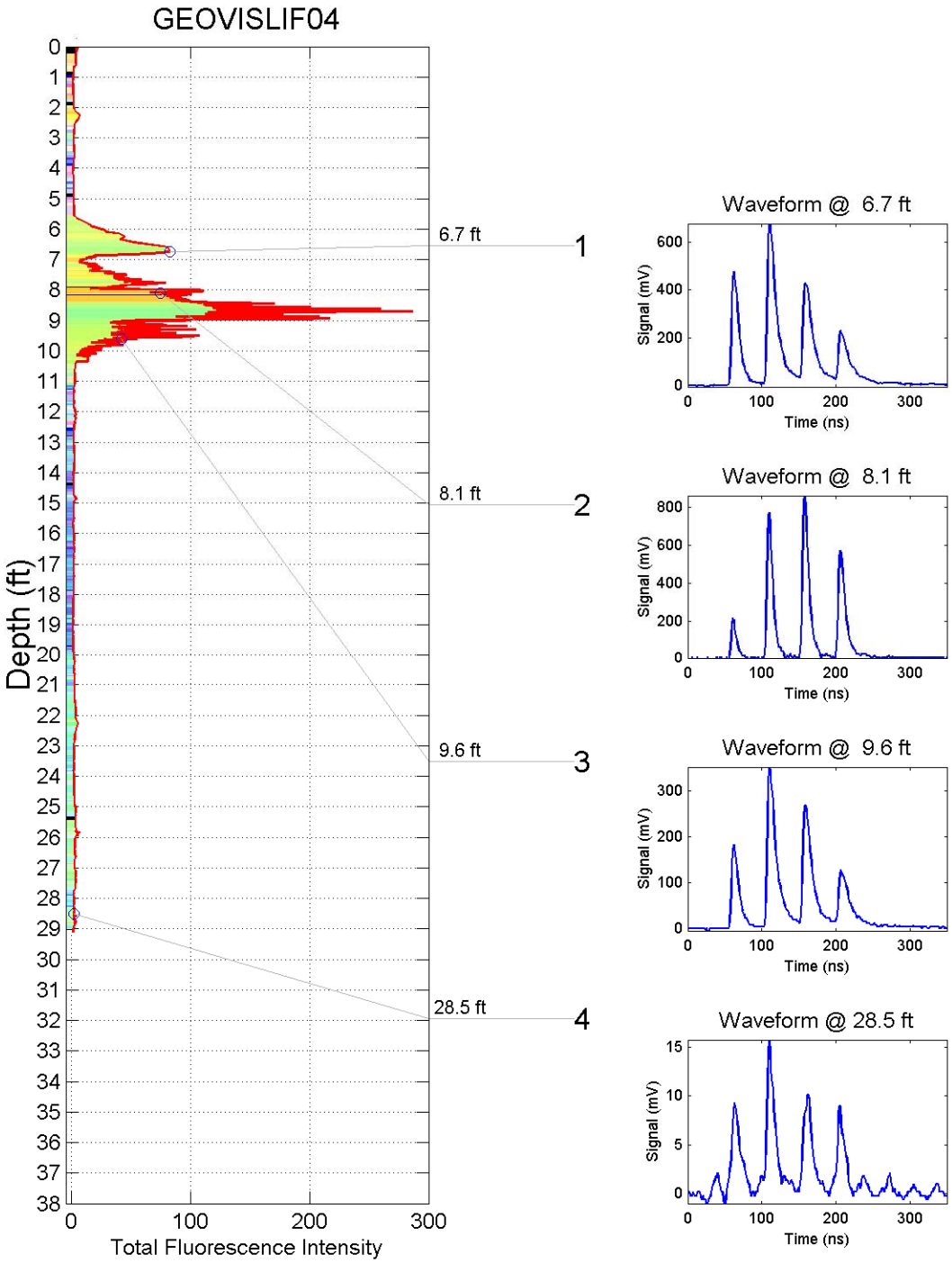

Figure 50. Colorized FVD from location #4

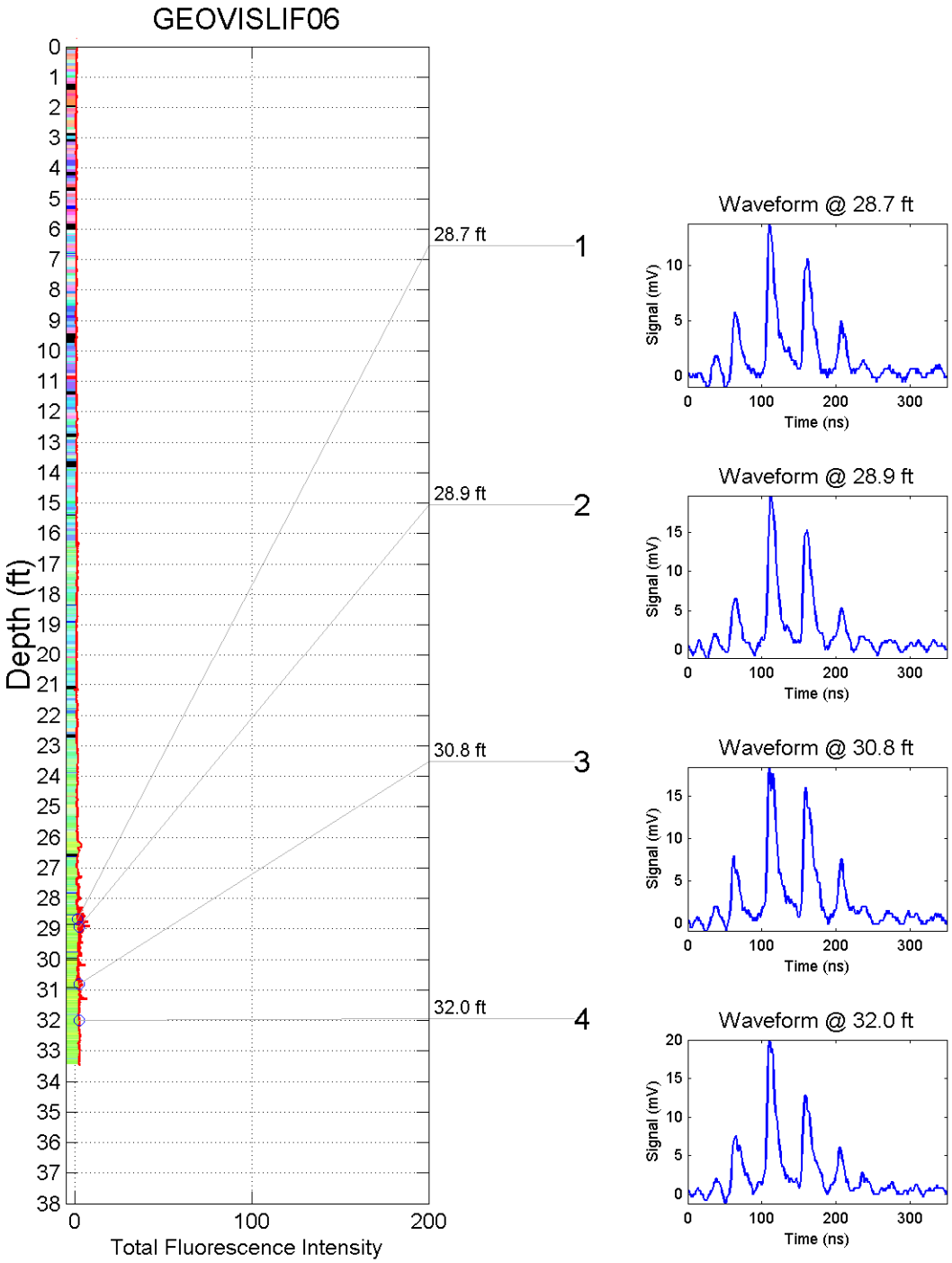

Figure 51. Colorized FVD from location #6

Figure 52 illustrates the LIF data change after depth-correction and interpolation of the raw data. Notice the fairly large jumps in depth and the window offset in the raw data. One can clearly

recognize where penetration velocities changed when the push crew changed from LIF screening mode to hyper-LIF/GeoVIS mode.

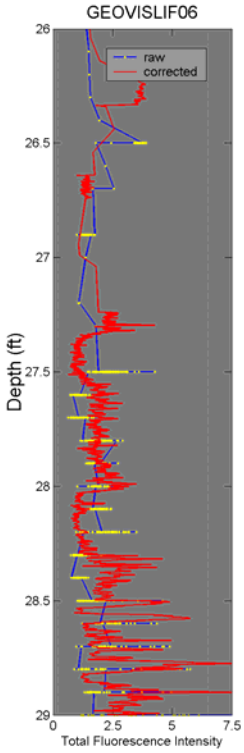

Figure 52. Depth correction example data from LIF log #6

Figure 53 illustrates the probe advancement velocity changes during push #2. The freedom to change speeds aids the search for DNAPL by allowing investigators to slow down when encountering suspect signals, then speed up and push the probe to the next "suspect" area. Real-time display of the LIF serves as a continuous indicator to prevent "missing" suspect zones. This ability to switch speeds enhances productivity substantially since GeoVIS requires relatively slow penetration rates as opposed to standard LIF speeds of 20 mm/sec. Figure 53 illustrates the adaptive velocity changes made during push and it's clear where the probe was slowed to examine suspect zones more closely.

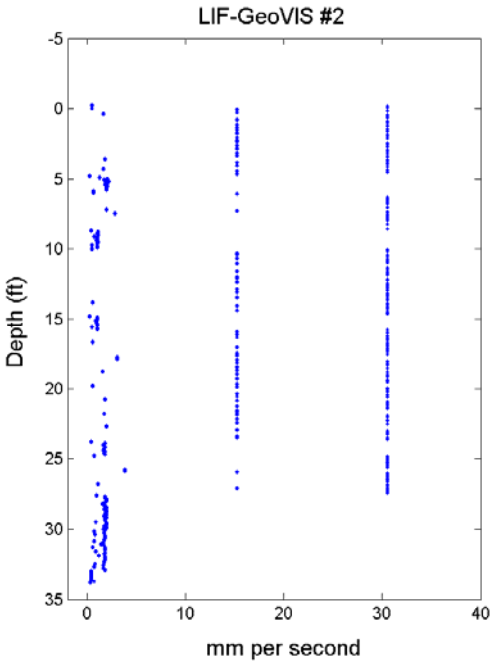

Figure 53. Velocity vs. depth for push location #2

Figure 54 shows the four logs side by side magnified to show the LIF's "spiky" behavior in the zone where DNAPLs were indicated with XSD. DNAPL globules are expected to behave in this spiky manner. A histogram of the differences between consecutive data points for GEOVISLIF06 is shown in Figure 55. The Gaussian distribution of the differences indicates well-behaved random error in the baseline values. The red line indicates the mean and blue lines indicating the 95% confidence intervals.

Figure 56 shows GEOVISLIF06 highlighted with blue circles where the LIF values exceeded the 95% confidence interval in Figure 56. This type of simple computer-driven analysis could be routinely performed to eliminate some of the guesswork and arbitrary nature of examining the LIF logs for indication of DNAPL. Intensity alone is not able to serve as an indicator. Notice that some of the log's baselines "wander" in general intensity due to background (soil/water) fluorescence changes, laser intensity, fiber optic bend radii losses, etc. making a set fluorescence limit a poor choice for making decisions on where to sample for suspected DNAPL.

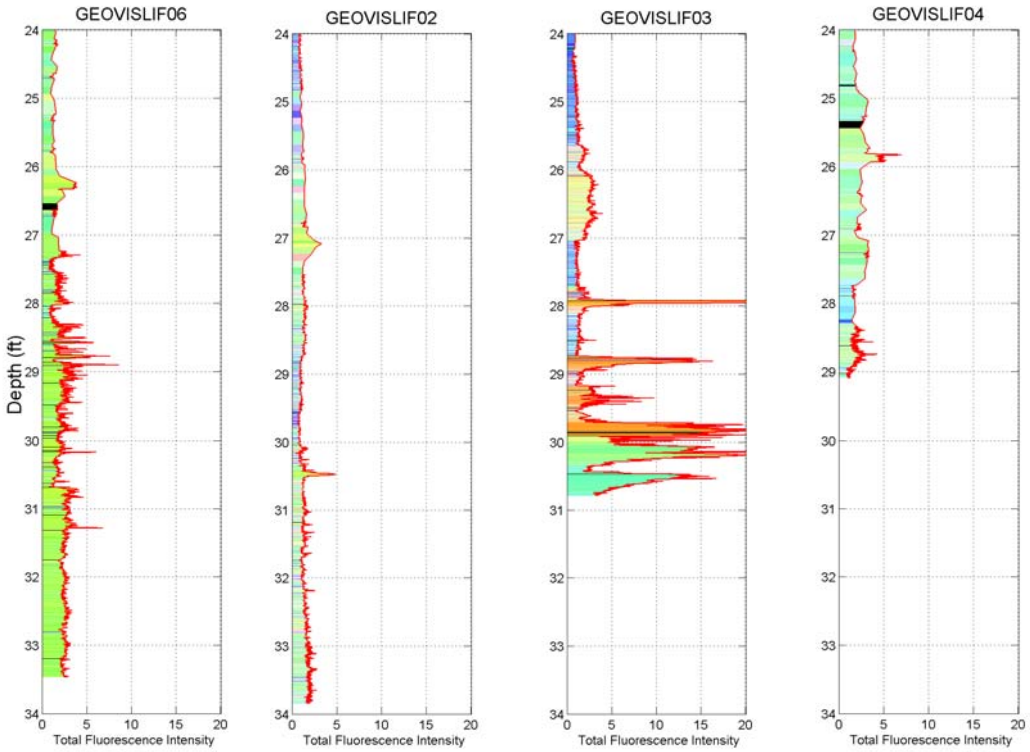

Figure 54. Four logs from transect with focus on XSD indicated suspect DANPL depth

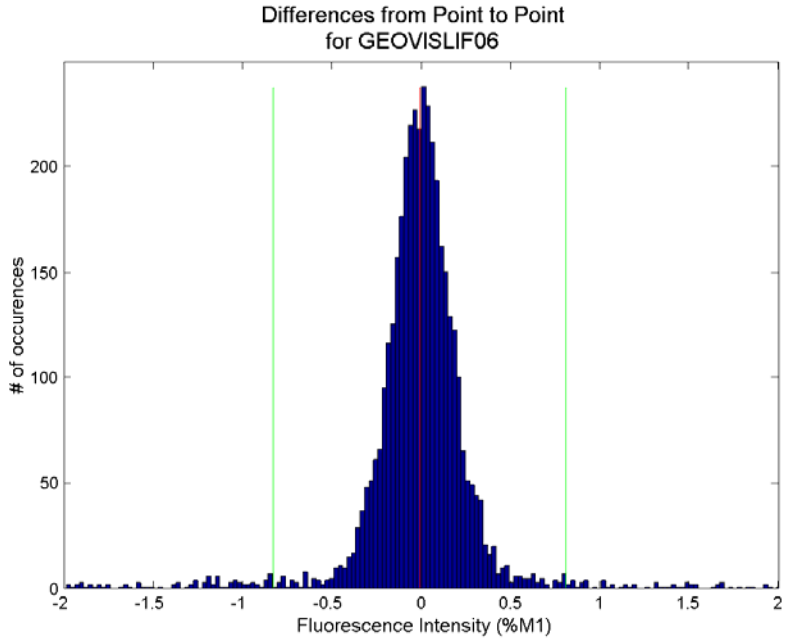

Figure 55. Histogram of differences between subsequent LIF data points for log GEOVISLIF06

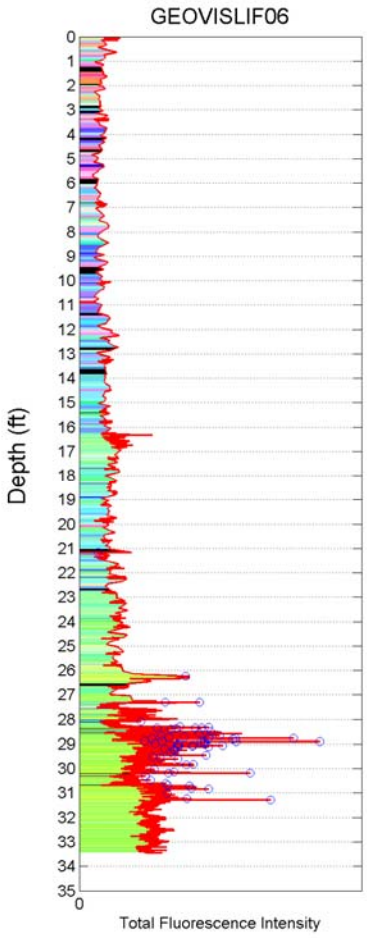

Figure 56. Colorized FVDs with highlighted rapid signal changes indicating possible DNAPL

4.3.1.3 Summary of NAS North Island Data

4.3.1.3.1 XSD

- XSD clearly showed several areas that were heavily impacted by halogenated compounds.
- XSD indicated heavy dissolved phase halogenated compounds in areas not determined in extensive previous studies (>34 ft in #6).
- XSD showed very high halogen concentrations in shallow regions along with several sharp features in deeper regions. XSD indicated saturated halogen conditions below 30 feet that was confirmed with water validation samples. Unable to confirm DNAPL existence in soil samples.
- Push #4 did not show strong signals that were expected based on other observations of LIF and confirmatory samples. It cannot be confirmed whether XSD was suffering from some sort of unidentified performance problem for this push.
- Calibration system worked well, some improvements needed.
- First MIP membrane was not badly punctured. Rather, water got into the return line, which effectively restricted the gas flow. The gas then was being pushed out of the MIP

membrane. Tests of this membrane in the lab after the demo confirmed that it was not torn or punctured.

- Water sample correlation with downhole measurements was poor but this was expected.
- Correlation between uphole XSD-MIP measurements of water samples and laboratory measurements was quite good.
- Two water samples, both from areas below heavily impacted area's did not show good agreement with either uphole or downhole measurements. Furthermore, both samples were from the same hole, which raised the concern about contamination being dragged down.
- Averaging XSD signal, especially when contaminate layers are thin, effectively dilutes the XSD signal levels. Averaging does not give a representative signal for the XSD when narrow bands are encountered.

4.3.1.3.2 LIF

- LIF confirmed existence of highly fluorescent LNAPL layer at 8 to 14 ft bgs which is consistent with previously attained site information.
- LIF log data showed "spiky" signals that caused us to suspect NAPL at 28 to 32 ft bgs for all locations except GEOVISLIF04, with the highest likelihood signals occurring at location GEOVISLIF03.
- Inability to conclusively confirm the existence of DNAPL globules via dye tests and visual examination left us unable to determine if "hyper" mode is paying off in the form of better DNAPL detection technique.

4.3.1.3.3 Combined XSD-LIF System

- Butterfly-style plots show similarities and contrasts between the data. Several questions that remain unanswered after examining them include:
    - Why didn't the XSD experience full-scale response when LIF indicated copious amounts of LNAPL at 8-12 range?

A relatively consistent "offset" seem to exist between LIF and XSD (XSD seemed to be showing response 0.25 to 0.75 ft deeper than LIF.

4.3.2 Camp Lejeune

4.3.2.1 XSD Data

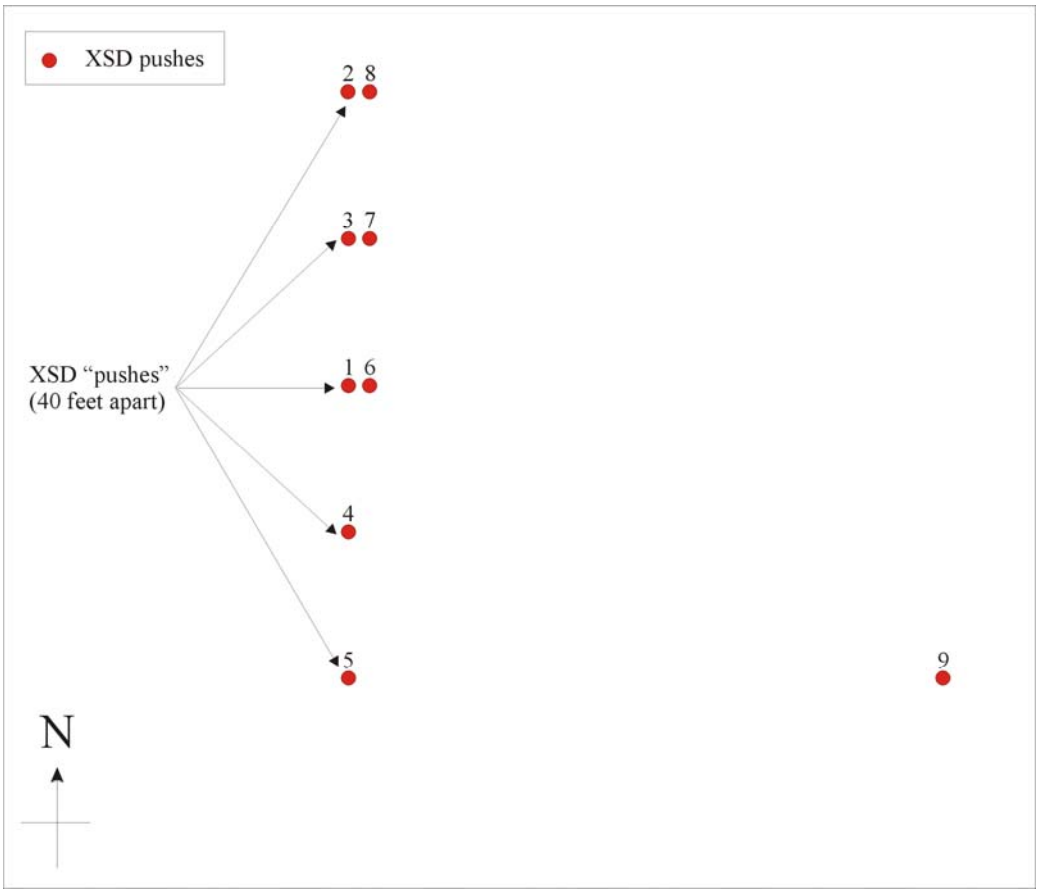

Figure 57. . Map of XSD push locations at Camp Lejeune, North Carolina.

Numerous areas of contamination were noted in Push 1(Figure 58). The largest continuous area ranged from ten to eighteen feet. Lower levels of contamination were noted from four to eight feet. The push was terminated at 18.15 feet.

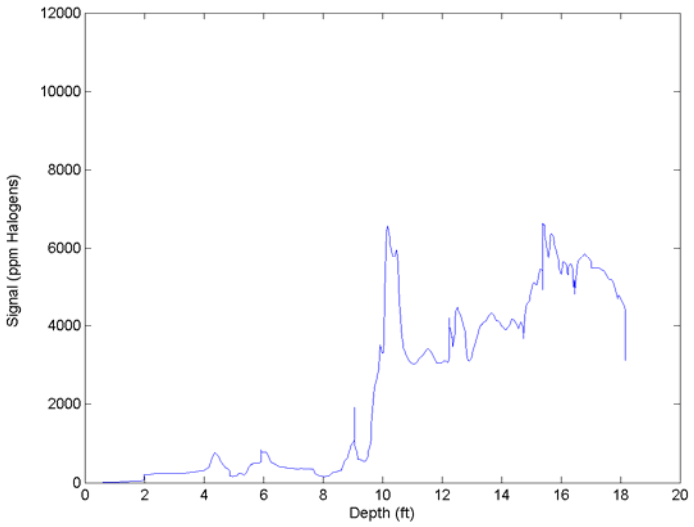

Figure 58. XSD Push 1 profile

A single area of contamination was noted during Push 2 (Figure 59) from 1.8 to 3 feet. The push was terminated at 18.37 feet.

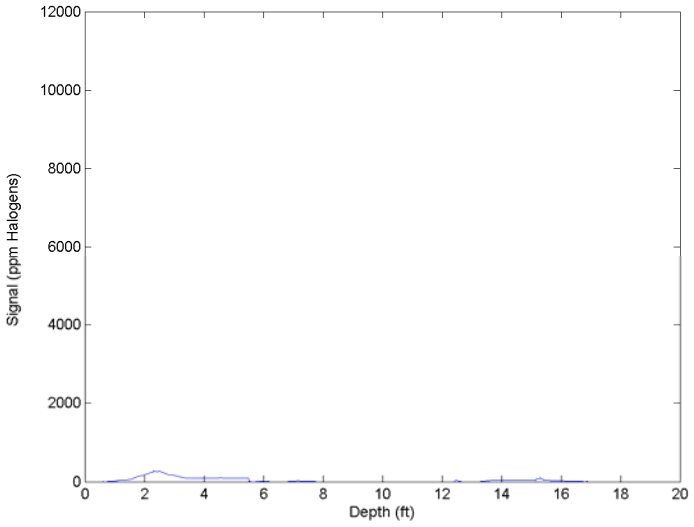

Figure 59. XSD Push 2 profile

Some areas of contamination were noted in Push 3 (Figure 60). The largest continuous area ranged from nine to seventeen feet. A smaller area of low-level contamination was noted from six to eight feet. The push was terminated at 17.62 feet.

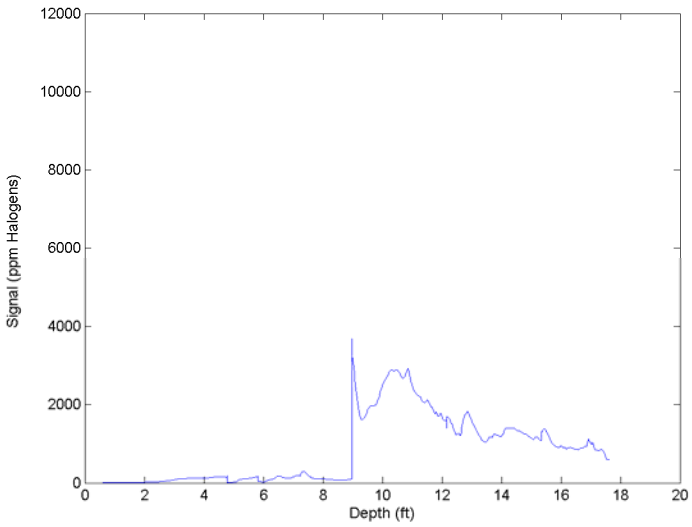

Figure 60. XSD Push 3 profile

Contamination was noted throughout the depth range in Push 4 (Figure 61). The push was terminated at 18.22 feet.

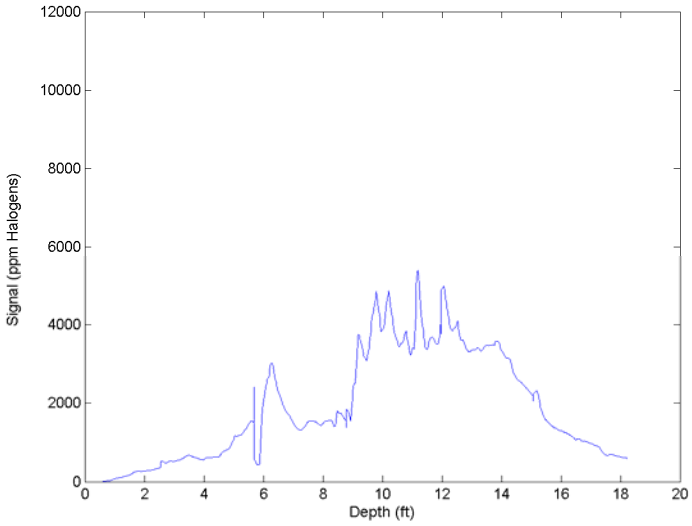

Figure 61. XSD Push 4 profile

Two moderate areas of contamination were noted during Push 5 (Figure 62). The two contamination areas were from six to ten feet and from ten to fifteen feet. The push was terminated at 15.91 feet.

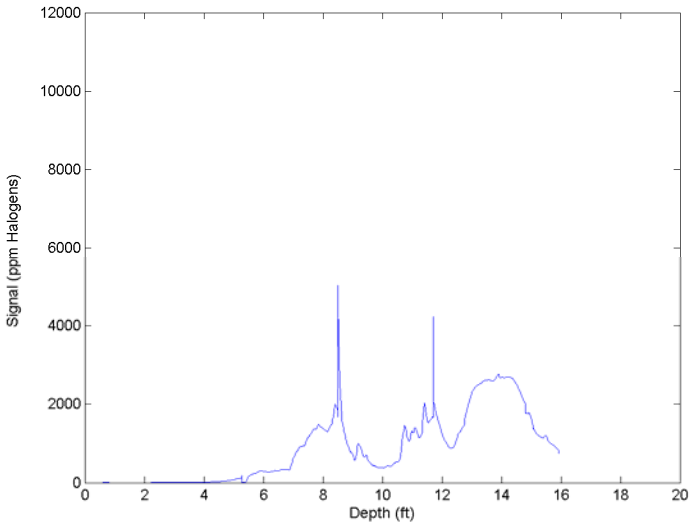

Figure 62. XSD Push 5 profile

Replicate push of Push 1 location. Several areas of contamination were noted in Push 6 (Figure 63). Contamination regions were noted from 1 to 8 feet, 8.5 to 12 feet and from 12 to 17.65 feet. The concentration levels indicated by the XSD-MIP system at the depth range from twelve to sixteen feet are near the saturation level for 1,1,2,2-tetrachloroehtane, indicating the possible presence of DNAPL. The push was terminated at 17.65 feet.

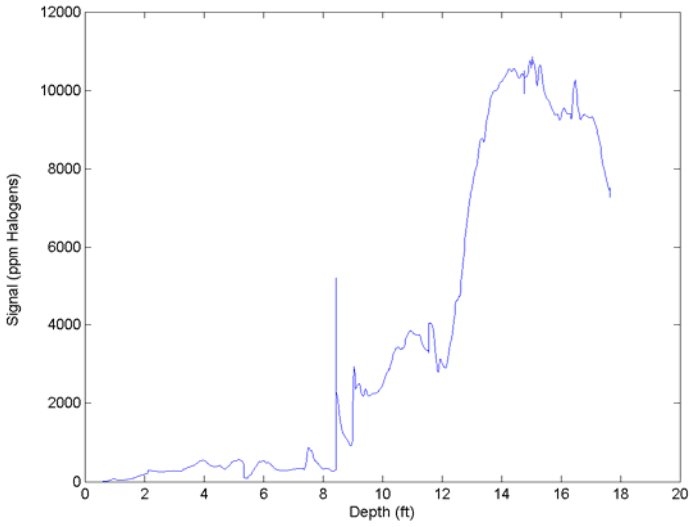

Figure 63. XSD Push 6 profile

Replicate push of Push 3 location. Some areas of contamination were noted in Push 7 (Figure 64). The largest continuous area ranged from nine to seventeen feet. A smaller area of low-level contamination was noted from six to eight feet. The push was terminated at 17.39 feet.

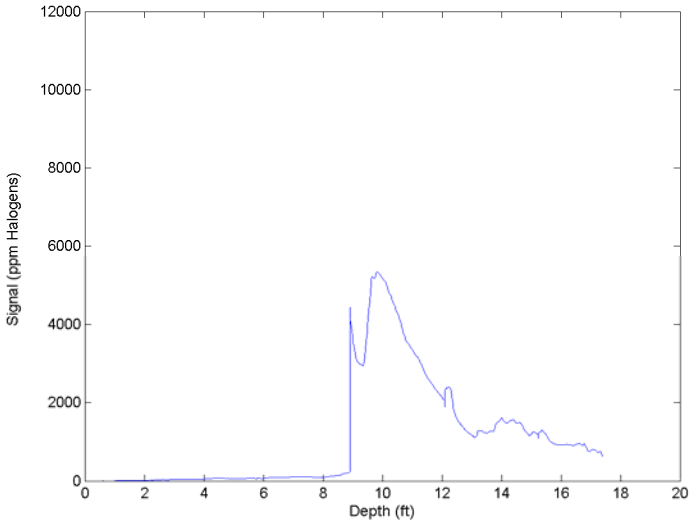

Figure 64. XSD Push 7 profile

Replicate push of Push 2 location. A single area of contamination was noted during Push 8 (Figure 65) from 1.8 to 3 feet. The push was terminated at 17.84 feet.

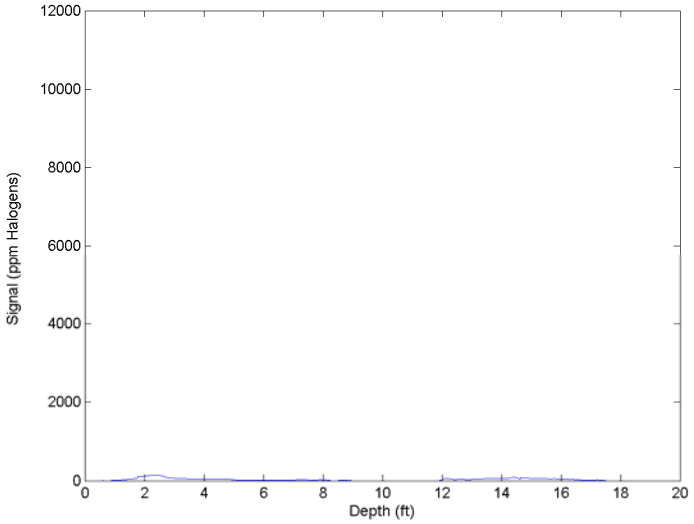

Figure 65. XSD Push 8 profile

Several areas of contamination were noted in Push 9 (Figure 66). Contamination regions were noted from 3.5 to 6 feet, 7.5 to 10 feet and from 12 to 15.33 feet. The concentration levels indicated by the XSD-MIP system at the depth range from thirteen to fourteen feet are near the saturation level for 1,1,2,2-tetrachloroehtane, indicating the possible presence of DNAPL. The push was terminated at 15.33 feet.

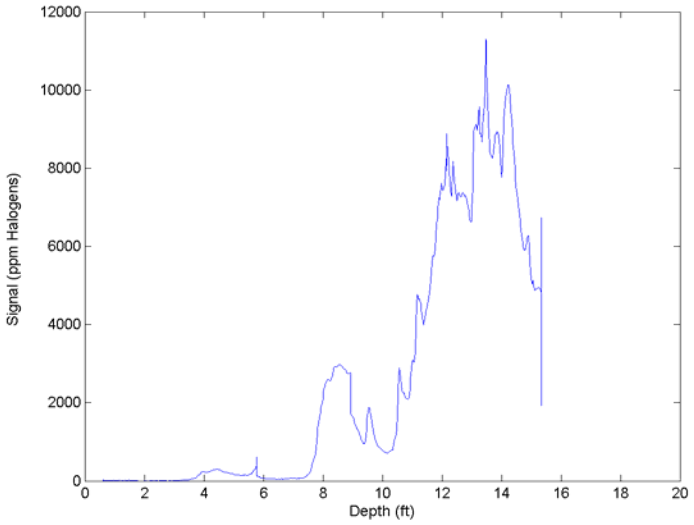

Figure 66. XSD Push 9 profile

Figure 67 shows the transect of the XSD pushes and results of the water sample data (blue "tees"). The amplitude of the "tee" indicates the total halogen concentration. The width of the "tee" denotes the depth interval over which the water samples were collected. Figure 68 shows the comparison of Push 9 with the water sample results.

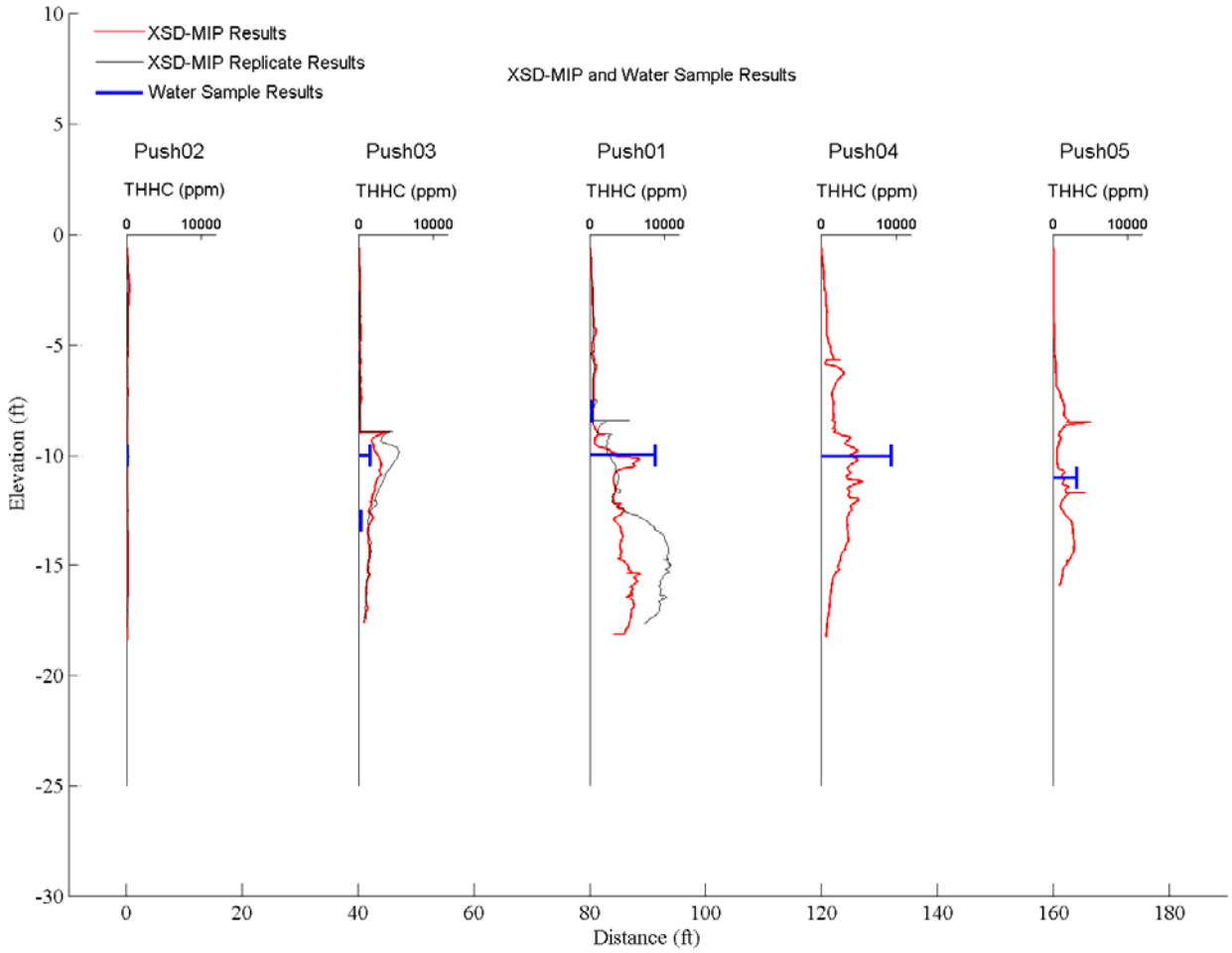

Figure 67. Transect of all XSD pushes and water samples at Camp Lejeune site 89

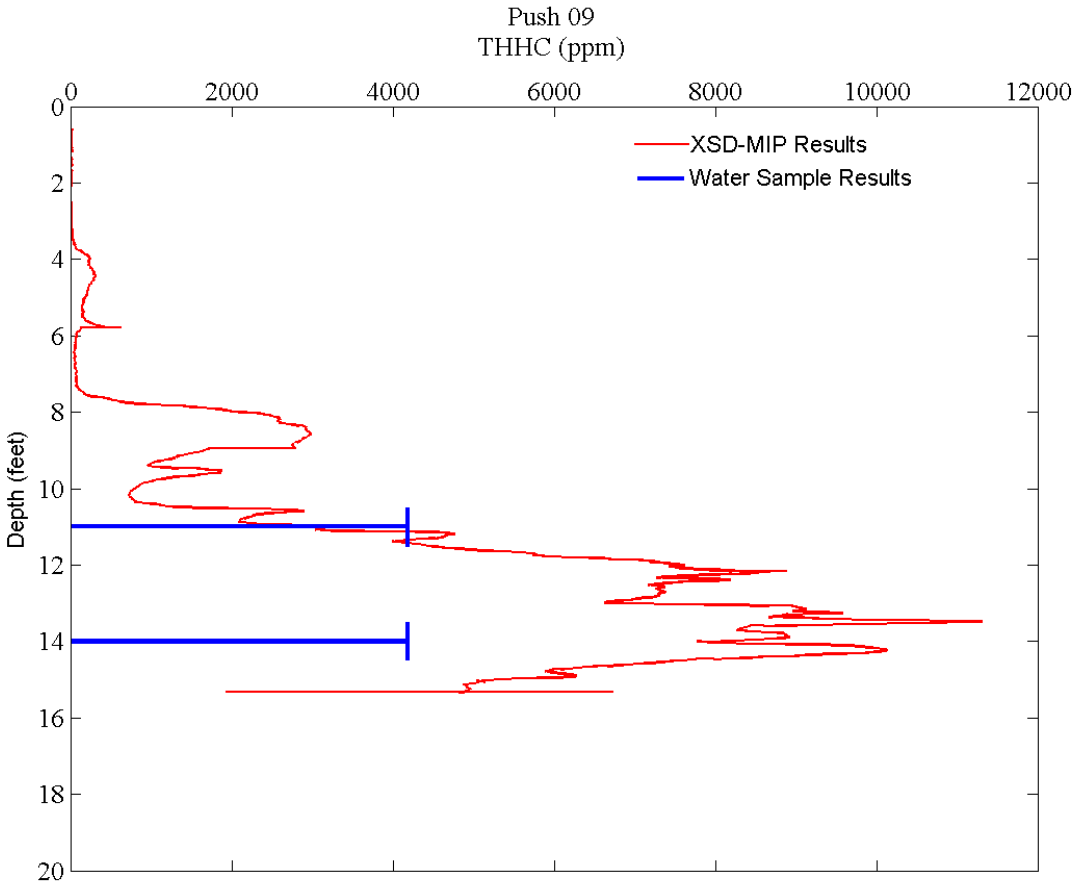

Figure 68. XSD Push 9 with water sample results at Camp Lejeune Site 89

4.3.2.1.1 Comparison of In-situ Measurements with Laboratory Water Samples

A comparison of the in-situ XSD measurements with the water samples was undertaken to identify any correlation. Since the water sample data was collected over discrete depth intervals and our data was collected continuously, the method to correlate our data was to average the XSD signal over the depth range of the water samples (Table 10). The push locations, depth regions, halogenated concentration, and averaged XSD signals are shown in Figure 69.

Table 10. Camp Lejeune water sample and XSD results at selected depths

XSD Push number	Depth (feet)	Total halogen concentration (ppm Halogens)	Average XSD signal (ppm Halogens)
01	7.5-8.5	334.3	232.45
01	9.5-10.5	8779	3978.83
02	9.5-10.5	17.71	-66.58
03	9.5-10.5	1493.58	2433.15
03	12.5-13.5	331.3	1385.67
04	9.5-10.5	9368.6	4189.71
05	10.5-11.5	3124.58	1255.35
09	10.5-11.5	4193.4	3215.12
09	13.5-14.5	4191	8894.56
06 (replicate of 01)	7.5-8.5	334.3	464.58
06 (replicate of 01)	9.5-10.5	8779	2645.91
08 (replicate of 02)	9.5-10.5	17.71	-14.03
07 (replicate of 03)	9.5-10.5	1493.58	4900.49

To compare the XSD-MIP signal with the water sample data, the total halogen concentration for each water sample was determined (see section 4.3.2.1 for details). In all cases during this demonstration the major contributor to the total halogenated concentration was 1,1,2,2-Tetrachloroethane. Figure 69 shows a scatter plot of the XSD signals vs. total halogenated concentration.

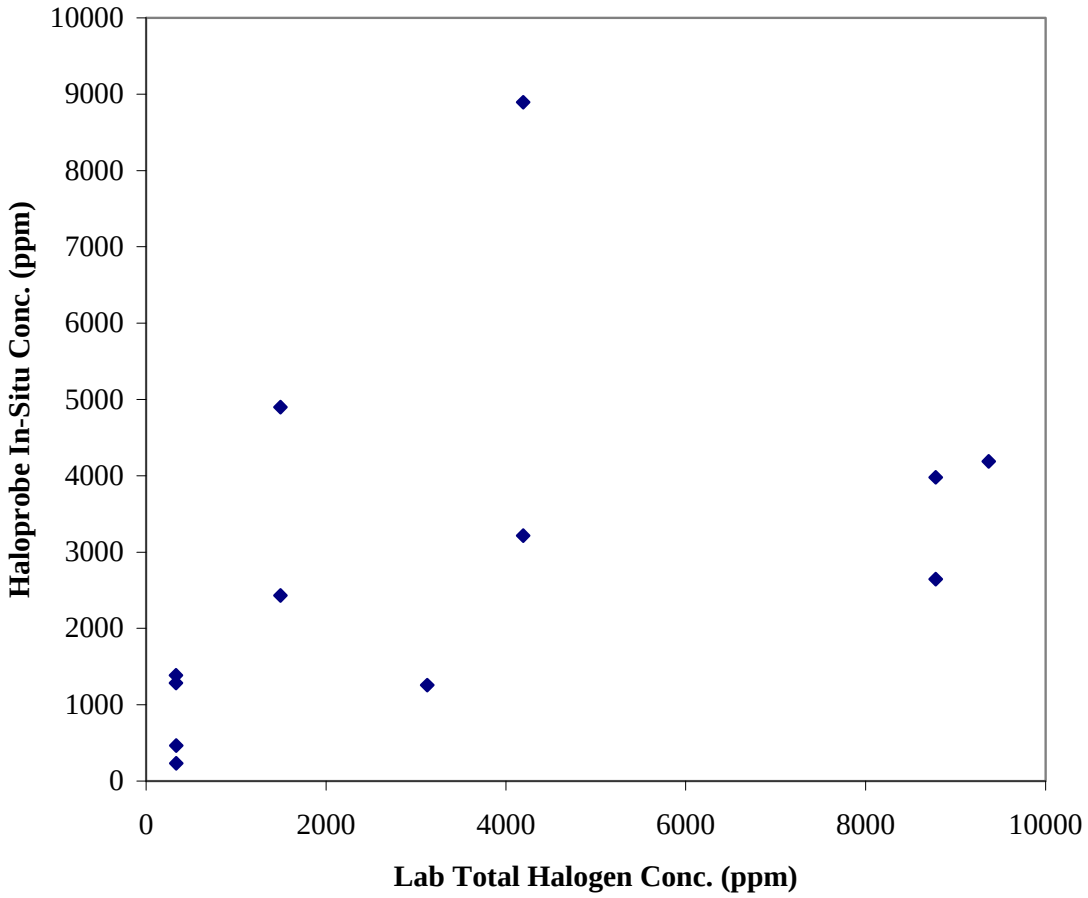

Figure 69. Total halogenated concentration vs. XSD signal

The correlation between the water sample data and the XSD signal levels is quite good. There are only two points that deviate substantially from the rest of the data points. A dye test of a soil sample taken at one of these points, corresponding to Push 9 at thirteen feet, indicated the presence of DNAPL. It is unclear why the water sample analysis did not show as strong of signals as the soil sample indicated. To validate that the XSD-MIP system reacts linearly to increasing halogen concentration, splits of the water samples taken at the Camp Lejeune site were analyzed with the XSD-MIP system in a mobile laboratory immediately after samples were acquired with the CPT rig. The procedure and results are discussed in the next sections.

4.3.2.1.2 Laboratory Analysis of Water Samples with XSD-MIP System

To evaluate whether the XSD-MIP system reacted linearly to the water samples collected at the site, splits were run on the XSD-MIP system in a field laboratory after the completion of the XSD-MIP in situ measurements. The sample introduction method discussed in the methods section of this report was used for all measurements.

4.3.2.1.2.1 Water Sample Analysis

Prior to the introduction of each water sample a single point calibration was done using multiple aliquots of the SRC solution. The results of each calibration were used to normalize the corresponding water sample data and to convert the XSD-MIP system's raw data to a halogen concentration.

Immediately following the calibration solution aliquots, the water samples were placed on the membrane. Again multiple sample aliquots were done to find an average value for the water samples.

Figure 70 shows the comparison of the laboratory water sample data with the XSD-MIP values for each sample location.

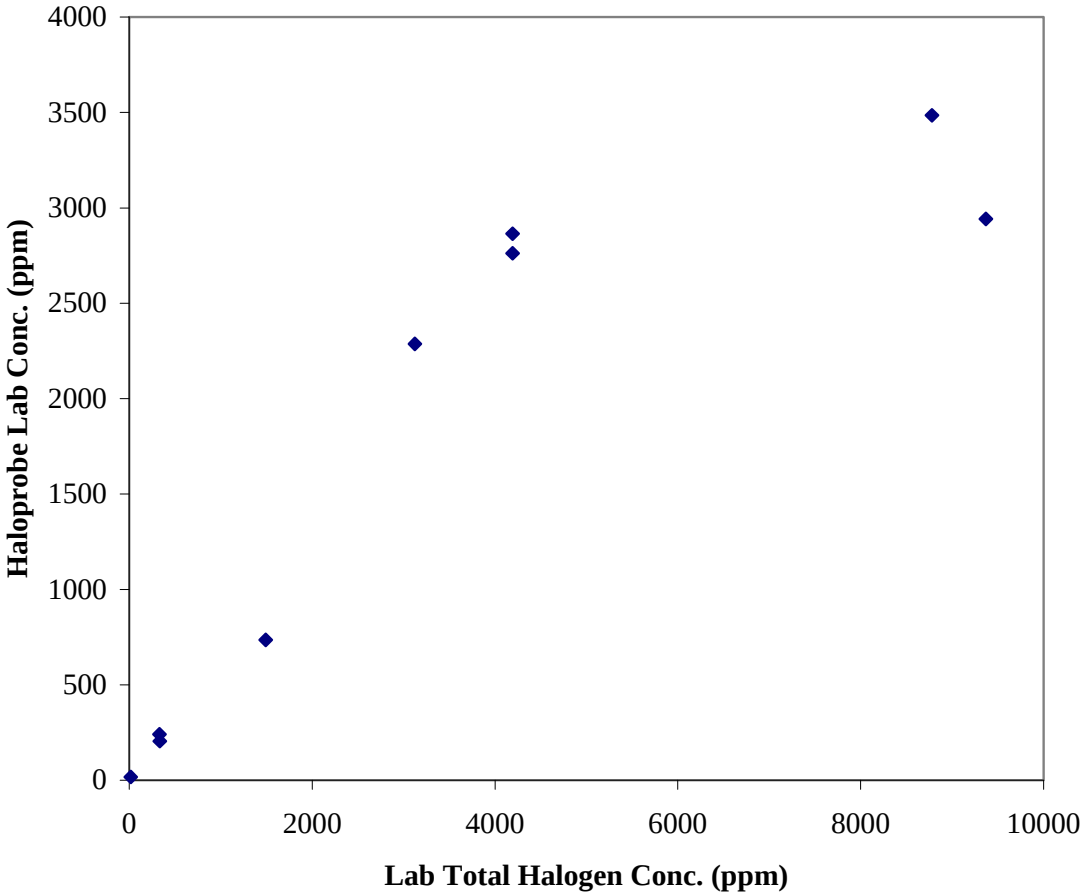

Figure 70. Comparison of laboratory water sample concentrations with XSD-MIP signals on water sample splits

There is good correlation between the laboratory water sample analysis and the XSD-MIP analysis. This data demonstrates that the XSD-MIP system is responding appropriately to chlorinated hydrocarbon contaminated water retrieved from the sub-surface. The system

responds faithfully to the true contamination content of the water and the only un-controlled aspect of the system remains the unavoidable variables inherent in the MIP mass transport of VOCs from the formation to the detector.

4.3.2.1.2.2 Comparison of In situ Measurements with Laboratory Soil Samples

A comparison of the in situ XSD measurements with the soil samples was also undertaken to identify any correlation. Since the soil sample data was collected over discrete depth intervals and our data was collected continuously, the method to correlate our data was to average the XSD signal over the depth range of the water samples. The push locations, depth regions, halogenated concentration, averaged XSD signals, and dye test results are shown in Table 11.

Table 11. Camp Lejeune soil sample and XSD results at selected depths

XSD Push number	Depth (feet)	Total halogen concentration (ppm Halogens)	Average XSD signal (ppm Halogens)	Dye Test
01	3.5-4.5	33.64	419.21	Negative
01	9.8-10.8	1888.68	4674.09	Negative
01	12.3-13.3	194480	3796.07	**Positive**
01	15.5-16.5	3840.7	5570.69	Negative
01	16.5-17.5	46.75	5561.26	Negative
02	9.6-10.6	0	-66.06	Negative
02	15.5-16.5	10.51	22.75	Negative
03	8-9	175.9	83.96	Negative
03	9-10	88.2	2055.40	Negative
03	13.5-14.5	45.44	1280.09	Negative
04	5.7-6.7	215.1	1924.36	Negative
04	9.5-10.5	661.6	4204.61	Negative
04	13.5-14.5	596	3297.79	Negative
05	3.5-4.5	2.61	13.23	Negative
05	7.5-8.5	168.86	1450.71	Negative
05	10.5-11.5	4186	1255.35	Negative
05	13.5-14.5	776.6	2654.62	Negative
09	10.5-11.5	1314.4	3215.12	Negative
09	12.5-13.5	3941	8174.65	**Positive**

To compare the XSD-MIP signal with the soil sample data, the total halogen concentration for each water sample was determined (see Methods for details). In all cases during this demonstration the major contributor to the total halogenated concentration was 1,1,2,2-Tetrachloroethane. Figure 71 shows a scatter plot of the XSD signals vs. total halogenated concentration.

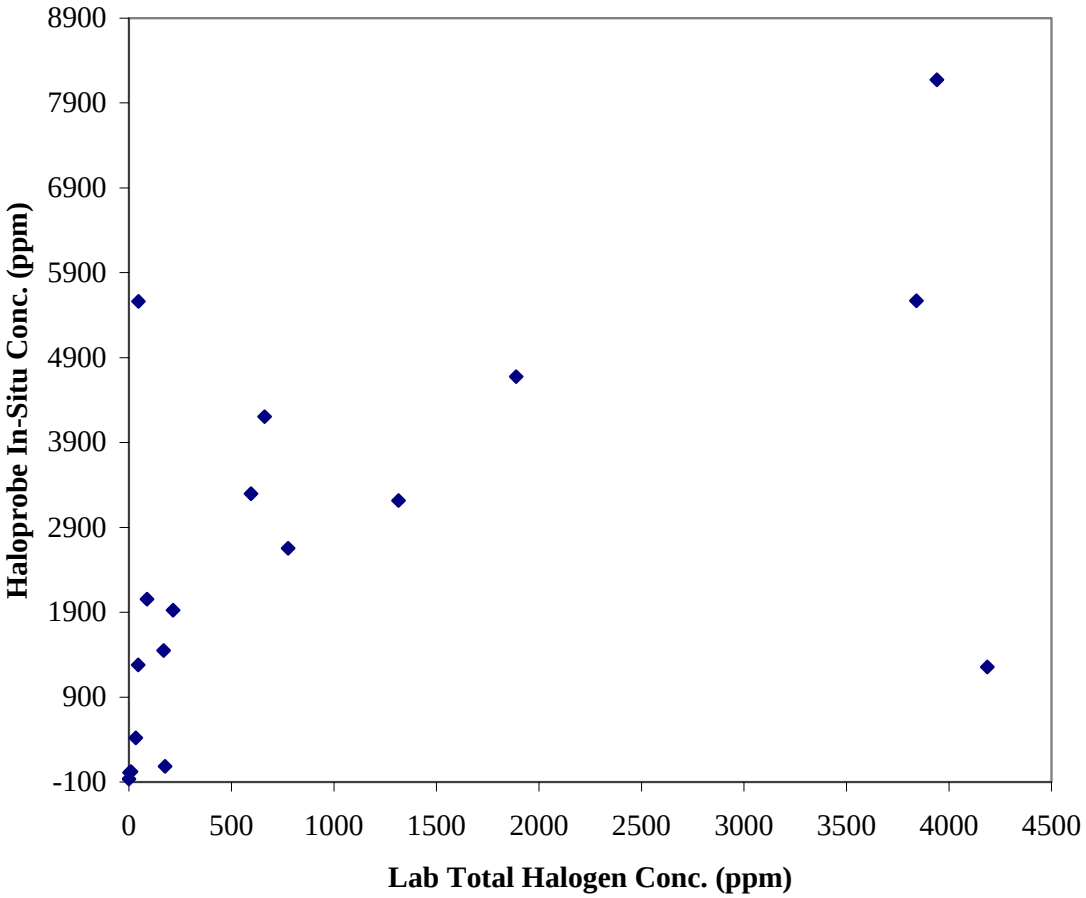

Figure 71. Total halogenated concentration vs. XSD signal

The correlation between the soil sample data and the XSD signal levels is quite good for field conditions. One of the depth locations corresponding to a positive dye test (Push 01, 12.5 feet) was left out of the plot because of the high concentration that was found at this point. There are only two points that deviate substantially from the rest of the data points. At one of these points (Push 01, 17 feet) the XSD indicated strong signals while the soil sample showed little contaminant present. However, the second deviated point (Push 05, 11 feet) showed high contaminant levels in the soil sample while the XSD showed little contaminant present. Dye tests were performed on all soil samples with only two positive results. The XSD indicated that both of these areas were heavily contaminated with chlorinated solvents. Figure 72 shows the transect of the XSD pushes and results of the soil sample data (blue "tees"). The amplitude of the "tee" indicates the total halogen concentration. The width of the "tee" denotes the depth interval over which the soil samples were collected. Figure 73 shows the comparison of Push 9 with the soil sample results. Also in both figures, the depths where positive dye tests were noted are shown with green asterisks.

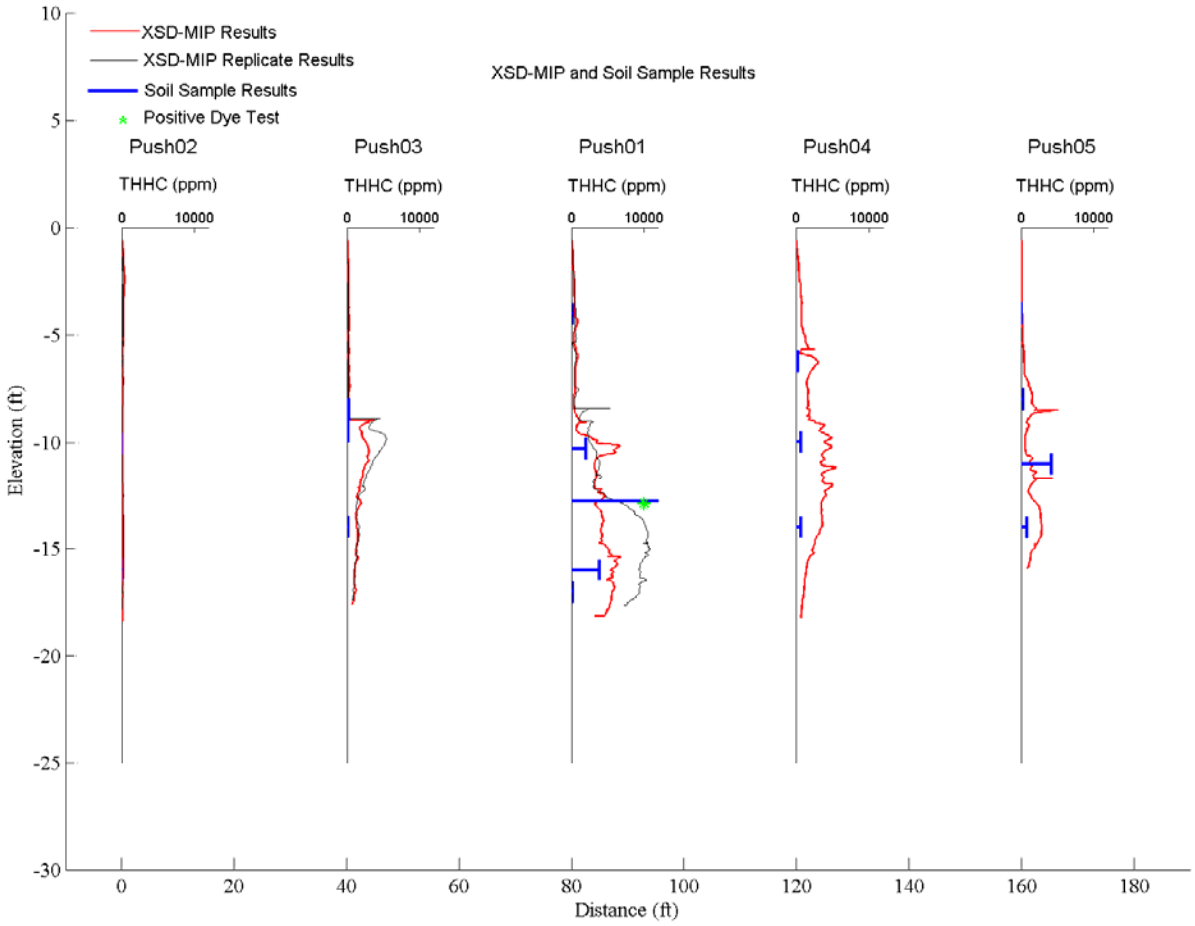

Figure 72. Transect of all XSD pushes and soil samples at Camp Lejeune site 89

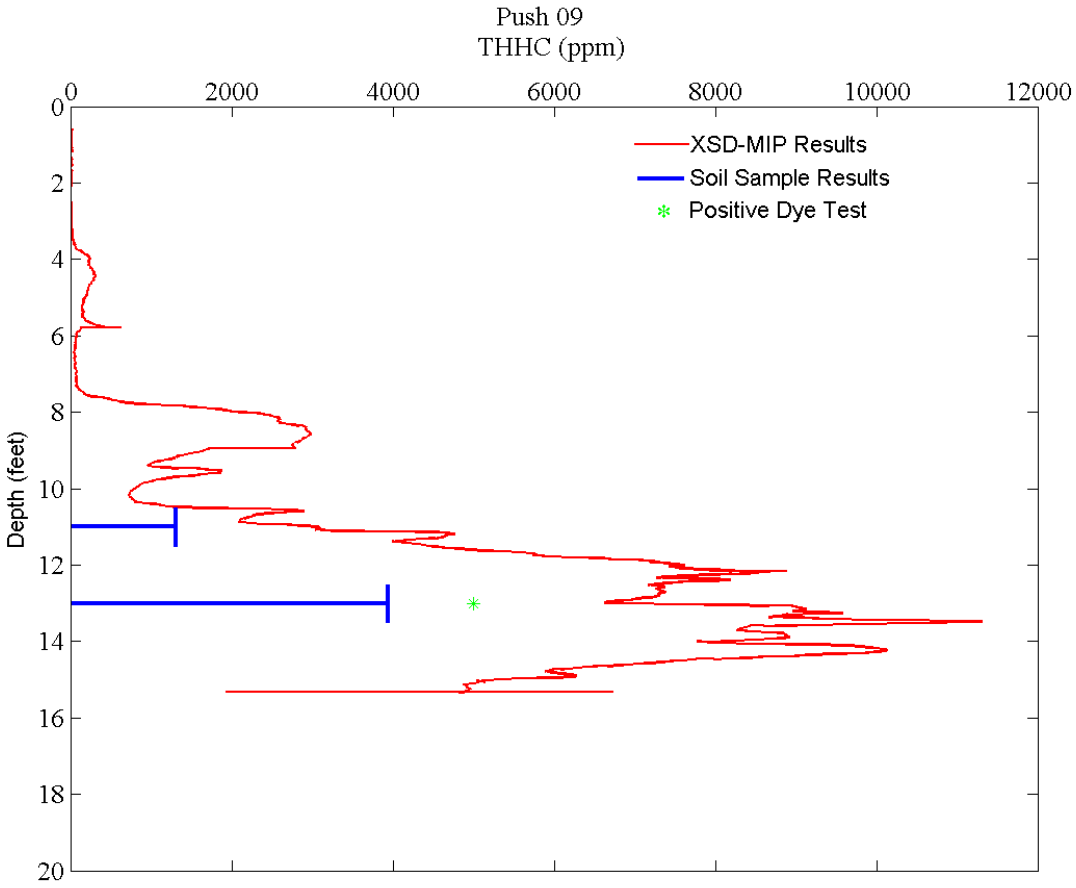

Figure 73. XSD Push 9 with soil sample results at Camp Lejeune Site 89.

4.3.2.1.3 Comparison of Laboratory Soil and Water Sample Analysis

The final analysis conducted was to compare the results of the laboratory water samples with the laboratory soil samples. Since we were comparing the XSD-MIP results to both, it was important to determine whether these two sampling methods correlated to one another. Figure 74 shows the correlation between the water sample data and the soil sample data. It can be seen that the correlation between the water samples and the soil samples is not as good as one would expect. This causes us concern since we must choose one of these methods to validate our data against.

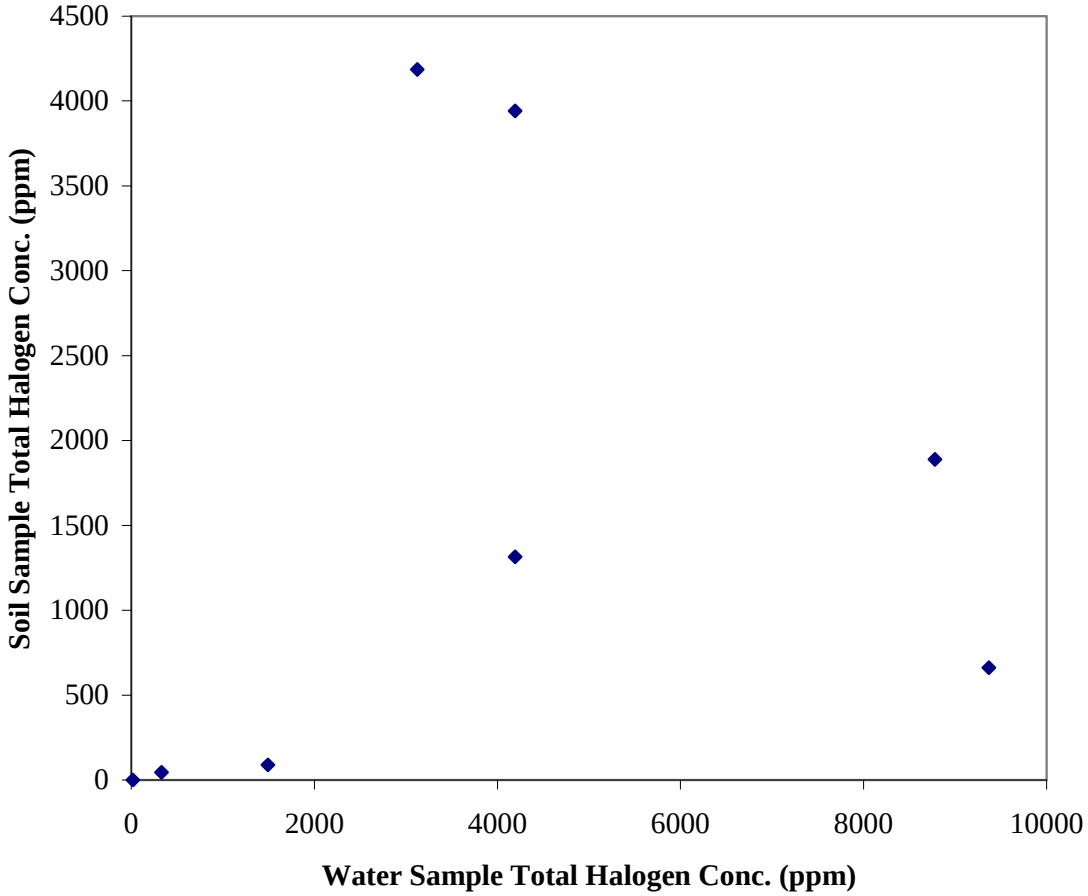

Figure 74. Water Sample vs. Soil Sample comparison.

4.3.2.2 Laser Induced Fluorescence

As discussed earlier, the depth information for ROST was provided via a RS-232 data-tap of the depth feed to the GeoVIS recording system. The data stream being sent is accurate for the GeoVIS video window, which is located 3.125" below the LIF window. This required that the LIF data be depth adjusted to 3.125" less than originally recorded. The resolution of the depth data stream was upgraded since the North Island demo to send depth to the nearest 0.01 foot. This was nearly adequate to properly encode the LIF data since the data density was on the order of 0.003 ft (during the slower GeoVIS/high resolution push mode). Constant velocity was assumed between all the depths recorded and a linear interpolation of depth was done for the ROST data stream where duplicate depths were recorded. The LIF depth data was then converted to the nearest 0.001 ft.

LIF logs printed in the field immediately following each test. The logs showed a variety of elevated signal fluorescence levels in narrow zones. Validation sampling zones were selected by examining the XSD and LIF logs side-by-side in an effort to maximize the chance of sampling in areas of DNAPL presence. Sampling areas were chosen in an attempt to establish DNAPL presence where XSD and/or LIF indicated its possible existence. Several additional sampling

locations were chosen in low-level signal zones as well in order to validate that the XSD was not recording false positives.

Several signals that occurred in the LIF logs indicated the possibility of NAPL impacted soils. Figure 75 contains the original field log printed just after location 01 was completed. Figure 76 shows this same log with both multi-wavelength waveforms and GeoVIS frame grabs taken from key areas. The waveforms are color-coded to match the colored cursors framing the depths on the FVD. This portrayal allows us to gain insight into any possible correlation between physical appearance of the soil matrix and the LIF waveforms.

The elevated signal at 4 feet in CLLIFGV01 appears to be associated with a foamy region of soil detected with the GeoVIS. The shallow depth at which this material was located and the relatively low signal observed with the XSD precluded us from taking any validation samples in this region. The elevated signal at 8 feet was minor, but the waveform shape (fluorescence distribution) is similar to that seen in the foamy region at 4 feet. Again, the lack of XSD signal indicated there was no need to co-sample this feature.

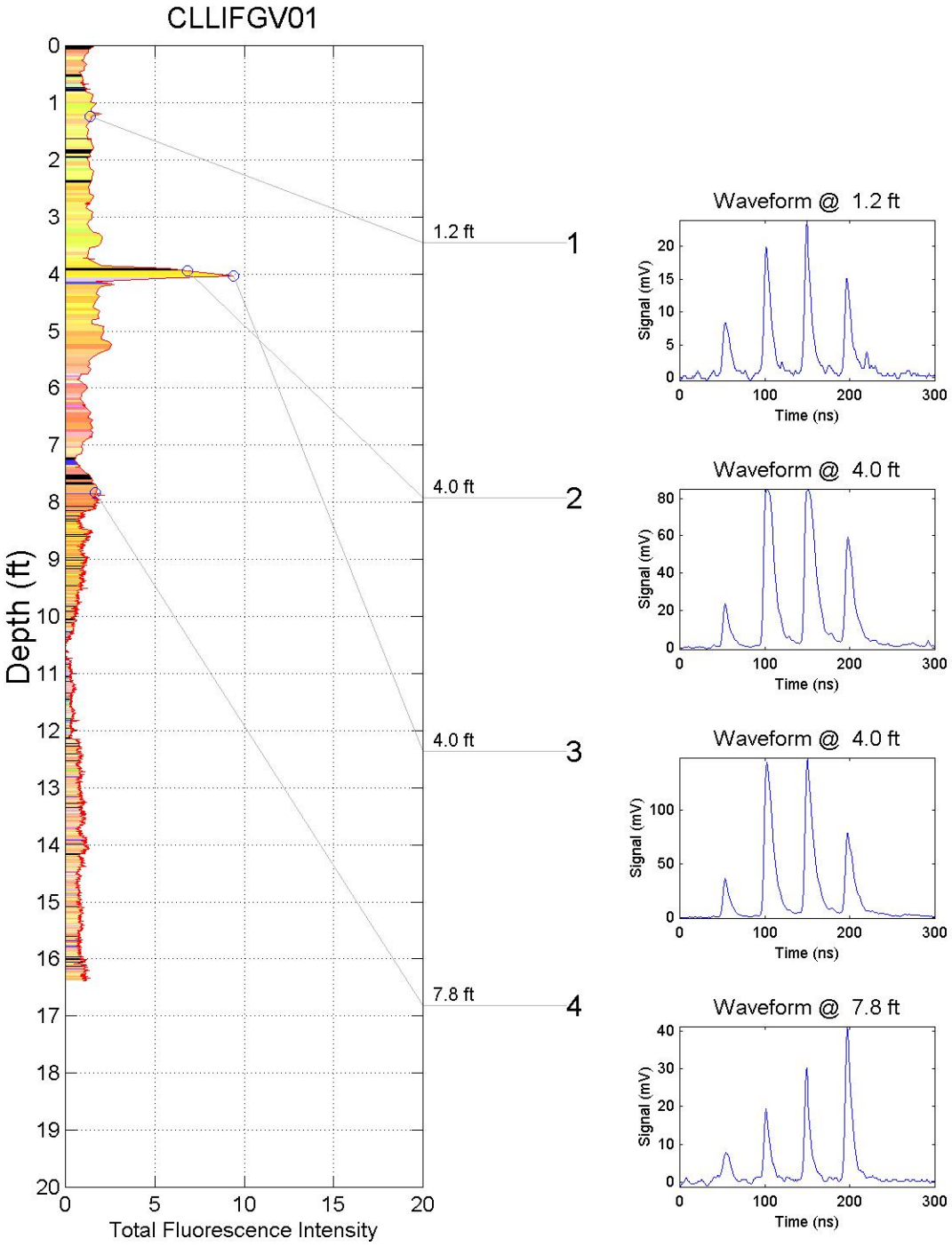

Figure 75. Field log from location # 01

The drop in fluorescence at ~10.5 feet and its continued low response to 12 feet appears to be associated with iron oxide staining as indicated by the orange soils seen in the GeoVIS frame at this depth. One possible explanation of this could be the quenching of dissolved phase humic/fulvic fluorescence from the metal salts in solution. It is interesting that co-sampling

found DNAPL at 12.3 feet, which is where the transition between iron oxide staining to non-stained gray soils took place. It is possible that the transition in soils types seen here indicates the location of a soils horizon that is acting to hold the DNAPL up at this depth. Unfortunately, LIF failed to detect any fluorescence from the DNAPL in this zone.

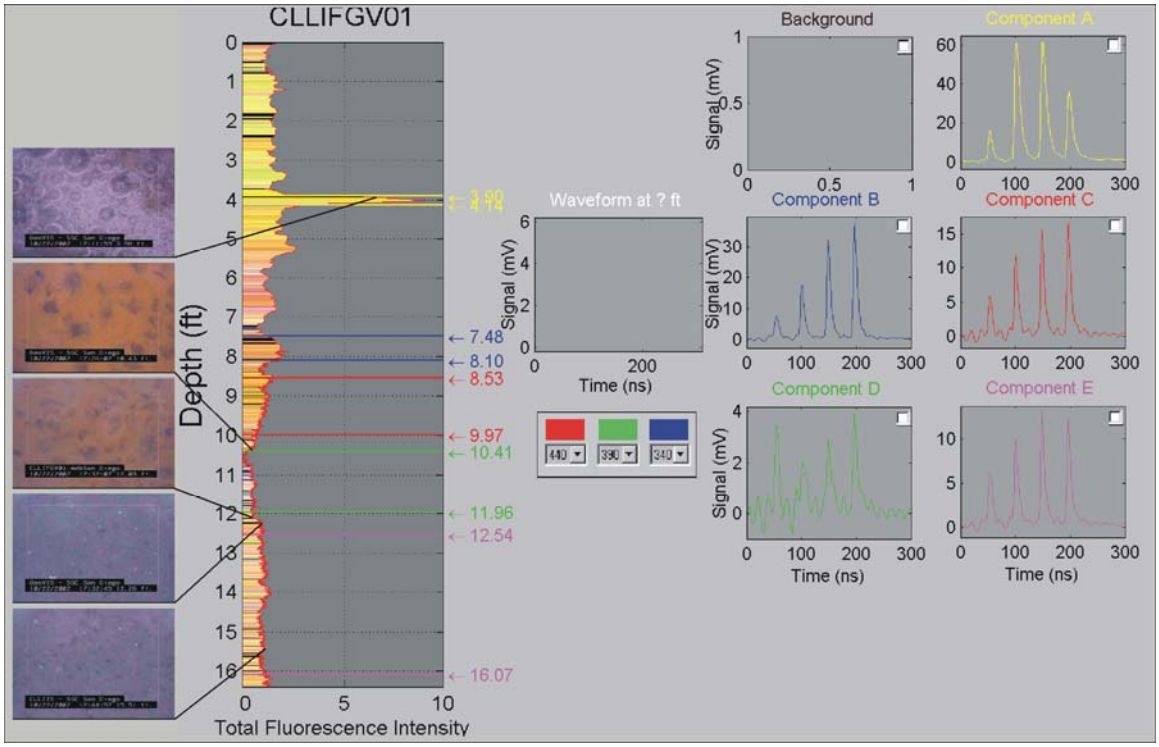

Figure 76. Averaged waveforms and GeoVIS frame grabs from select portions of # 01

The field log generated for CLLIFGV02 is shown in Figure 77. This location showed low XSD signals and is considered the "clean" location. No significant LIF signals were encountered with the exception of the humps located in the 7-8 foot region. Figure 78 shows the combined GeoVIS video frame grabs and waveforms for zones of interest at CLLIFGV02. The humps located in the 7-8 foot region appear to be associated with an increased "milkiness" of the groundwater observed in the free pore space of the soils. Again, as in # 01, the appearance of orange iron oxide occurs in the region of reduced fluorescence and ends when the probe passes into the tight gray soils seen from 13 feet to the bottom of the location.

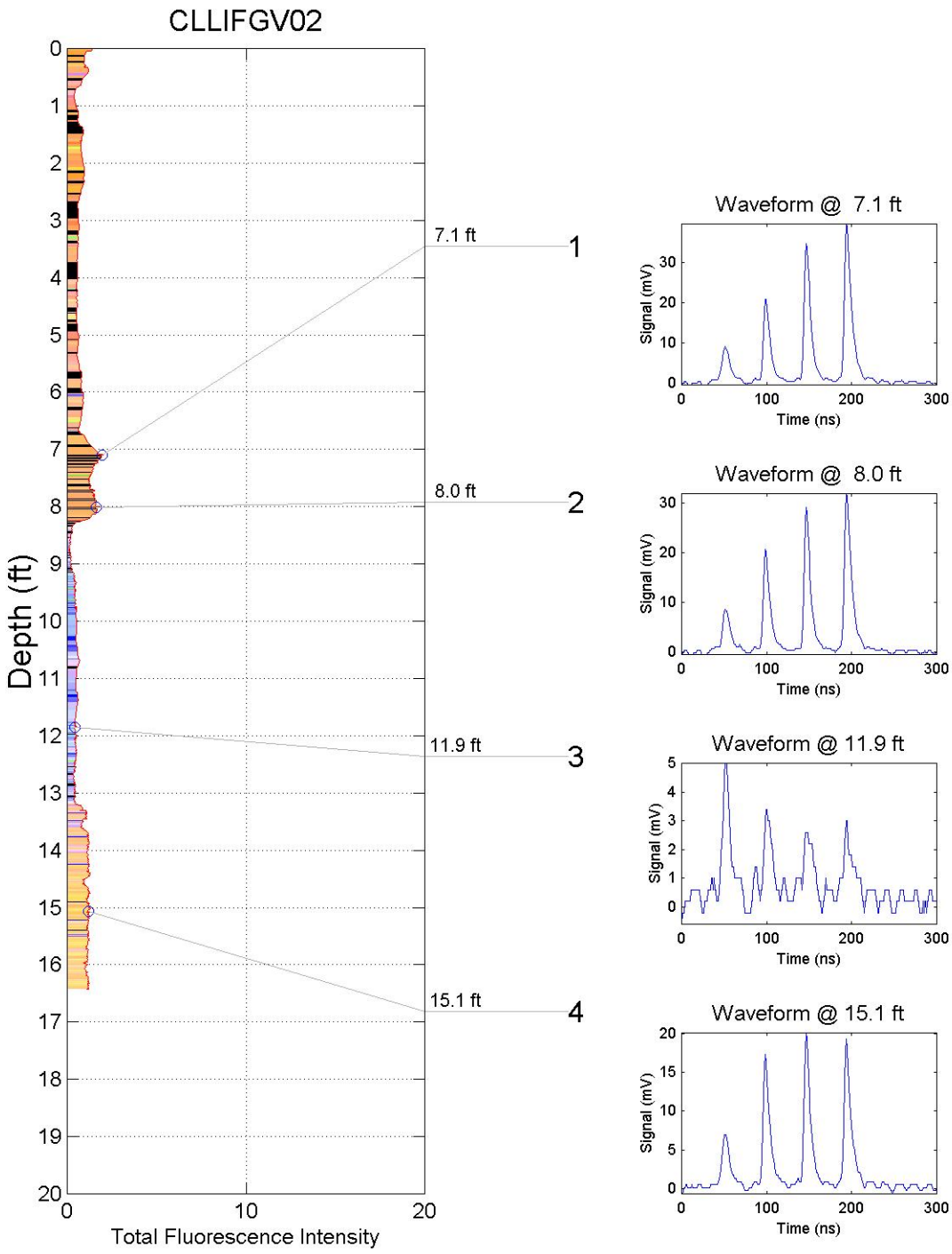

Figure 77. Field log from location # 02

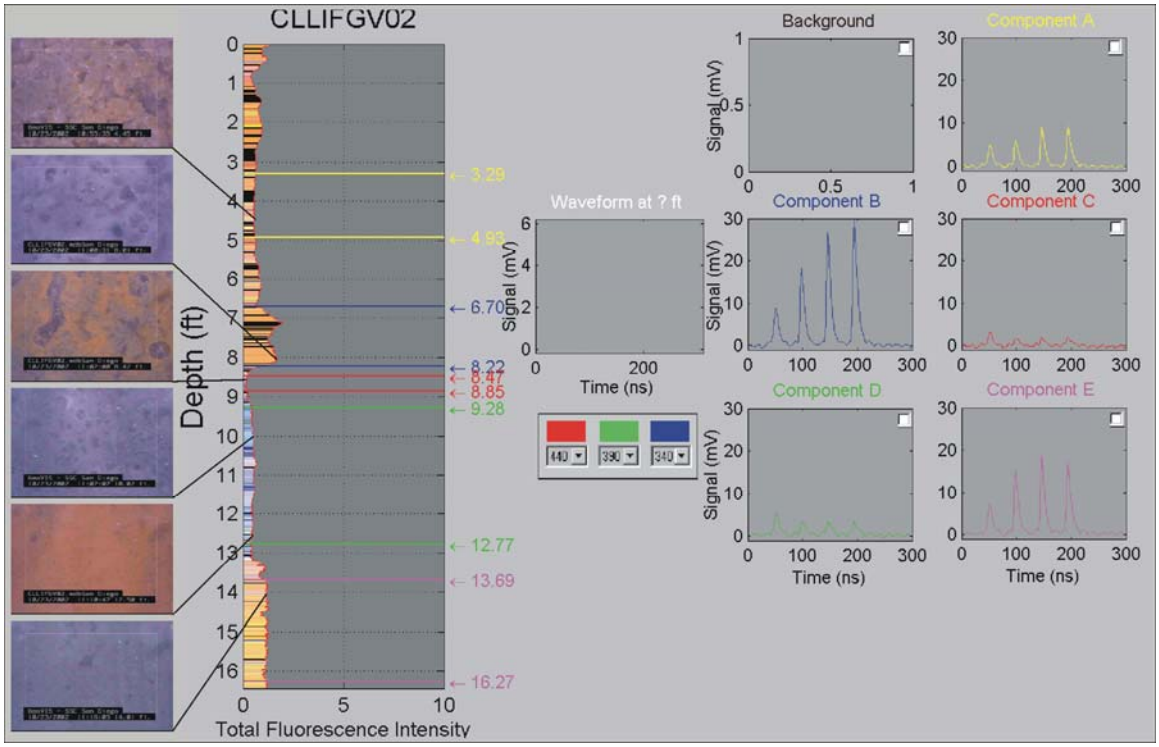

Figure 78. Averaged waveforms and GeoVIS frame grabs from select portions of # 02

Figure 79 contains the field log for push CLLIFGV03. The associated combination graph with GeoVIS video frame grabs and associated waveforms is shown in Figure 80. The obviously elevated signal at 9 feet is well above the signal levels previously encountered from mineral or humic/fulvic interferents. Calcite sands (sea shells/coral) have been previously observed yielding signals of this magnitude and wood fragments can also give rise to such signal levels. While LIF signal levels for XSD and validation tests indicated high dissolved phase, validation sampling failed to confirm DNAPL. Therefore, the source of the elevated LIF signal was not established. It is possible that the validation and XSD pushes, collocated within a foot of this location, happened to miss a narrow vein of DNAPL, but this is impossible to confirm. The clear bubbles shown in the GeoVIS frames at 9 feet appear to be gaseous, not liquid, but this is also difficult to establish with any confidence. It is frustrating to see such high LIF signals without being able to pinpoint their origin.

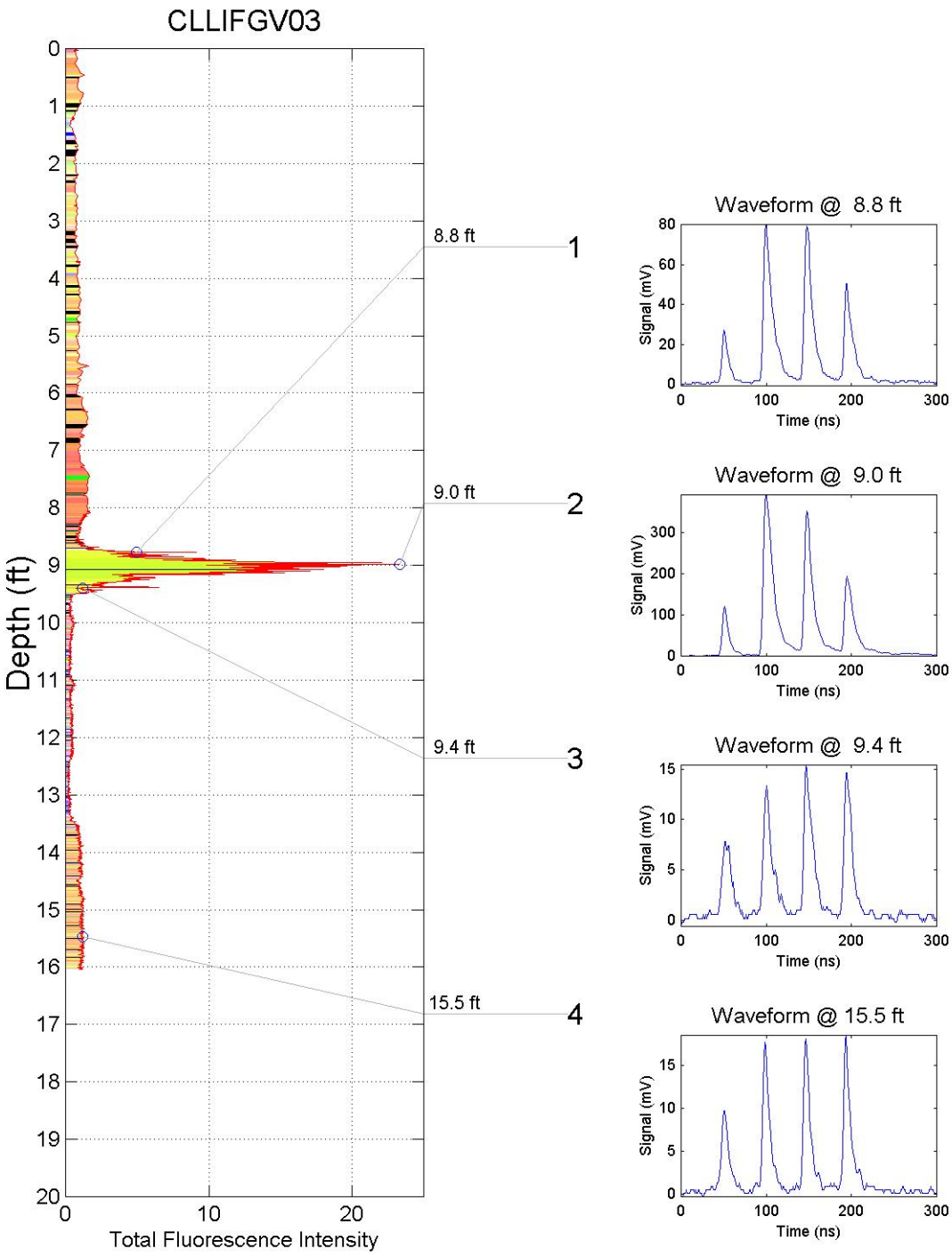

Figure 79. Field log from location # 03

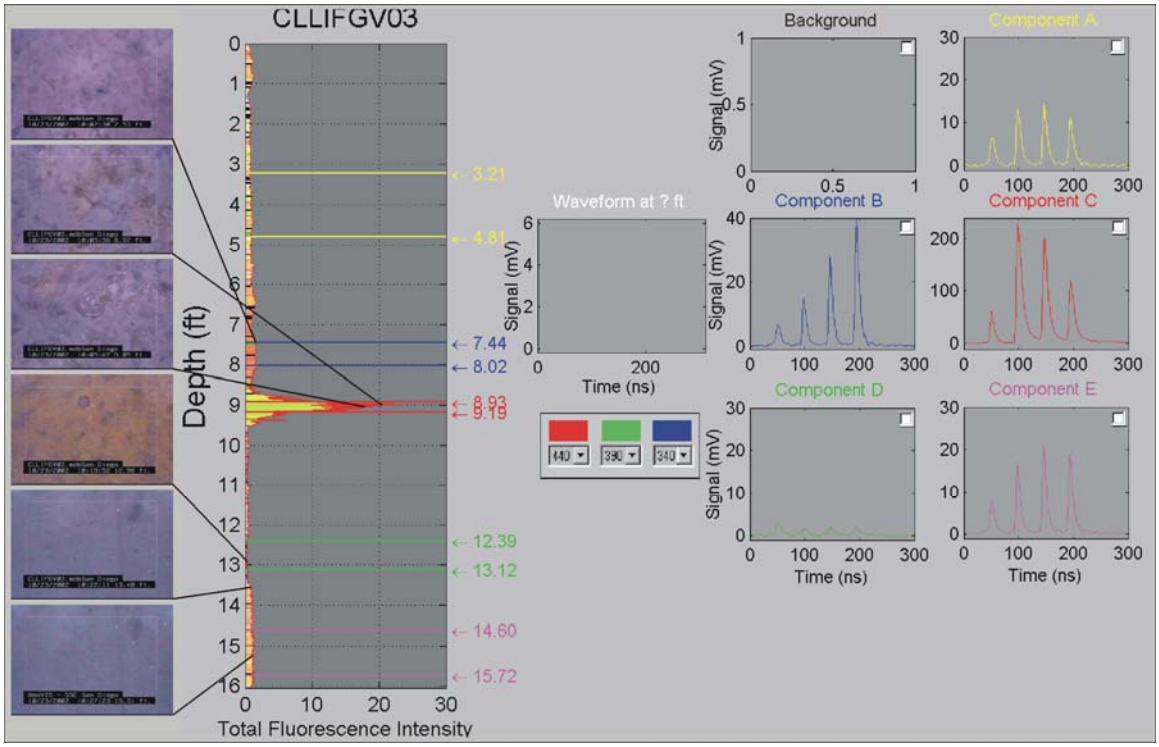

Figure 80. Averaged waveforms and GeoVIS frame grabs from select portions of # 03

The field log and combination data set for CLLIFGV04 are shown in Figure 81 and Figure 82, respectively. The elevated signal at 10 feet, in concert with the elevated signal levels shown with the XSD at the same depth, indicated this zone should be sampled for confirmation of suspected DNAPL. The waveform shape is similar to waveforms seen at other depths, so the spectral characteristics of the material causing the rise in signal in this very narrow seam is not unique. This makes it more difficult to confirm that the LIF was elevated due to DNAPL. Also, the dye test failed to show positive. Again, spatial variability makes it difficult to sample the exact zones penetrated with the tool and/or confirmation sampling, making conclusive validation difficult if not impossible. Our examination of the GeoVIS frames in this region did not yield conclusive evidence of DNAPL ganglia. Nonetheless, it is encouraging that the small zone at ~10 feet in which the LIF was elevated did prove positive for DNAPL.

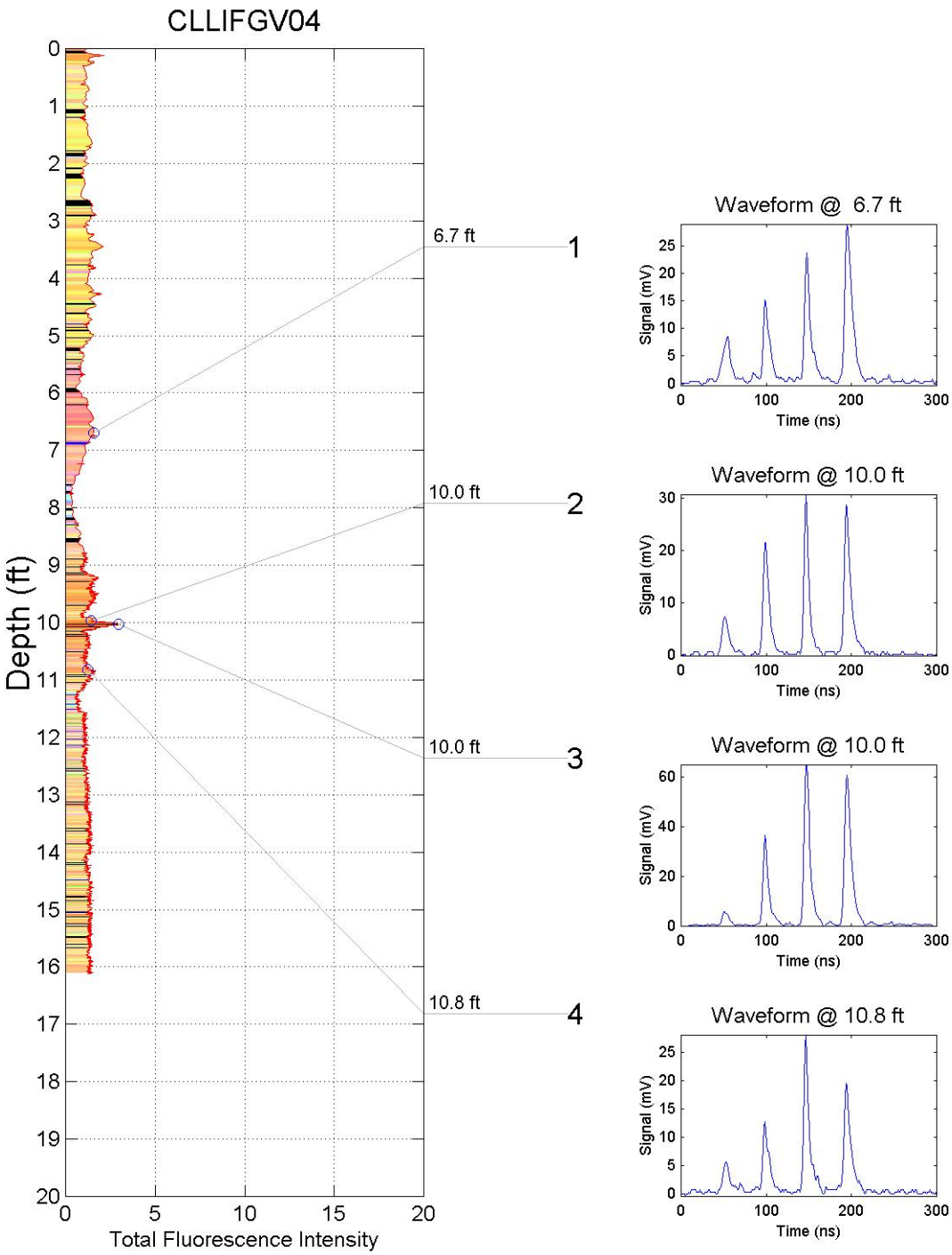

Figure 81. Field log from location # 04

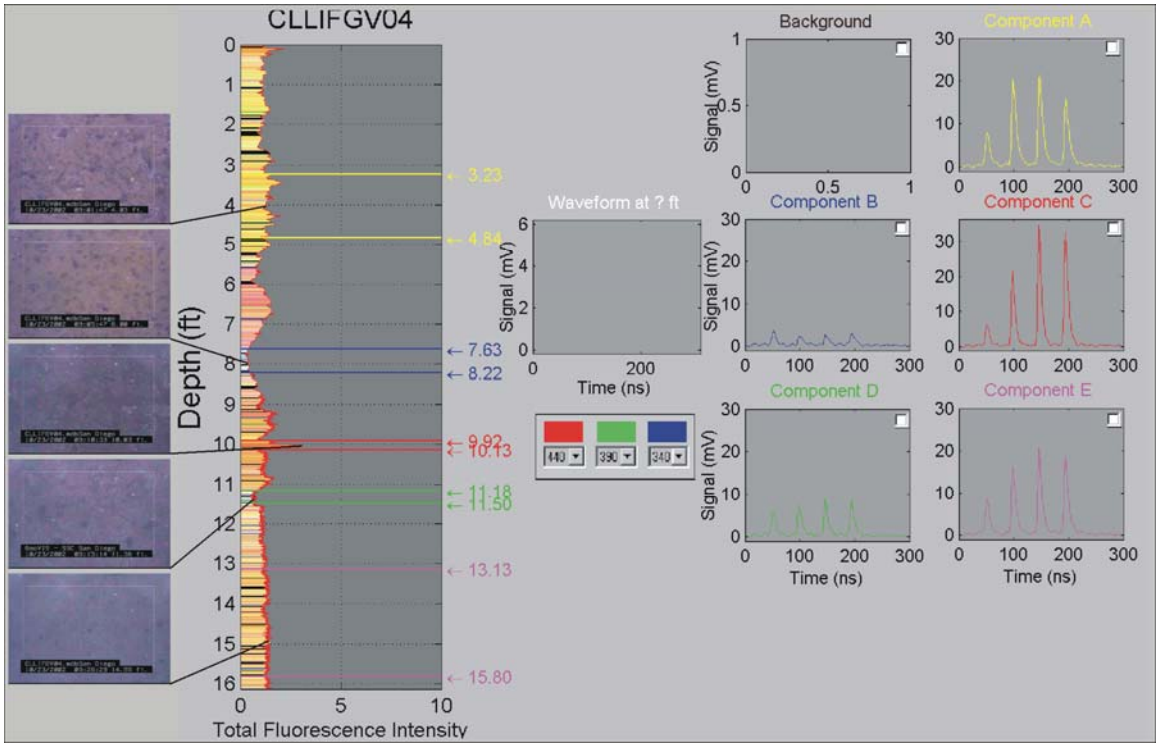

Figure 82. Averaged waveforms and GeoVIS frame grabs from select portions of # 04

The field log and combination data set for CLLIFGV05 are shown in Figure 83 and Figure 84, respectively. The elevated signal that occurs at 3 to 5 feet is very similar to that seen in CLLIFGV01, with relatively long decay times and peak heights. Again this signal appears to coincide with a bubbly-foamy soil condition, indicating the possible presence of proteins due to high biological activity. No validation samples were acquired due to lack of XSD signal. The two elevated signals at 11 and 12. 4 feet occurred in fine grain soils and no DNAPL or ganglia were detectable upon examination of the GeoVIS frames at these depths. White particles occasionally appearing in the GeoVIS video, possibly shell fragments, suggest that the source of these elevated signals could be fluorescent calcite.

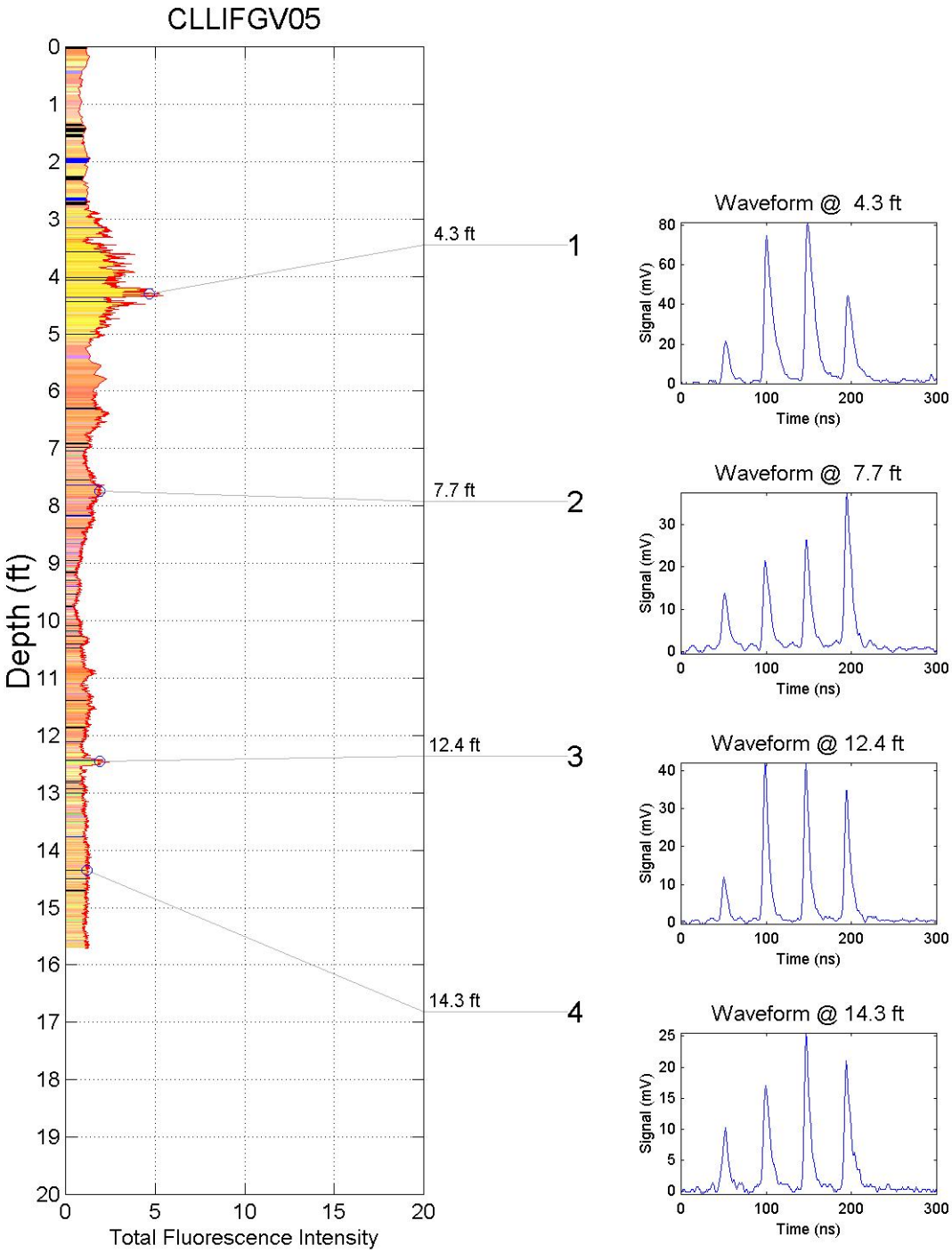

Figure 83. Field log from location # 05

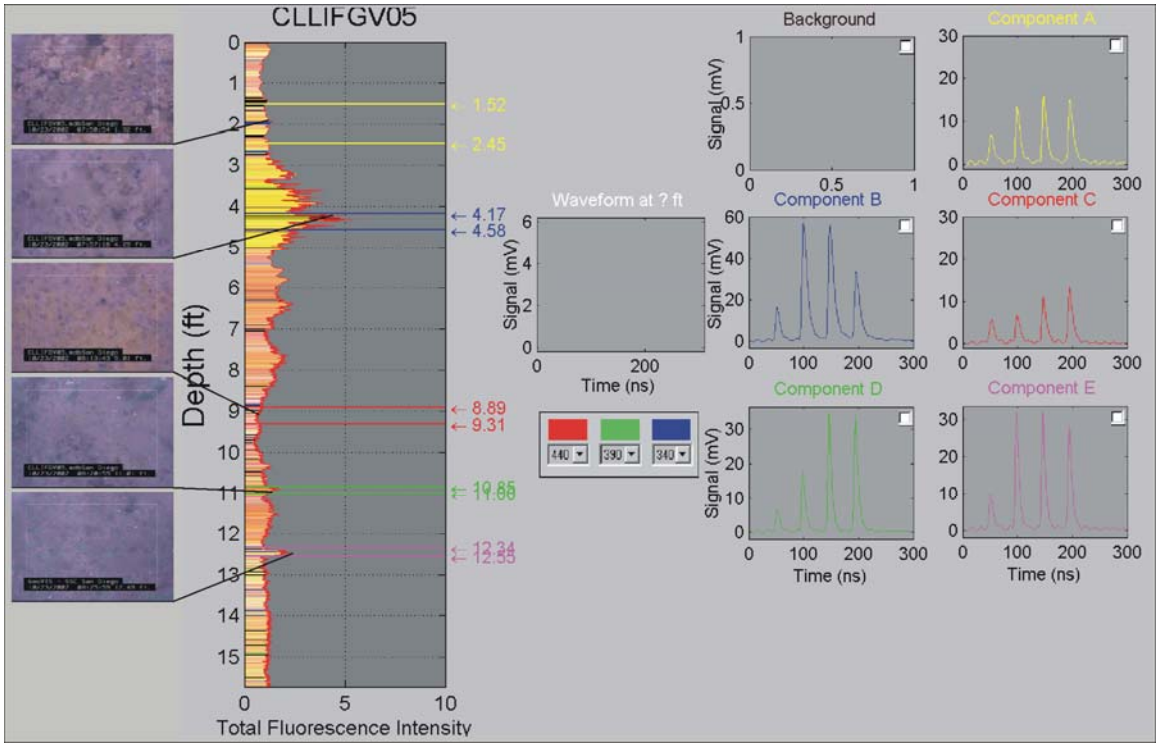

Figure 84. Averaged waveforms and GeoVIS frame grabs from select portions of # 05

The field log and combination data set for CLLIFGV09 are shown Figure 85 in and Figure 86, respectively. The elevated signal that occurred at 2 feet was not co-sampled due to low XSD signal. It is possible that wood fragments caused the rise because wood fragments were observed in the GeoVIS video in some regions of the site. The elevated signal that occurred at 10.6 feet was quite intense and the waveform was unique to the other waveforms observed at the site. Unfortunately the GeoVIS was moving too quickly to observe the soils in this region. Watching the video you can see that there is a distinct band of pale colors and textures streaming past the window at this depth, but freezing the video for frame grabs results in blurry frames leaving one without sufficient knowledge of the soil conditions in this zone. Push # 09B was an attempt to gain insight into this soil horizon, but site inhomogeneity caused us to miss this material on the second push at this location.

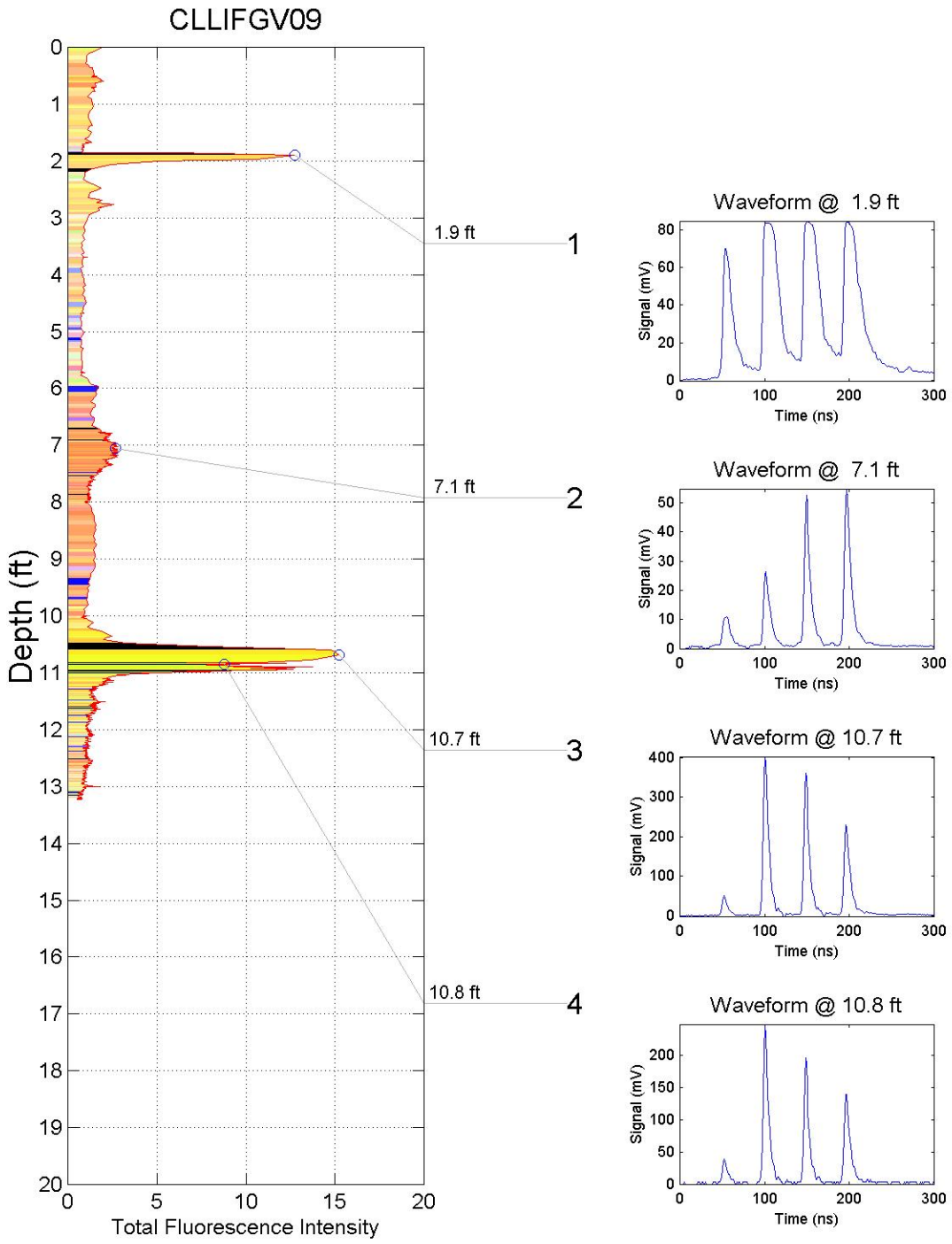

Figure 85. Field log from location # 09

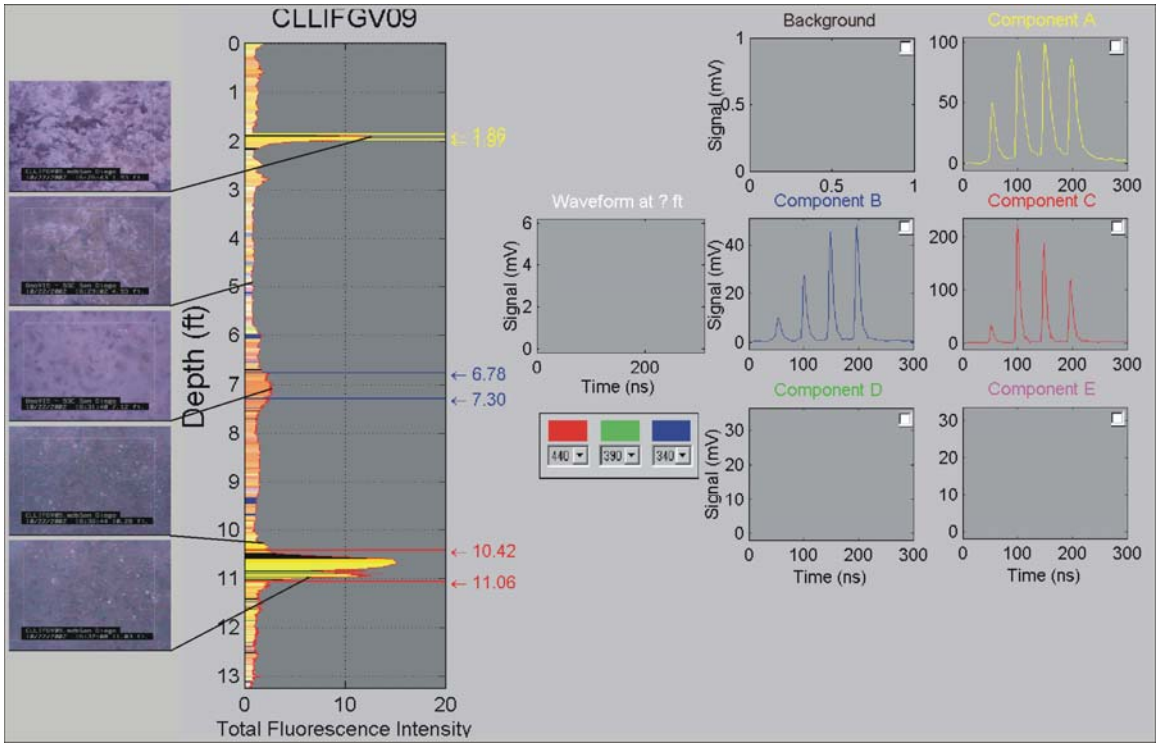

Figure 86. Averaged waveforms and GeoVIS frame grabs from select portions of # 09

The LIF log conducted at CLLIFGV09B was conducted in an effort to better examine the material that gave rise to large signals at 10.6 feet on # 09. Figure 87 and Figure 88 illustrate the results. Again an elevated signal was observed at shallow depth. GeoVIS observed a light buff-colored waxy substance of unknown origin. The elevated signals at 11 and 12 feet showed the same unique waveform as that seen at this depth on # 09, but the signal was dramatically lower. GeoVIS video shows clear quartz sand grains with possible murky off-color droplets of an immiscible liquid mixed in with clear water. It is believed that the unique waveforms observed here are due to the DNAPL that was confirmed via dye tests and water sampling at 13 feet via validation efforts.

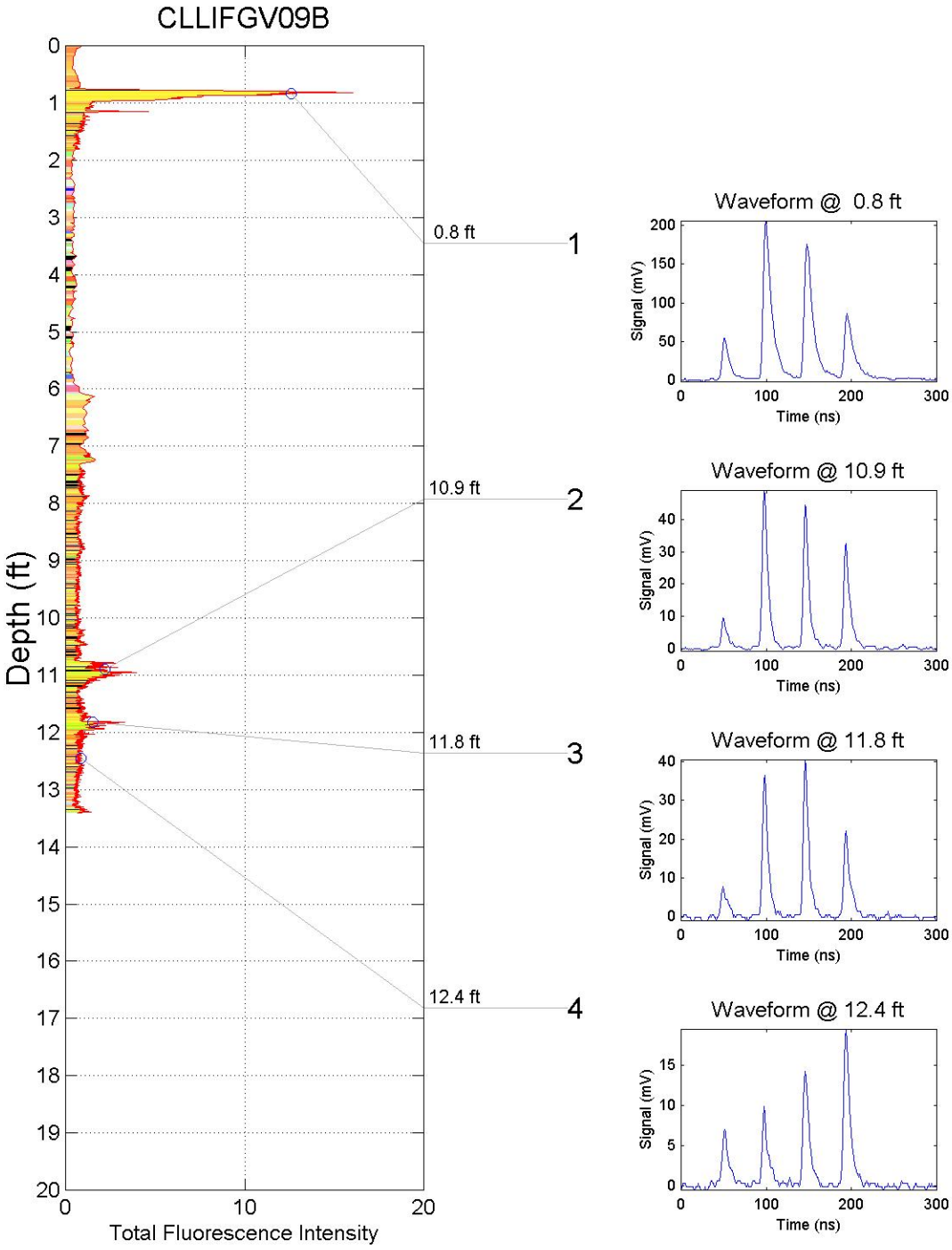

Figure 87. Field log from location # 09B

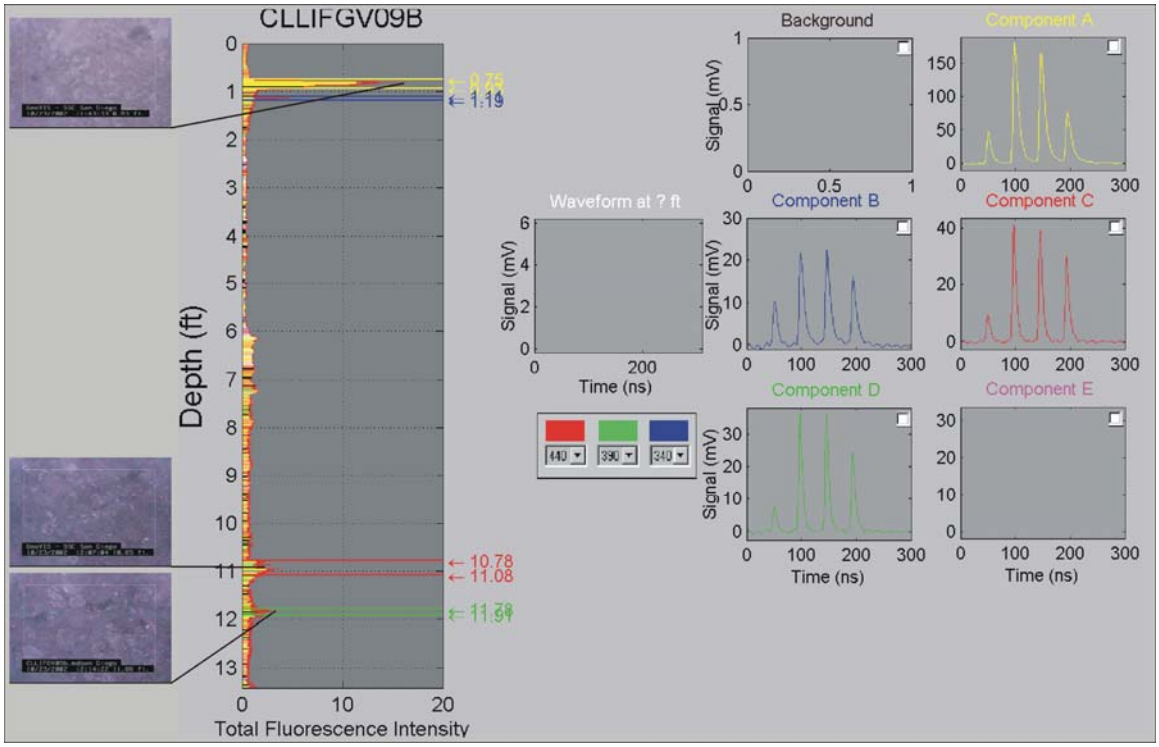

Figure 88. Averaged waveforms and GeoVIS frame grabs from select portions of # 09B

4.3.3 Summary of Camp Lejeune Data

4.3.3.1 XSD

- XSD clearly delineated zones of chlorinated VOC contamination and water sampling confirmed the relative accuracy of the XSD concentration vs. depth profiles.
- Maintaining an acceptable MIP temperature was difficult. While this negatively affected mass transport since we were dealing with a compound (1,1,2,2-tetrachloroethane) that has a high boiling point (146 ºC) and relatively low vapor pressure (6.36 torr), successful profiling was still accomplished.
- XSD signal levels were not saturated at Camp Lejeune, even in areas later found to have DNAPL. It is unclear at this time if this was because of the deviation from the normal operating conditions, inability to maintain higher MIP temperature, or if it takes longer for 1,1,2,2-tetrachloroethane to pass through the membrane.
- Calibration system worked well, some minor improvements needed, most notably, temperature stabilization of saturated response calibration solution.
- Water sample correlation was good with some minor deviations.
- Correlation between uphole XSD-MIP measurements of water samples and laboratory measurements was very good.
- Averaging XSD signal when contaminate layers relatively homogenous over a large depth range produces a good correlation with water sample data.

4.3.3.2 LIF

- False positives were encountered; elevated LIF responses did not always prove positive indicator for DNAPL; fairly high heterogeneity (as demonstrated in replicate push at location # 09) could explain inability to confirm DNAPL at some locations.
- Elevated response at locations 09, 09B, and 04 appear to have been result of DNAPL fluorescence.
- Elevated LIF responses were sometimes seen when GeoVIS passed through at high speed; LIF and GeoVIS window positions should be swapped for optimum performance as a DNAPL validation system.

4.3.3.3 Combined XSD-LIF-GeoVIS Approach

- GeoVIS-LIF system's ability to confirm DNAPL was mixed due to false positives (LIF), which are difficult to substantiate due to heterogeneity.

4.3.4 Travis AFB

4.3.5 Delivery Vehicle

The main modification during the 3rd field demonstration was to demonstrate that the XSD-MIP could be transitioned from a cone penetrometer test (CPT) platform to an anchored (when necessary) Geoprobe platform. A secondary goal of this demonstration was to show that the XSD-MIP (halogen-specific detector - membrane interface probe) system could be effectively used to completely map the source term area of a halogenated VOC site.

Transitioning from a CPT platform to an anchored Geoprobe platform makes economic sense because of the limited availability of CPT platform and their high capital and maintenance costs. To fully realize the broad application of the XSD-MIP system, it is imperative that the system be deployed from a more cost-effective and generalized platform. Geoprobe Systems (Salina, KS) direct push machines fulfill this requirement because of their lower cost as well as their widespread use around the world. Dakota Technologies, Inc. (DTI) owns and operates a Geoprobe Model 5400 system, so the transition process was carried out entirely at DTI's facilities prior to mobilization.

4.3.6 Design

The XSD-MIP sensor consists of several components housed in a downhole assembly that is advanced continuously through the subsurface. The assembly is mounted just behind the cone penetrometer tip and sleeve sensors. The main components of the XSD-MIP are 1) the MIP that samples the soil matrix for VOCs, 2) a water removal system, and 3) a halogen specific detector. As the heated membrane is advanced past the soil, the MIP continuously samples the VOCs that come across the membrane from the soil formation. The effluents from the MIP are passed directly to the water removal system via a short (ca 6 inch) transfer line. By placing the drying system directly behind the MIP, the amount of water that condenses out in the transfer lines is greatly reduced if not eliminated.

After passing through the drying system, the gas stream passes into the XSD for analysis. The total distance that the effluents travel from the MIP to the detector is approximately eighteen

inches, which corresponds to less than 2 seconds of lag time between sample collection and analysis. Since the probe is typically operated at advancement rates of 0.5-1.0 cm/sec the spatial distortion between collection and analysis is typically on the order of 1-2 inches.

Placing all of the sensing components of the XSD-MIP downhole offers several important advantages. First, the adsorption losses in the transfer lines are virtually eliminated with the short transfer lines. Second, the halogen detector's active sensing element operates at elevated temperatures (800-1000 °C), which effectively warms the transfer lines and reduces the risk of analyte carryover or drag. Finally, depth correlation is straightforward since spatial distortion is only 1-2 inches. These features of the XSD-MIP effectively allow true dynamic logging of halogenated VOCs with depth.

DTI personnel traveled to Travis AFB for the demonstration at Site DP039 (Building 755). A grid of push locations was laid out across the site to characterize the suspected source term area. The grid (Figure 89) was laid out in such a way as to evenly space the holes across the site. Upon completion of the grid layout, calibration of the system and XSD-MIP pushes were commenced.

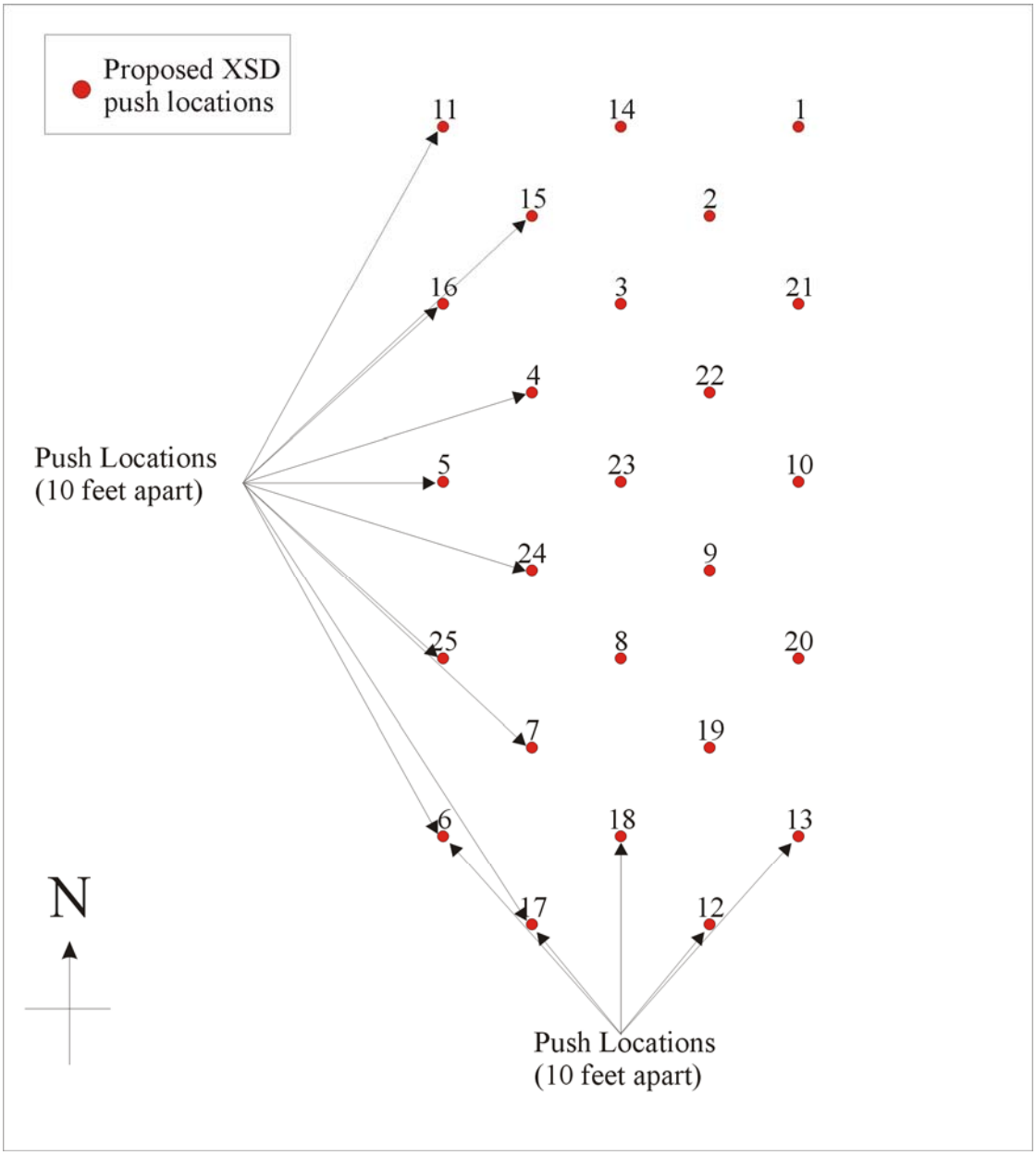

Figure 89. Proposed push locations at Site DP039

Prior to each in situ measurement, a calibration of the system was done using the saturated response calibration (SRC) solution and the aliquot injection method described above.

At the end of each push, the SRC data was used to normalize all field data to correct for any changes in responsivity and baseline. The SRC process allowed us to convert the XSD-MIP system's signal from its native data format (volts) to a total halogen concentration (ppm halogens). Application of this factor corrected for any system drift and changed the data to a format that could be readily compared to water sample data. This allowed us to view the entire project data set in a normalized context at project completion with confidence that any drift in system responsivity had been accounted for.

The first push (Push 01) was attempted at location 01 using an anchoring system to insure that the hydraulic ram would be immobilized sufficiently. When the probe reached 5.89 feet, considerable resistance was met which was great enough to begin pulling the anchor from the subsurface. The push was terminated at this point. No contamination was encountered during this push.

A second push (Push 01a) was then attempted at location 01 but before this push was started a pre-probe was used to create a small diameter hole to 20 feet below ground surface. The XSD-MIP push was commenced in this hole but the probe again met refusal at 9.79 feet. No contamination was encountered during this push.

The Geoprobe platform was then moved to location 21 and another series of pushes were attempted. The first push (Push 02) was attempted without pre-probing, which resulted in refusal at a depth of 9.74 feet. No contamination was encountered during this push.

A second push was then attempted at location 21 using the pre-probe to a depth of 20 feet. The XSD-MIP push was commenced in this hole but the probe met refusal at a depth of 11.93 feet. No contamination was encountered during this push.

The Geoprobe platform was then moved to location 8 and another push was attempted. However, before this push was started the pre-probe was used to create a pilot hole for the anchoring system. With the aid of the pilot hole the anchor was able to reach a depth of 10 feet. The additional depth reached with the anchoring system was able to exert considerably more force on the foot of the Geoprobe ram.

Push 03 (Figure 90) was then commenced at this location. Several areas of contamination were encountered in the depth regions from 25 to 34 feet. The contamination levels at these areas ranged from 5 to 65 ppm total halogens. The probe met refusal at 34.0 feet at which point the push was ended.

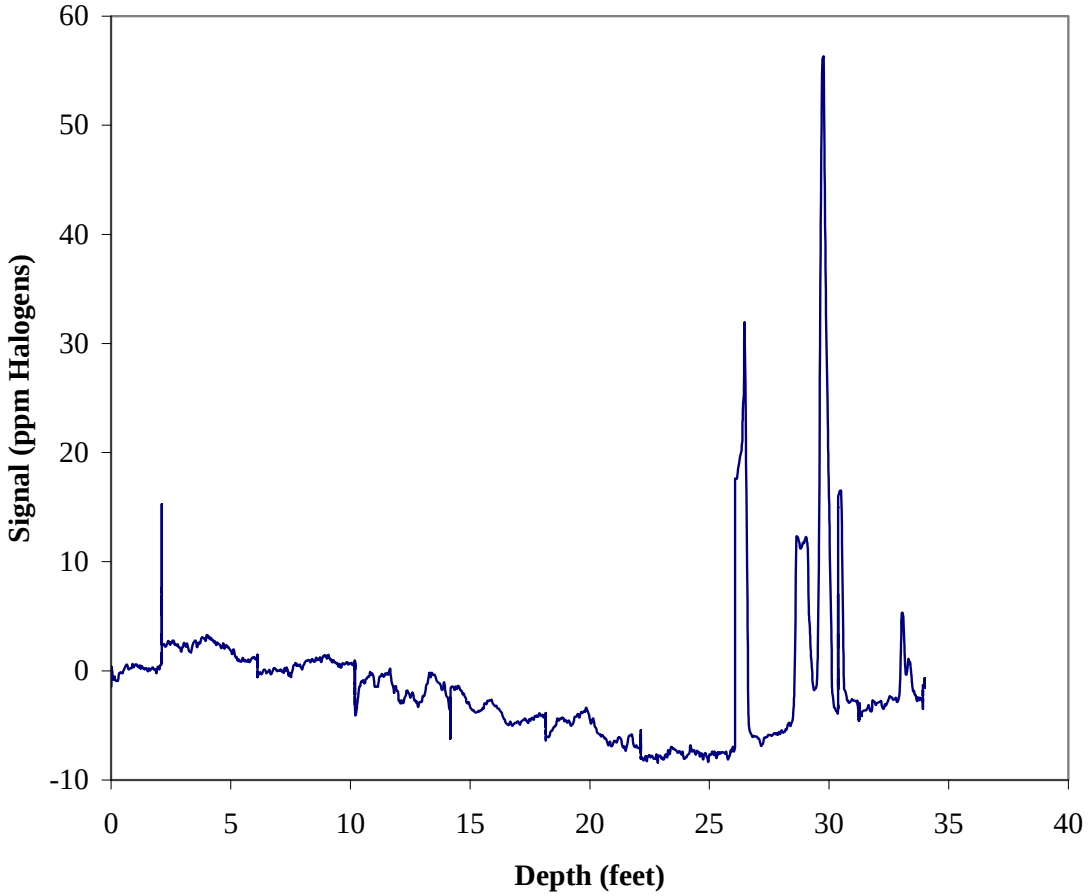

Figure 90. XSD-MIP log at location 08

4.3.7 Problems Encountered

Upon completion of Push 03 the applicability of Site DP039 as a viable demonstration location was reviewed. By the end of the first day of pushing it had become apparent that the geological conditions at the site were much more difficult than had been anticipated. A slightly cemented, loamy soil of unknown thickness was encountered at approximately six feet that was causing considerable resistance to the probe. The geological data collected to date at this site, which had been reviewed by both DTI's geologist and the Travis AF Base geologist, did not indicate that this layer was present.

The difficult soil conditions caused several issues of concern. First, the hydraulic ram of the Geoprobe was being subjected to so much force that the mounting brackets were beginning to bend. Second, the push rods used for advancing the probe were bending during the push, which raised the possibility of breaking off the probe. Finally, the chains and mounting system used to attach the anchor to the hydraulic ram were becoming fatigued and stretched. All of these issues raised concerns about the likelihood of a catastrophic failure with the possible outcome the loss of an XSD-MIP probe, major damage to the Geoprobe platform, or injury to the personnel involved. Upon considering these issues it was determined to abandon further efforts at this site.

Analytical results from the XSD sensor will be compared to laboratory results from Method 8260b using standard regression analysis. The standard regression analysis will include an ANOVA table, coefficients, standard error of y estimate, r^2 values, number of observations, and standard error of coefficients.

The HRF and GeoVIS data will be compared to results from visual observations and Sudan Red dye tests. Because of the qualitative nature of this data a standard contingency analysis will be used to report the data. The final results for each technology (HRF and GeoVIS) will be stated in terms of percent (%) agreement with the lab method (visual and Sudan Red) by summing he number of true positives and true negative observations and dividing by the total number of samples. The final report will include the overall % agreement for each technology summed over all sites.

4.3.7.1 Redesign of the XSD-MIP for High sensitivity mode

The development of the of the XSD-MIP system (hereafter referred to as the Haloprobe system) was originally funded by a Strategic Environmental Research and Development Program contract (SERDP CU-1089) for the delineation of chlorinated dense non-aqueous phase liquids. Under this contract, DTI successfully designed and tested the Haloprobe system for use with a Geoprobe delivery vehicle and successfully conducted two demonstrations at sites with dissolved phase chlorinated VOC concentrations (<10 ppm). In these demonstrations the detector was operated in high sensitivity mode, which yields a limit of detection (LOD) of 100 ppb. Since the Haloprobe's sensitivity is directly related to the operating temperature, the higher the temperature, the more sensitive the detector and the lower the LOD. By successfully demonstrating the ability of the Haloprobe system to operate in this mode, DTI was confident that transitioning to the low sensitivity (i.e. DNAPL sensing) mode would be a straightforward process.

During the summer of 2001, DTI and SPAWAR System Center, San Diego began the transition process of the Haloprobe system from the Geoprobe delivery platform to a CPT delivery platform. Under the ESTCP contract, DTI and SPAWAR were tasked with demonstrating the applicability of the Haloprobe system for delineating DNAPL contaminated areas. The Haloprobe detector (Figure 91) was used successfully to identify DNAPLs at two sites (North Island Naval Station, CA and Camp Lejeune Marine Corp Base, NC). At both of these demonstrations, the Haloprobe system was operated in low sensitivity (DNAPL) mode.

Figure 91. Original Haloprobe Detector

4.3.7.1.1 Problems/Challenges encountered with original Haloprobe System

In May 2003, construction of a second Haloprobe system was begun for Mr. Jerry Hansen of the Air Force Center for Environmental Excellence (AFCEE). This system was to be integrated into the Kansas City Army Corps of Engineers SCAPS truck and used in both high and low sensitivity modes. During the construction and testing process several problems were encountered when the detector was operated in high sensitivity mode, including:

1. Insufficient thermal protection of the power, thermocouple and CPT lines that bypassed the detector's sensing element
2. Failure of the K-type thermocouple used to monitor and control the detector's temperature
3. Ability to reproducibly fabricate the detector's reactor core assembly
4. Connection of the various power, thermocouple, and signal lines to the detector assembly
5. Serviceability of the detector during field operations

These problems were severe enough to cause the failure of two Haloprobe detectors during the initial integration effort. After the loss of the second detector, the Haloprobe system was removed from the COE truck and brought back to DTI for further analysis.

4.3.7.1.2 Description of new Haloprobe System

In light of the problems encountered during the construction and operation of the initial AFCEE Haloprobe system, DTI requested and received approval from both ESTCP and AFCEE to redesign the Haloprobe to correct the system's shortcomings.

Table 12 describes the solutions adopted for correcting the original Haloprobe system's shortcomings.

Table 12. Revised Haloprobe System Improvements

Problem	Solution
1. Insufficient thermal protection	Implemented use of microporous insulation. Lab and field tests have shown that the insulating properties of this insulation is far superior to the insulation used in previous versions. Temperature profiles in the MIP and CPT bypass areas are under 140 ºC which is well below their maximum rated value (200 ºC)
2. Control thermocouple failure	The K-type thermocouple was replaced with a B-type thermocouple which offered two advantages. First, this thermocouple type can withstand much higher temperatures (1700 ºC) than all other thermocouple types (other than RTDs). Second, changing to two different thermocouple types automatically color codes the detector and MIP thermocouples so they cannot be accidentally switched.
3. Fabrication reproducibility	A special jig was designed for construction of the interior components of the detector. This jig has allowed us to reliably build detector assemblies that are interchangeable with one another.
4. Connection of input lines	A custom connector assembly (Figure 92)) was developed to eliminate the need for silver-soldering any of the detector's thermocouple, power or electrode lines.
5. Field Serviceability	A modular design was developed to allow for straightforward switching of components during field operation (Figure 93).

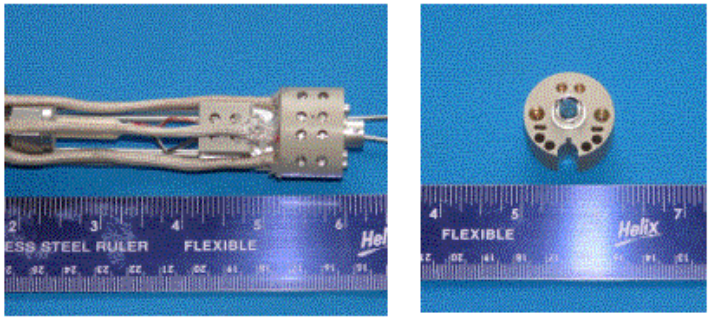

Figure 92. Haloprobe Custom connector assembly

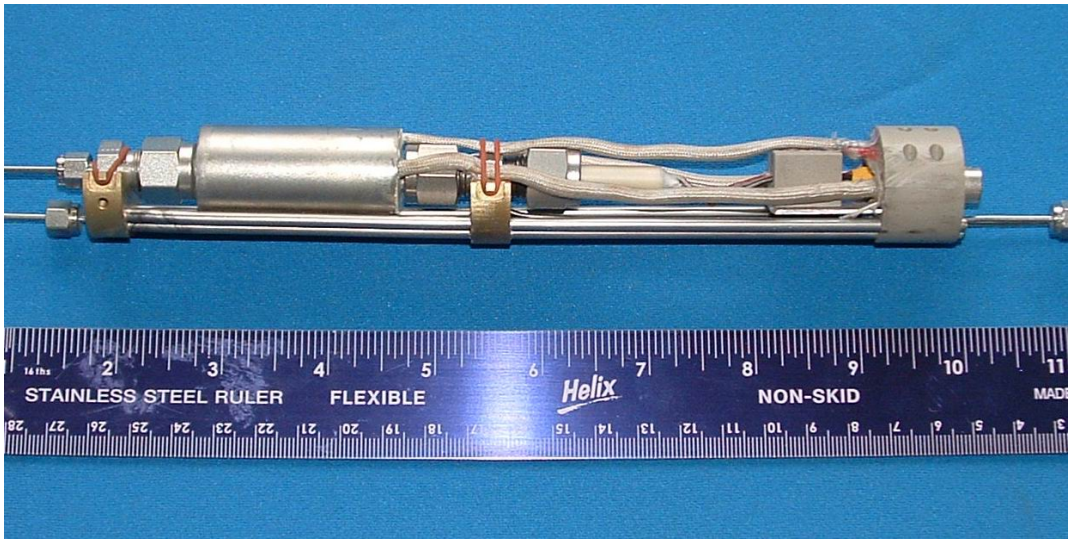

Figure 93. Revised Haloprobe detector with modular design

The redesigned Haloprobe system was successfully tested in December, 2003 at Rickenbacker International Airport in Columbus, OH. During this 1-week demonstration, the system was integrated into the KC COE CPT truck and operated in high sensitivity mode with no problems encountered. This effort showed that the redesign was successful in addressing the last remaining issues required to transition the Haloprobe system to end-users in the direct push industry.

5 Cost Assessment

5.1 Cost Reporting

Costs analysis associated with direct push sensor systems has already been performed for direct push petroleum hydrocarbon sensors ([17],[6, 18]) and metal sensors [18, 19]). This effort will document and compare the costs for delineating DNAPL source zones using direct push sensor systems.

5.2 Cost Analysis

5.2.1 Cost Reporting.

Cost comparisons are reported on a fee-for-service basis. The estimate of the fee-for-service rate is based on an average obtained from commercial service providers for similar operations with CPT delivered MIP systems with standard uphole detection systems. This cost comparison focuses mainly on the XSD-MIP but includes the LIF confirmation tool and two previously tested SCAPS metal sensors for comparison. No significant changes in technology or labor rates have occurred since LIF estimates were assembled in earlier ESTCP reports {Steve L's earlier

LIF reference here} so previous ESTCP demonstration rates were left unchanged. Quoted rates can vary by approximately a factor of two depending on productivity. The average rate used for cost comparisons in this report of $4,675/10 hr day appears to represent a fairly conservative estimate that would cover not only operations but also account for basic data analysis and reporting. This rate is based on a CPT truck equipment rate of $2,750/day (includes the CPT equipped 20-ton penetrometer system plus two support vehicles, push room operator, push room helper), XSD-MIP data logging service with data acquisition specialist ($1,500/day), and labor for a project geologist or project manager charged at $67.50 hr for 10 hr day.

5.2.2 Cost Analysis

Major cost drivers for CPT deployed XSD-MIP operations include equipment charges (including capital equipment costs, equipment repair and maintenance), labor, material (including grout material, carrier gases, misc. expendables), permitting, utility location, location surveying, IDW disposal, work plan and report preparation and equipment mobilization and demobilization. As described in Section 5.1, costs are reported here on a fee-per-service basis in order to facilitate comparisons with conventional site assessment methodology. The primary source of uncertainties in cost estimates provided here is related to variations in the number of feet pushed per day that result from pushing in different geological materials. At sites where pushing is difficult because of tough geological material or large number of cobbles, the push rate may be reduced or the probe may be refused and it may be necessary to move the push vehicle to a new push location several times in order to achieve penetration. In these situations, the push rate could be reduced by a factor of 25 to 50% or more. A decrease in production rate of 50% would of course increase the cost per sample report in Table 14 by a factor of two. It should be noted however, that if pushing is difficult or limited for the XSD-MIP-CPT sensor it will also be difficult for the direct push sampling system and may also slow the conventional hollow-stem auger and split spoon sampler system. Although the MIP probes used in this study were equipped with strain gauges to monitor the tip and sleeve friction during pushes (also useful for avoiding breaking the probe) pushing in difficult geology also puts the probes at greater risk and increases the chances of damaging or breaking the expensive sensor probe. In extreme cases, it may become necessary to charge a surcharge for repair of damaged probes (the equipment charges cover normal “wear and tear” which includes periodic replacement of MIP membranes and other wear items). Other variations in production rate (number of feet pushed per day) arise from differences in the depth pushed at each push location. In general, production rates increase as the depth of the push increases because the setup time required to move the truck to a new location is reduced.

The fee for service costs reported include the capital equipment costs and costs for normal wear and tear and maintenance. Table 13 provides estimates of the capital costs of the XSD-MIP, 2 SCAPS metal sensor technologies [20], and LIF for comparison. Estimates provided in Table 13 indicate that the capital equipment costs for XSD-MIP are about half of the cost of the other technologies. The relatively expensive lasers and other opto-electronic devices required for the other sensors drive costs up considerably. Although the XSD-MIP has a rather complicated downhole assembly, the component cost of these parts is relatively inexpensive vs. laser, optical fibers, etc. and this brings the costs into agreement with other downhole sensors in the Probe/Umbilical cost category. Based on previous experience with LIF systems operated by government and commercial service providers it is estimated that the life cycle for the instrumentation system is expected to be approximately 5 to 7 years and the XSD-MIP should be

comparable. Environmental/Safety training is also expected to be similar to that for LIF systems currently in operation in government and commercial systems.

Table 13. Capital equipment costs for XSD-MIP, two SCAPS metal sensor systems, and a commercial LIF system.

	XSD-MIP	FO-LIBS	DL-LIBS	LIF
Up hole Instrumentation System	$29K	$72.5K	$62K	$97.5K
Probe/Umbilical	$16K	$19K	$27K	$15K
TOTAL	$45K	$91.5K	$89K	$112K

- Cost Basis: Quantitative costs comparisons will be performed on a per sample basis. In addition, attempts will be made to estimate cost savings that result from the availability of real-time field data that facilitates optimization of sampling plans in the field and possible reduction or elimination of additional sampling operations.

-Cost Drivers: Factors affecting the cost of the direct push sensor operations include, labor, material, travel, permitting, utility location, location surveying, work plan and report preparation and equipment mobilization and demobilization. Geology of the subsurface will also influence the applicability and costs of using direct push sensor technology at a specific site.

- Life Cycle Costs: Life cycle costs for direct push sensor systems include the capital cost of the sensor systems, startup, operations and maintenance, and mobilization and demobilization costs. Depending on locality some fees are sometime required for "drilling permits." Based on previous experience with other direct push sensor systems, 5 years is estimated as an appropriate life-cycle period for cost comparison.

5.2.3 Cost Comparison

This demonstration has focused on judging the effectiveness of CPT delivered XSD-MIP technology to perform field screening at hazardous waste sites containing halogenated DNAPLs. Table 14 presents a direct comparison between the costs using an XSD-MIP sensor versus conventional drilling, sampling, and laboratory analysis for field screening. This program has focused on the effectiveness of the XSD-MIP technology to perform field screening for DNAPL contamination and its associated dissolved phase VOCs. Table 14 presents a direct comparison between the costs using XSD-MIP sensor versus conventional drilling, sampling, and laboratory analysis for field screening. For a site investigation with 10 holes to a depth 30 feet, the Table 14 shows the cost for XSD-MIP sensor is approximately 36% of the cost of conventional sampling with a sampling ratio of 60 to 1 in favor of XSD-MIP sensor. On a per sample basis, Table 14 shows that XSD-MIP technologies offer approximately a 99% cost savings compared with conventional soil borings and laboratory analyses and a 98% cost savings compared to

Direct push with Off-site laboratory analysis. The cost savings realized from direct push methods compared to conventional drill rigs are due to: (1) the speed with which direct push techniques access depth versus drilling methods, (2) the low amount of investigation derived waste produced by the direct push methods, and (3) the ability of direct push technique to acquire near continuous data. Further savings not documented in Table 14 may be realized using the SCAPS sensors because onsite real-time data acquisition allows the sampling strategy to be modified in the field to more accurately delineate the extent of contamination. In contrast, traditional sampling strategies depend on results from laboratory analyses that are usually not available for days or weeks after samples are collected and often require return trips to the field when initial results indicate that further sampling is required to complete delineation of the contaminated zone. Also, the greater vertical sampling rates provided by the SCAPS sensors compared to conventional sampling methods (every one to two inches compared to every 5 feet) minimizes the chances that significant zones of contamination are missed because five foot sampling intervals performed with soil boring do not provide the resolution necessary to resolve some contaminant layers. For the XSD-MIP sensor technique, regulators may require a minimum number of confirmatory samples, which can be obtained using CPT sampling devices. This will increase the XSD-MIP sensor cost as presented in Table 14 but only 3 or 4 samples would be required at less than $1,000 additional cost.

Table 14. Cost Comparison of XSD-MIP sensor with Conventional Sampling and Direct Push Sampling.

XSD-MIP Measurement		Conventional Drilling (hollow stem auger, split spoon, and offsite analyses)		Direct Push and Offsite Analysis	
10 Pushes to 30 ft. Relative hVOC and geotechnical data	Cost	10 Borings to 30 ft (60 soil or water samples for GC analysis)	Cost	10 Borings to 30 ft (60 soil or water samples for GC analysis	Cost
2 10 hr field days @ $4,675/day	$9,350	Drilling and sampling @ $50/ft for 300 ft (approx three 10hr days)	$15,000	Drilling and sampling for 300 ft. (approx tow 10hr days)	$3000
1 sample/inch for VOCs = 3600 total samples	Included in basic cost	GC laboratory @ $50 per sample x 60 samples	$3000	GC laboratory @ $50 per sample x 60 samples	$3000
1 sample/inch for geotechnical Data	Included in basic cost	Geotechnical laboratory analysis @ $100/sample x 5 samples	$500	Geotechnical laboratory analysis @ $100/sample x 5 samples	$500
4 waste drums @ $40/drum	$160	28 Waste drums @ $40/drum	$1120	1 Waste drum @ $40/drum	$40
Decon water testing	$1000	Decon water testing	$1000	Decon water testing	$1000
Waste Soil testing	$0	Waste soil testing	$3000	Waste soil testing	$0
Waste Soil not produced	$0	Waste soil disposal 20 drums @ $100/drum	$2000	Waste Soil not produced	$0
Decon water disposal for 4 drums @ $100/drum	$400	Decon water disposal	$800	Decon water disposal for 1 drum @ $100/drum	$100
4 man crew	Included in cost	Geologist @ $75/hr x 36 hrs	$2700	Geologist @ $75/hr x 36 hrs	$2700
		Technician @ $40/hr x 40 hrs	$1600		
TOTAL	**$10,910**	**Total**	**$30,720**	**Total**	**$10,340**
Per Sample Cost for 3600 samples	$3.03/sample	Per Samples cost for 60 samples	$512/sample	Per Sample Cost for 60 samples	$172/sample

6 Implementation Issues

6.1 Environmental Checklist

From previous experience with direct push technologies permitting requirements are expected to vary with individual locality. Some regulators require "drilling permits" and associated fees for direct push investigations. Other regulators do not require permits or payment of fees and only require notification usually via submittal of a test plan. The RPM (remedial program manager) at NAS North Island has agreed to handle all permitting requirements with local regulators.

6.2 Cost Observations

Factors affecting the cost of the XSD-MIP CPT operations include labor, material, travel, permitting, utility location, location surveying, work plan and report preparation, and equipment mobilization. Mobilization fees can also vary widely since the geographic coverage of CPT services are limited mainly to coastal population centers. Additional cost may also be incurred for coring if the media surface is too hard for penetration (cement) or when the sensor probe is frequently refused because of lithologies that are difficult to push. SCAPS CPT/METAL SENSOR or standard SCAPS Membrane Interface Probe (MIP) costs has been quoted as approximately $6,380 per 10-hour day plus per diem. The operating costs for commercially operated CPT services (such as Gregg Drilling and Fugro Geosciences) are less expensive than the government owned SCAPS and typically range from $2,500 to $3,000 per day with a crew of two. Combined with commercially offered XSD-MIP sensor logging service, the overall service price of $4,675 per 10-hour day plus per diem is lower than SCAPS. The higher G&A and administrative costs typically endured by any government service is likely the major driver for the difference.

6.3 Performance Observations

The primary performance objective for XSD-MIP in this evaluation was that it provides semi-quantitative data necessary to locate halogenated DNAPL along with the high VOC concentrations that strongly indicate the presence of DNAPL. As summarized in Figure 43 and Figure 71for NAS North Island and Camp Lejeune respectively were somewhat mixed with inconclusive correlations for North Island and quite good correlations at Camp Lejeune results also showed that spatial heterogeneity can contribute to high variability in results. The higher sampling rates associated with *in situ* sensor systems such as the XSD-MIP may provide improved delineation of contaminant zones compared to information derived from a small number of discrete samples.

6.4 Scale up

Unlike remediation technologies there are very few scale up issues anticipated in moving from demonstration to full-scale implementation of this field screening system. Direct push platforms capable of deploying the sensor systems used in these demonstrations are readily available from several commercial vendors with Fugro Geosciences and Gregg Drilling being two examples.

The capability for deploying the XSD-MIP sensor from platforms of opportunity was demonstrated during this project by deploying the sensors from two different penetrometer platforms (the SSC San Diego SCAPS system and the Navy Publics Works Center SCAPS out of Norfolk, VA). DTI has previously integrated this and several other direct push sensors into commercial CPT systems. DTI has recently outfitted the U.S. Army Corps of Engineer's SCAPS truck in Kansas City with a fully operational XSD-MIP system. DTI is also prepared to offer the XSD-MIP service in cooperation with commercial vendors of CPT service. Although no commercial jobs have been conducted with private party funding, we have submitted proposals for DNAPL characterization along with Fugro Geosciences who will be supplying the CPT service portion.

6.5 Other Regulatory Issues

Lack of regulatory acceptance by both Federal and State regulatory agencies has traditionally been cited, as major obstacle to implementation of innovative site characterization techniques on DOD sites. ESTCP has previously funded (or partially funded) efforts to help establish regulatory acceptance of the SCAPS Laser Induced Fluorescence (LIF) sensor for rapid subsurface detection of petroleum, oil and lubricants and SCAPS Heavy Metal Sensors for mapping subsurface metal contamination. Significant lessons were learned from these efforts. Most notably, there appears to be no single path to gain universal acceptance of new technology by the regulatory community. The LIF sensor for petroleum hydrocarbons was the first major chemical sensor system developed for this SCAPS system. During the early stages of technology transfer of the LIF sensor a common question raised by potential user was: "Is the technology approved by the regulators?" From this question grew the concept that if the LIF technology were "approved" by the regulatory community then the users would embrace it. The quest for regulatory approval led to a successful multi-year effort to gain regulatory acceptance for the SCAPS LIF sensor technology based on assembling a comprehensive set of field measurements that directly compare the performance of the sensor system with traditional US EPA methods for a variety of contaminants under different hydrogeological conditions. The cornerstone of obtaining as broad an acceptance as possible was the linking these technical efforts with multi-state and national certification/verification programs such as the US EPA Consortium for Site Characterization Technology "verification" program and "certification" by the California EPA Department of Toxic Substance Control's Technology Certification Program (Cal Cert). For the case of the SCAPS nitrogen laser LIF sensor system, these opportunities were subsequently linked to the Western Governors Association, Demonstrating Onsite Innovative Technologies (WGA/DOIT) project. Interest by the WGA/DOIT project subsequently led to the establishment of a SCAPS-LIF Interstate Technology and Regulatory Cooperation (ITRC) workgroup, Technology Specific Task Group (TSTG) with the goal to achieve acceptance by each of the seven TSTG member-states (Utah, Nebraska, New Mexico, Louisiana, New Jersey, Idaho, California) and using California Certification (Cal Cert) as the protocol. For the SCAPS nitrogen laser LIF system these efforts resulted in the successful certification by the Cal Cert Program [21], verification by the US EPA [22], 1997) and endorsement of the Cal Cert certification by the WGA [23].

However, experience has shown that obtaining regulatory acceptance does not automatically insure user acceptance. While regulatory acceptance is a desirable goal, the users must be convinced that the new technology will enable them to do their jobs faster, better, and cheaper.

Experience from the SCAPS LIF program suggests that user acceptance is built one user at a time. Discussions with both government and commercial LIF service providers indicate that the key to growing the business is to provide a product that meets the customers needs at a competitive price (personal communications, Tim Shields, PWC San Diego, San Diego California; Racyp Yilmaz, Fugro Geoscience, Inc., Houston, Texas). Satisfied users generate repeat business and tell other perspective customers. In retrospect, experience seems to suggest that many perspective users that initially expressed reluctance to use SCAPS LIF because of "lack of regulatory acceptance" may have found other reasons not to use a new technology even if the regulatory community approved the technology.

Based on lessons learned from the SCAPS LIF sensor technology it appears the most effective means to promote acceptance of a new field screening technology is to aggressively market the technology and grow a user base for the technology. Because of the high turnover in personnel, both the user and regulatory community experience suggests that a long term and persistent marketing effort is required to establish a new technology. In general, a motivated commercial vendor has the capability to rally more marketing savvy (knowledge and experience) for a product or service than does a government technology developer. While the SCAPS LIF ESTCP project focused almost exclusively on gaining acceptance of the technology by regulators, the efforts of the SCAPS metal sensor ESTCP project were directed more towards generating a link with commercial partners that ultimately take the lead for marketing the technologies to both users and regulators. It is believed that this strategy has the advantage of offering a longer term solution to the difficult problem of nurturing a new technology through its' infancy than the previous approach that focused almost exclusively on the single issue of regulatory acceptance at the expense of other factors required for successfully establishing a new technology in the marketplace. Finally, experience from the SCAPS LIF and metals sensor project has shown that users are often slow to accept new methods and technologies due to limited exposure, inadequate technical understanding, and lack of high quality validation data that support developers and/or vendor claims. Ultimately, acceptance requires exposure leading to understanding, as well as comprehensive data validation of the type that is generated in ESTCP demonstrations.

6.6 End-User Issues

Two parallel paths exist for the transition of the technologies that will be demonstrated as part of this effort. One path is to transition the technology directly to government owned/operated systems. The DoD currently operates 5 cone penetrometer systems (three Army SCAPS systems and 2 Navy SCAPS systems). In addition the Department of Energy (DOE) and Environmental Protection Agency each operate a CPT system. All five DoD systems are operated on a fee per service basis for work at government facilities. The operators of these are motivated to expand the sensing capabilities that they offer because it helps to generate new business. As part of this Dem/Val program we plan to keep these users informed of our efforts and to invite them to attend the field demonstrations so that they can view the technologies in operation in the field. The SCAPS user community holds a user meeting as least once a year. We intend to have a representative attend the SCAPS user meeting to update all DoD, DOE and US EPA users on the status of the technologies that will be demonstrated as part of this effort.

The second path for transition of the technologies presented in this effort is directly to the commercial sector. This will be directly facilitated via DTI's efforts to commercialize these

technologies and through the use of CRADA's for transferring the technology to the commercial sector. DTI is currently negotiating licensing agreements with Fugro Geosciences, Inc for the use of LIF technologies. DTI already has a license for the use of the MIP with downhole sensors. DTI is a service provider on its own GeoProbe platform. SSC-SD currently has a CRDA with Fugro Geosciences Inc. for the technology transfer of the GeoVIS video imaging system.

6.7 Other Significant Observations

Temperature control of the MIP during continuous logging appears to be one of the key factors in obtaining consistent quantitative performance. Sandy water-saturated soils are sometimes difficult to heat to sufficient temperatures, possibly due to the relatively high water content and the resulting high thermal conductivity of this matrix. It is very important to maintain even temperatures above boiling in order to produce the "steam" that seems to be necessary for efficient mass-transport of the HVOCs into the carrier stream behind the MIP and ultimately into the XSD for measurement. The MIPS used in this demonstration operated at 50V. An 110V version of the MIP has recently become available from Geoprobe. This higher voltage version has since been tested by DTI and this higher-powered version has had the ability to provide more raw heating power to the matrix and therefore maintain the proper temperatures more consistently.

While trends were not clearly definable from the limited data produced in this demonstration, matrix effects from differing soil types (sands, silts, clays) clearly have an impact on the efficiency of the mass transfer of HVOCs across the membrane. This has a direct effect on the signal observed from the XSD. While these effects can be significant, the logs still show the relative distribution of possible DNAPL, dissolved phase "hotspots", and their trends sufficiently enough to isolate and identify the most probable depths and locations of the DNAPL source term.

6.8 Lessons Learned

The XSD-MIP logs generated during this demonstration have the same innate ability to convey relative concentrations of contaminant vs. depth as SCPAPS and ROST LIF. The XSD-MIP logs provide an intuitive graphical representation of HVOC concentrations vs. depth. Even though the logs are not analytically accurate in a quantitative sense, they are invaluable in their ability to instantly paint a picture of the subsurface HVOC distribution. The CPT delivered XSD-MIP system provides an unparalleled ability to "hunt and seek" DNAPL and its associated high dissolved phase HVOCs. It is difficult to fully convey the benefits of the immediate feedback the logs give the geologist in the hunt for DNAPL source terms when one is necessarily constrained to follow up the logging with validation and confirmation sampling. Deciding where to place a transect, conducting tests along that transect, and then sampling and comparing soils and waters retrieved from that transect, are obviously necessary and desirable for the purposes of a demonstration like this. But the true value of tools such as the XSD-MIP are their ability to be used in a real-time sense to adaptively move about the site, follow gradients toward locations with higher signal levels both laterally and horizontally, and finally pinpoint the true hotspots and likely DNAPL source term areas. While DNAPL source terms were successfully located along some of the transects, the true value of this and other SCAPS type tools is only realized when free ranging characterization is allowed. Until a demonstration format is developed that

allows this aspect of the technology to dominate, the demonstrations will never be capable of fully conveying the technology's promise.

6.9 End-User Issues

DTI has been a leading researcher and commercial vendor of various CPT and Geoprobe logging equipment for the past decade. Even with close working relationships with CPT service vendors such as Fugro Geosciences of Houston, TX and Geoprobe Systems of Salina, KS, commercialization has been difficult. Restrictive licensing issues with the sapphire window based technologies (LIF, LIBS, etc.) have prevented the technology from being utilized. Other MIP-based technologies, including the XSD-MIP discussed here, have been hampered by criticisms concerning the repeatability of the soil/water-to-MIP interface and subsequent consistency of the transport of VOCs across the membrane of the MIP with varying temperature, pressure, and other variables.

While DTI has offered the XSD-MIP as a product and has, in fact, provided estimates for full XSD-MIP systems to companies such as Fugro, we have yet to make any commercial sales of the system. Any discussion of the system's performance inevitably leads to questions as to whether the system can yield data that are 'equivalent' to traditional sample grabs and lab analysis. Of course the answer is no, since it is after all a screening tool and is incapable of achieving analytical performance in real time on the inherently heterogeneous matrix of the subsurface. There has been an insistence by both the potential commercial providers and their customers that the XSD-MIP is capable of providing "ground truth" quantitative accuracy or the data will not be valuable. Honest admission that it simply isn't capable of such accuracy has inevitably resulted in a reluctance to purchase the equipment or use it on sites. Until the environmental community begins to accept a screening tool's limitations and embrace its positives, without getting buried in discussions of meeting/matching grab sample and lab analyses approaches, their commercial application will remain limited and it will be difficult to sustain any service/business based on them.

6.10 Approach to Regulatory Compliance and Acceptance

As described earlier, the XSD-MIP sensor evaluated as part of this effort represents only one of a suite of sensor systems that have been developed or that are still under development for deployment with direct push systems. The LIF sensor for petroleum hydrocarbons was the first major chemical sensor system developed for this system. During the early stages of technology transfer of the LIF sensor a common question raised by potential user was: "Is the technology approved by the regulators?" From this question grew the concept that if the LIF technology were "approved" by the regulatory community then the users would embrace it. The quest for regulatory approval led to a successful multi-year effort (partially funded by ESTCP) to gain regulatory acceptance for the SCAPS LIF sensor technology based on assembling a comprehensive set of field measurements that directly compare the performance of the sensor system with traditional EPA methods for a variety of contaminants under different hydrogeological conditions. The cornerstone of obtaining as broad an acceptance as possible is linking these technical efforts with multi-state and national certification/verification programs such as the US EPA Consortium for Site Characterization Technology "verification" program

and “certification” by the California EPA Department of Toxic Substance Control’s Technology Certification Program (Cal Cert). For the case of the SCAPS nitrogen laser LIF sensor system, these opportunities were subsequently linked to the Western Governors Association, Demonstrating Onsite Innovative Technologies (WGA/DOIT) project. Interest by the WGA/DOIT project subsequently led to the establishment of a SCAPS-LIF Interstate Technology and Regulatory Cooperation (ITRC) workgroup, Technology Specific Task Group (TSTG) with the goal to achieve acceptance by each of the seven TSTG member-states (Utah, Nebraska, New Mexico, Louisiana, New Jersey, Idaho, California) and using California Certification (Cal Cert) as the protocol. For the SCAPS nitrogen laser LIF system these efforts resulted in the successful certification by the Cal Cert Program [21], verification by the US EPA [22] and endorsement of the Cal Cert certification by the WGA [23].

Significant lessons were learned from the Tri-Service SCAPS Program in the process of obtaining regulatory acceptance of the SCAPS LIF sensor. Specifically, there appears to be no single path to gain universal acceptance of new technology by the regulatory community. However, and probably more importantly, it was learned that obtaining regulatory acceptance does not guarantee user acceptance. While regulatory acceptance is a desirable goal, if the users cannot be convinced that the new technology will enable them to do their jobs faster, better, and cheaper then it will be slow to establish itself in the marketplace. Experience from the SCAPS and ROST LIF programs suggests that user acceptance is achieved one user at a time. Discussions with both government and commercial LIF service providers indicate that the key to growing the business is to provide a product that meets the customer’s needs at a competitive price (personal communications, Tim Shields, PWC San Diego, San Diego California; Recep Yilmaz, Fugro Geosciences, Inc., Houston, Texas). Satisfied users generate repeat business and tell other perspective customers. Regulatory approval by itself may not generate user acceptance. In retrospect, experience seems to suggest that many perspective users that initially expressed reluctance to use SCAPS or ROST LIF because of “lack of regulatory acceptance” may have found other reasons not to use a new technology even if the regulatory community approved the technology.

Based on lessons learned from the SCAPS LIF sensor technology it appears the most effective means to promote acceptance of a new field screening technology is to aggressively market the technology and grow a user base for the technology. Experience suggests the need to convince individual users and regulators of the merits of the technology coupled with the fact that there is often high turnover in both communities requires a long-term and persistent marketing effort. In general, a motivated commercial vendor has the capability to rally more marketing savvy (knowledge and experience) for a product or service than does a government technology developer. It is believed that a strategy of commercialization based mainly on customer need and not necessarily on the views or formal acceptance of regulators has the advantage of offering a longer term solution to the difficult problem of nurturing a new technology through its’ infancy than the previous approach that focused almost exclusively on the single issue of regulatory acceptance at the expense of other factors required for successfully establishing a new technology in the marketplace.

During the SCAPS LIF ESTCP project, it also became apparent that, in general, regulators and users are often slow to accept new methods and technologies due to limited exposure, inadequate technical understanding, and lack of high quality validation data that support developers and/or vendor claims. Ultimately, acceptance requires exposure that leads to understanding, as well as

comprehensive data validation. With the goal to document the performance of these sensor systems under various conditions with "hard data," a comprehensive effort was conducted to make available the results of this demonstration/validation program as well as related work. To inform regulators, government agencies, and commercial users, the XSD-MIP technology should be presented in national and international environmental conferences and peer-reviewed, scientific journals. The XSD-MIP technology should also demonstrated at the annual SCAPS User's meetings.

7 References

1. Schwille, F., *Dense Chlorinated Solvents in Porous and Fractured Media*. 1988, Chelsea, Michigan: Lewis Publishers, Inc. 146.

2. Pankow, J.F. and J.A. Cherry, *Dense Chlorinated Solvents and other DNAPLs in Groundwater: History, Behavior, and Remediation*. 1996, Portland, Oregon: Waterloo Press. 522.

3. Feenstra, S., J.A. Cherry, and B.L. Parker, *Conceptual Models for the Behavior of Dense Non-Aqueous Phase Liquids (DNAPLs) in the Subsurface*, in *Dense Chlorinated Solvents and other DNAPLs in Groundwater: History, Behavior, and Remediation*, J.A. Cherry, Editor. 1996, Waterloo Press: Portland, Oregon. p. 53-88.

4. Benson, M., *State EPA Study Finds PCE in Many Wells*, in *The Wall Street Journal*. 1966.

5. Fountain, J.C., *Technologies for Dense Nonaqueous Phase Liquid Source Zone Remediation: Technology Evaluation Report*. 1998, Ground-Water Remediation Technologies Analysis Center: Pittsburg, PA.

6. ESTCP, *ESTCP Cost and Performance Report: Tri-Service Site Characterization and Analysis System (SCAPS) Thermal Desorption Sampler for Volatile Organic Compounds.* 2001, Environmental Security Technology Certification Program: Arlington, VA. p. 32.

7. Interstate Technology and Regulatory Cooperation Work Group - DNAPLs/Chemical Oxidation Work Team, *Dense Non-Aqueous Phase Liquids (DNAPLs): Review of Emerging Characterization and Remediation Technologies*. 2000. p. 59.

8. Brown and Caldwell, *Initial Assessment Study of Naval Air Station North Island, San Diego.* 1983.

9. Jacobs Engineering Group, I., *Naval Air Station North Island, North Island, San Diego, California, RI/RFI Report, Site 9, Chemical Waste Disposal Area.* 1995.

10. Kennedy, *Geology of the San Diego Metropolitan Area, California.* California Division of Mines and Geology, 1975. **Bulletin 200**.

11. Baker Environmental Inc., *Remedial Investigation, Operable Unit No. 16 (SITES 89 AND 93), MCB Camp Lejeune, North Carolina*. 1998: Coraopolis, Pennsylvania. p. 258.

12. Cardinell, A.P., S.A. Berg, and L.O.B. Jr., *Hydrogeologic Framework of U.S. Marine Corps Base at Camp Lejeune, North Carolina.* 1993, USGS. Water-Resources Investigations.

13. Baker Environmental Inc., *Letter Report for Operable Unit No. 16, Site 89*. 1999. p. 22.

14. Costanza, J. and W. Davis, *"Rapid Detection of Volatile Organic Compounds in the Subsurface by Membrane Introduction into a Direct Sampling Ion Trap Mass Spectrometer.* Field Analytical Chemistry and Technology, 2000. **4**(5).

15. Feenstra, S. and J.A. Cherry, *Diagnosis and Assessment of DNAPL Sites*, in *Subsurface. In Dense Chlorinated Solvents and other DNAPLs in Groundwater: History, Behavior, and Remediation*, J.A. Cherry, Editor. 1996, Waterloo Press: Portland, Oregon. p. 395-465.

16. Lieberman, S.H., *Direct Push Chemical Sensors for DNAPLS Demonstration/Validation, Technology Demonstration Plan at Site 9 Naval Air Station North Island*. 2001, SSC San Diego: San Diego, CA. p. 60.

17. Schroeder, J.D., S.R. Booth, and L.K. Trocki, *Cost effectiveness of the Site Characterization and Analysis Penetrometer System*. 1991, Los Alamos National Laboratory.

18. ESTCP, *ESTCP Cost and Performance Report: POL Sensor Validation of SCAPS*. 1997, Environmental Security Technology Certification Program: Arlington, Virginia. p. 25.

19. ESTCP, *ESTCP Cost and Performance Report: SCAPS Heavy Metals Sensors*. In Press, Environmental Security Technology Certification Report: Arlington, Virginia.

20. Lieberman, S.H., et al., *Environmental Security Technology Certification Program (ESTCP)*
Site Characterization and Analysis Penetrometer System (SCAPS) Heavy Metal Sensors Demonstration/Validation: Cost and Performance Report, in *ESTCP*. 2002. p. 42.

21. California Environmental Protection Agency Department of Toxic Substances Control, *Final Hazardous Waste Technology Certification Program Report: Site Characterization and Analysis Penetrometer System with Laser-Induced Fluorometry (SCAPS-LIF) as an in-situ field screening technology for the detection of PNA-containing Petroleum Hydrocarbons*. 1996. p. 47 pages.

22. Bujewski, G. and B. Rutherford, *Innovative Technology Verification Report: The Site Characterization and Analysis Penetrometer System (SCAPS) Laser-Induced Fluorescence (LIF) Sensor and Support System*. 1997, US Environmental Protection Agency, National Exposure Research Laboratory: Las Vegas, Nevada. p. 83 pages.

23. Cone Penetrometer Task Group Report, *Multi-State Evaluation of an Expedited Site Characterization Technology: Site Characterization and Analysis Penetrometer System Laser-Induced Fluorescence (SCAPS-LIF)*. 1996, Western Governors' Association DOIT Initiative, Interstate Technology and Regulatory Cooperation Workgroup. p. 12 pages.

8 Points of Contact

POINT OF CONTACT Name	ORGANIZATION Name Address	Phone/Fax/Email	Role In Project
Dr. Stephen H. Lieberman	SSC-SD 2112, 53475 Strothe Rd., San Diego, CA 92152	619-553-2778 voice 619-553-2778 FAX stephen.lieberma@navy.mil	Principal Investigator
Dr. Greg Gillispie	Dakota Technologies, Inc 2201A 12th St. N., Fargo, ND 58102	701-237-4908 voice 701-237-4926 FAX, gillispie@dakotatechnologies.com	Co-Principal Investigator
Mr. Randy St.Germain	Dakota Technologies, Inc 2201A 12th St. N., Fargo, ND 58102	710-237-4908 701-237-4926 FAX stgermain @dakotatechnologies.com	Technical Lead-High Res. Fluorescence
Mr. Paul Jarski	Dakota Technologies, Inc 2201A 12th St. N., Fargo, ND 58102	701-237-4908 voice 701-237-4926 FAX, pjarski@dakotatechnologies.com	Technical Lead-XSD Detector
Mr. Jed Constanza	Georgia Tech 200 Bobby Dodd Way Atlanta, GA 30030	(404) 894-3087 jed64@bellsouth.net	Technical consultant

Appendices

Appendix A: Analytical methods Supporting the Experimental Design

Method SW-848 Method 8260b Volatile Organic Compounds by Gas Chromatography/Mass Spectrometry (GC/MS)

The complete method is available at the following web site:
http://www.epa.gov/epaoswer/hazwaste/test/8260b.pdf

Appendix B: Analytical Methods Supporting the Sampling Plan

D3441-05 Standard Test Method for Mechanical Cone Penetrometer Tests of Soil

The complete method D3441-98 is available at the ASTM web site at: http://www.astm.org/cgi-bin/SoftCart.exe/DATABASE.CART/PAGES/D3441.htm?L+mystore+gbse7944

Appendix C: Quality Assurance Project Plan (QAPP)

The quality assurance (QA) plan for this demonstration specifies procedures that will be used to ensure data quality and integrity. Careful adherence to these procedures will ensure that data generated from the demonstration will meet the desired performance objectives and will provide sound analytical results.

1 Purpose and Scope

The primary purpose of this QA plan is to outline steps that will be taken by SSC-SD, Dakota Technologies and Georgia Tech and the confirmatory analytical laboratory to ensure that data resulting from this demonstration are of known quality and that a sufficient number of critical measurements are taken. This section of the demonstration plan addresses the key elements that are required according to guidelines in the US EPA guidance document "A Guidance Manual for the Preparation of Site Characterization Technology Demonstration Plans" (EPA 1995).

2 Quality Assurance Responsibilities

The SSC-SD Program Manager is responsible for coordinating the preparation of the QA plan for this demonstration and for its approval. The SSC-SD Program Manager, in conjunction with the DTI, and Georgia Tech project teams, will ensure that the QA plan is implemented during all demonstration activities. The Georgia Tech technical consultant, Mr. Jed Costanza, will review and approve the QA plan and will provide independent QA oversight of all demonstration activities.

Data will be collected and analyzed in two ways: on site by the SCAPS direct push sensor technologies (XSD, HRF, and GeoVIS) using quantitative and qualitative field methods, and off site by analysis of soil samples collected and shipped off site for analysis by the confirmatory laboratory using a quantitative US EPA laboratory method. Many individuals will be responsible for sampling and analysis quality assurance/quality control (QA/QC) throughout the demonstration. Primary responsibility for ensuring that sampling activities comply with the requirements of the sampling plan (Section 5) will rest with the Georgia Tech QA manager. QA/QC activities for the three direct push DNAPL sensor technologies will include those activities required to assure the demonstrations will provide data of the necessary quality.

QA/QC activities for the confirmatory laboratory analysis of samples will be the responsibility of the analytical laboratory's QA officer. If problems arise or any data appear unusual, they will be thoroughly documented and corrective actions will be implemented as specified in Sections 4

and 5 of this QA plan. The QA/QC measurements made by the confirmatory laboratory are dictated by the analytical methods being used.

3 Data Quality Parameters

The data obtained during the demonstration must be of sound quality for conclusions to be drawn on the three SCAPS direct push DNAPL sensor technologies. For all measurement and monitoring activities conducted, data quality parameters should be established based on the proposed end uses of the data. Data quality parameters include five indicators of data quality: representativeness, completeness, comparability, accuracy, and precision.

Data generated by the three SCAPS sensor technologies will be compared to the data generated from US EPA Method 8260b and visual observations supplemented with visual observations enhanced with Sudan Red dye [15].. High quality, well-documented confirmatory laboratory results are essential for meeting the purpose and objectives of this demonstration. Therefore, the following indicators of data quality will be closely evaluated to determine the performance of the technology when measured against data generated by the confirmatory laboratory.

3.1 Representativeness. Representativeness refers to the degree to which the data accurately and precisely represent the conditions or characteristics of the parameter represented by the data. In this demonstration, representativeness will be ensured by executing consistent sample collection and handling procedures, including sample locations, sampling procedures, sample storage, sample packaging, sample shipping, and sample equipment decontamination (Section 5). Representativeness also will be ensured by using each method at its optimum capability to provide results that represent the most accurate and precise measurement it is capable of achieving.

Note that soil stab sampling was chosen for this demonstration because it is currently the standard method being used during site characterization by the SCAPS CPT. In general site characterization, sampling is not performed with the density of samples (approx. 1 per foot collected throughout the boring) conducted in this demonstration, and so the contaminant location is typically not as well documented. This sampling plan was constructed to provide as precise a measurement of the plume location as possible using the stab sampling method

The sampling plan was also constructed to sample soil from as close to the push locations (horizontally) as possible. It is well known that variations in the contamination level can occur over short horizontal distances (less than 1 foot). To insure that the soil samples are representative of the region sampled by the two direct push sensor probes, the push used for

collection of soil samples will be located within approximately 12 inches from the other two pushes. (Pushes will be positioned so that the push locations form a triangle approximately 12 inches on a side).

3.2 Completeness. Completeness refers to the amount of data collected from a measurement process compared to the amount that was expected to be obtained. For this demonstration, completeness refers to the proportion of valid, acceptable data generated using each method. The overall completeness objective for data generated during this demonstration is 90 percent.

It is anticipated that less than 100 percent completeness of the three SCAPS direct push sensors' data and discrete sample analysis results will occur. A broken, cracked or obstructed sapphire window or a problem with the MIP sampling interface would disqualify the push. Likewise, identification of any broken part of a probe upon retraction would disqualify the push. In addition, a push that was refused due to contact with cobbles, boulders, or a buried obstruction would also be disqualified. A substitute push would be advanced in these cases, generally within 8 inches horizontally of the disqualified push. If slippage greater than 3 inches of the push rod in the hydraulic ram is noted during a push, the data from the push will be disqualified due to excessive depth measurement inaccuracy.

The operating procedure criteria are designed such that the behavior of the three SCAPS sensor technologies is watched closely during a site characterization effort. As a result, the SCAPS metal sensor technologies' operators tend to fix problems before questionable data are generated. If a SCAPS sensing probe were to malfunction, however, such as occurs when a sapphire window becomes cracked, or the MIP sampling port becomes clogged in the case the XSD sensor, the data generated would not be acceptable and the operators would recommend that the sampling location be pushed again after the probe is repaired.

It is also anticipated that less than 100 percent completeness of the discrete soil samples collected will be attained. The data quality officer may note or "flag" those soil samples believed to be collected from disturbed depths. Consequently, these flagged samples would decrease the completeness to below 100 percent.

3.3 Comparability. Comparability refers to the confidence with which one data set can be compared to another. A primary objective of this demonstration is to evaluate how well the SCAPS DNAPL sensing in situ technologies perform in comparison to conventional analytical methods used by a confirmatory laboratory based on the experimental design discussed in

Section 5. Additional QC for comparability will be achieved by analyzing QC samples and blanks for the confirmatory methods in accordance with the confirmatory analytical laboratory's SOPs to be provided in an Addendum upon analytical laboratory selection and by adhering to methods for sample preparation and instrument operation for the SCAPS CPT.

Because an in situ measurement will be compared with a conventional laboratory measurement, it is not possible to ensure absolute comparability of the two measurement methods. It is believed, however, that the proposed approach of pushing the soil stab sampling push in close proximity to the SCAPS metal sensor push holes will minimize, but not necessarily eliminate, potential noncomparability issues that result from the sampling process. The following subsection regarding accuracy further describes issues involved in comparing in situ, field methods with laboratory methods.

It should be noted that the analytical and SCAPS CPT deployed methods for quantifying and qualitatively determining DNAPL contamination discussed in this document (namely the analytic method, US EPA 8260b (GC/MS)), and the SCAPS methods XSD, HRF, and GeoVIS) measure and quantify the amount of contaminant differently. The analytical method tests a digested sample that represents an "average" result for that sample, whereas, the SCAPS sensors test a small and discrete sample spot. Additionally, sharp vertical and horizontal boundaries of the contamination plume may cause each sensor to have different results due to spatial differences in the samples being evaluated in situ and in the laboratory. In order to attempt to account for some of this small scale spatial variability in situ data will be averaged over several measurements that correspond to the depth interval of the core sample that is shipped to the laboratory for analysis.
The GC/MS method employs a solvent extraction technique to remove and concentrate the contaminant from the soil. The measurement from the extract is compared to a curve generated by standards made with known concentrations of analytes. These in situ methods do not use an extract from the soil sample, but measure the contaminant in situ as it is comes in contact with the membrane sampling system or the window of the sensor. For this reason, the in situ sensors can be more sensitive to matrix effects.

3.4 Accuracy. Accuracy refers to the degree of agreement of a measurement to the true value. With conventional laboratory-based measurements, the accuracy of the method is a function of both the sampling errors and errors associated with the measurement method. To evaluate the accuracy of a laboratory method, the conventional approach is to compare the results obtained from analysis of a spiked sample of known concentration. Errors related to sampling are not addressed. Because there is no independent measure of the subsurface value of

contaminant concentration, it will be necessary to evaluate the accuracy of the in situ measurement by comparing in situ results with results from conventional methods that may not provide a true value of the subsurface contaminant distribution because of errors associated with the sampling process itself. However, this sampling problem should be minimized by comparing the averaged in situ sensor data with the analytical laboratory's results for the homogenized soil samples.

Another difference between in situ and conventional laboratory-based measurements is that laboratory measurements usually employ extraction or matrix simplification procedures, whereas in situ measurements offer limited opportunities for controlling matrix effects. Because it is not possible to account for all sources of variability that affect sensor response at this time, the sensors are intended to operate as field screening methods, and will provide only semi-quantitative data on the distribution of DNAPL contamination.

Recognizing the limitations stated above, the accuracy of the SCAPS DNAPL sensors will be evaluated by directly comparing in situ data with data from samples analyzed by a traditional laboratory method (GC/MS). This comparison will be made by collecting soil samples for laboratory analysis directly adjacent to the DNAPL sensors push locations using the SCAPS CPT equipped with a soil stab sampler. US EPA Method 6820b will be used to evaluate the accuracy of the three SCAPS DNAPL sensors as field screening methods for DNAPLs because it represents the most frequently used laboratory method employed to delineate subsurface distributions of DNAPLs in soils.

The approach for evaluating accuracy presented here depends on direct comparison of in situ sensor data with analysis of discrete samples collected as close as possible to the soil sample measured by the in situ sensor and on comparison of reevaluation of the homogenized soil samples. Although it is believed that this approach provides the best opportunity for evaluating the accuracy of the in situ measurement, it should be noted that it will not be possible to account for all variability associated with the uncertainty in depth from which the discrete samples are collected. It is possible that the depth of the discrete sample may be in error by up to 3 inches in the vadose zone. In stratified conditions, this sampling error could lead to poor comparisons between in situ data and laboratory data. In addition, because there will be several inches of horizontal offset between the push location and the location of the stab sampler, there may also be some small-scale horizontal variability of up to 4 inches that will not be accounted for. Both the vertical uncertainty and a smaller-scale horizontal variability may also be a factor when comparing the laboratory method because the soil samples will be obtained from different locations within the same 6.6-inch hollow tube. Thus, these soil samples will be homogenized in

order to minimize differences due to sample location and heterogeneity. Accuracy for the confirmatory laboratory methods will be evaluated by the QA/QC data generated by the analytical laboratory while adhering to the SOPs for the methods provided in an Addendum.

3.5 Precision. Precision refers to the reproducibility of measurements of the same characteristic, usually under a given set of conditions. Because the three SCAPS sensors' primary utility is for in situ sensing as the probe is pushed into the ground, it will not be possible to obtain precision data for the sensor under conditions that exactly duplicate the manner in which in situ measurements are made in the subsurface. The main difference is that for in situ measurements the standard operating procedure for the SCAPS DNAPL sensor systems automatically integrates signals as the probe is being pushed into the ground. Therefore, the standard in situ measurement integrates the resulting signal (effectively averaging) from a series of discrete locations on the soil.

Although there is no method currently available that can duplicate the above measurement procedure, the precision of the method can be estimated from static measurements made with the probe on the surface. The estimate of the precision of the method will be obtained by placing a standard sample containing a known concentration of a chlorinated hydrocarbon (for example, 1 parts per million (ppm) TCE solution flowed over the MIP) and measuring the sample using the same system settings as that will be used during pushing. This procedure should, therefore, provide a best-case estimate of the precision of the method. Experience indicates that precision of better than ±10 % (1 standard deviation) can be obtained using the appropriate integration times for the XSD sensor.

Precision for the confirmatory laboratory methods will be evaluated by the QA/QC data generated by the analytical laboratory while adhering to the SOPs for the methods provided in an Addendum once the analytical laboratory has been selected.

4 Calibration Procedures, Quality Control Checks, and Corrective Action

Calibration procedures, method-specific QC requirements, and corrective action associated with nonconformance QC for the three SCAPS DNAPL sensor technologies and the reference methods are described in the following subsections.

4.1 XSD calibration. At the start of each day and after each push, a calibration of the XSD is performed to characterize the performance of the XSD. The calibration procedure utilizes a dual reservoir flow cell to flow a known concentration calibration solution containing a

chlorinated solvent (whichever solvent is appropriate for the site being analyzed) over the MIP. The procedure for calibration of the MIP/XSD is given below:

4.1.1. Initial Startup of MIP and XSD

- Set flow rate of air to system between 20-40 mL/min. (Do not exceed 30 psi back pressure). Confirm flow from umbilical cable return line. If flow is low or absent, refer to Gas Flow Troubleshooting in Corrective Action section.
- Attach flow cell to MIP. Turn MIP and XSD heater controllers on. If either the MIP or XSD fail to respond, refer to the appropriate Corrective Action section.
- Start data collection program; monitor signal vs. time and XSD temperature vs. time. Visually monitor MIP temperature
- Continue data collection until baseline signal and XSD temperature have been stable for five minutes
- Stop run, record data file name in logbook
- Save the data file to a floppy disk and print out three copies of the raw graphical data. Place one printout in logbook.
- If the baseline signal levels are greater than ±25% of previously collected data, consult the appropriate Corrective Action section below.

4.1.2 XSD-MIP Saturation Response Calibration (SRC) Process:

A calibration flow cell is placed over the MIP and a controlled flow of water containing the SRC calibrant is flowed over the membrane in a continuous fashion. The calibrant flow system, consisting of reservoirs, tubing, and a peristaltic pump assures consistent delivery of fresh SRC calibrant to the flow cell. This allows stable signals to be achieved without the drop in signal due to loss of analyte that would occur with "splash" applications of fixed volumes of SRC calibrant. Clean water is also flowed across the MIP for baseline (zero) determination. The entire SRC process is documented here (4.1.2 in original proposal):

SRC profile acquisition:

- Prepare a very large volume of SRC stock solution by allowing water to be in contact with DNAPL (neat TCE here) for no less than 48 hours. This solution will be used for all of the subsequent calibrations for the demonstration. The SRC reservoir will also contain neat TCE to keep the TCE concentration constant over time.
- Pour the SRC solution prepared in the previous step into the calibration bottle of the dual reservoir. Fill the clean water reservoir bottle and place on the pump system.

- Make sure pump inlet is set to clean water bottle.
- Start data collection program. Monitor signal vs. time and MIP temperature vs. time.
- Collect three minutes of baseline. At three minute mark, turn on flow cell system. Inspect flow cell system for leaks; tighten as necessary to obtain a leak free system.
- Continue water flow until the MIP temperature returns to the setpoint. Allow water to flow for one additional minute. Record average baseline signal of XSD.
- Switch valve to calibration solution. Record time (from program) in logbook.
- Monitor XSD signal, allow signal to come to steady state, record time from program in logbook. Collect two additional minutes of stable signal.
- Switch pump valve to water bottle, record time in logbook. Allow XSD signal to return to baseline signal. Collect two additional minutes of baseline.
- End run, turn off water flow, and record data file name in log book.
- Save the data file to a floppy disk and print out three copies of the raw graphical data. Place one printout in the logbook.
- Repeat replicate run of another SRC solution.
- If the baseline signal or the analyte signal levels are greater than ±25% of previously collected data, consult the appropriate Corrective Action section below.

Data normalization process:

- Background correct each SRC profile by subtracting the average baseline signal collected at the start of the run.
- For each SRC profile, take the average SRC signal over the range in the profile where the SRC solution was producing a stable signal.
- Calculate the mean SRC value by finding the average of all of the individual SRC averages.
- Divide the mean SRC analyte signal by the average SRC value for each SRC profile in order to create a correction factor for each in-situ profile. (This allows normalization without loss of the mV units)
- Background correct each in-situ profile using the average baseline signal collected at the start of the run.

Multiply the in-situ profiles by its associated SRC correction factor.

4.1.3 Analytical procedure for MIP/XSD for in-situ measurements

- Insure that the XSD is at a stable operating temperature (800-1000 °C)
- Insure the MIP is hot (110-130 °C)
- Push MIP membrane to level of ground surface. Record depth. This will be the ground zero depth for the ensuing push.

- Begin data acquisition program
- Begin probe advancement at 0.5 cm/sec.
- Continue probe advancements until maximum probe depth is achieved, probe advancement is rejected, or deepest suspected contamination level is surpassed
- End run and record data file name in logbook.
- Save the data file to a floppy disk and print out three copies of the raw graphical data. Place one printout in the logbook.
- Extract probe from subsurface maintaining sufficient temperature of MIP to minimize water intrusion during extraction.

4.1.4 Analytical procedure for MIP/XSD after extraction

- Upon extraction, place MIP in standby mode. Allow MIP temperature to reach 50 °C.
- Clean off membrane with steel brush. Wash off membrane with distilled water. Visually inspect membrane for damage.
- Place Flow cell on MIP.
- Place MIP in run mode.
- Perform one calibration of the MIP/XSD following procedure given in Calibration of MIP/XSD system.

4.1.5 Corrective Action

4.1.5.1 XSD Troubleshooting

- Check power supply to see if current is being supplied to XSD. If power supply fails to turn on, check if 120 VAC is being supplied. If it is, check fuse of power supply

    - If power supply is operating correctly, check thermocouple connection to temperature controller
        - If loose or disconnected, tighten and try again
        - If tight, XSD thermocouple has developed short, replace XSD

    - If power supply is on but current is not being supplied, check output connections of power supply (IMPORTANT: Turn off power supply and unplug before checking connections)

        - If output connections are loose or disconnected, tighten and reattempt startup

- If problem still persists, disassemble system
    - Check continuity of reactor core
        - If there is no continuity, reactor core has burned out, replace XSD
        - If continuity is present, check umbilical connections

4.1.5.1 MIP Troubleshooting

- Pour water on MIP
    - If MIP block is hot, IMMEDIATELY turn off system. Thermocouple has developed a short. Locate short and repair. If short is inside XSD, replace entire XSD.
    - If MIP block is not hot, move to next step
- Check that breaker is on
    - If breaker is not on, turn on and reattempt heating procedure
    - If breaker is on, move to next step
- Check temperature controller is fully plugged into its wall mount
    - If temperature controller is loose, tighten and reattempt heating procedure
    - If temperature controller is tight, move to next step
- Check MIP output connections
    - Check output connection going into MIP controller box. (IMPORTANT: This should be done only with power supply off and unplugged)
        - If loose or disconnected, tighten and retry
        - If tight, move to next step
- Disassemble system,
    - Test continuity between heater leads of MIP
        - If open, MIP heater element has burned out; replace MIP
        - If closed, reattach umbilical leads and retry heating.

4.1.5.3 XSD Baseline Troubleshooting

- **XSD baseline signal hovering at 0-20 mV XSD is at normal operating temperature**

- Make sure analog to digital converter (ADC) is on

- Make sure all appropriate connections between ADC and computer are tight

- Check Bias connection
    - Measure battery potential, if low, replace.
    - Measure potential between positive lead and ground of signal cable.
        - If not 45 V, disassemble system and test umbilical.
        - If umbilical connection is sound, bias wire has broken, replace XSD

- Check signal connection
    - Measure resistance between center conductor and ground of BNC connector.
        - If 1 MΩ, current-voltage converter is functioning properly skip next step.
        - If less than 1 MΩ, disassemble system and replace current-voltage converter.

- Check signal connection to ADC
    - If loose or disconnected, tighten and reattempt
    - If tight, move to next step

- Check ground connections
    - Make sure all components are at the same, earth ground

- **XSD baseline signal low, analyte signal levels consistent with historical data**
- This is a normal function of the aging process of the probe head
    - While not absolutely necessary, the baseline signal levels can be returned to previous levels by increasing the XSD temperature at 10 °C increments until baseline signals are at desirable levels.
- **XSD baseline signal erratic or noisy**
    - Check all ground connections.
        - Ground loops and insufficient grounding is the single largest factor for noisy or erratic signal levels. Care must be taken to ensure that all components of the system are at the same, earth ground

    - Check umbilical connections
        - If loose, tighten and retry
        - If tight, move to next step

- If problem still persists, probe head has broken, replace XSD.

4.1.5.4 XSD Signal Troubleshooting

4.1.5.5 Gas Flow Troubleshooting

4.2. HRF Calibration Procedures. The HRF probe will be deployed in a detect/non-detect mode to screen for DNAPL droplets. Because this requires the system to be operated at peak sensitivity, without regard to linear response criteria, a single point calibration is sufficient. This calibration measurement will be conducted immediately prior to each push. This calibration consists of applying a reference emitter solution (M1, a proprietary fluorescent solution in quartz cuvette) against the cleaned window and acquiring a 500 shot average of the resulting fluorescence waveform. This waveform is automatically stored to disk along with all profiles acquired during the push. The total fluorescence intensity, which is simply the summed waveform voltages over time (pico-Volt-seconds (pVs)) is calculated by the computer, recorded and displayed. This value is used to normalize the entire ensuing log. All subsequent waveforms in the push are summed, divided by the calibration value, and displayed as a percentage of this reference emitter. This is referred to as Total Fluorescence Intensity (%) and represents the quantitative aspect of the HRF tool. A reference reading will also take place upon retrieval of the rod string and proper function of the system will be assumed if the post-push reference reading falls within 20% of pre-push reading. If not, the data will be examined to determine if the failure was gradual or sudden, and a determination will be made as to whether all or a portion of the data is viable.

The process of calibrating the HRF system also serves as an end-to-end check of the system function. The shape of the waveform itself is examined to determine that it is consistent with previous experience with M1 and it's maximum intensity falls within acceptable limits of between 800 and 1200 mV peak response. If the reference emitter waveform is not consistent with previous experience or the maximum intensity does not fall within 800 and 1200mV system checkout and debugging will ensue. If the waveform intensity is too high the neutral density filters can be used to attenuate the beam. If the intensity is too low the launch fiber can be moved closer to the excimer beam focal point. The scope should be adjusted so that the

waveform fits within a time window of 300 ns and baseline level signal exists for a minimum of the first 25 ns of the selected time window. A minimum operating energy of 0.6 mJ/pulse will be maintained. If the excimer laser falls below this value a recharge will be conducted and energy levels exceeding 0.6 mJ/pulse will be confirmed.

4.3. GeoVIS Calibration Procedures. The only calibration that is required for the GeoVIS system is to place scale over the viewing window for the camera system and to adjust the focus and electronic scales that is imposed on the images collected with the video system.

4.4 Strain Gauge Calibration. Strain gauge calibration is performed in accordance with ASTM standard D3441. A load cell device and an automated software procedure are used to determine the scale and offset converting strain gauge output in millivolts to tons per square foot, for both the sleeve and cone tip strain gauges. This procedure is required each time a different probe assembly is used or when strain gauge zero checks (performed after each push) differ from zero by more than 1 ton per square foot (TSF) for the sleeve and 10 TSF for the cone tip.

The initial calibration procedure for the reference methods is found in US EPA Method 8260b. The confirmatory analytical laboratory SOPs for this method will be provided in an Addendum once an analytical laboratory has been selected.

4.5 Performance Evaluation Materials. Performance evaluation (PE) samples will not be used for this demonstration. Because the three SCAPS DNAPL sensing technologies are in situ measurement techniques, PE samples cannot be inserted into these dynamic measurement processes.

4.6 Duplicate Samples. Due to the nature of the in situ measurement, duplicate samples cannot be measured in situ by the three SCAPS DNAPL sensors. In an homogeneous environment, nearby pushes are an approximate duplicate measurement.

At the confirmatory analytical laboratory, duplicate samples will be analyzed by the reference methods and 10 percent of the samples will be analyzed in duplicate. This will provide a qualitative assessment of the heterogeneity of the soil matrix. This 10 percent will not be selected randomly; only the samples containing detectable DNAPL contamination will be analyzed in duplicate.

5 Demonstration Procedures

The XSD and HRF sensors require an initial startup period of about 30 minutes each day, then can run without interruption. The GeoVIS does not require a warm-up period. No maintenance is required for any of the sensors except in case of equipment failure. Most components for all three sensors are replaceable in the field in about an hour.

The SCAPS DNAPL sensor operators will verify the completeness of the appropriate data forms and the completeness and correctness of data acquisition and reduction. The confirmatory laboratory or field team supervisor will review calculations and inspect laboratory logbooks and data sheets to verify accuracy, completeness, and adherence to the specific analytical method protocols. Calibration and QC data will be examined by the individual operators and the laboratory supervisor. Laboratory project managers and QA managers will verify that all instrument systems are in control and that QA objectives for accuracy, completeness, and method detection limits have been met.

Analytical outlier data are defined as those QC data lying outside a specific QC objective window for precision and accuracy for a given analytical method. Should QC data be outside of control limits, the confirmatory laboratory or field team supervisor will investigate the cause of the problem. If the difficulty involves an analytical problem, the sample will be reanalyzed. If the problem can be attributed to the sample matrix, the result will be flagged with a data qualifier. This data qualifier will be included and explained in the final analytical report. A copy of the confirmatory laboratory's Quality Assurance Manual will be included along with the laboratory procedure SOPs in an Addendum once an analytical laboratory is selected.

5.1 Data Reporting. The following data will be reported:

1. Field data plots from all pushes, including the three SCAPS DNAPL sensors, cone pressure, sleeve friction, and soil classification, each with respect to depth. All push data displaying the raw data collected during the pushes as well as analog and digital video data.

2. System check and calibration sample concentrations; tabulated raw system check and calibration sample data; average system check response for each push; background, noise, and sensitivity calculated from calibration data.

3. Stab sampling logs indicating soil sample collection information, including sample numbers, depth of samples, location of water table, and other relevant information concerning the collection of the soil samples; chain-of-custody documentation associated with soil samples.

4. Laboratory results for GC/MS measurements of soil samples, including the standard analytical results and quality control data. Field/laboratory results for visual and Sudan Red dye enahanced insepections of soil samples for evidence of free phase product.

The data for each SCAPS DNAPL sensor and the confirmatory analytical laboratory will be held by Gerogia Tech. Gerogia Tech will provide independent QA oversight of all demonstration activities.

Calculation of Data Quality Indicators
Completeness is defined as follows for all measurements:

$$\%C = 100\% \times (V / T)$$

where: %C = percent completeness
V = number of sample measurements judged valid
T = total number of discrete sample measurements.

6 Performance and System Audits

The following audits will be conducted during this demonstration. These audits will determine if this demonstration plan is being implemented as intended.

6.1 Performance Audit. PE samples will not be used in this demonstration. Because the three SCAPS DNAPL sensing technologies are dynamic, in situ measurement techniques, PE samples cannot be inserted into the three SCAPS DNAPL measurement processes. PE samples may be used for the laboratory samples.

6.2 On-Site System Audits. On-site system audits for sampling activities, field operations, and laboratories are not a part of the SSC-SD test plan but may be carried out at the direction of the ESTCP project manager. On-site system audits and inspections will take place in the field while the demonstration is being conducted or at the confirmatory laboratory and will be formally reported by the auditors to the project manager. Separate audit reports will be completed after the audits and provided to the participating parties through the Gerogia Tech coordinator.

6.3 Contingency Laboratory. A contingency laboratory would be used if the QC data from the reference laboratory indicate a problem with the data quality. A contingency laboratory has not been identified.

7 Quality Assurance Reports

QA reports provide management with the necessary information to monitor data quality effectively. Proper QA begins with integration into the test plan. The SSC-SD, DTI, and Gerogia Tech data quality managers will ensure that QA is an integral part throughout all phases of this demonstration project, the test plan, field operations, validation sampling, analytical laboratory analysis, and final reporting. Status and audit reports will be prepared as required as part of this demonstration project and are described below.

7.1 Status Reports. The SSC-SD project manager, in conjunction with DTI and Gerogia Tech will prepare written status. These reports will discuss project progress, problems and associated corrective actions, and future scheduled activities associated with the demonstration. When problems occur, SSC-SD, DTI and Gerogia Tech project managers will discuss them, estimate the type and degree of impact, and identify the corrective actions to be taken to mitigate the impact and to prevent a recurrence of the problems.

7.2 Audit Reports. As part of this demonstration project, SSC-SD, DTI and Georgia Tech will follow the QA procedures for the three SCAPS DNAPL sensors detailed in this test plan. The analytical laboratory will follow QA procedures that will be detailed in an Addendum to be submitted upon selection of the analytical laboratory. The resulting QA information will be included as part of the technology evaluation report. Independent QA audits are not a part of this test plan, but may be carried out at the direction of the ESTCP project manager. QA audits and inspections will take place in the field while the demonstration is being conducted or at the confirmatory laboratory and will be formally reported by the auditors to the project manager. The Georgia Tech coordinator will forward independent audit reports to SSC-SD, DTI and Georgia Tech for review and appropriate actions.